THE SYNTHESIS AND CHARACTERIZATION OF Ni(II) AND Cu(II) CYANOXIMATES

A Masters Thesis

Presented to

The Graduate College of

Missouri State University

In Partial Fulfillment

Of the Requirements for the Degree

Master of Science, Chemistry

By

Adedamola Abraham Opalade

July, 2016

THE SYNTHESIS AND CHARACTERIZATION OF Ni(II) AND Cu(II) CYANOXIMATES

Chemistry

Missouri State University, July, 2016

Master of Science

Adedamola Abraham Opalade

ABSTRACT

The design of one-dimensional nickel wires were attempted. Metal complexes of hydrated Cu(II) and Ni(II) with several cyanoximates were synthesized and characterized by elemental analysis, thermal analysis, IR-, electronic- (solid state diffuse reflectance) spectroscopy, and the X-ray analysis (powder diffraction and single crystal studies). Hydrolysis of the HECO and HMeCO cyanoxime ligands leads to the formation of another dianionic cyanoxime – $AACO^{2-}$, which forms multimetallic Cu(II) and Ni(II) complexes and oxamide as a side product. The crystal and molecular structures of 8 compounds were determined (6 metal complexes and 2 organic compounds). Two Ni metal complexes have distorted octahedral structures with the cyanoximes acting as a chelating ligand, one Cu metal complex has distorted square pyramidal structure and three metal complexes of Cu and Ni were found to be multimetallic with two different environments: penta- and hexa-coordinated which correspond to distorted square pyramidal and octahedral geometries. The trimetallic complexes of Ni(II) and Cu(II) with $AACO^{2-}$ are isostructural. The tri-copper(II) complex demonstrates significant antiferromagnetic interactions between the cyanoxime-bridged metal centers at room temperature. All metal complexes have both coordinated, and crystallization water molecules, which are essential for the crystal packing via the system of H-bonds. The hydrated complexes of Ni(II) of selected cyanoximes were dehydrated, and respective anhydrous complexes were obtained and characterized. Electronic spectroscopy and XRD powder diffraction studies of the anhydrous complexes evidenced the retention of geometry of the central Ni atom after dehydration which suggests bridging function of cyanoximes in the lattices even after water loss. These results show the design of the desired one-dimensional nickel wire systems are feasible.

KEYWORDS: cyanoximes, Ni(II) and Cu(II) complexes, crystallohydrates, TG/DSC, IR-, Uv-Vis spectroscopy, X-ray single crystal analysis, XRD powder diffraction, antiferromagnetic

This abstract is approved as to form and content

_____

Dr. Nikolay N. Gerasimchuk Chairperson,
Advisory Committee Missouri State University

THE SYNTHESIS AND CHARACTERIZATION OF Ni(II) AND Cu(II)

CYANOXIMATES

By

Adedamola Abraham Opalade

A Masters Thesis
Submitted to the Graduate College
Of Missouri State University
In Partial Fulfillment of the Requirements
For the Degree of Master of Science, Chemistry

July, 2016

Approved:

_____
Dr. Nikolay N. Gerasimchuk

_____
Dr. Richard N. Biagioni

_____
Dr. Reza Sedaghat-Herati

_____
Dr. Diann Thomas

_____
Julie Masterson, PhD: Dean, Graduate College

ACKNOWLEDGEMENTS

I would like to thank Dr. Nikolay N. Gerasimchuk for the great deal of time and effort he invested in making my journey through my graduate program a successful one. Not only has he been my research advisor, but he has also been a good mentor to me.

I would like to thank the committee members for their patience, time and energy invested to look over my research project.

I would also like to thank Dr. Sergey V. Lindeman, Marquette University, for the powder X-ray data; Dr. Bruce Noll, Bruker AXS; for recording the powder XRD patterns as well; Prof. Amitava Choudhury, Missouri University of Science and Technology, for his help with solid state diffusion reflectance spectra and Prof. Mikhail Barybin from The University of Kansas for his help with a single sample magnetic susceptibility studies.

I would also like to thank the Missouri State University Graduate College and Chemistry Department for research funding and other assistances.

Finally, I would extend my appreciations to a co-student in Dr. Gerasimchuk's research group – Snow Popis for being a wonderful research partner.

TABLE OF CONTENTS

LIST OF TABLES

LIST OF FIGURES

I. INTRODUCTION

I.1. One-dimensional Compounds

Extended compounds such as coordination polymers can be classified as one, two- or three-dimensional based on dimensionality of the structure. Solid brings to mind the idea of three dimensional space (volume or depth) and it may, therefore, seem strange to discuss solids that exist, or be described as one dimensional. This concept, however, is quite relevant and, in fact, refers to a situation in which chemical bonds exhibit a high degree of directional anisotropy (changes in properties with change in direction). One-dimensional solids on microscopic scale are polymeric compounds composed of stacked sheets or chains, fibers, or ladders that are extended in one direction only. The term '1D' should be more accurately prefixed by 'quasi' - [1]. To be one-dimensional, the pattern of the complex compound must advance in one direction. One-dimensional metal wires can have different patterns of arrangement of the metal centers in coordination compounds. The arrangement could be such in a way that they line up to give straight 'poker chip' stacks as in the case of Magnus' green salt, $[Pt(NH_3)_4][PtCl_4]$. The arrangements can be more complex such as those in zig-zag, helical, ribbon, and or ladder motifs, all extending in one-direction [2].

In the past, a number of extended in one dimension materials and coordination compounds were studied intensely. These include $K_2Pt(CN)_4X_{0.3}\cdot 3H_2O$, where X = Cl, Br (KCP), tetracyanoquinodimethane (TCNQ) salts and the purely inorganic sulfur-nitrogen polymer $[(SN)_x]$ [3]. The compound KCP(Br), or Krogmann's salt – $[K_2Pt(CN)_4Br_{0.3}\cdot 3H_2O]$ is the most extensively studied organo-metallic quasi one-

dimensional solid. Its precursor $K_2Pt(CN)_4$ has a highest occupied electron band produced by the overlap of the platinum electron orbitals (d_z^2 orbitals) in a linear array and because this band is full, the compound is an insulator. In KCP(Br) the mixed valence polymer is formed, and bromide anions are included interstitially between the Pt(II)---Pt(IV) chains. These Br^- compensate for extra '+' charge of partially oxidized to Pt(IV) state metal centers [1]. A removal of the d_z^2 electrons from the metal centers introduces a hole along the Pt-----Pt 'wire' and thus facilitates free electron motion in it. This property leads to electrical conduction in one dimension.

Oxalato anion based complexes, for example, $[K_{1.6}Pt(C_2O_4)_2 \cdot 1.2H_2O]$ originally prepared in 1888 by German chemist H.G. Soderbaum, are also one-dimensional conductors with analogous structures [3]. Certainly, mixed valency is important because of conducting 1D solids. This includes integral and non-integral oxidation state metal complexes with columnar structures. Tetra-coordinated planar complexes have featured strongly in this field where the central metal atom with d^8 and d^4 electronic configuration shows columnar structure formation with pronounced metallophilic interactions, and has the desired chemical and physical properties. Thus Rh^I, Ir^I, $Pd^{II,}$ and Pt^{II} satisfy the d^8 requirements and consequently received increased attention [4].

One-dimensional conductors based on platinum are very common, with the cyano complexes best known. Thus $K_2[Pt(CN)_4] \cdot 3H_2O$ is a very stable colourless solid but by appropriate partial oxidation it is possible to obtain bronze-coloured, 'cation-deficient', $K_{1.75}[Pt(CN)_4] \cdot 1.5H_2O$ and other partially oxidized compounds like $K_2[Pt(CN)_4X_{0.3}] \cdot 3H_2O$. In these, square planar $[Pt(CN)_4]^{n-}$ ions are stacked (Figure 1) to give linear chain of Pt atoms in which Pt – Pt distances of 280 – 300 pm compared to 348

pm in the original $[K_2[Pt(CN)_4]\cdot 3H_2O]$ and 278 pm between the metals itself allow strong overlap of d_z^2 orbitals. This account for metallic 1D conductance of these materials only along the 'metal – metal wire'. Indeed, there is considerable current interest in such one-dimensional electrical conductors [5] as molecular electronics materials. One-dimensional metals exhibit unusual collective behavior such as an abrupt decrease of conductivity due to Peierls instability at low temperatures [3].

A major shortcoming in the field of 1D compounds described above 'metal wires' research is the inability to create systems with systematically varied and predictable structures to establish the relationship between structure and properties [6]. Another big problem was their poor solubility in common solvents. Afterall, those 1D solids were coordination polymers.

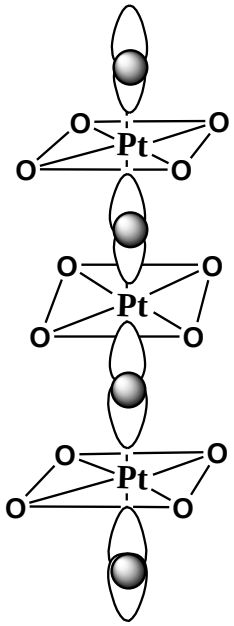

O - C of CN

Figure 1. Stacking of square-planar units in $[Pt(CN)_4]^{n-}$ showing possible overlaps of d_z^2 orbitals [5].

I.2. Classification of One-dimensional Solids

One-dimensional solids may be classified into the following categories:

One-dimensional Conductors: e.g TTF-TCNQ, $[K_2Pt(CN)_4X_{0.3}\cdot 3H_2O]$ (X = Cl or Br), $NbSe_3$ and $BaVS_3$ [3].

One-dimensional insulators: Several insulating ABX_3 solids ($A = Rb^+$, Cs^+, Tl^+ or $(CH_3)_4N^+$; $B = Mn^{2+}$, Fe^{2+}, Co^{2+} or Ni^{2+} and $X = Cl^-$, Br^- or I^-) crystallizes in one-dimensional structure containing chains of B atoms. These chains are separated from one another by large A cation. These solid exhibit quasi one-dimensional magnetic behavior, with $(CH_3)_4NMnCl_3$ being well studied [7].

One dimensional metals and polymers: One dimensional metals and polymers have strong orbital overlap with neighbouring atoms along a chain, have negligible interaction between chains (anisotropy) and also a partially filled conductance band.

I.3. Columnar Metal Chain Compounds

Integral oxidation state compounds exhibits insulating and semi-conducting properties and non-integral oxidation state compounds exhibit varied properties including metallic conductivity [4]. To form a metal atom chain columnar structure, a co-planar monomeric 'building block' complex is required. Tetra-coordinate square planar complexes including a central metal ion with d^8 electronic configuration such as Ni^{II}, Pd^{II} and Pt^{II} may be used. The central atom 3d, 4d or 5d electrons extend to neighboring monomers allowing orbital overlap whereby electron delocalization along the metal atom chain may occur at the appropriate conditions. There exist a potential electrically conducting chain of metal ions surrounded by insulating ligands. The insulating ligand helps to separate columns and the monomer-monomer inter-ligand interactions usually lead to a staggered plane conformation. They also affect the metal atom chain electronic states [4].

The energy gap is dependent on metal ion separation. Conductivity has been shown to increase with decreasing metal-metal separation in cyanoplatinates. Large

organic ligand groups cause an increase in metal separation due to mutual complex repulsion and hence lead to a decrease in conductivity. To have a desirable conductivity; small ligands are preferable [4]. Variation in the metal-metal distance can be a key factor in altering the electrical conductivity and optical properties of 1D metal compounds [8,9].

I.4. Applications of One-dimensional Compounds

Interest has grown in one-dimensional solids because of their high electrical and optical anisotropy and potential utility in molecular sensing, nanotechnology and photovoltaic devices [10]. Recently the 1D polymeric platinum cyanoximate has been shown to exhibit near infra-red emission, making it interesting for the further NIR applications in industry, science, military and medicine as new optical devices [11,12], sensors [13], contrast agent [14 – 15] and imaging techniques [16 – 17]. The 1D polymeric platinum cyanoximate of 2-cyano-2-oximino-N,N'- dimethylaminoacetamide, DECO, emits beyond 1000 nm and was first reported in 2015 [18].

II. LITERATURE REVIEW

II. 1. Ligands for Coordination Compounds

Ligands represent Lewis bases with at least one electron pair that can be donated to metal atoms or metal ions, which are Lewis acids through coordinate covalent bonds. Coordination compounds are formed as a result of Lewis acid – base reactions between ligands and metal atoms/ions. There are numerous different classes of organic ligands employed in coordination chemistry, one of which include oximes (compounds with the >C = N – OH fragment). Cyanoximes are subclass of oximes and have general formula HONC(CN)-R, where R is an electron-acceptor/ withdrawing group containing O, N or S donor atoms. This can be NC, amide, thioamide, keto groups, carboxylic ester, substituted aryl, and heteroaryl fragments [19 – 23]. There are 42 cyanoximes known today (Figure 2). Cyanoximes are more acidic than their aldoxime, ketoxime and dioxime (Figure 3) [24] counterparts by a magnitude of about 10^3 - 10^5 [25 -26]. The increased relative acidity of cyanoximes is due to the presence of a strongly electron - withdrawing cyano group next to the oxime moiety [27, 28]. This was revealed in one of the previous works where Cu^{2+} and Ni^{2+} ions complexes of 2- (hydroxyimino)propanamide , 2-(hydroxyimino)propanoic acid, 2-cyano-2-(hydroxyimino)acetamide and 2-cyano-2-(hydroxyimino)acetic acid (Figure 4) were prepared and the stability constant of both Cu^{2+} and Ni^{2+} ions complexes with 2-cyano-2-(hydroxyimino)acetamide and 2-cyano-2-(hydroxyimino)acetic acid were several orders of magnitude lesser than those of the counterpart 2-(hydroxyimino)propanamide and 2-(hydroxyimino)propanoic acid complexes because of the increased acidity of the cyano carrying species which

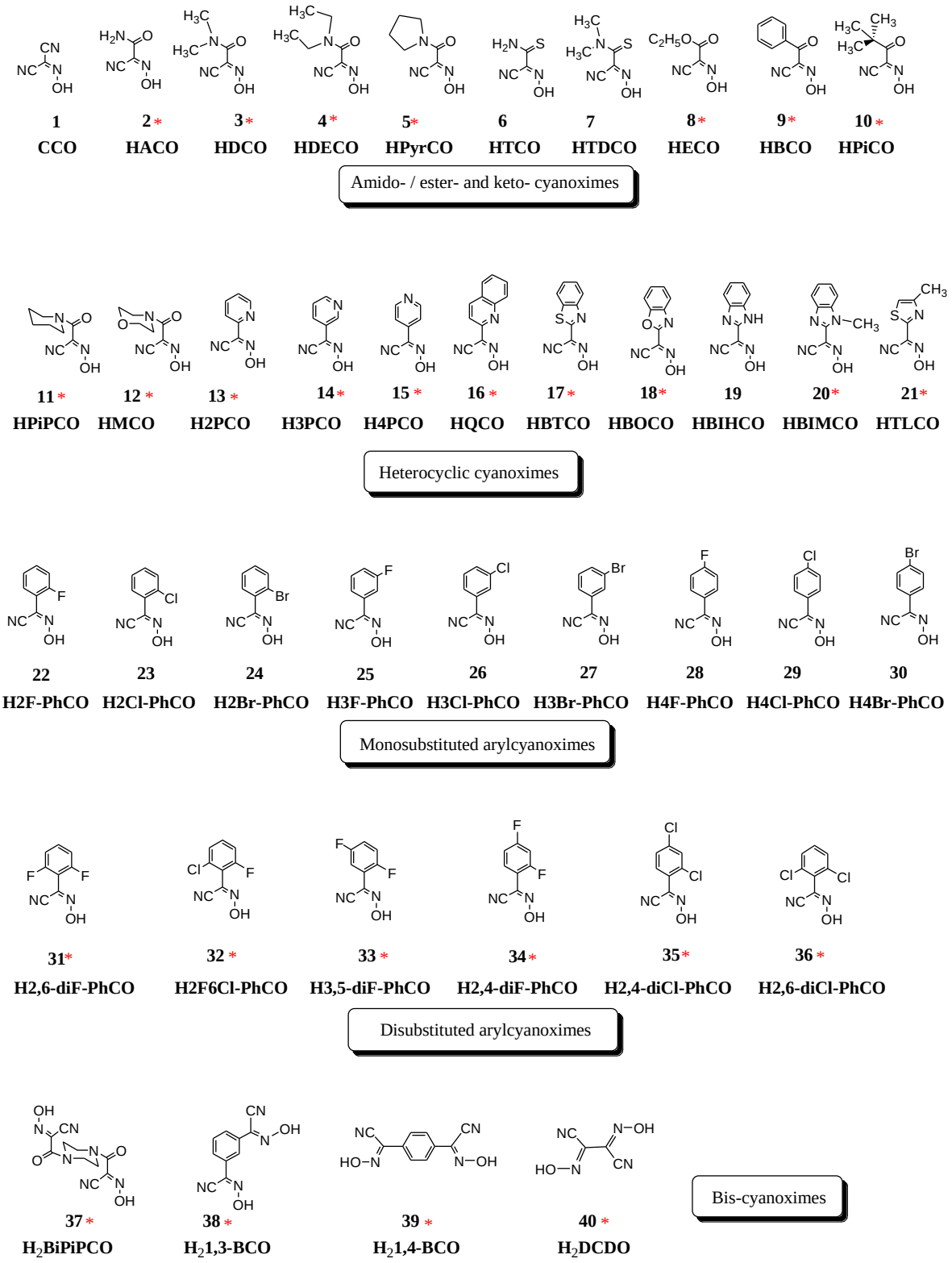

Figure 2. List of cyanoxime ligands. * - Crystal structures were determined.

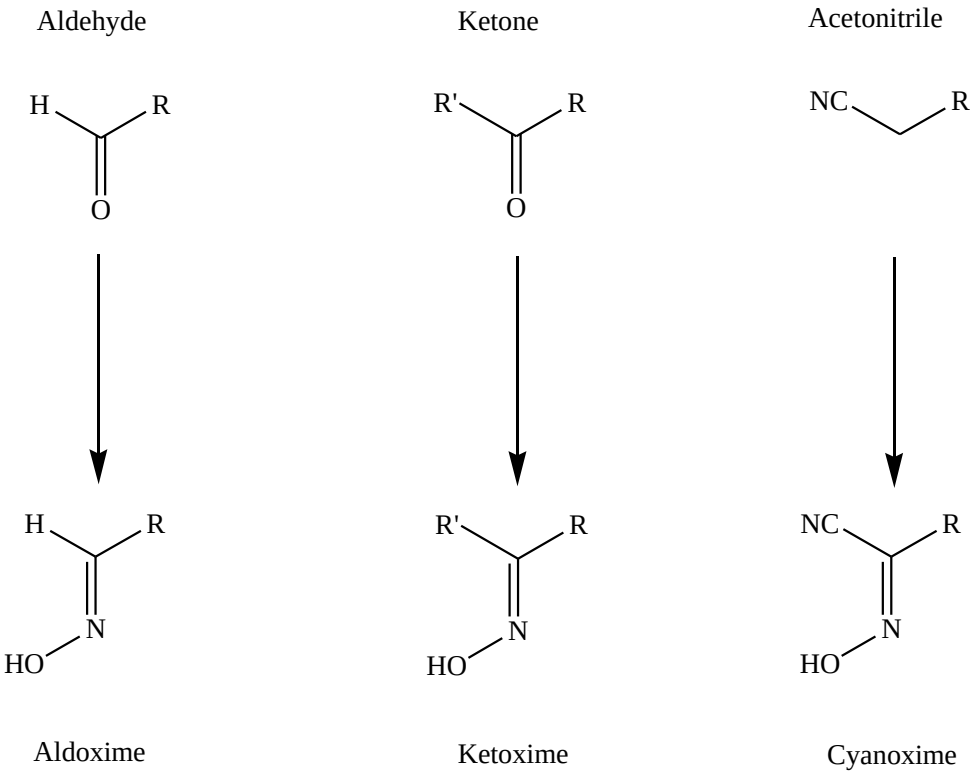

Figure 3. Classes of oximes.

consequently, lead to a decreased stability [28, 29].

The presence of the cyano group makes deprotonation of the cyanoxime in alkaline medium very facile in aqueous and non-aqueous solutions to form yellow coloured stable cyanoximate anions [26, 30, 31] (Figure 5). The colour originates from ground state to a low lying excited state $n \rightarrow \pi^*$ in the *nitroso*-chromophore in the visible region of the spectrum, similar to the transitions [32] found in the NO_2^- and $ONC(CN)_2^-$ anions [26, 33, 34, 35]. The negative charge is delocalized throughout the cyanoximate and the cyanoximate can be represented by four mesomeric forms for most of these anions that also includes the *nitroso* – structure [20, 36] (Figure 6). The cyanoximate ion can also exist in different conformations due to rotation around the C – C bond between the alkyl group and cyanoxime fragment, and thus the presence of rotational isomers of the NO group

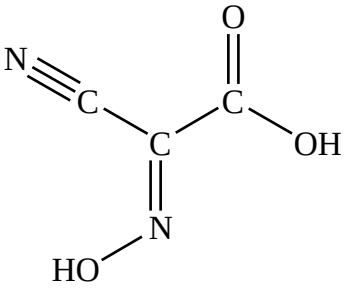

2- Cyano-2-(hydroxyimino)acetic acid

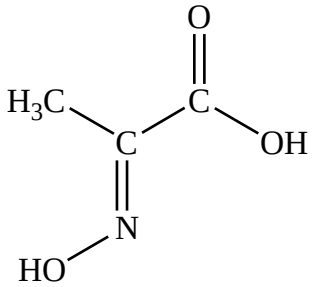

2-Hydroxyiminopropanoic acid

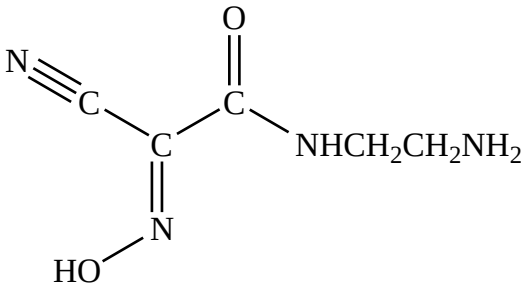

N-(2-Amino-ethyl)-2-cyano-2-hydroxyimino-acetamide

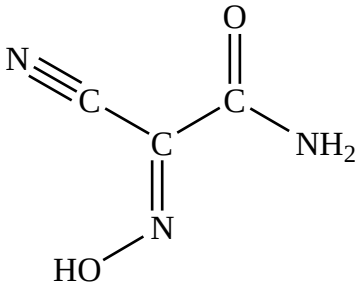

2-Cyano-2-hydroxyimino-acetamide

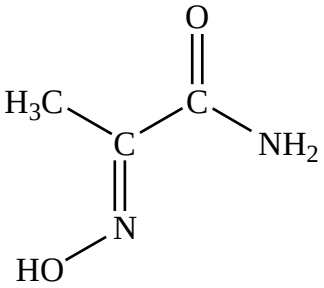

2-Hydroxyimino-propionamide

Figure 4. Oxime ligands used for the previous studies [28].

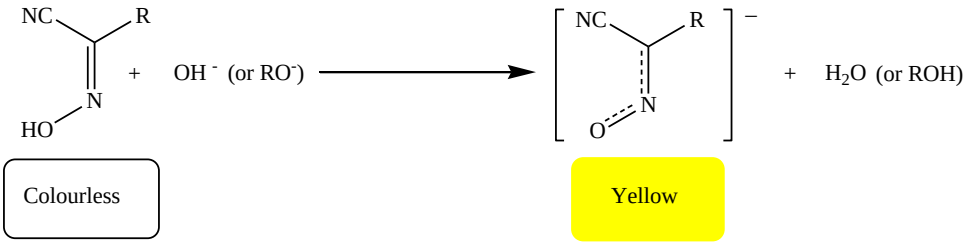

Figure 5. Deprotonation of cyanoximes.

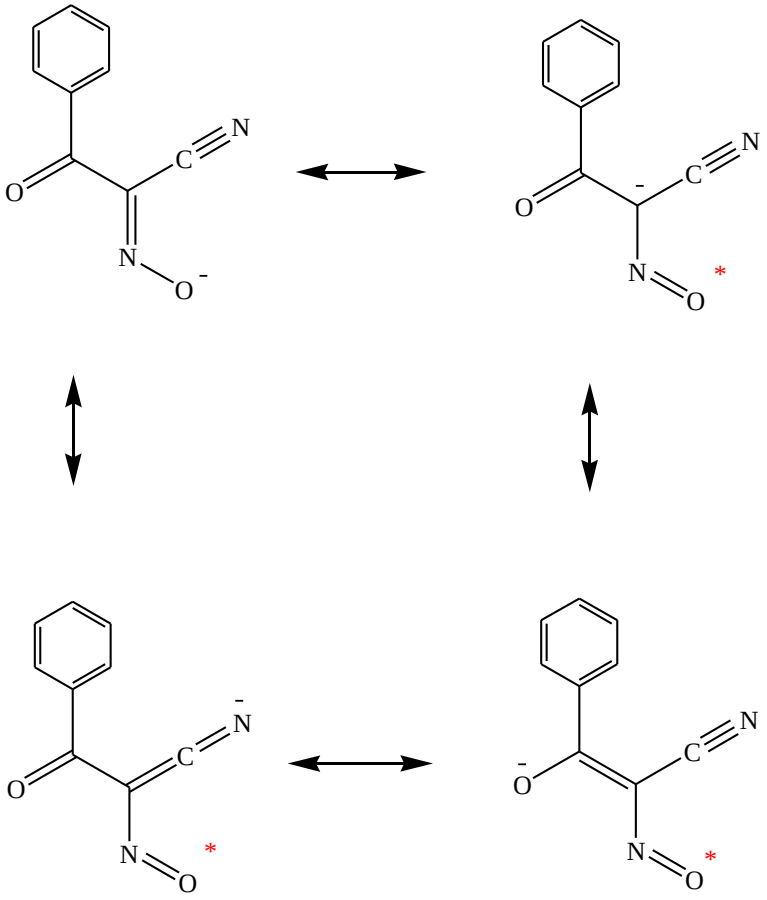

Figure 6. Four mesomeric forms for acido-cyanoximes; * - nitroso – forms.

(Figure 7). Therefore, elevated acidity combined with the solubility of alkali-metal salts

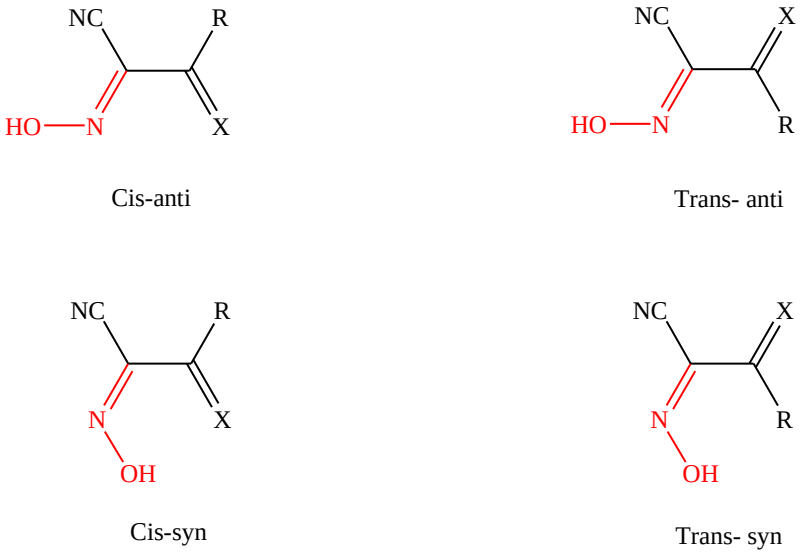

Figure 7. Geometrical isomers of cyanoximes.

and ability to act as ambidentate ligands makes them attractive for coordination chemistry [26, 36].

Cyanoximes were found to be excellent ligands because of their propensity to coordinate to different metal ions and their ability to adopt several conformations [25, 26]. These abilities make cyanoximes in general to be considered as models for ambidentate biological receptors. Their ability to form stable metal complexes with different chemical properties in aqueous or non-aqueous media together with variety of coordination modes make cyanoximes suitable for development of selective sorbents [26]. In deprotonated form, all cyanoximes are known to readily form various coordination compounds [37], in which they demonstrate different coordinating modes. In 3d-metal complexes, the amide containing cyanoxime acido-ligands: $[ONC(CN)C(S)NH_2]^-$ and $[ONC(CN)C(O)NH_2]^-$ exhibit chelating function, forming five-membered metallocycles by coordination via

nitrogen atoms of *nitroso* groups and via sulfur atoms [38, 39] or oxygen atoms [32] of the amide fragment.

The interest in cyanoximes and their coordination compounds is aroused due to their established biological activities and antimicrobial activities [24, 40 – 43]. Cyanoxime ligands with heterocyclic substituents are used in analytical chemistry. For example, almost all of the cyanoximate ions form intensely colored stable anionic tris-complexes with Fe^{2+} cations, and this effect finds use in analytical chemistry [30, 44].

II.2. Preparation of Cyanoxime Ligands

Cyanoximes are prepared by the Meyer reaction by using substituted acetonitriles and source of NO group such as KNO_2, $NaNO_2$ or organic nitrites [34]. The Meyer reaction can be carried out using three different routes. The easiest routes are **1** and **2** (Figure 8) while route **3** requires an alkyl nitrite and basic conditions. The choice of the route completely depends on the activity of the initial substrate $R – CH_2 – CN$ (Figure 3, 8).

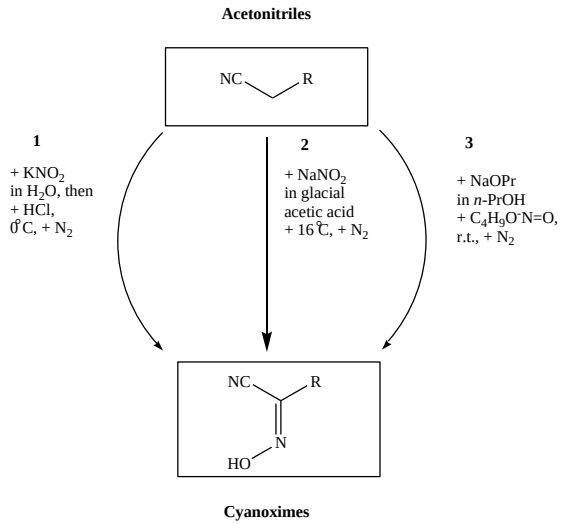

Figure 8. Cyanoximes synthetic routes from substituted acetonitrile.

II.3. Metals Used for Studies

II.3.1. Nickel: Its Chemistry and Applications. Nickel was discovered by the Swedish chemist Baron Axel Fredrik Cronstedt in the mineral niccolite (NiAs) in 1751 when he was trying to extract copper from kupfernickel at a cobalt mine in the Swedish village of Los and instead extracted a white metal [45]. Today, most nickel is obtained from the mineral pentlandite (NiS.2FeS). The name 'nickel' originates from the German word 'Kupfernickel' (devil's copper), derived from the German word for copper [46]. Nickel has electronic structure [Ar] $3d^8$ $4s^2$ and has oxidation states –I, 0 (well characterized but less important states), +II (the most important oxidation states because they are the most abundant and stable), +I and +IV oxidation states which are unstable, or in doubt. Ni(-I) is found in the carbonyl anion $[Ni_2(CO)_6]^{2-}$, the zero-valent is found in $[Ni^0(CO)_4]$ (Table 1) [47]. The Ni(+I) is found in $K_4[Ni^I_2(CN)_6]$. The Ni(+II) is very prevalent and is found in a lot of compounds, for example, $[Ni(H_2O)_6]^{2+}$, $[Ni(CN)_4]^{2-}$ and so on. Ni(+III) is found in compounds like $K_3[NiF_6]$, $Ni_2O_3 \cdot 2H_2O$ which decompose to NiO on dehydration. +III is also found in NiOOH – used in NICAD and nickel metal hydride batteries. The Latimer diagrams for nickel in acidic and basic solutions are shown in Figure 9 [48]. Ni(+IV) is rare but is found in compound like $K_2[NiF_6]$, which is strongly oxidizing and liberates O_2 with water [49]. The d^8 electronic configuration of Ni(II) ion is as shown in Figure 10.

II.3.1.1. Application of Nickel**.** About 46 % of nickel produced is used in stainless steel production to produce ductile, stable and corrosion resistance material. 14 % goes into electroplating with 34 % going into nonferrous and super alloys production and 6 % into other uses [49, 50]. End uses were as follows: transportation, 30 %; fabricated metal

products, 14 %; electrical equipment, 12%; petroleum industry, 10 %; chemical industry, construction, household appliances, and industrial machinery, 8 % each; and others, 2 % [49].

Table 1. Oxidation states and stereochemistries of nickel compounds [5]

Oxidation state	Coordination number	Stereochemistry	Ni Compound
-1	4	Trigonal prism	$[Ni_2(CO)_6]^{2-}$
0 (d^{10})	3	Planar	$[Ni\{P(OC_6H_4\text{-}2\text{-}Me)_3\}_3]$
	4	Tetrahedral	$[Ni(CO)_4]$
1 (d^9)	4	Tetrahedral	$[NiBr(PPh_3)_3]$
	3	Trigonal planar	$[Ni(NPh_2)_3]^-$
2 (d^8)	4	Tetrahedral	$[NiCl_4]^{2-}$
		Square planar	$[Ni(CN)_4]^{2-}$
	5	Trigonal bipyramidal	$[Ni(PPhMe_2)_3(CN)_2]$
		Square Pyramidal	$[Ni(CN)_5]^{3-}$
	6	Octahedral	$[Ni(H_2O)_6]^{2+}$
		Trigonal prismatic	NiAs
	7	Pentagonal bipyramidal	$[Ni(dapbH)_2(H_2O_2)]^{+2}$ [1]
3 (d^7)	4	Square planar	-
	5	Trigonal bipyramidal	$[NiBr3(PEt_3)_2]$
	6	Octahedral	$[NiF_6]^{3-}$
4 (d^6)	6	Octahedral	$[NiF_6]^{2-}$
	8	'Piano-stool'	-
5 (d^5)	6	Octahedral	-
6 (d^4)	6	Octahedral	-

A. $NiO_2 \xrightarrow{+1.68\ V} Ni^{2+} \xrightarrow{-0.25\ V} Ni$

[1] dapbH = 2,6-diacetylpyridinebis(benzoic acid hydrazone)

B. $NiO_2 \xrightarrow{+0.49\ V} Ni(OH)_2 \xrightarrow{-0.72\ V} Ni$

Figure 9. The Latimer diagrams for Ni in acidic (1 M H^+) (A) and basic (1 M OH^-) (B) solutions [48].

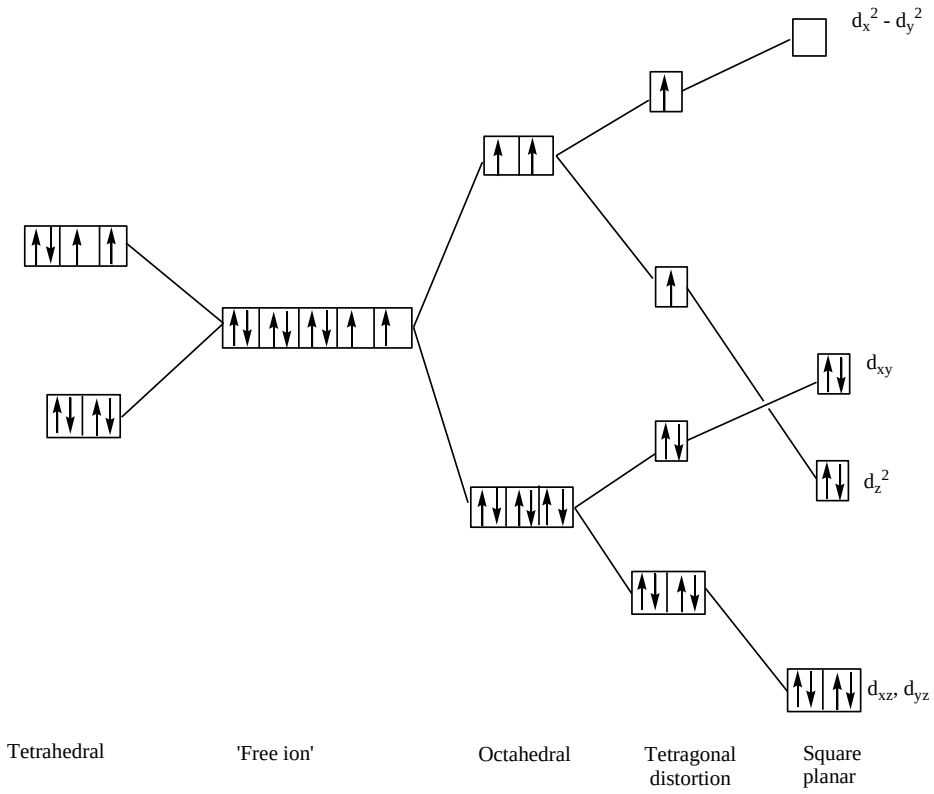

Figure 10. The splitting of d^8 ion orbitals in fields of different symmetries [5].

Nickel's biological role was not recognized until the 1970s. Nickel plays an important role in biological microorganisms and plants [51, 52]. The hydrogen gas oxidizers 'NiFe-hydrogenases' contain nickel in addition to iron-sulphur clusters. Cofactor F430, which is a nickel-tetrapyrrole coenzyme, is present in methyl coenzyme M reductase which powers methanogenic archaea [53]. Other nickel containing enzyme is the rare bacterial class of superoxide dismutase and glyoxalase I enzymes in bacteria and several

parasitic eukaryotic trypanosomal parasites [54] (In higher organisms and mammals, these enzymes use Zn^{2+}) [55 - 57].

II.3.1.2. Identification of Nickel. Nickel complexes can be identified and subsequently analyzed by making use of dimethylglyoxime ($dmgH_2$) [58]. This dioximic organic reagent was introduced by Russian chemist Chugaev [59]. It gives a flocculent magenta-red coloured precipitate complex of $[Ni(dmgH)_2]$, a very poorly soluble square-planar complex (Figure 11) which would precipitate out of solution. This method has been used in the gravimetric determination of Ni. Additionally, $[Ni(dmgH)_2]$ complex can be extracted by non-polar solvents from aqueous solutions. The Pd and Pt complexes form similar complexes as well. Table 2 contains some useful properties of nickel.

Table 2. Some properties of nickel [5, 47]

Property	Value
Covalent radius (Å)	1.15
Ionic radius (Å)	M^{2+} = 0.69
	M^{3+} = 0.60[2]
Pauling's electronegativity	1.8
Electrical resistivity (20 °C) μ ohm cm	6.84
MP/ °C	1455
BP/ °C	2920

[2] High spin value

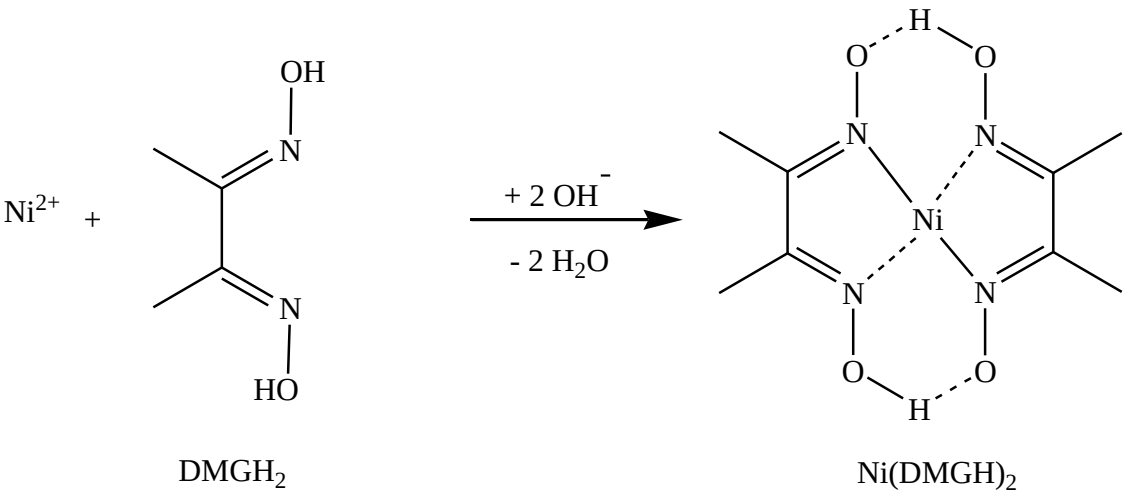

Figure 11. The formation of square-planar magenta-coloured complex of [$Ni(DMGH)_2$].

II.3.1.3. Selected Coordination Chemistry of Ni Complexes. Nickel (II) ion forms numerous stable complexes and can exist with varieties of coordination numbers which frequently demonstrate a very interesting coordination chemistry. Tetrahedral and square planar complexes are very common. Square pyramid and trigonal bipyramid complexes have been found as well, while octahedral complexes are by far the most abundant. Equilibria often exist between penta-coordinated complexes [5].

The most intriguing feature of changing coordination numbers 5 and 6 in Ni-complexes, especially in hydrated ones, is the reaction of acetylacetone with $Ni(NO_3)_2$ in the presence of a base, which gives the blue - green diaquo complex $Ni(acac)_2 \cdot 2H_2O$ with coordination number of 6, having two molecules of water attached axially (Figure 12). Dehydration of the complex by heat with the use of the Dean-Stark trap by azeotropic distillation leads to the trimerization because $Ni(acac)_2$ is coordinatively unsaturated [59]. Hence, the formation of the emerald green trimeric $[Ni(acac)_2]_3$ complex afford coordinatively saturated nickel(II) in a distorted octahedral environment (Figure 13).

Upon exposure to the moist atmosphere, $[Ni(acac)_2]_3$ converts back to the chalky green monomeric dihydrate [59, 60]. At about 80 K $[Ni(acac)_2]_3$ exhibit normal paramagnetism with μ_{eff} = 3.2 BM close to the spin-only moment value of 2.9 – 3.3 BM expected of an

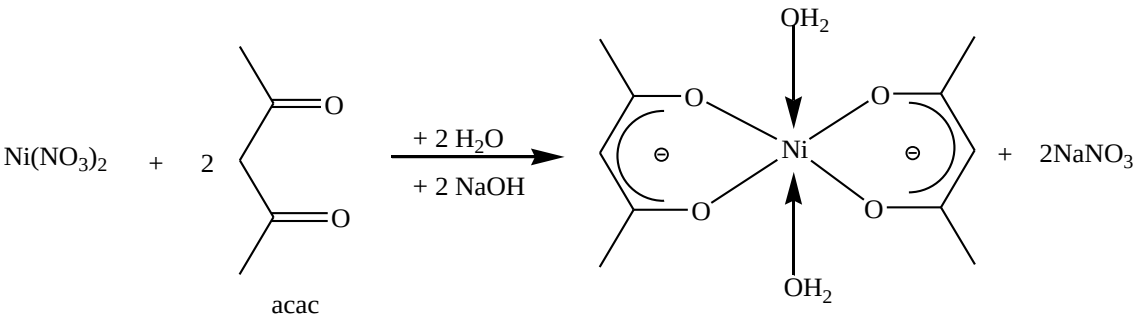

Figure 12. Synthesis of octahedrally coordinated diaquo $Ni(acac)_2 \cdot 2H_2O$

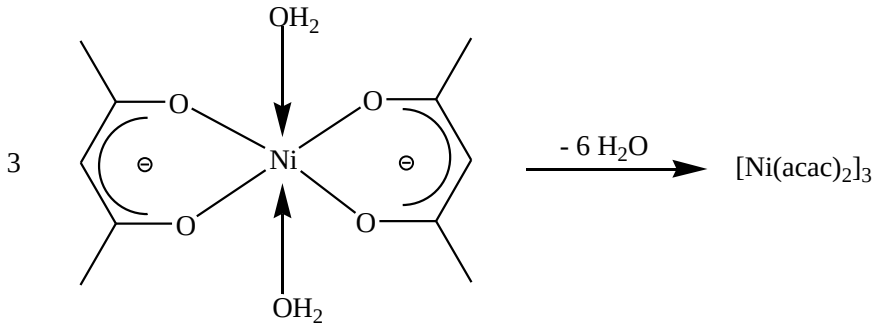

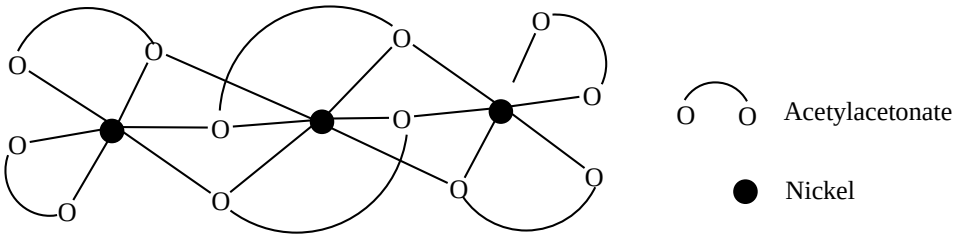

Figure 13. $Ni(acac)_2$ after dehydration showing octahedrally Ni atoms.

ion with d^8 configuration with two unpaired electrons in an octahedral environment. At 4.3 K the μ_{eff} = 4.1 BM due to ferromagnetic exchange interactions involving all the three nickel ions [5, 61]. Making use of substituted acetylacetone by replacing the $–CH_3$ group of acetylacetone with $–C(CH_3)_3$ prevents the formation of the trimer but instead the red square-planar monomeric complex is formed [5].

The described above case of $Ni(acac)_2$ is common for other acac – type system. Furthermore, nickel acetylacetonate ($Ni(acac)_2$) is only found to be monomeric at temperatures around 200 °C in non-coordinating solvent such as *n*-decane. Octahedral monomeric species are formed in solvents such as pyridine at room temperature but in the solid state $Ni(acac)_2$ exist as trimer as shown in (Figure 13) where Ni atoms are in distorted octahedral environment.

II.3.2. Copper: Chemistry and Applications. Copper is a chemical element with element symbol Cu and atomic number 29. Its electronic structure is [Ar] $3d^{10}$ $4s^1$. The oxidation states of Cu are +I, +II and +III (Table 3). The most important oxidation state is +II. The +I oxidation state is well-characterized but less important and +III are unstable, or in doubt [47]. In the oxidation state of +II, copper provides the most extensive inorganic and coordination chemistry of this element. Simple salts are formed with most known anions except CN^- and I^-, which instead form covalent Cu(I) compounds insoluble in water. The salts are significantly water soluble and the blue colour of their solutions arise from the single electron transition in visible spectrum at ~ 600 – 800 nm. Salts of Cu(II) frequently crystallize as hydrates [5]. The reduction potential of copper in acid and basic solution is as shown in Figure 14. The most common coordination number of copper (II) are 4, 5 and 6. In the latter there is a clear manifestation of Jahn-Teller distortion. A

Table 3. Oxidation states and stereochemistries of copper [5]

Oxidation State	Coordination Number	Stereochemistry	Cu Compunds
0 (d^{10} s^1)	3	Planar	$[Cu(CO)_3]$ (10 K)
	4	-	$[(CO)_3CuCu(CO)_3]$ (30K)
< +1	8		
	10		
	12	Icosahedral	
1(d^{10})	2	Linear	$[CuCl_2]^-$, Cu_2O
	3	Trigonal planar	$[Cu(CN)_3]^{2-}$
	4	Tetrahedral	$[Cu(py)_4]^+$
		Square planar	
	6	Octahedral	
2 (d^9)	4	Tetrahedral	$Cs_2[CuCl_4]$
		Square planar	$[EtNH_3]_2[CuCl_4]$
	5	Trigonal bipyramidal	$[Cu(bipy)_2I]^+$
		Square pyramidal	[3]$[\{Cu(dmgH)_2\}_2]$
	6	Octahedral	$K_2Pb[Cu(NO_2)_6]$
	7	Pentagonal bipyramidal	[4]$[Cu(H_2O)_2(dps)]^{2+}$
	8	Dodecahedral (dist.)	$[Cu(O_2CMe)_4]^{2+}$
3 (d^8)	4	Square planar	$[CuBr_2(S2CNBu^t_2)]$
	5	Square pyramidal	$[CuCl(PhCO_2)_2(py)_2]$
	6	Octahedral	$[CuF_6]^{3-}$
4 (d^7)	6	?	$[CuF_6]^{2-}$
5 (d^6)	6	Octahedral (?)	

[3] $dmgH_2$ = dimethylglyoxime
[4] dps = 2,6-diacetylpyridine bissemicarbazone

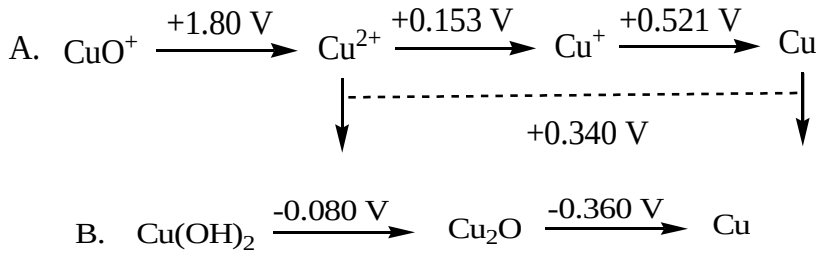

Figure 14. The Latimer diagrams of Cu in acidic (1 M H^+) (A) and basic (1 M OH^-) (B) solution [48].

distinction between square-planar and tetragonally distorted octahedral coordination is generally not easily made as a result of the above effect [62]. In the $KAlCuF_6$; for instance, there is a compression of the octahedron with two short axial bonds and four longer equatorial ones [62]. The usual result, however, is just the opposite: an elongation of the two axial bonds. In the most extreme case, lengthening of the axial bonds leads to the loss of the axial ligands and a formation of square-planar complexes [62]. The effect of configurational mixing of higher lying s-orbitals into the ligand field d-orbital basis set is also likely to favour elongation rather than compression [63]. The splitting of the d^9 ion is shown in Figure 15. Some important and relevant properties of copper are highlighted in Table 4.

II.3.2.1. Biological Significances, Uses and Applications of Cu. Copper is essential to life and adult humans contain about 100 mg. Though small amounts of copper are essential, larger amounts are toxic. About 4-5 mg of Cu are required in the daily diet and its deficiency will lead to the inability to make use of the iron stored in the liver which will then lead to anemia. Copper is present in the body bound to protein as either metalloproteins or enzymes [47]. Examples include various oxidases and blue protein. Copper is important in lysine oxidase, which affects the elasticity of aortic walls,

dopamine hydroxylase which affect brain function, tyrosinase, which affects skin pigmentation and ceruloplasmin, which plays a role in iron metabolism. Haemocyanin is

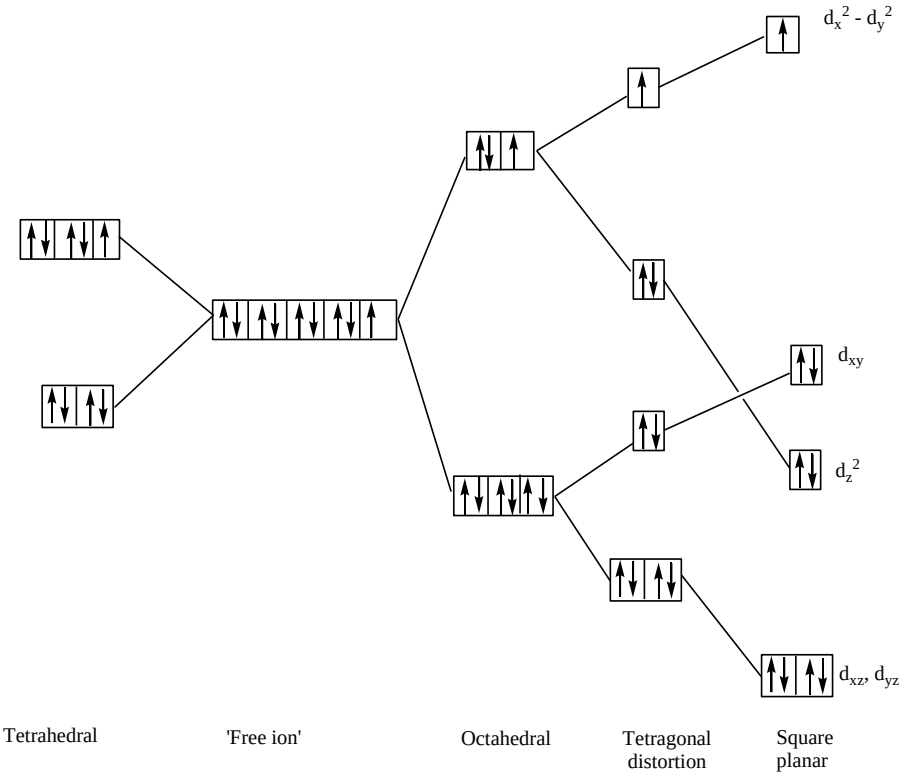

Figure 15. The splitting of d orbitals in fields of different symmetries and the resulting electronic configuration of the Cu^{II} d^9 ion [5].

Table 4. Some properties of copper [5, 47]

Property	Value
Covalent radius (Å)	1.17
Ionic radius (Å)	$M^+ = 0.77$ $M^{2+} = 0.73$ $M^{3+} = 0.54$[5]
Pauling's electronegativity	1.9
Electrical resistivity (20 °C) μ ohm cm	1.673
MP/ °C	1083
BP/ °C	2570

[5] Low spin value

a copper containing protein which is important as an O_2 carrier in invertebrate animals [47]. The blue protein act as electron transfer agent by means of a Cu^{2+}/Cu^{+} couple. Examples include plastocyanin and azurin [47]. Copper wire is used in the power industry, in electrical equipment [64] and it has also found application in construction [65]. Copper oxides are also used in the production of high temperature superconductors of which $YBa_2CU_3O_7$ is the most common [5].

II.3.2.2. Determination of Copper. Copper can be determined photometrically by using monosodium glutamate (MSG). The method is relatively simple, inexpensive, quantitative and makes use of readily available reagents. Copper (II) ion rapidly reacts with glutamate in aqueous solution at pH 10 to form a blue complex [66]. This serves as a basis for the determination of the copper (II) ion in the range of 10-500 µg/ml. This technique could be applied to determine copper (II) concentration in ore samples. Methods with other reagents like dithizone and diethyldithiocarbamate can be complicated and time consuming [66].

II.4. Coordination Chemistry of Cu(II) and Ni(II) Ions with Oximes and Cyanoximes

Modification of the amino group into the oxime functional group had been shown to lead to a very effective chelating agent. Oximes of amino acids and peptides have been shown to be a specific and efficient coordinating agent with Ni^{2+} and Cu^{2+} [67, 68]. The complexes formed are stable and water soluble [29]. Also, there is an extensive formation of dimers for Cu^{2+} systems above a pH of 5.

Previous work done on the copper (II) and nickel (II) complexes with oxime

analogues of amino acids using potentiometric, spectroscopic and x-ray studies of complexes of this metal ions with 2-cyano-2-(hydroxyimino)acetic acid and its ethane-1,2-diamine derivative (Figure 4) showed that 2-cyano-2-(hydroxyimino)acetic acid was found to be an effective ligand for Ni^{2+} and Cu^{2+} ions over a very broad pH range. Potentiometric and spectroscopic data revealed the formation of dimeric complexes with Cu^{2+} ions and the X-ray structural analysis revealed again that the dimeric structures were formed [28]. The deprotonation of the oxime group allowed the formation of dimeric species both for dipeptide and amino acid derivatives. Potentiometric and spectroscopic data obtained for copper (II) complex with 2-cyano-2-(hydroxyimino)acetic acid (HL) (Figure 4) suggest the formation of monomeric $CuHL_2$ and CuL_2, as well as dimeric species $Cu_2H_{-1}L_2$, $Cu_2H_{-2}L_2$ and $Cu_2H_{-3}L_2$ complexes. The formation of dimeric species was supported by EPR method in which signals became reduced in intensity because of the dimeric species. The dimeric species are predominant at pH above 3.5 and the monomeric species predominant at pH below 3.5. Nickel (II) ions form monomeric complex species only: $NiHL_2$, NiL_2, $NiH_{-1}L_2$. The $NiH_{-1}L_2$ specie was not found for the 2-(hydroxyimino)propanoic acid (Figure 4). All three nickel (II) species have distorted octahedral geometry [28]. In both cases where copper (II) and nickel (II) complexes of the 2-cyano-2-(hydroxyimino)acetic acid and 2-(hydroxyimino)propanoic acid were prepared, it was found that the 2-(hydroxyimino)propanoic acid complexes were more stable than the 2-cyano-2-(hydroxyimino)acetic acid complexes. This is because of the lower basicity of the 2-cyano-2-(hydroxyimino) acetic acid due to the strong electron withdrawing effect of the cyano group.

Studies were conducted with two effective chelating agents: oxime and ethane-

1,2-diamine, in one molecule forming a terdentate (N-(2-aminoethyl)-2-cyano-2-(hydroxyimino)acetamide) (Figure 4) chelating agent for copper (II) ions [69]. At pH from 4.5-9.0, the dimeric species $Cu_2H_{-1}L_2$ were predominant and above pH 9.0, the monomeric species $CuH_{-1}L$ were predominant. Spectroscopic data indicated that in both complexes the Cu^{2+} ions were complexed to three nitrogen donors $\{N_{oxime}, N^-, NH_2\}$ [69]. In the dimeric complex, one of the oxime oxygens undergoes deprotonation and bridges two Cu^{2+} ion species. Deprotonation of the second oxime OH group leads to the formation of the monomeric species with same $\{N_{oxime}, N^-, NH_2\}$ binding mode [28].

In essence, it was shown that the binding activity of the oxime towards Cu^{2+} and Ni^{2+} ions may easily be modified by the substituent attached to vicinal 2-carbon and rearrangement of electron density from oxime oxygen to the oxime nitrogen due to deprotonation would make the oxime nitrogen very efficient in metal-ion coordination with the deprotonated oxime oxygen responsible for the formation of dimeric copper (II) complexes [28]. The coordination ability of oxime derivatives of the amino acid can be improved by conjugation with strong chelating agents like ethane-1,2-diamine. The oxime nitrogen would serve as a low pH effective metal-ion anchoring site while conjugated ethane-1,2-diamine completes the coordination with its two strongly bonding nitrogen donors. The hydrolysis of the amide bond in N-(2-aminoethyl)-2-cyano-2-(hydroxyimino)acetamide might be catalyzed by the bound copper (II) metal ion [28].

Spectroscopic and theoretical studies of the interaction of Ni(II) and Cu(II) with 2-cyano-2-(hydroxyimino)acetic acid have shown that the transition metal complex of 2-cyano-2-(hydroxyimino)acetic acid have trans bidentate square-planar geometry with the different protonation state of the oximic group [28]. This is similar to the structures in

solution determined by potentiometric and spectroscopic studies [70].

Copper (II) complexes with N,N – dimethylacetamidocyanooximate ion (DCO^-) (Figure 2) were also investigated [71]. The diaquo complex $Cu(DCO)_2 \cdot 2H_2O$ was dehydrated to give $Cu(DCO)_2$. The intermediate $Cu(DCO)_2 \cdot H_2O$ was also obtained and studied. Single crystals were not obtained for the dihydrate and the anhydrous complexes but single crystal for the monohydrate was obtained by storing the mother liquor of $Cu(DCO)_2 \cdot 2H_2O$ in a dessicator charged with concentrated H_2SO_4.

The magnetochemical measurements performed on the $Cu(DCO)_2 \cdot 2H_2O$ and anhydrous $Cu(DCO)_2$ to test the hypothesis of the complex arrangement on the adjacent complex layer such that there exists a contact between the copper centers to afford magnetic exchange revealed mononuclear octahedral structure for $Cu(DCO)_2 \cdot 2H_2O$ with lack of exchange interactions between the copper (II) atoms. Lower μ_{eff} for $Cu(DCO)_2$ complex suggested a polymeric structure with exchange interactions between the paramagnetic copper centers but variable temperature magnetic measurement from 296 K to 363 K showed that the μ_{eff} of this anhydrous complex is independent of temperature hence suggest lack of magnetic interaction without excluding the possibility of polymeric structure [71].

The IR analysis revealed coordination to the copper (II) ion using the nitrogen atom of the nitroso group. An interesting observation in the case of the $Cu(DCO)_2$ and $Cu(DCO)_2 \cdot 2H_2O$ is the comparison of positions of ν(CN) in spectra. In the case of the anhydrous complex, the ν(CN) shift to a lower vibrational frequency and that can be viewed as a result of weak electrostatic interaction between the copper atom and the CN group of the adjacent molecule of the complex [71]. This can be described as a 'side-on'

coordination [72] through the system of multiple CN bonds. The monohydrate has H-bonding in between the H atoms of H_2O and O of the nitroso group of the adjacent complex along the y-axis. The nitrile is linear but the angle made by the nitrile group with the α-C atom of the oxime is 174°. Additional interaction between the Cu and the N atom of the nitrile of neighboring complexes with the N occupying a vacant position in the Cu^{2+} coordination polyhedron and it is situated *trans* to the aqua-ligand making an angle of 86.9 ° with Cu^{2+} ion. These angular interactions suggest electrostatic rather than coordination [71]. However, the structure of the $Cu(DCO)_2 \cdot 2H_2O$ and $Cu(DCO)_2$ still remain a suggestion but the structure of the intermediate monohydrate was determined by X-ray crystal structure analysis.

It has been shown that the stability of metal complexes in a series of oxime ligands is dependent upon the basicity of nitrogen atom of the oxime group [28, 73]. The 2-thiazolyloxime complexes with Ni(II) and Cu(II) ion was studied. The 2-thiazolyloxime coordinates to these metals using the nitrogen atoms of the oxime group and the thiazole ring forming MN_4 (M = Cu, Ni) complexes (Figure 16).

The explanation for lower stability for Cu^{2+} complexes was given as the negative inductive effect of the thiazole and nitrile substituents as well as intramolecular attractive interaction between the oxygen atom of the oximic group and sulphur atom of the thiazole group in the thiazolyloxime. In the case of Ni^{2+} complexes, square-planar complexes were formed and it is the reason why thiazolyl ligand is more effective in metal ion binding than simple 2-(hydroxyimino)propanoic acid forming only octahedral species. The thiazolyl ligand is a distinctly better ligand for Ni^{2+} than 2-(hydroxyimino)propanoic acid while with Cu^{2+} ion, the stability of the thiazolyl ligand

is lower compared to the 2-(hydroxyimino)propanoic acid species [73].

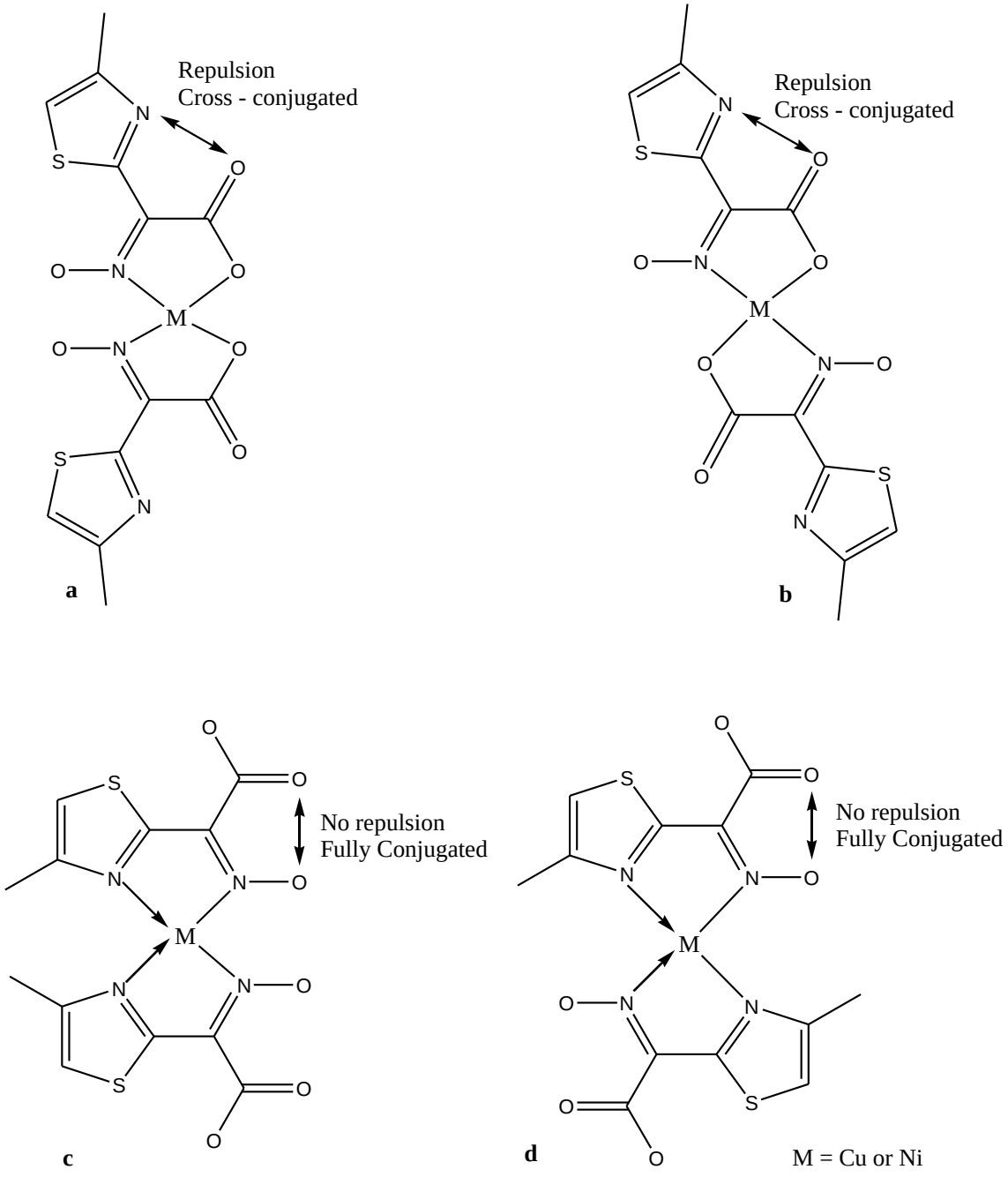

Figure 16. Favorable MN_4 conformation in 2-thyazolyloxime [73].

The coordination mode of oxime analogues of amides and peptides are to a large extent determined by the presence of a planar RC(=NOH)CONH framework which

allows the formation of different chelate ring with virtually no change in conformation. The formation of bis-complexes of $MH_{-1}L_2$ type having *cis* ligand coordination stabilized by hydrogen bonding between the oxime oxygens is the most characteristic feature of complexes with amino acid or amide analogues. The deprotonation of the first proton of the bis- complex of Ni^{2+} has a critical impact on the binding ability of the neighbouring nitrogen [29]. Like in the case of 2-(hydroxyimino)propanamide (HL) (Figure 4) complexes, the NiL_2 species having both oxime of the hydroxyl groups protonated is octahedral while its deprotonated specie $NiH_{-1}L_2$ is square-planar [27, 29]. There is no change of binding groups during the deprotonation process. The only change possible is the change in the distribution of charge density from the deprotonated hydroxyl group of the oxime moiety towards the neighbouring oximic nitrogen [29]. With amide oxime 2-cyano-2-(hydroxyimino)acetamide, the acidity of the oxime hydroxyl changes considerably the coordination mode of the oxime ligand with Cu^{2+} and Ni^{2+} ions. The donor atoms were the same as those reported for the non-cyano amide oxime: 2-(hydroxyimino)propanamide (Figure 2), where the two molecules of the propanamide ligand are bound in the *cis* position but in the 2-cyano derivative, the ligands are *trans* to each other. The determining factor for the *cis* positions of the ligand molecule in the major complex $MH_{-1}L_2$ formed with the oxime analogues of amino acids is the hydrogen bond between the two hydroxyl oxygens. The hydrogen bond is not present in the corresponding complex of the 2-cyano derivative, $MH_{-2}L_2$, due to the very acidic oxime hydroxyl group [29].

The nickel (II) and Cu(II) complexes of 2-pyridylcyanoxime (HPCO) (Figure 2) were also synthesized and studied in aqueous and non-aqueous solution [74]. The nickel

compounds $[Ni(HPCO)_2](ClO_4)_2$ and $[Ni(HPCO)_2]Cl_2$ were reported to possess distorted-tetrahedral structures based on the appearance of the crystalline samples of the complexes and a significant increased magnetic moment of the $[Ni(HPCO)_2](ClO_4)_2$ complex which is typical of tetrahedral complexes of Ni^{2+}. Ni^{2+} tetrahedral complexes' magnetic moments are known to be temperature dependent [74]. In the variable magnetic moment measurement of the $[Ni(HPCO)_2](ClO_4)_2$ at around 220 K and there was an unexpected break and below 163 K, the magnetic moment increased drastically. This effect was attributed to the appearance of significant ferromagnetic interactions between the central nickel (II) atom in this complex which was assumed to be mediated by the bridging effect of the oxygen atom of the nitroso group which result in the coordination number of the Ni^{2+} ion in the complex to be increased to 6. The unexpected break at 220 K was explained to be polymorphic transition involving the approach and contact between structural units which lead to a ferromagnetic exchange interaction between Ni^{2+} centers below 163 K. However, the $[Ni(HPCO)_2]Cl_2$ has magnetic moment of 2.96 B.M which is lower than what is expected for a tetrahedral complexes disagreeing with the diffuse reflection spectra which shows three transitions at 21,400, 12,760 and 12,000 cm^{-1} [74].

The $Ni(PCO)_2 \cdot 2H_2O$ lost two molecules of H_2O at 110 °C in two steps to give an anhydrous $Ni(PCO)_2$ with the dehydration being irreversible. One of the water molecules was reported to be unbound while the other one is coordinating making the Ni(II) ion having a penta-coordinated square pyramidal environment [74]. This is confirmed by the electronic spectra of the solutions and crystalline samples [75]. This was also confirmed by magnetic moment measurement of the diaquo complex giving a $\mu_{eff} = 3.05$ BM typical of high spin square-pyramidal Ni(II) complex [74]. There was no change in coordination mode

of the anion after dehydration as evident from the vibrational spectra of the diaquo and the anhydrous complex in the range of 2300 to 900 cm^{-1}. However the magnetic moment of the anhydrous complex $Ni(PCO)_2$ is temperature dependent dropping from 2.69 to 2.07 BM as temperature varies from 300 to 92 K showing the presence of strong antiferromagnetic interaction between the Ni^{2+} ion centers which was proposed to be a direct Ni to Ni strong axial interaction resulting from stacked polymeric structure of the $[Ni(PCO)_2]$ complex with the acido-ligand situated in the plane of tetrahedrally distorted octrahedra with extended, sufficiently strong axial Ni ---- Ni bonds [74].

The diffuse reflection spectra of $[Cu(HPCO)_2]Cl_2$ indicates a distorted tetrahedral structure and undoubted tetragonal structure for $[Cu(HPCO)_2](ClO_4)_2$ with $CuN_4(O_2)$ chromophore [76]. The nitrogen atoms of the coordinated HPCO were seen to be situated in the plane tetrahedrally distorted with the ClO_4^- ion occur at a large distance from the central Cu^{2+} ion. This conclusion was confirmed by the μ_{eff} of these complexes. A value of 1.98 BM for $[Cu(HPCO)_2](ClO_4)_2$ showed the presence of spin-orbit couplings in copper atoms which is typical of tetragonal and square-planar complexes [75]. A lower value of 1.78 BM for $[Cu(HPCO)_2]Cl_2$ shows the presence of mononuclear specie [74].

Novel open chain oxime ligand N,N'-bis(2-hydroxyiminopropionyl)propane-1,3-diamine (H_2pap) complexes of Cu(II) and Ni(II) were studied spectroscopically and potentiometrically in solution. Open chain oximes coordinating to metal ions using two nitrogens from oxime and two nitrogens from amide are shown to be very effective ligand in coordinating Ni(II) and Cu(II) ions. Amide nitrogen have a strong effect on binding abilities while hydrogen bonds between oximic oxygens is less important than in

simple oximes. However, these hydrogen bonds close the open chain structure into closed macrocylic system [77].

A study of the Ni(II) and Cu(II) complexes of 2-Oxyiminopivaloylacetonitrile, HPiCO (an α - ketocyanoxime) (Figure 2) indicated that the ligand coordinates with the metal ions using the nitroso nitrogen atom and oxygen atom of the carbonyl group of the ligand forming a five-membered chelate ring [78]. This mode of ligand coordination in complexes with 3d metal of other ligand complexes is well known for other cyanoximes [79]. The diffuse reflection spectra of Cu^{2+} and Ni^{2+} complexes, $Ni(PiCO)_2$, $Cu(PiCO)_2$ and $NiPy_2(PiCO)_2$ revealed octahedral environment around the metal ions. However, $Ni(PiCO)_2 \cdot 6H_2O$ electronic spectra recorded in nitromethane showed that it has a square-planar configuration in the solution. The magnetic moment measurements of the complexes: $Cu(PiCO)_2 \cdot 2H_2O$, $Cu(PiCO)_2 \cdot 2Py$, $Ni(PiCO)_2 \cdot 6H_2O$ and $Ni(PiCO)_2 \cdot 2Py$ revealed that these complexes are mononuclear with distorted octahedral geometry. TGA data showed that the water molecules in $NiPy_2(PiCO)_2 \cdot 4H_2O$ are uncoordinated [78].

III. RESEARCH GOALS

My work initiates new research in Dr. N. Gerasimchuk's laboratory. It was aimed at the design and preparation of the extended 1D solids-coordination polymers based on metal ions other than Pd and Pt due to their high cost. Therefore, we wanted to investigate the simple preparative and structural coordination chemistry of the first element of the Ni-triad with a group of selected cyanoximes (Figure 17) that are known to form chelates with transition metals. Literature review revealed that there were some studies of Cu(II) and Ni(II) complexes with several cyanoximes in the past. However, no significant comparative investigations of these metal ions with a series of chelating cyanoximes has been done. It was unknown what happens to the hydrated Cu and Ni cyanoximes upon H_2O removal. Thus the goal of current research project were:

1. To synthesize series of Ni(II) complexes with chelating cyanoxime ligands as hydrates and their anhydrous complexes, investigate structural rearrangement in the complexes upon dehydration (Figure 18) and perform oxidation of the anhydrous Ni-complex in order to form mixed valence system as shown in Figure 19.

2. Prepare, characterize and study a series of analogous Cu(II) cyanoximates and compare them with Ni(II) complexes in a hope that the application of the EPR spectroscopy and magnetochemistry will allow such comparison.

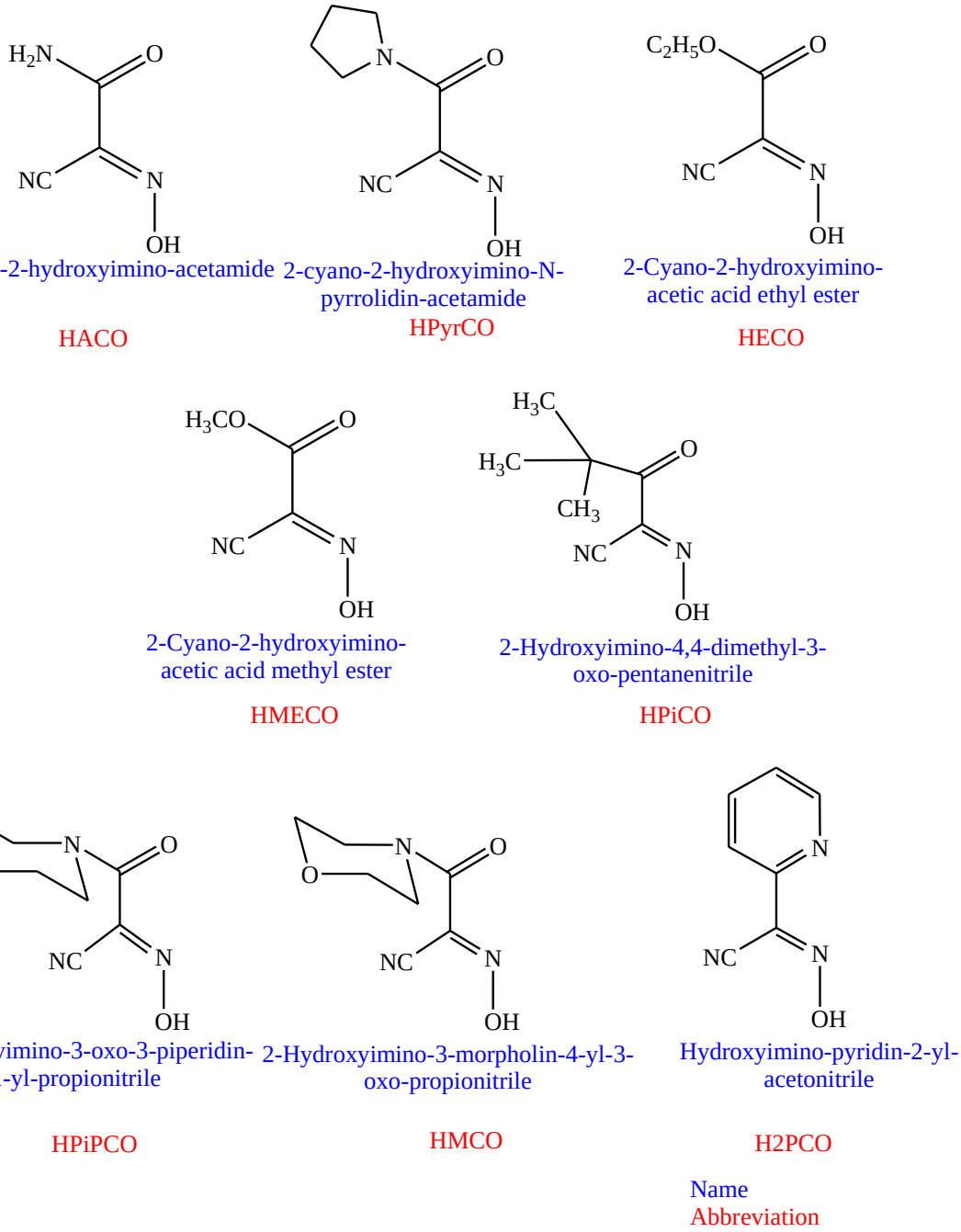

Figure 17. Cyanoxime ligands used for our studies.

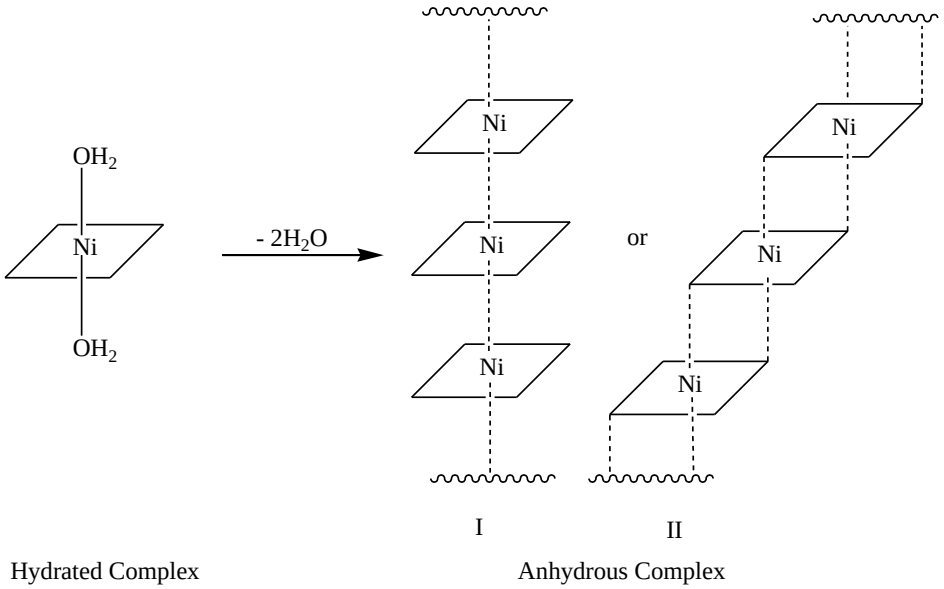

Figure 18. Possible structural rearrangement after dehydration of Ni(II) complexes with chelating cyanoximes.

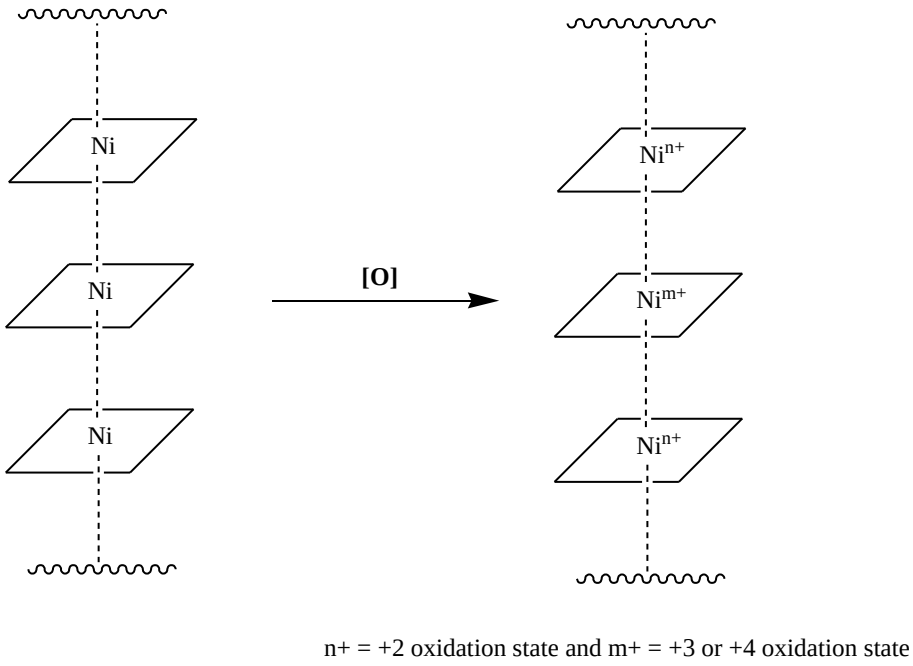

Figure 19. Oxidation of anhydrous complex with direct Ni----Ni interaction to create a multivalent Ni- system.

IV. EXPERIMENTAL

Reagents used are; nickel nitrate hexahydrate ($Ni(NO_3)_2 \cdot 6H_2O$), copper sulfate pentahydrate ($CuSO_4 \cdot 5H_2O$), concentrated sulfuric acid (H_2SO_4), ethylcyanoacetate ($C_5H_7NO_2$), morpholine (C_4H_9NO), acetonitrile (CH_3CN) are all reagent grades from Aldrich. Common organic solvents were: hexane, ethylether and acetone.

The cyanoxime ligands used for this research project syntheses were made by Dr. Gerasimchuk and his previous research students. The exception was the preparation of needed amount of HMCO and HECO which was carried out during this research. Melting point and thin-layer chromatography (SiO_2 plates with a UV-indicator) were used for the identification and verification of the purity of each cyanoximes. The values were compared to those of reported in the literature when freshly prepared for a match. A detailed synthetic procedure for these ligands syntheses can be found in previous writings [80, 81].

The instruments used for this research are as follows: a custom-built high vacuum station Dream-1 (Appendix A-1) which was used for dehydration of prepared complexes. Spectroscopic studies included UV-visible (both solution and solid state) and IR spectroscopy. For the first method, a HP 8453 diode array spectrophotometer operating in the 200 – 1100 nm range was used for solutions, while a Cary 100 Bio with integrating sphere (Appendix A-2) installed was employed for studies of reflectance spectra in the range of 200 nm – 800 nm of the obtained compounds. The baseline was recorded using a White Millipore HA 0.45 μm 20 mm diameter filter attached with a transparent Scotch tape (Appendix A-3). The sample was applied on the Millipore filter paper membrane

and held down by the tape. The spectra were recorded in % reflectance mode which was then converted to more common appearance as absorbance mode.

The IR spectra were obtained using a Bruker Vertex 70 Spectrophotometer in KBr disks pressed at 9 tons pressure by a Carver hydraulic press. The TG/DSC measurements of Ni and Cu – complexes were carried out under N_2 (UHP grade) flow using a TA Q-600 instrument. The X-ray analysis of single crystals grown in current studies was conducted using APEX 2 diffractometer (Mo K_α radiation, $\lambda = 0.70092$ Å) in Omega – scans mode with 0.5° step covering the full sphere of reflections. X-ray powder diffraction studies were carried out using an Oxford diffractometer equipped with Cu tube ($\lambda = 1.54$ Å). Solid-state volume magnetic susceptibility (χ_v) was measured on a Johnson Matthey MSB-1 balance at 292.5 K using only one complex ($K_2[Cu_3(AACO)_4.4H_2O].4H_2O$) obtained in sufficient quantities for studies. The elemental analyses to determine the % composition of carbon, hydrogen and nitrogen (CHN) of compounds were done at Atlantic Microlab at Norcross, Georgia.

IV.1. Synthesis of HMCO

IV.1.1. Synthesis of 3-Morpholin-4-yl-3-oxopropionitrile (the HMCO Cyanoxime Precursor)

Figure 20**.** The synthesis was performed in neat condition using reagents (method **1**), using dichloromethane (method **2**) as solvent and using chloroform as solvent (method **3**) as shown in Figure 20.

Under neat conditions (method **1**): 1.000 g (11.5 mM) of morpholine was mixed with 1.000 g (7.99 mM) of ethylcyanoacetate in a 25 mL capacity amber glass with stirring and nitrogen gas protection (Figure 20). After 5 minutes, stirring was stopped and

the mixture was covered and cooled at temperature around 0 °C in a freezer for 96 – 120 hours. Crystalline compound appeared in the mixture and was filtered and then washed with 25 mL of toluene and then 25 mL of hexane. The crystals were then dried in a dessicator charged with concentrated sulfuric acid for 5 days. The yield was 57 % (0.7769 g); m.p. = 80 – 81 °C.

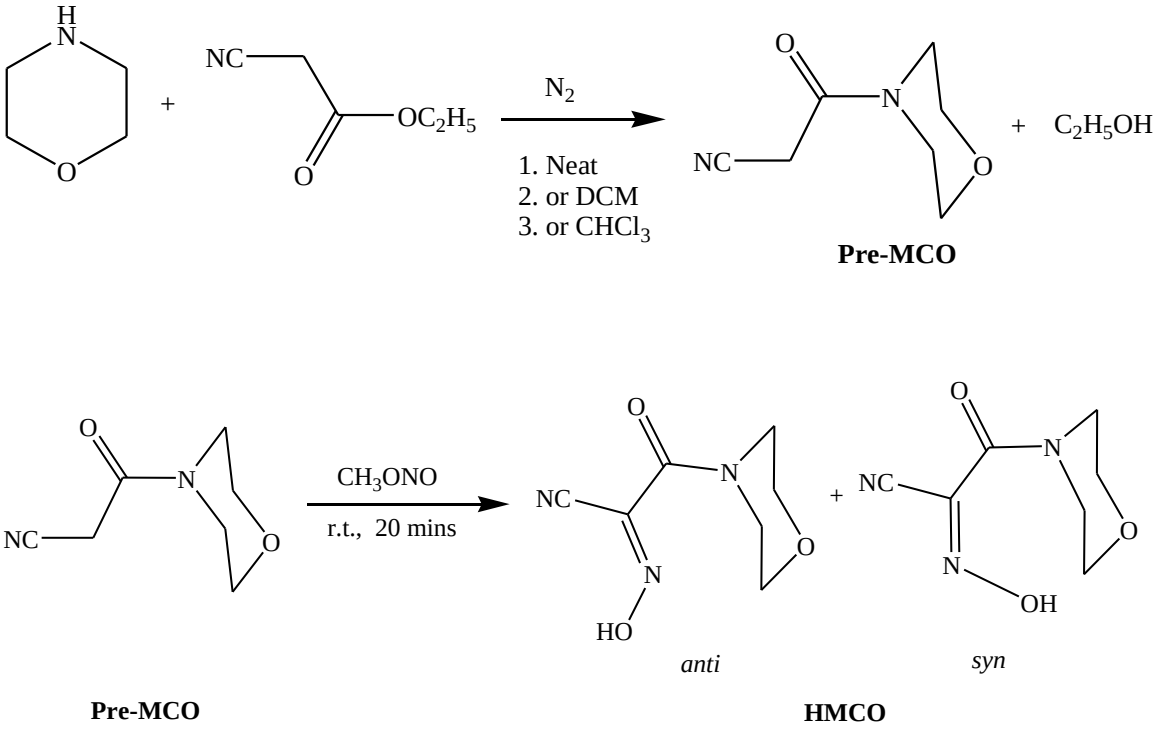

Figure 20. Synthesis of the HMCO from its precursor obtained in three different ways.

Preparation using dichloromethane (method **2**) as a solvent: a mixture of morpholine, ethylcyanoacetate and dichloromethane was prepared in a ratio of 1:1:1 respectively in an amber glass 25 mL capacity bottle. Nitrogen gas was bubbled into the mixture under stirring for 5 minutes (Figure 20) and the bottle was placed in the freezer at temperature around 0 °C for 96-120 hours. Crystallization of the desired acetonitrile pre-

MCO occurred from the mixture. The crystals were washed with 25 mL of toluene and then 25 mL of hexane, and dried in a dessicator charged with concentrated sulfuric acid for 5 days. The yield was 97 % (1.327 g) based on the amount of ethylcyanoacetate used; m.p. = 82-84 °C.

Preparation using chloroform (method **3**) as a solvent: a mixture of morpholine, ethylcyanoacetate and chloroform was prepared at a ratio of 1:1:1 respectively in an amber glass 25 mL capacity bottle. This reaction was essentially as described above (Figure 20). Crystallization of the acetonitrile pre-MCO occurred from the mixture. The crystals were dried in a dessicator charged with concentrated sulfuric acid for 5 days. The yield was 52 % (0.7079 g) based on the amount of ethylcyanoacetate used; m.p. = 83-84 °C.

Values of melting points are close to the value reported earlier [80]. The TLC was carried out and only one spot was detected with R_f = 0.12 (after method **1**), 0.14(after method **2**), 0.12 (after method **3**). The ^{1}H NMR spectra are analogous to those recorded previously [80].

IV.1.2. Synthesis of the HMCO from its Precursor. Nitrosation of the pre-MCO was performed at room temperature with gaseous methylnitrite at basic condition according to published procedures [80] as shown in Figure 20. Yield of the final product was 55 % (1.3296 g) from 2.0349 g of pre-MCO, m.p.: 156 -157 °C, and R_f = 0.44 in EtOAc/hexane = 2:1 mobile phase. The ^{1}H NMR and ^{13}C NMR spectra, of the HMCO, were recorded in dmso-d_6 and showed the presence of *syn* and *anti*-diastereomers; similarly, to reported in [81] case.

IV.2. Synthesis of HECO Ligand

The synthesis (Figure 21) was carried out by reacting 5.700 g (82.6 mM) of $NaNO_2$ dissolved in 71 mL of H_2O with 10.000 g (88.4 mM) of ethyl cyanoacetate in a round bottom flask according to the reaction below. The 3.6 mL of 1 M H_3PO_4 was added dropwise over 45 minutes to the reaction mixture and the temperature was kept at 3-4 °C using an ice bath. After the addition was completed, the temperature was raised to 40 °C and the reaction was quenched with 7.3 mL of fuming HCl at 65 °C and left to cool to room temperature. The reaction mixture was then kept in the refrigerator. The mixture was filtered using filter paper and gravity filtration. The precipitate was dried under vacuum. The filtrate was extracted with ethyl acetate after the mixture was treated with solid NaCl to facilitate extraction. The solution was off-yellow, and the colour was maintained in the organic phase, while the water phase was colourless. The dried precipitate was 7.153 g. An additional amount of 3.042 g was obtained after the extraction. The total yield of HECO was 10.195 g (81 %); m.p = 129.4-132.4 °C.

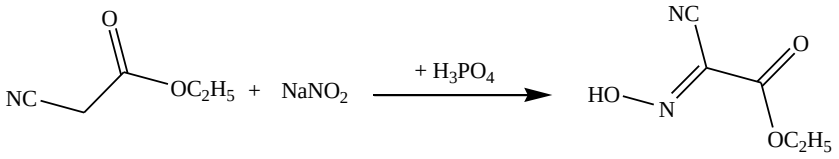

Figure 21: Synthesis of HECO

IV.3. Syntheses of 2-Cyano-2-hydroxyimino Acetamide (HACO) Complexes of Ni(II) and Cu(II)

The cyanoxime ligand of HACO was available from the bank of prepared ligands for research in Dr. Gerasimchuk's lab.

The 0.300 g (1.21 mM) of the sodium acid salt of HACO of the composition $NaH(ACO)_2$ was dissolved in 5 mL of deionized water in a 25 mL beaker and then 1.21 mL (1.21 mM) of 1M KOH solution was added for the complete deprotonation of the ligand to form the anion. The colour of solution changed to a deep yellow. The 0.3515 g (1.21 mM) of $Ni(NO_3)_2 \cdot 6H_2O$ was dissolved in 5 mL of deionized water in a 25 mL beaker. The nickel nitrate solution was added dropwise to the fully deprotonated ACO^- ligand solution. Cloudy pink mixture was slowly formed, which was allowed to stand for ~ 2 hours under continuous stirring (Figure 22). The mixture was filtered on a filter paper using gravity filtration technique. The colour of the filtrate was bright pink and the precipitate was bright pink as well as seen in Figure 23. The filtrate was kept in a dessicator charged with concentrated sulfuric acid and silica gel for almost a month for crystal growth. The precipitate was allowed to dry at room temperature for a week, giving 0.3266 g of $[Ni(ACO)_2.2H_2O]$ complex at 85 % yield.

The same preparation procedure was repeated for Cu(II) complex of HACO using the sodium acid salt. The amount used were: 0.300 g (1.21 mM) of $NaH(ACO)_2$ in 5 mL of deionized water, 1.21 mL of 1 M KOH, 0.1929 g of $CuSO_4 \cdot 5H_2O$ dissolved in 5 mL of deionized water. The precipitate was filtered using filter paper and gravity filtration. The colour of the filtrate was deep green and the precipitate deep green as well (Figure 23). The filtrate was kept in a dessicator charged with concentrated sulfuric acid and silica gel for almost two months for crystal growth. The precipitate was allowed to dry at room temperature for a week to give 0.1850 g of $Cu(ACO)_2 \cdot H_2O$ complex at 50 % yield. Table 5 shows the result of the elemental CHN analyses of the complexes.

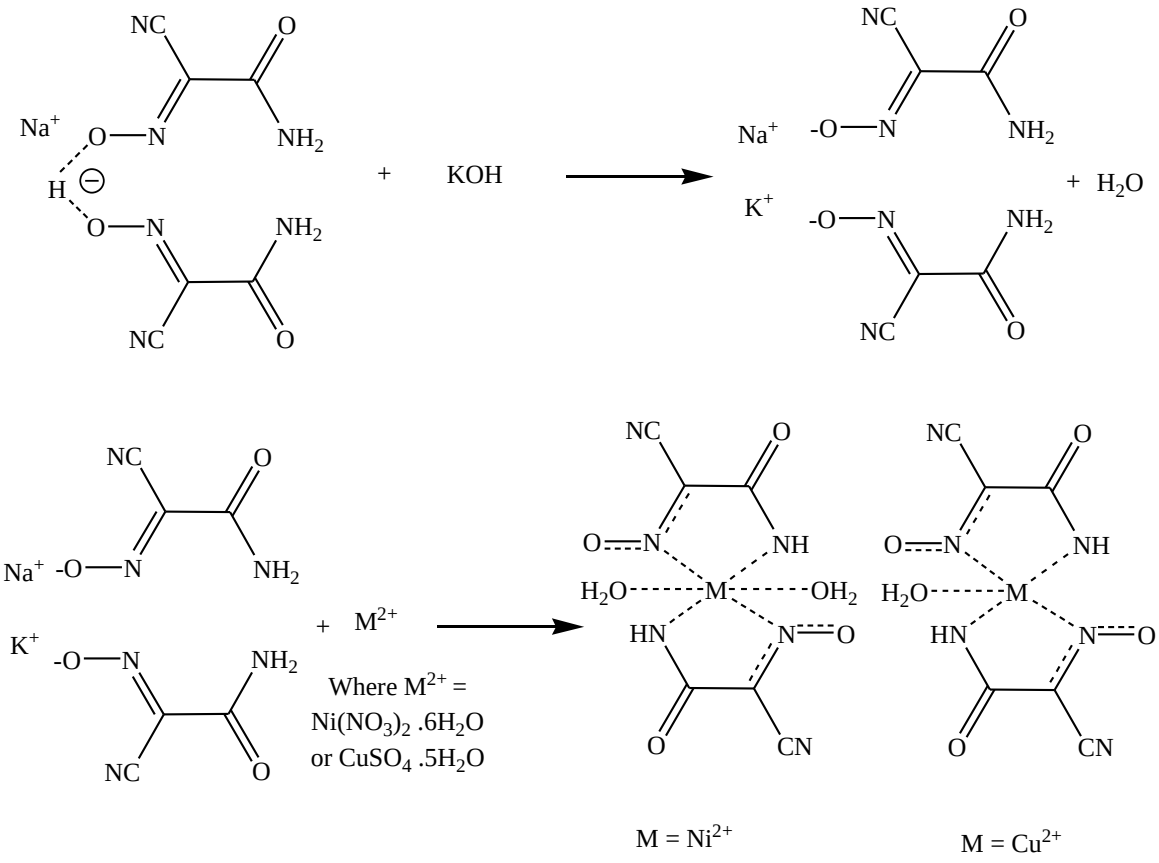

Figure 22. Syntheses of Ni (II) and Cu(II) complexes of HACO ligand.

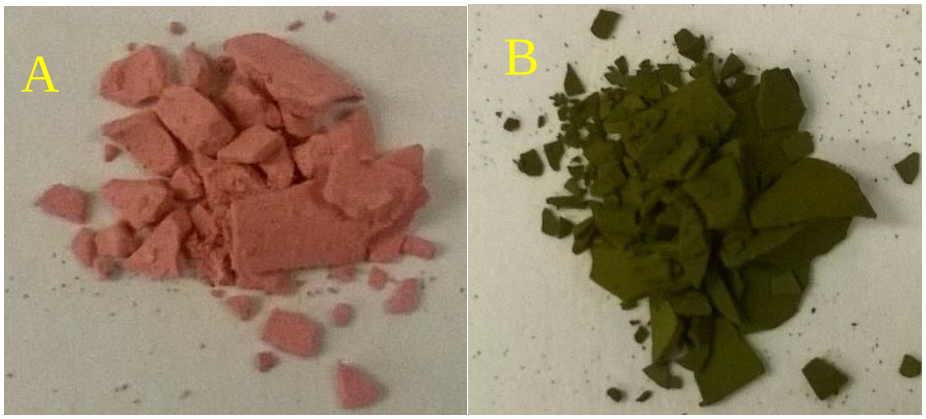

Figure 23. Bulk precipitates of the [$Ni(ACO)_2 \cdot 2H_2O$] (A) and [$Cu(ACO)_2 \cdot H_2O$] (B) Complexes. Photograph taken using Motic Microscope at 40x magnification.

Table 5. The elemental analyses for the ACO^- based complexes.

Complex	C, % Calc. (Found)	H, % Calc. (Found)	N, % Calc. (Found)
$[Ni(ACO)_2 \cdot 2H_2O]$	22.60 (22.80)	2.53 (2.38)	26.36 (26.61)
$[Cu(ACO)_2 \cdot H_2O]$	23.57 (24.44)	1.98 (1.57)	27.49 (28.28)

IV.4. An Attempt of Syntheses of 2-Cyano Hydroxyimino Acetic Acid Ethyl Ester (HECO) Complexes of the Ni(II) and Cu(II)

The 0.300 g (2.11 mM) of the HECO (Figure 17, 24) was dissolved in 5 mL of deionized water in a 25 mL beaker and then 2.11 mL (2.11 mM) of 1M KOH solution was added for the deprotonation of the ligand. The colour changed to deep yellow. The solution was then stirred using a magnetic stirrer continuously for 5 minutes. The 0.3069 g (1.06 mM) of $Ni(NO_3)_2 \cdot 6H_2O$ was dissolved in 5 mL of deionized water. This solution was then added dropwise to the deprotonated ECO^- ligand solution. Clear deep brown solution was formed but unexpectedly no precipitate. The mixture was allowed to stand for ~ 2 hours under continuous stirring. The mixture was kept in a dessicator charged with concentrated sulfuric acid and silica gel for almost two weeks for crystal growth.

A very similar preparation was carried out for Cu(II) complex. The amounts used were: 0.300 g (2.11 mM) of HECO, 2.11 mL of 1 M KOH, and 0.1685 g (1.06 mM) $CuSO_4 \cdot 5H_2O$. After mixing all the reactants as depicted in Figure 24, no precipitate formed, which was unexpected. Clear green solution was left in a dessicator charged with concentrated H_2SO_4 for possible crystal growth.

It turned out that the 'products' in Figure 24 were complexes of $AACO^{2-}$ dianion; resulted from the hydrolysis of the initial ECO^- cyanoximate, and an oxamide.

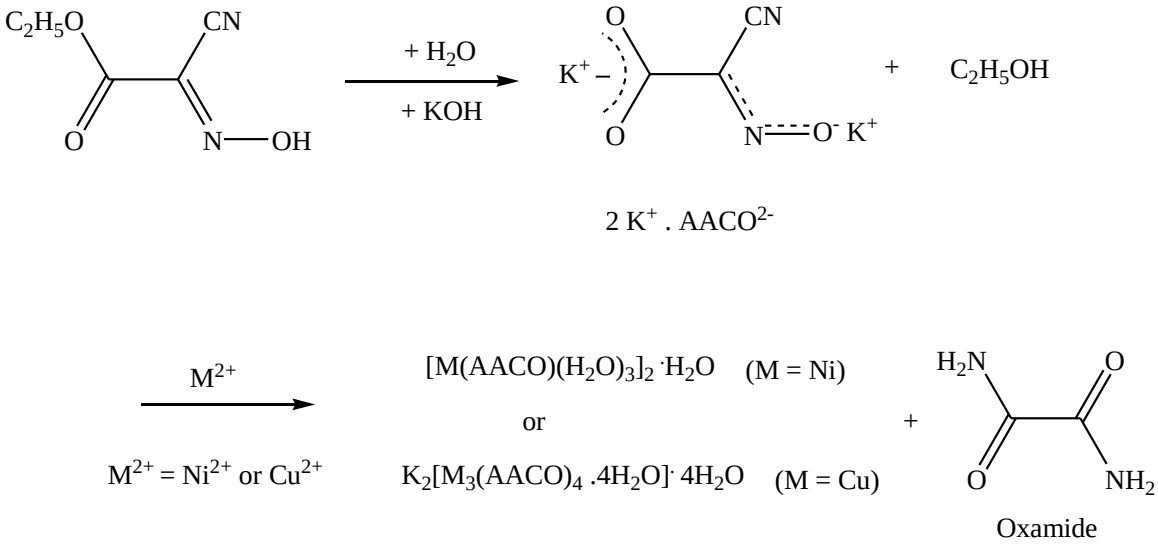

Figure 24. Syntheses of Ni(II) and Cu(II) complexes of ECO^-.

IV.5. Syntheses of Ni(II) and Cu(II) Complexes of 2-Hydroxyimino-4,4-dimethyl-3-oxo-Pentanenitrile (HPiCO)

These complexes were obtained using the same general method shown in Figure 25. Actual appearance of bulk compounds as microscope photographs are shown in Figure 26.

The 0.300 g (1.95 mM) of HPiCO (Figure 17, 25) was dissolved in 5 mL of deionized water in a 25 mL beaker and then 1.95 mL (1.95 mM) of 1M KOH solution was added for the deprotonation of the ligand. The colour of the solution changed to deep yellow. The 0.2829 g (0.97 mM) of $Ni(NO_3)_2 \cdot 6H_2O$ was then added dropwise to the deprotonated $PiCO^-$ ligand solution. A cloudy green mixture was formed, then allowed to stand for ~ 2 hours under continuous stirring, and was then filtered using filter paper and gravity filtration. The colour of the filtrate was light green and the precipitate was deep green (Figure 26). The filtrate was kept in a dessicator charged with concentrated sulfuric

acid and silica gel for almost two months for crystal growth. The precipitate was allowed to dry at room temperature for a week. The percent yield was calculated based on the amount of bulk precipitate and found to be 41 % (0.3158 g).

The Cu(II) complex with $PiCO^-$ was obtained in a similar way. The amount was: 0.300 g (1.95 mM) of HPiCO (in 5mL H_2O); 1.95 mL of 1 M KOH solution, and 0.1553 g (0.97 mM) of $CuSO_4 \cdot 5H_2O$ in 5 mL of H_2O. The green precipitate that was formed was allowed to dry at room temperature for a week. The percent yield was calculated based on the amount of bulk precipitate and found to be 35 % (0.2742 g). Table 6 shows the result of the elemental analyses of the complexes.

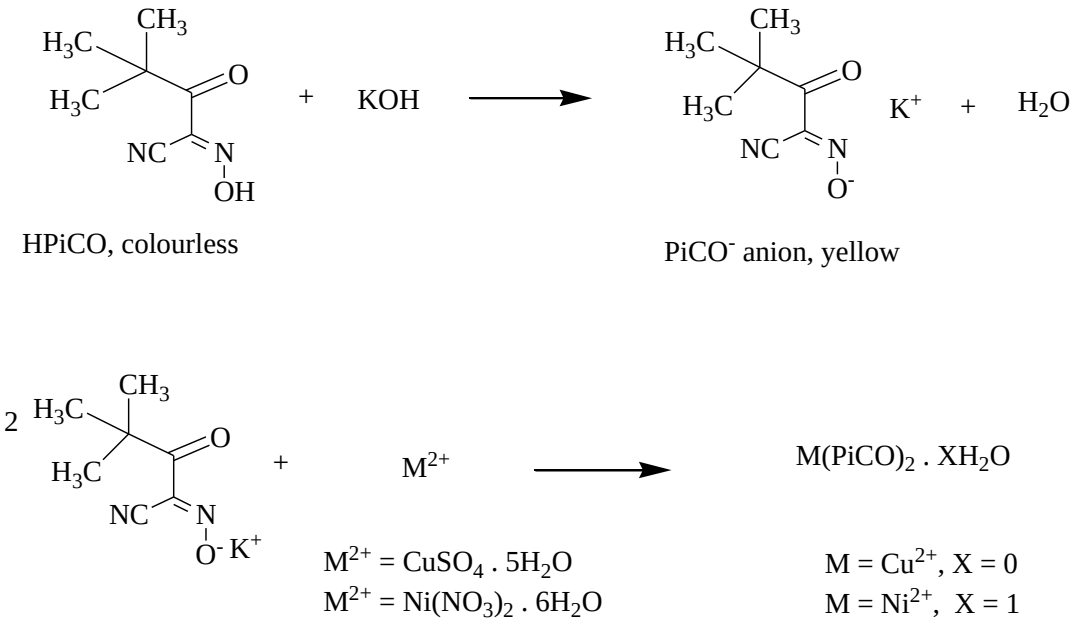

Figure 25. Syntheses of $Ni(PiCO)_2 \cdot H_2O$ and $Cu(PiCO)_2$.

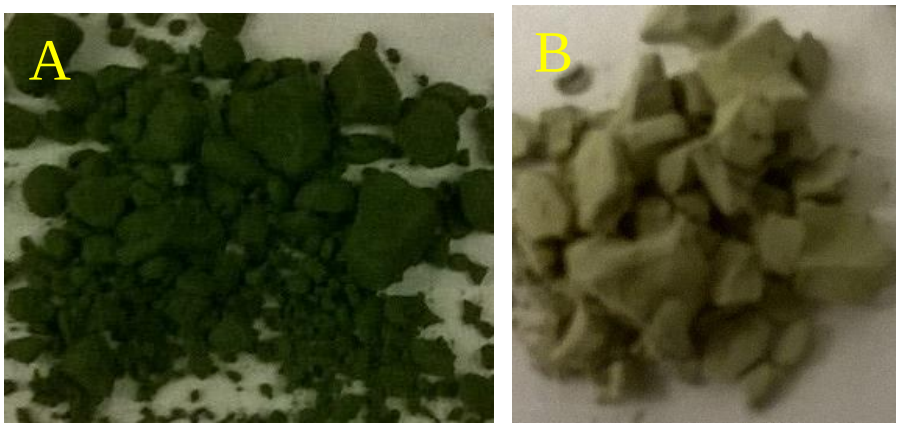

Figure 26. Microscope photographs of bulk precipitate of $Ni(PiCO)_2 \cdot H_2O$ (A) and $Cu(PiCO)_2$ (B) obtained at 40x magnification.

Table 6. The elemental analyses for $PiCO^-$ based complexes

Complex	C, % Calc. (Found)	H, % Calc. (Found)	N, % Calc. (Found)
$Ni(PiCO)_2 \cdot H_2O$	43.90 (44.46)	5.26 (5.24)	14.63 (14.60)
$Cu(PiCO)_2$	45.46 (44.99)	4.91 (5.46)	15.15 (15.07)

IV.6. An Attempt of Syntheses of the Ni(II) and Cu(II) Complexes of 2 - Cyano- 2 - hydroxyimino-acetic acid Methyl Ester (HMeCO)

With Cu(II) and Ni(II), the formation of $AACO^{2-}$ anions was observed due to hydrolysis of $MECO^-$ anion in solution, similarly to the aforementioned preparations based with ECO^- anion.

The 0.300 g (2.34 mM) of HMeCO (Figure 17, 27) was dissolved in 5 mL of deionized water in a 25 mL beaker and then 2.34 mL (2.34 mM) of 1M KOH solution was added for the deprotonation of the ligand. The colour of the solution changed to deep yellow. The solution was then stirred using a magnetic stirrer continuously for 5 minutes.

The 0.3407 g (1.17 mM) of $Ni(NO_3)_2 \cdot 6H_2O$ was dissolved in 5 mL of deionized water, and added dropwise to the deprotonated $MECO^-$ ligand solution. Clear deep brown solution was formed and was allowed to stand for ~ 2 hours under continuous stirring at room temperature. The clear deep brown solution was then kept in a dessicator charged with concentrated sulfuric acid and silica gel for almost two months for crystal growth.

A similar reaction between deprotonated $MECO^-$ anion and $CuSO_4.5H_2O$ resulted in the formation of small amount of green precipitate (Figure 28) and green solution. The amount of reagent used were: 0.300 g (2.34 mM) of HMeCO in 5 mL of H_2O; 2.34 mL of 1 M KOH, 0.1870 g (1.17 mM) of $CuSO_4 \cdot 5H_2O$. The green solution was kept in a dessicator charged with concentrated H_2SO_4 for crystal growth. The percent yield was calculated based on the amount of bulk precipitate and found to be 16 % (0.1322 g). It turned out that the obtained complexes did not contain desired $MECO^-$ anion, but instead $AACO^{2-}$ dianion as the result of hydrolysis of the former. This situation is similar to as described for the ECO^- system described above.

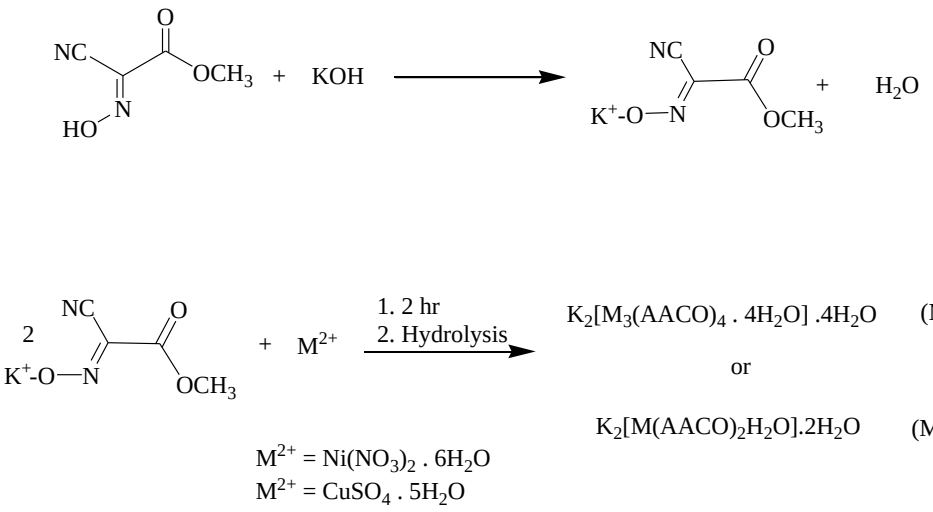

Figure 27. Syntheses of Ni (II) and Cu(II) complexes of $MeCO^-$

Figure 28. The microscope picture of the bulk precipitate of $K_2[Cu(AACO)_2H_2O]\cdot 2H_2O$ at 40x magnification.

IV.7. Syntheses of the Ni(II) and Cu(II) Complexes of Hydroxyimino-pyridin-2-yl-acetonitrile (H(2PCO))

The nickel and copper complexes of H(2PCO) cyanoxime were synthesized. The ligand was obtained from the compounds' bank available for research in Dr. Gerasimchuk's lab.

The 0.300 g (2.03 mM) of H(2PCO) (Figure 17, 29) was dissolved in 5 mL of deionized water in a 25 mL beaker and then 2.04 mL (2.03 mM) of 1 M KOH solution was added for the deprotonation of the ligand. The colour of the solution changed to deep yellow. The 0.2965 g (1.02 mM) of $Ni(NO_3)_2\cdot 6H_2O$ was dissolved in 5 mL of deionized water and was added to the deprotonated ligand solution. Light reddish-brown solution and precipitate of the same colour was formed. The mixture was allowed to stand for ~ 2 hours under continuous stirring at room temperature. After 2 hours; the solution was filtered using paper filter and gravity filtration technique. The filtrate was kept in a plastic centrifuge tube and the precipitate retained in the filter paper. The colour of the filtrate

and precipitate was pink (Figure 30). The filtrate was kept in a dessicator charged with concentrated sulfuric acid and silica gel for almost a month for crystal growth. The precipitate was allowed to stand at room temperature for a week to get dried. The percent yield was calculated based on the amount of bulk precipitate obtained and found to be 49 % (0.1941 g).

The Cu(II) ion complex with H(2PCO) cyanoxime was obtained in similar way using the following amounts of reagents: 0.300 g (2.04 mM) H(2PCO), in 5 mL of H_2O, and 2.04 mL of 1 M KOH; 0.1627 g (1.02 mM) $CuSO_4 \cdot 5H_2O$ in 5 mL of H_2O. Mixing under stirring resulted in the formation of a small amount of olive green precipitate (Figure 30) and clear solution of the same colour. The yield of $Cu(2PCO)_2$ was 64 % (0.3777 g). Table 7 shows the result of the elemental analyses of the complexes.

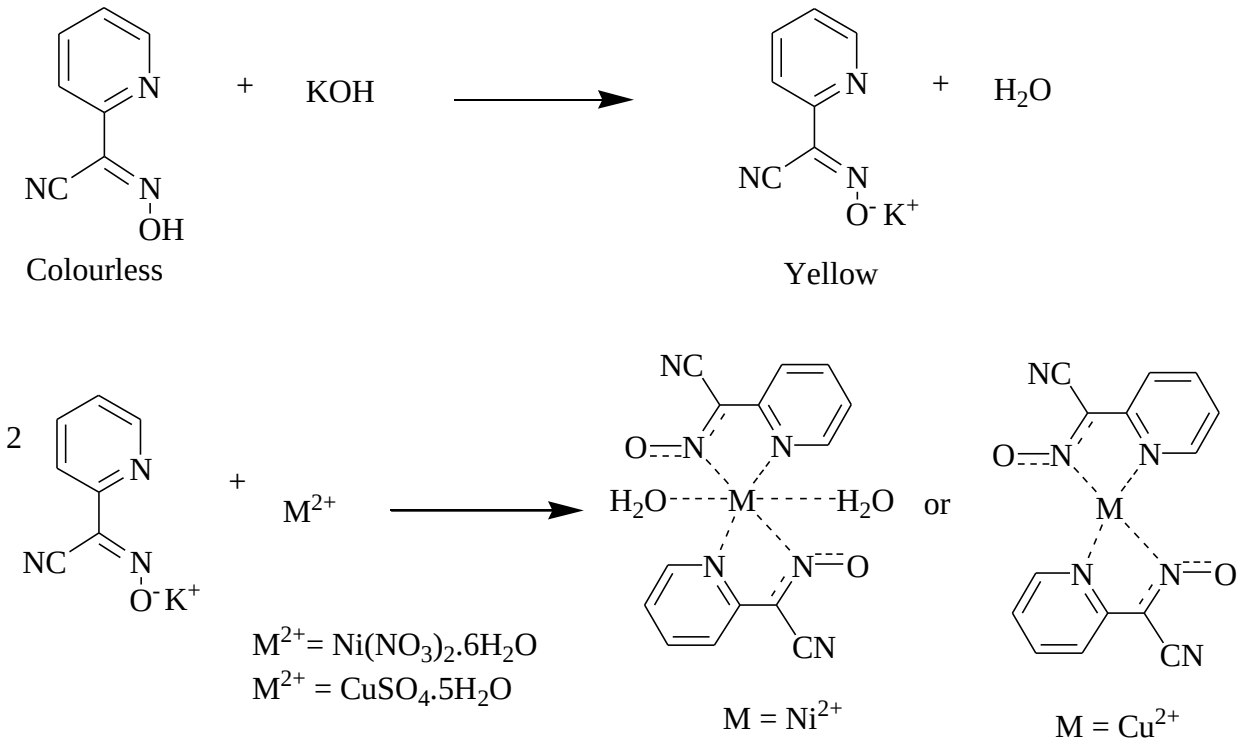

Figure 29. Preparation of Ni(II) and Cu(II) complex of H(2PCO) cyanoxime.

Figure 30. Bulk precipitate of $[Ni(2PCO)_2 \cdot 2H_2O]$ (A) and $Cu(2PCO)_2$ (B) at x40 magnification.

Table 7. The elemental analyses results for $2PCO^-$ - based complexes.

Complex	C, % Calc. (Found)	H, % Calc. (Found)	N, % Calc. (Found)

$Ni(2PCO)_2 \cdot 2H_2O$	39.75 (39.14)	3.81 (2.95)	19.87 (19.63)
$Cu(2PCO)_2$	47.26 (46.83)	2.27 (2.39)	23.62 (23.28)

IV.8. Syntheses of the Ni(II) and Cu(II) complexes of 2-Hydroxyimino-3-oxo-3-pyrrolidin-1-yl-propionitrile (HPyrCO)

The nickel and copper complexes of the HPyrCO used for this research were synthesized using the HPyrCO ligand previously made in Dr. Gerasimchuk research laboratory.

The 0.300 g (1.79 mM) of HPyrCO (Figure 17, 31) was dissolved in 5 mL of deionized water in a 25 mL beaker and then 1.79 mL (1.79 mM) of 1M KOH solution was added for the deprotonation of the ligand. The colour of solution also changed to deep yellow as in previous cases of other cyanoximes. The 0.2609 g (0.90 mM) of $Ni(NO_3)_2 \cdot 6H_2O$ was dissolved in 5 mL of deionized water, and then added drop-wise to the deprotonated $PyrCO^-$ solution. Murky reddish-brown mixture was formed and after which mixture was filtered using filter paper and gravity filtration technique. The colour of the filtrate was brown and the precipitate was reddish-brown (Figure 32). The filtrate was kept in a dessicator charged with concentrated sulfuric acid and silica gel for crystal growth. The precipitate was allowed to stand at room temperature for a week to get dried. The percent yield was calculated based on the amount of bulk precipitate and found to be 52 % (0.3403 g).

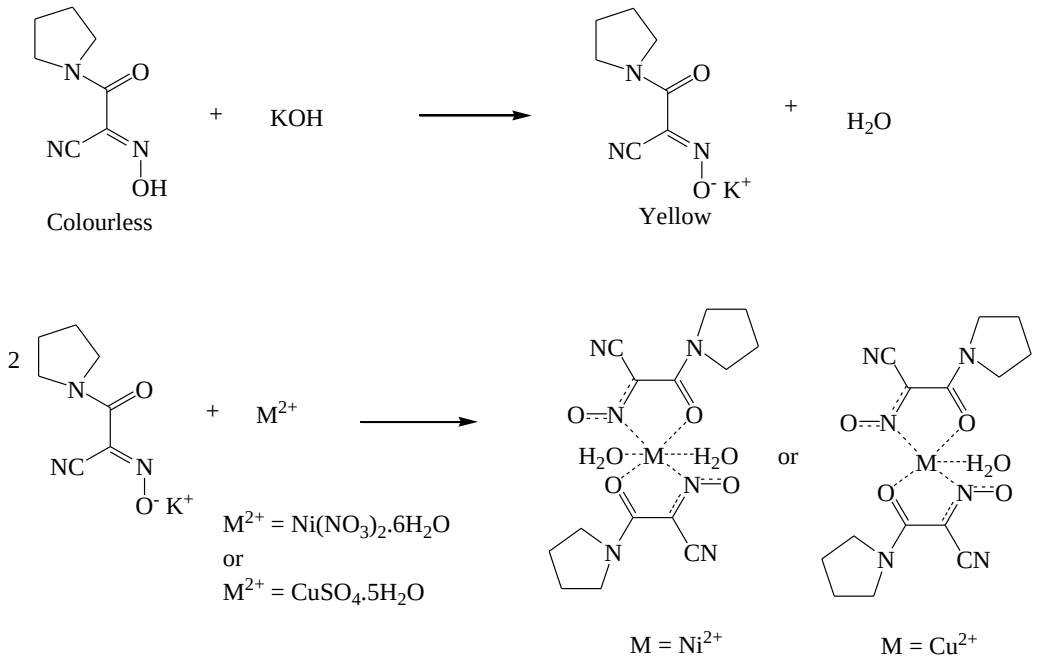

Figure 31. Syntheses of $Ni(PyrCO)_2.2H_2O$ and $Cu(PyrCO)_2.H_2O$.

The Cu(II) complex was obtained in a similar manner using the following amounts of reagent: 0.300 g (1.79 mM) of HPyrCO, 5 mL H_2O, 1.79 m L of 1 M KOH, 0.1432 g (0.90 mM) $CuSO_4 \cdot 5H_2O$ in 5 mL H_2O. Green solution and green precipitate (Figure 32) were formed. Mother liquor was left in plastic tube for crystal growth, while precipitate was collected and dried. Yield was 47 % (0.1751 g). Table 8 shows the result of elemental CHN analyses of the complexes.

Figure 32. Microscope photographs of bulk Precipitate of $Ni(PyrCO)_2 \cdot 2H_2O$ (A) and $Cu(PyrCO)_2 \cdot H_2O$ (B) at x40 magnification.

Table 8. The elemental analyses for the $PyrCO^-$ - based complexes.

Complex	C, % Calc. (Found)	H, % Calc. (Found)	N, % Calc. (Found)
$Ni(PyrCO)_2 \cdot 2H_2O$	39.38 (38.75)	4.72 (4.00)	19.68 (19.54)
$Cu(PyrCO)_2 \cdot H_2O$	40.63 (40.36)	4.38 (4.03)	20.31 (20.06)

IV.9. Syntheses of the Ni(II) and Cu(II) Complexes of 2-Hydroxyimino-3-morpholin-4-yl-3-oxo-propionitrile (HMCO)

The 0.0800 g (0.44 mM) of HMCO was dissolved in 2.5 mL of deionized water in a 25 mL beaker and then 0.44 mL (0.44 mM) of 1M KOH solution was added for the deprotonation of the ligand. The colour of the solution changed to deep yellow. The 0.0637 g (0.22 mM) of $Ni(NO_3)_2 \cdot 6H_2O$ was dissolved in 5 mL of deionized water, and then added dropwise to the deprotonated MCO^- ligand solution. Clear brown solution was formed, but no precipitation occurred even within extended period of time.

The reaction mixture was kept in a dessicator charged with concentrated sulfuric acid and silica gel for crystal growth, but unfortunately, no crystals were obtained as well. Therefore, an attempt to prepare [$Ni(MCO)_2 \cdot 2H_2O$] complex was unsuccessful, perhaps due to high stability of the compound in water.

An attempt to prepare Cu(II) complex of this cyanoxime was nevertheless successful. The Cu(II) complex was obtained in a similar manner using the following amounts of reagents: 0.0800 g (0.44 mM) of HMCO dissolved in 5 mL of deionized water; 0.437 mL of 1 M KOH solution; 0.0350 g (0.22 mM) of $CuSO_4 \cdot 5H_2O$ in 5 mL of H_2O. Green murky solution was obtained. The solution was filtered using filter paper and gravity filtration technique. Deep green filtrate and precipitate were obtained (Figure 33). The precipitate was allowed to dry at room temperature and the percent yield was found to be 23 % (0.0231 g). The filtrate was kept in a plastic centrifuge tube and placed in a dessicator charged with concentrated sulfuric acid for months for crystal growth. Unfortunately, no suitable crystals were obtained.

The elemental analysis of the MCO^- complex with Cu(II) gave:

- % Carbon – calculated: 31.37, found: 31.74
- % Hydrogen – calculated: 5.27, found: 3.79
- % Nitrogen – calculated: 15.68, found: 15.87

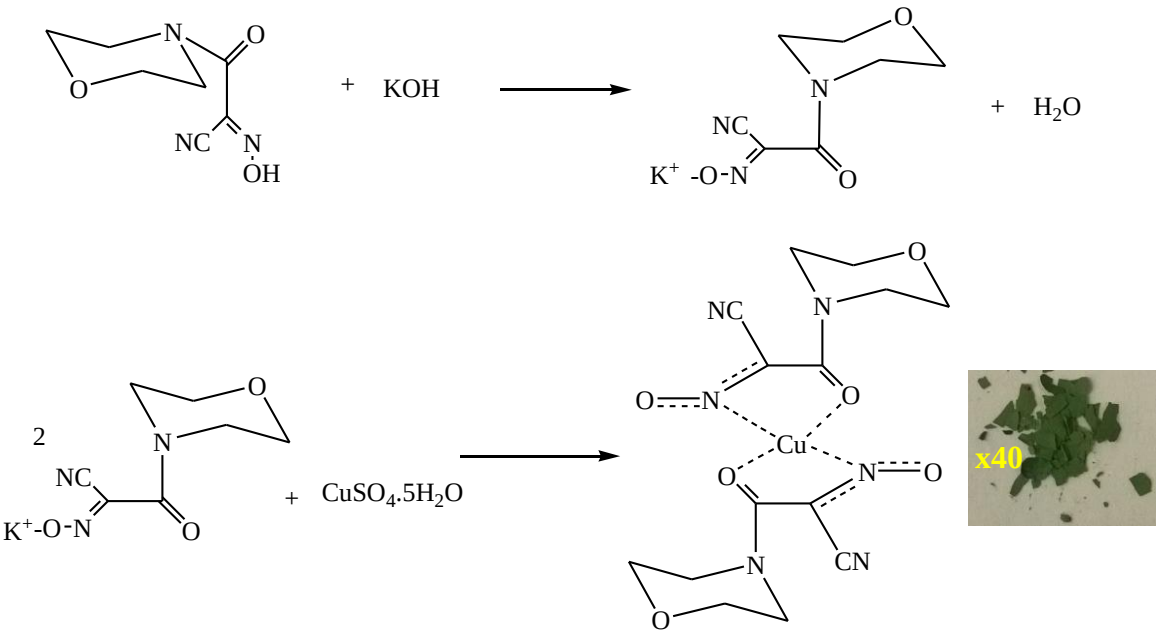

Figure 33. Synthesis of the Cu (II) complex with HMCO cyanoxime.

IV.10. Syntheses of the Ni(II) and Cu(II) Complexes of 2-Hydroxyimino-3-oxo-3-piperidin-1-yl-propionitrile (HPiPCO)

The reaction route was similar to previously described preparations. The 0.300 g (1.66 mM) of HPiPCO (Figure 17, 33) was dissolved in 2.50 mL of deionized water in a 25 mL beaker and then 1.66 mL (1.66 mM) of 1M KOH solution was added for the deprotonation of the ligand. The colour of the solution changed to deep yellow. The 0.2407 g (0.83 mM) of $Ni(NO_3)_2 \cdot 6H_2O$ was dissolved in 5 mL of deionized water, then added dropwise to the deprotonated $PiPCO^-$ ligand solution. Murky cream brown reaction mixture was formed. The mixture was allowed to stand for approximately 2 hours under continuous stirring prior to filtration (Figure 34).

The colour of the filtrate was clear very light brown and the precipitate was cream-brown in appearance (Figure 35). The precipitate was allowed to stand at room

temperature for a week to get dried. The percent yield was calculated based on the amount of bulk precipitate obtained and found to be 42 % (0.3154 g).

For the Cu(II) complex, the following amount were used: 0.300 g (1.66 mM) of HPiPCO in 5 mL of H_2O, 1.66 mL of 1 M KOH, 0.1321 g (0.83 mM) $CuSO_4 \cdot 5H_2O$ in 5 mL H_2O. Green filtrate and precipitate (Figure 35) were obtained and the yield was 66 % (0.2415 g). Table 9 shows the result of elemental CHN analyses of the complexes.

Unfortunately, no suitable crystal of this complexes were obtained.

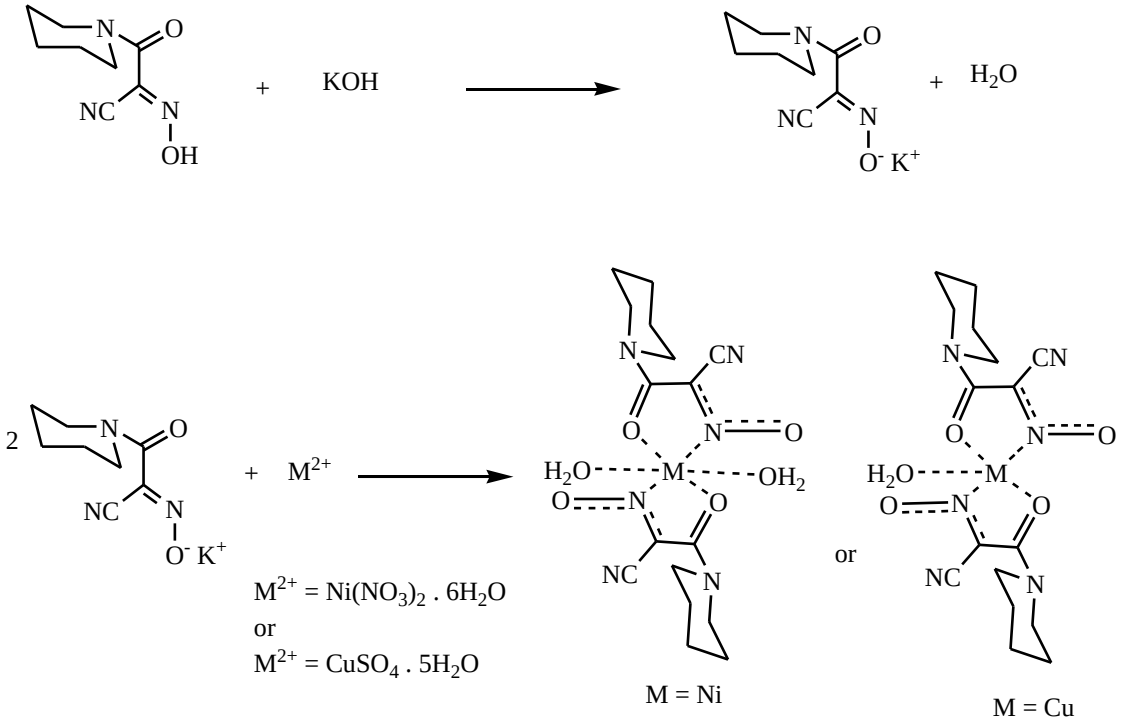

Figure 34. Syntheses of the Ni (II) and Cu(II) complexes of HPiPCO cyanoxime.

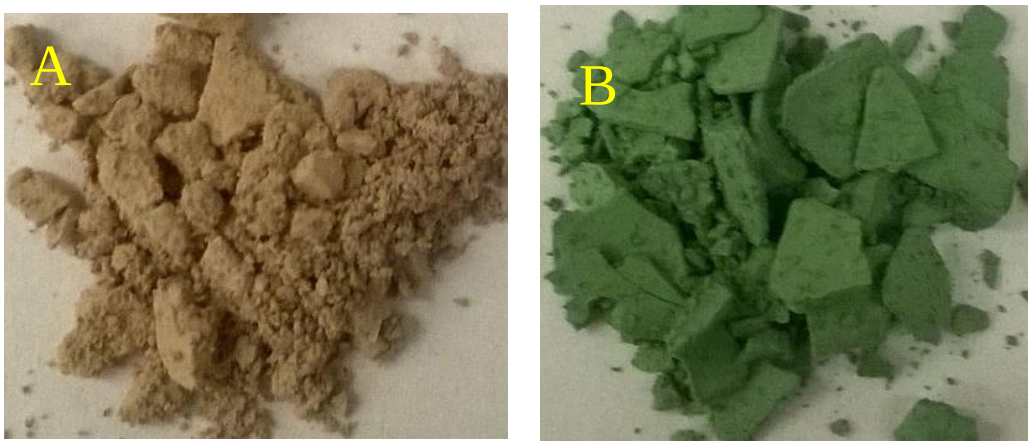

Figure 35. Microscope photographs of bulk precipitate of $Ni(PiPCO)_2 \cdot 2H_2O$ (A) and $Cu(PiPCO)_2 \cdot H_2O$ (B), taken at x40 magnification.

Table 9. The elemental analyses for $PiPCO^-$ based complexes.

Complex	C, % Calc. (Found)	H, % Calc. (Found)	N, % Calc. (Found)
$Ni(PiPCO)_2 \cdot 2H2O$	42.23 (42.00)	5.32 (4.89)	18.47 (18.44)
$Cu(PiPCO)_2 \cdot H_2O$	43.48 (43.81)	5.02 (4.90)	19.02 (19.05)

V. RESULTS AND DISCUSSIONS

V.1. Crystal Structure of HECO

The crystal specimen used for the X-ray crystallographic analysis was a clear light colourless plate-like specimen. The crystal specimen turned out to be a rotational twin. Individual components were selected with the aid of CELL_NOW program [82]. Application of the detwinning procedure followed by absorption correction with the help of TWINABS [83] led to a successful structure solution and refinement. All H-atoms were found objectively on electron difference map and were refined. The space group of the crystal is P21/c and the crystal system is monoclinic. The unit cell dimensions are a = 6.336 Å, b = 13.549 Å, c = 7.928 Å, $\alpha = 90°$, $\beta = 94.418°$, $\gamma = 90°$ (Table 10).

The compound is in a cis-anti-conformation (Figure 36). Thus, the oxime fragment and carbonyl group are on the same sides of the molecule along C1 – C3. All atoms in the HECO molecule are in a plane except for the H – atoms attached to C4 and C5 atom that stick out of the plane. The bond lengths C1 – N1 = 1.287 Å and N1 – O1 = 1.363 Å and bond angle N1 – C1 – C2 = 123.0° (Table 11) is normal for cyanoxime [26, 81, 84]. Molecules of HECO packed in the unit cell exhibit hydrogen bonding (Figure 37) (Appendix C-2) [85]. Literature contains data about the crystal structure of this cyanoxime [86] which was determined at room temperature in the rhombic crystal system. A two positional disorder was noted in that published structure. We determined that the HECO crystallized in monoclinic P lattice at 120 K, and is a valuable addition to the discovery of polymorphism in solid state structures of cyanoximes. The first indication of presence

of this phenomenon in this class of compounds was published just a couple of years ago [80]. CCDC 1473516 contains the supplementary crystallographic data for this compound.

Table 10. Crystal data and structure refinement data for the structure HECO

Parameter	HECO	
Chemical formula	$C_5H_6N_2O_3$	
Formula weight	142.12 g/mol	
Temperature	120(2) K	
Wavelength	0.71073 Å	
Crystal size	0.113 x 0.192 x 0.342 mm	
Crystal system	Monoclinic	
Space group	P21/c	
Unit cell dimensions	a = 6.336(2) Å	α = 90°
	b = 13.549(4) Å	β = 94.418(5)°
	c = 7.938(3) Å	γ = 90°
Volume	679.4(4) $Å^3$	
Z	4	
Density (calculated)	1.389 g/cm^3	
Absorption coefficient	0.117 mm^{-1}	
F(000)	296	
Theta range for data collection	2.98 to 26.37°	
Refinement method	Full-matrix least-squares on F^2	
Refinement program	SHELXL-2013 (Sheldrick, 2013)	
Goodness-of-fit on F^2	1.146	
Final R indices	1016 data; I>2σ(I)	R1 = 0.0545, wR2 = 0.1017
	all data	R1 = 0.0836, wR2 = 0.1118
Weighting scheme	$w=1/[\sigma^2(F_o^2)+(0.0242P)^2+0.7372P]$	
	where $P=(F_o^2+2F_c^2)/3$	
R.M.S. deviation from mean	0.063 $eÅ^{-3}$	

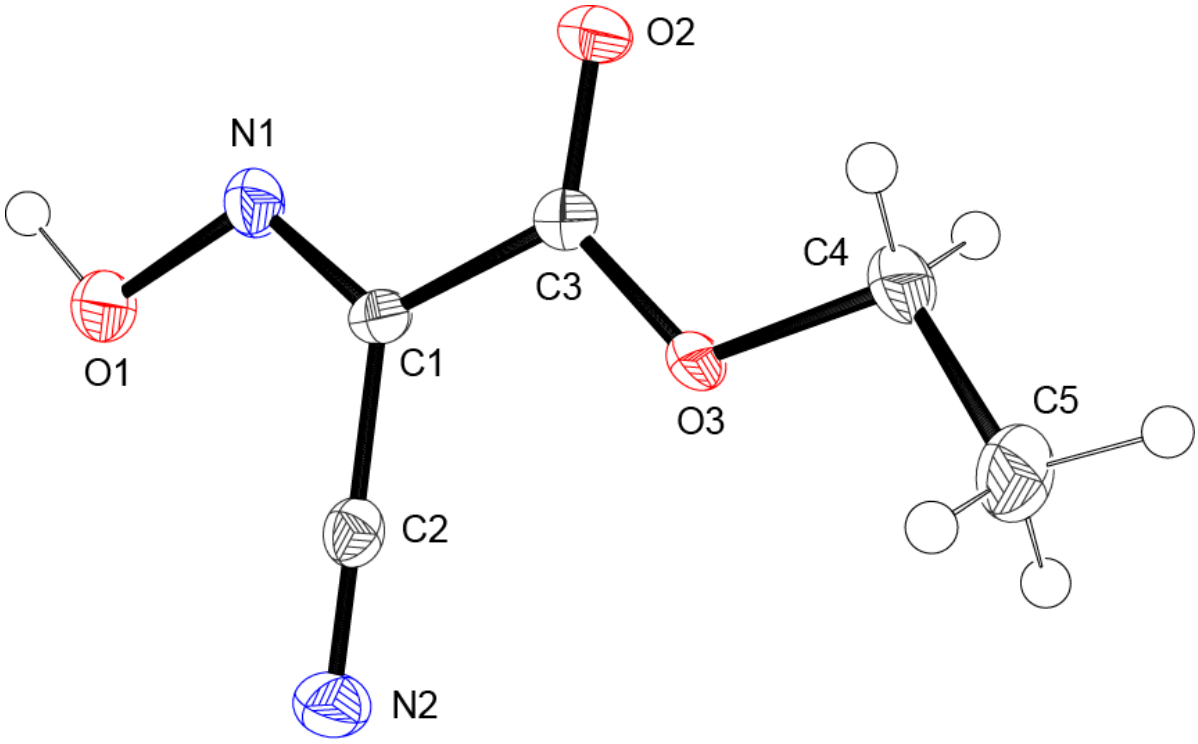

Figure 36. The ASU in the structure of HECO; thermal ellipsoids are drawn at 50% probability level.

Table 11. Selected bond lengths (Å) and bond angles (°) in HECO cyanoxime.

Bonds	(Å)	Bonds	(Å)	Angles	(°)
C1-N1	1.287(3)	C3-O3	1.318(3)	N1-C1-C2	123.0(2)
C1-C3	1.492(3)	C4-C5	1.491(4)	C2-C1-C3	119.5(2)
C3-O2	1.217(3)	C4-H4B	0.98(3)	O2-C3-O3	125.5(2)
C4-O3	1.477(3)	C5-H5B	0.99(3)	O3-C3-C1	110.48(19)
C4-H4A	0.96(3)			N1-C1-C3	117.5(2)
C5-H5A	0.96(3)			N2-C2-C1	179.3(3)
C5-H5C	0.98(3)			O2-C3-C1	124.0(2)
N1-O1	1.363(3)			O3-C4-C5	107.1(2)
C1-C2	1.444(3)			C1-N1-O1	111.72(19)
C2-N2	1.147(3)			C3-O3-C4	116.50(18)

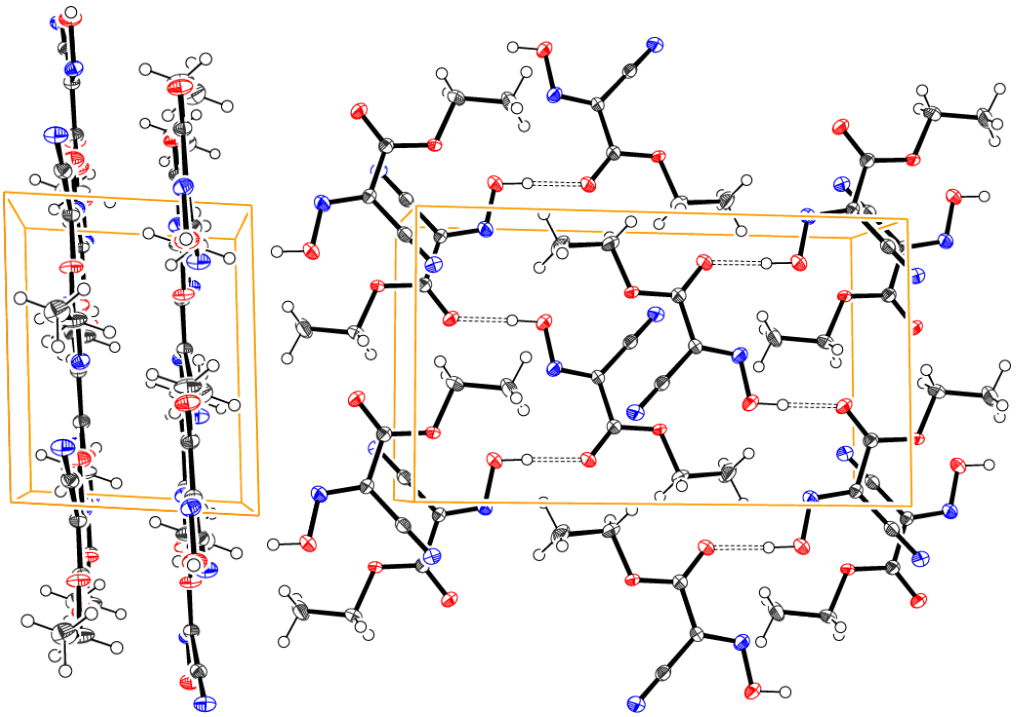

Figure 37. A perspective view of the unit cell content in the structure of cyanoxime HECO: two perspective views. Left - along *a* and *b* directions, right - showing H-bonding and layered structure of the compound.

V.2. Elemental Analysis CHN Results

The elemental CHN analyses results of the prepared complexes were reported in chapter IV - Experimental. Thus complexes of Ni(II) with cyanoximes were obtained and had the following compositions: $Ni(ACO)_2 \cdot 2H_2O$, $Ni(2PCO)_2 \cdot 4H_2O$ (two molecules of H_2O non-coordinating), $Ni(PiCO)_2 \cdot H_2O$, $Ni(PiPCO)_2 \cdot H_2O$, $Ni(PyrCO)_2 \cdot 2H_2O$. Also the product of hydrolysis: $[Ni(AACO) \cdot (H_2O)_3]_2 \cdot H_2O$ and $K_2[Ni_3(AACO)_4 \cdot (H_2O)_4].4H_2O$.

Similarly, Cu(II) complexes were obtained as: $Cu(ACO)_2 \cdot H_2O$, $Cu(2PCO)_2$, $Cu(PiPCO)_2 \cdot H_2O$ and $Cu(PyrCO)_2 \cdot H_2O$. Also, product of hydrolysis of the $MeCO^-$ and ECO^- anions employed for the preparation of complexes: $K_2[Cu_3(AACO)_4 \cdot (H_2O)_4] \cdot 4H_2O$ and $K_2[Cu(AACO)_2 \cdot H_2O] \cdot 2H_2O$.

V.3. Results of Differential Scanning Calorimetry – Thermal Gravimetry Analysis (DSC – TGA)

The DSC-TGA analysis of the bulk precipitate of the complexes were performed and will be briefly described below (Table 12). Typical thermogram are shown in Figure 38. Other thermograms of the complexes can be found in the appendix section (Appendix B1-B9).

V.4. Dehydration and Rehydration

The dehydration experiment was successfully performed using the information from the DSC – T GA studies. Data of thermal analysis indicated the loss of H_2O molecules from Ni – cyanoximates. It was important to investigate whether water can rehydrate anhydrous complexes. Result of analysis proved that the dehydrated complex of Ni(II) with ACO^- ($Ni(ACO)_2$**),** and $2PCO^-$ ($Ni(2PCO)_2$), $PyrCO^-$ ($Ni(PyrCO)_2$) are essentially 100 % reversible with the dehydrated complex being able to regain the lost two molecules of water as evident from % change in masses. The rehydration of the dehydrated Ni(II) complex with $PiPCO^-$ ($Ni(PiPCO)_2$) is only partly reversible with the dehydrated complex being able to regain a molecule of water to form $Ni(PiPCO)_2 \cdot H_2O$. However, the colour of the rehydrated Ni(II) complex with $2PCO^-$ differs from the parent hydrated complex but, the colour is similar to that of the dehydrated complex (Figure 39). Whereas, the rehydrated Ni(II) complex of ACO^- has the same colour with the parent hydrated complex (Figure 40). The hydrated, dehydrated and rehydrated Ni(II) complex with $PiPCO^-$ and $PyrCO^-$ cyanoximate ion have similar colours (Figure 41 and 42).

Results of thermal analysis studies provided valuable information about the

Table 12. DSC/TGA analysis of metal complexes

Complex	Process, Temp (°C)	Products and weight (%)	Effect
$Ni(ACO)_2 \cdot 2H_2O$	Loss of two molecules of H_2O, 173	$Ni(ACO)_2$; calc: 88.7, found: 88.5	Endothermic
$Cu(ACO)_2 \cdot H_2O$	Loss of a molecule of H_2O, 214	$Cu(ACO)_2$; calc: 94.11, found: 97.57	Exothermic
	Decomposition, 306	$CuCO_3$; calc: 40.42, found: 39.81	Endothermic
$Ni(PiCO)_2 \cdot H_2O$	Loss of a molecule of H_2O, 114	$Ni(PiCO)_2$; calc: 95.30, found: 95.53	Endothermic
$Cu(PiCO)_2$	Decomposition with loss of 2 CH_3CN, 218	(?); calc: 77.80, found: 79.42	Endothermic
	Decomp, 328	CuO; calc: 21.51, found: 25.01	Exothermic
$Ni(2PCO)_2 \cdot 4H_2O$	Loss of 1st two molecules of H_2O, 146	$Ni(2PCO)_2 \cdot 2H_2O$; calc: 91.48, found: 91.78	Endothermic
	Loss of 3rd molecule of H_2O, 263	$Ni(2PCO)_2 \cdot H_2O$; calc: 87.22, found: 89.88	Exothermic
$Cu(2PCO)_2$	Decomposition, 313	$CuCO_3$; calc: 34.72, found: 35.14	Exothermic
$Ni(PyrCO)_2 \cdot 2H_2O$	Loss of 1st molecule of H_2O, 138	$Ni(PyrCO)_2 \cdot H_2O$; calc: 95.78, found: 97.36	Endothermic
	Decomposition, 297	$Ni(NO_3)_2$; calc: 42.78, found: 40.51	Exothermic
$Cu(PyrCO)_2 \cdot H_2O$	Decomposition, 219	$Cu(OCN)_2$; calc: 35.66, found: 38.81	Exothermic
$Ni(PiPCO)_2 \cdot 2H_2O$	Loss of 1st molecule of H_2O, 155	$Ni(PiPCO)_2 \cdot H_2O$; calc: 96.04, found: 94.81	Endothermic
$Cu(PiPCO)_2 \cdot H_2O$	Loss of a molecule H_2O, 140	$Cu(PiPCO)_2$; calc: 95.92; found: 96.13	Exothermic

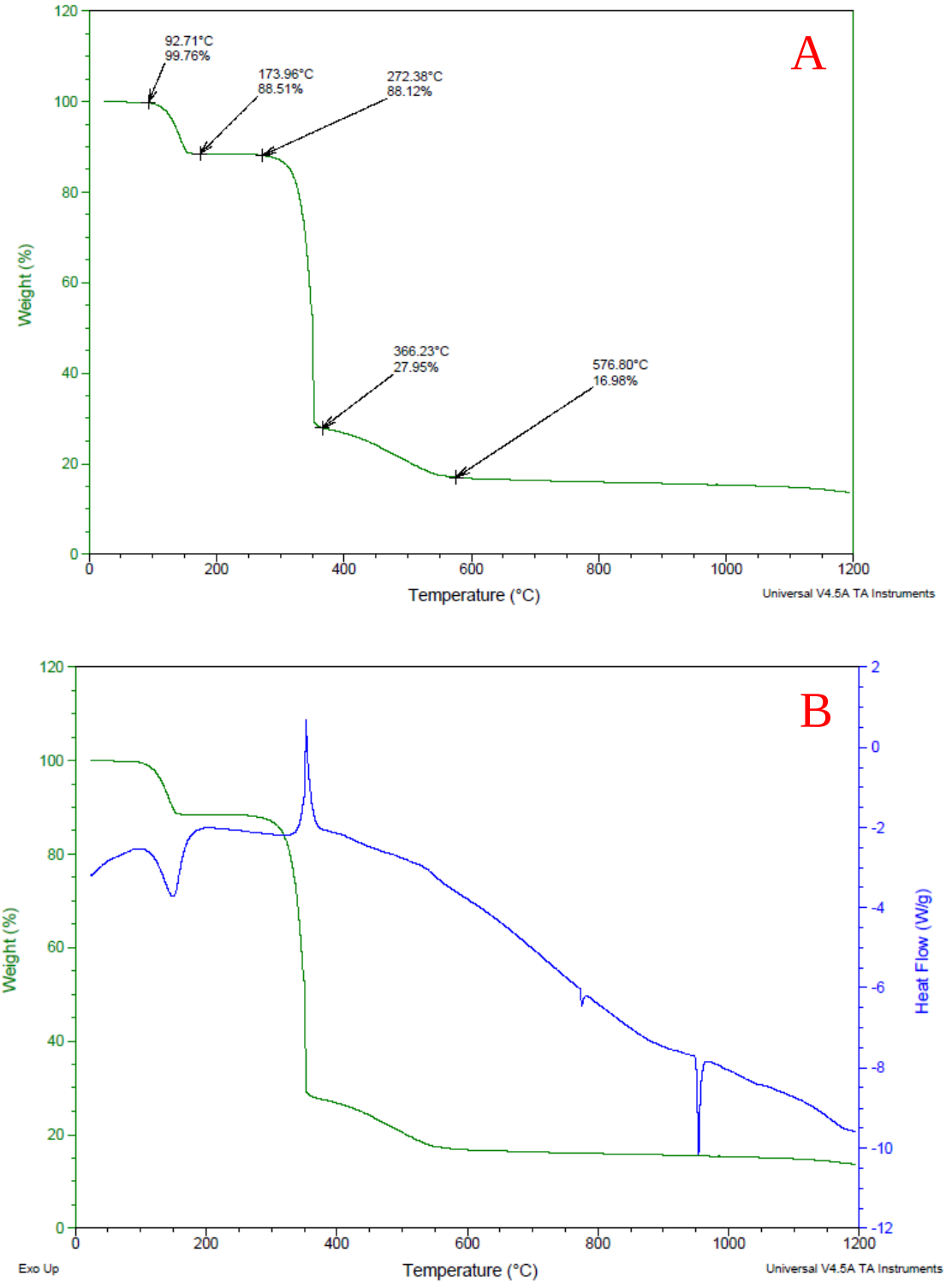

Figure 38. Results of thermal analysis study of $Ni(ACO)_2 \cdot 2H_2O$. Mass loss trace (A); combined weight loss and the heat flow curves (B).

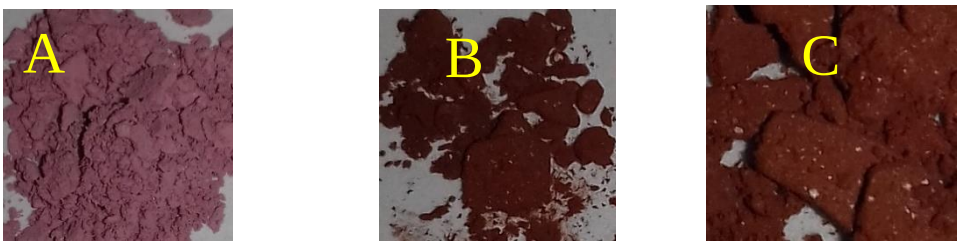

Figure 39. The microscope photographs of the hydrated $Ni(2PCO)_2 \cdot 2H_2O$ (A), anhydrous $Ni(2PCO)_2$ (B) and rehydrated $Ni(2PCO)_2 \cdot 2H_2O$ (C) complex at x40 magnification.

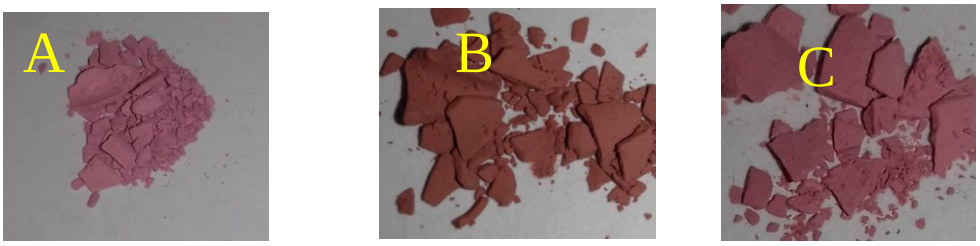

Figure 40. The microscope photographs of the hydrated $Ni(ACO)_2 \cdot 2H_2O$ (A), anhydrous $Ni(ACO)_2$ (B) and rehydrated $Ni(ACO)_2 \cdot 2H_2O$ (C) at x40 magnification.

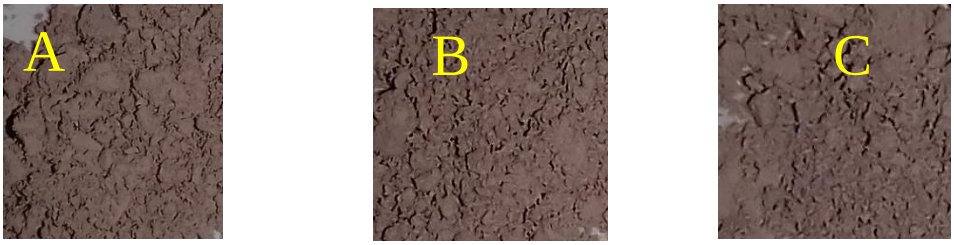

Figure 41. The microscope photographs of the hydrated $Ni(PiPCO)_2 \cdot 2H_2O$ (A), anhydrous $Ni(PiPCO)_2$ (B) and rehydrated $Ni(PiPCO)_2 \cdot 2H_2O$ (C) complex at x40 magnification.

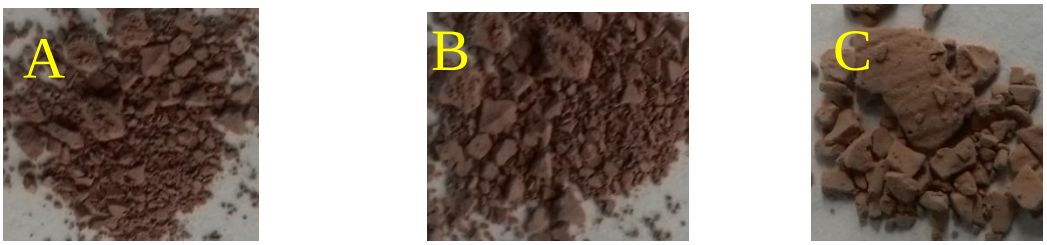

Figure 42. The microscope photographs of the hydrated $Ni(PyrCO)_2 \cdot 2H_2O$ (A), anhydrous $Ni(PyrCO)_2$ (B) and rehydrated $Ni(PyrCO)_2 \cdot 2H_2O$ (C) at x40 magnification.

temperatures of crystallization/coordination water loss. This data coupled with rehydration experiments gave sense of the lattice rigidity in studied Ni-cyanoximates. The Cu complexes were not performing in similar fashion to Ni compounds. Thus, after studies of the reversibility of dehydration ↔ rehydration process in Ni(II) cyanoximates, we realized the flexibility of crystal lattices of these complexes.

This finding lead to a conclusion that it is possible to construct 1D extended solids based on Ni(II) as we postulated at the end of research goal part on page 33 with potentially achievable goal of making mixed valence coordination polymer shown schematically on page 35.

V.5. Infrared Spectroscopy

The assignments of vibrational bands in the IR - spectra (Table 13) were made in reference to previous works done by previous students in the research group with the same ligands [87 – 90]. The vibrational frequencies provide information about the coordination modes of the ACO^-, $PiPCO^-$, $PyrCO^-$ and $PiCO^-$ cyanoximates with the Ni(II) and Cu(II) ions. The shift in ν(C=O) band positions of the ligands indicate bidentate chelating mode using the oxygen atom of the CO (Table 13). The high energy shifts of the ν(NO), ν(CNO) bands evidences the participation of the CNO fragment in coordination as well. Therefore, chelate binding modes are suggested. A comparison of vibrational frequencies in the spectra of complexes $^{6h}Ni(ACO)_2 \cdot 2H_2O$, $^{7a}Ni(ACO)_2$, $^{8r}Ni(ACO)_2 \cdot 2H_2O$ shows some structural changes after dehydration of $^{h}Ni(ACO)_2 \cdot 2H_2O$

[6] hydrated
[7] anydrous
[8] rehydrated

Table 13. Assignment of important vibrational frequencies (cm^{-1}) for ligand and their metal complexes.

Compounds	ν(N–H)	ν(C≡N)	ν(C=O)	ν(CNO)	ν(NO)	$\nu(C=N)_{Py}$	$\nu(C=N)_{ox}$
$NaH(ACO)_2$	3470, 3326	2247	1680	1246	1095		
$^{h}Ni(ACO)_2 \cdot 2H_2O$	3364, 3198	2227	1671	1303	1102		
$^{a}Ni(ACO)_2$	3418	2223	1658	1279	1174		
$^{r}Ni(ACO)_2 \cdot 2H_2O$	3366, 3199	2227	1670	1304	1103		
$Cu(ACO)_2 \cdot H_2O$	3334, 3241	2223	1658	1335	1190		
H(2PCO)		2229		1284	1252	1593	1476
$^{h}Ni(2PCO)_2 \cdot 2H_2O$		2218		1300	1265	1603	1463
$^{a}Ni(2PCO)_2$		2221		1301	1273	1601	1457
$^{r}Ni(2PCO)_2 \cdot 2H_2O$		2222		1300	1273	1601	1455
$Cu(2PCO)_2 \cdot H_2O$		2215		1319	1273	1603	1454
HPiPCO		2228	1624	1290	1182		1470
$^{h}Ni(PiPCO)_2 \cdot 2H_2O$		2211	1590	1295	1186		1450
$^{a}Ni(PiPCO)_2$		2211	1590	1295	1186		1450
$^{r}Ni(PiPCO)_2 \cdot 2H_2O$		2211	1590	1295	1189		1450
$Cu(PiPCO)_2 \cdot H_2O$		2205	1586	1300	1194		1471
HPyrCO		2240	1622	1217	1159		1462
$^{h}Ni(PyrCO)_2 \cdot 2H_2O$		2213	1574	1224	1153		1468
$^{a}Ni(PyrCO)_2$		2210	1588	1219	1155		1468
$^{r}Ni(PyrCO)_2 \cdot 2H_2O$		2211	1590	1219	1156		1468
$Cu(PyrCO)_2 \cdot H_2O$		2199	1582	1224^{vw}	1143^{vw}		1453
HPiCO		2166	1678	1217	1032		1484
$^{h}Ni(PiCO)_2 \cdot H_2O$		2214	1629	1232	1042		1463
$Cu(PiCO)_2 \cdot H_2O$		2217	1674	1232	1043		1481

^{h} – Hydrated, ^{a} – anhydrous, ^{r} – rehydrated, ^{vw} – very weak, $_{py}$ – pyridine, $_{ox}$ -oxime

to give the $^{a}Ni(ACO)_2$. This may indicate tighter binding of the anion in an anhydrous complex. The rehydrated complex $^{r}Ni(ACO)_2 \cdot 2H_2O$ has vibrational spectra similar to that of the parent hydrated complex $^{h}Ni(ACO)_2 \cdot 2H_2O$. In the $Cu(ACO)_2 \cdot H_2O$ vibrational spectra, a low energy shift of the ν(C=O) band position from 1680 cm^{-1} to 1658 cm^{-1} indicates coordination through the oxygen atom of the carbonyl group and a high energy shift of the ν(NO) band from 1095 cm^{-1} to 1190 cm^{-1} and ν(CNO) band from 1246 cm^{-1} to 1335 cm^{-1} evidences the participation of the CNO fragment in coordination as well. This indicates a bidentate chelation mode to the Cu(II) center.

It appears that Cu(II) and Ni(II) complexes of H(2PCO) exhibit bidentate chelate coordination mode as well using the nitrogen atom of the oxime and nitrogen atom of the pyridine. This is reflected by the increased vibrational frequencies of the $\nu(C=N_{)(Py)}$ and of ν(N – O) in the IR spectra of the complexes as compared to that of the H(2PCO) (Table 13). A comparison of vibrational frequencies of $^{a}Ni(2PCO)_{2,}$ $^{r}Ni(2PCO)_2 \cdot 2H_2O$ and $^{h}Ni(2PCO)_2 \cdot 2H_2O$ revealed that there were slight changes in coordination after dehydration and even after rehydration, this new coordination mode apparently persisted because the vibrational frequencies of the rehydrated complex are still very similar to those of the anhydrous complexes.

The Ni(II) and Cu(II) complexes of HPiPCO also exhibit bidentate chelate coordination mode as can be seen from the IR spectra vibrational that shifted to a lower energy when compared to that of the pure HPiPCO ligand (Table 13). This indicates a coordination using the oxygen atom of the carbonyl group. A high energy shift of the ν(NO), ν(CNO) bands indicate the participation of the CNO fragment in coordination as well (Table 13). The hydrated, anhydrous and rehydrated complex of Ni(II) with $PiPCO^{-}$

cyanoximate ion have very similar vibrational frequencies (Table 13). This could be that the coordination mode is the same in these complexes and arrangement of atoms are similar.

The Ni(II) and Cu(II) complexes of HPyrCO exhibit bidentate chelate coordination modes using the O-atom of the carbonyl group and N-atom of the oxime group. This is evident by the decreased vibrational frequency of ν(C=O) and increased vibrational frequencies of ν(CNO) and ν (NO) when compared to ν(C=O), ν(CNO) and ν(NO) in pure HPyrCO ligand (Table 13). There was no change in coordination mode after dehydration and upon rehydration as evident with apparently similar ν(C=O), ν(CNO) and ν(NO) vibrational frequencies in the hydrated, anhydrous and rehydrated complexes with those for dehydrated and rehydrated closer in values (Table 13).

V.6. UV-Visible Spectroscopy

The vast majority of synthesized complexes are poorly soluble in water. Also, dissolution of complexes in organic solvents leads to the change in integrity of compounds and the loss of solid state structures. Thus, we used solid samples to record electronic spectra of synthesized metallo-cyanoximates. However; for the presentation of spectra we converted the reflectance spectra to the most common and accepted format – absorbance. Two types of spectra and their relations are seen in Appendix B-10.

Diffuse reflectance spectroscopy of solid states of hydrated $Ni(ACO)_2 \cdot 2H_2O$, anhydrous $Ni(ACO)_2$ and rehydrated $Ni(ACO)_2 \cdot 2H_2O$ (Figure 43) showed transitions expected for d^8 electronic configuration of Ni(II) in a distorted octahedral environment. In this section of the thesis, two units for expression of values of peaks maxima in spectra

will be used: nm and cm^{-1}. For a d^8 ion in an octahedral environment, three spin allowed transitions $d - d$ transitions are expected: $^3A_{2g}$ to $^3T_{2g}$, $^3T_{1g}(F)$ and $^3T_{1g}(P)$ which generally fall within the ranges 1428 nm-769 nm (7000 cm^{-1}-13000 cm^{-1}), 909 nm-500 nm (11000 cm^{-1}-20000 cm^{-1}) and 526 nm-370 nm (19000 cm^{-1}- 27000 cm^{-1}) respectively [91].

Two of these transitions: $^3A_{2g} \rightarrow {}^3T_{1g}(P)$ and $^3A_{2g} \rightarrow {}^3T_{1g}(F)$ were seen on the spectra of $Ni(ACO)_2 \cdot 2H_2O$, anhydrous $Ni(ACO)_2$ and rehydrated $Ni(ACO)_2 \cdot 2H_2O$. The third transition: $^3A_{2g} \rightarrow {}^3T_{2g}$ is expected to be seen at near IR region which is beyond the wavelength range of the Cary 100 Bio spectrophotometer used. The assignment of the spectra is as shown in Table 14. The transitions $n \rightarrow \pi^*$ and $\pi \rightarrow \pi^*$ are transitions in the ligand (Table 14).

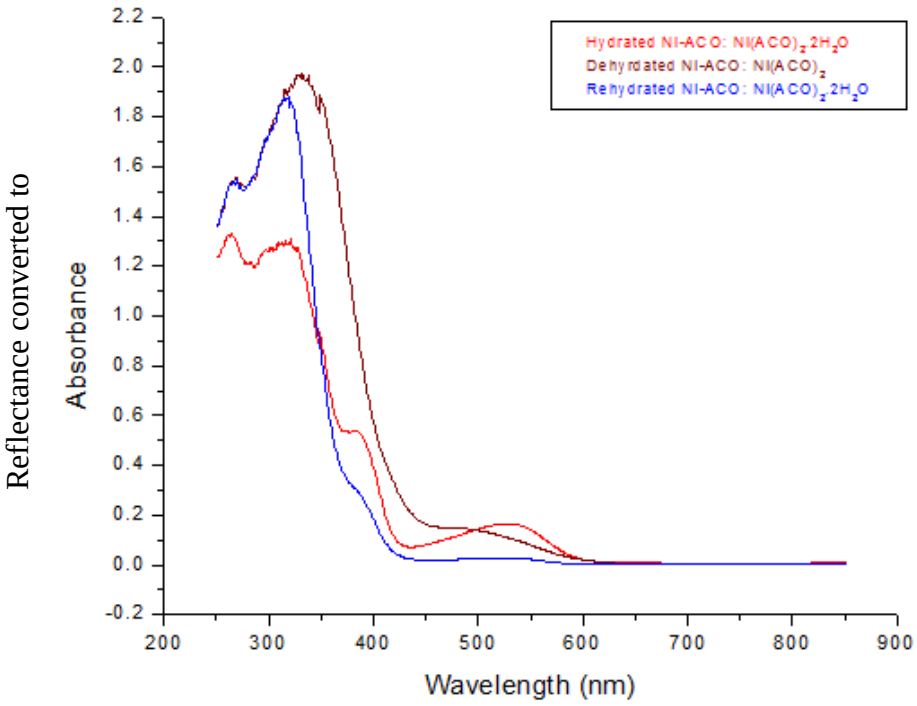

Figure 43. The solid state diffuse reflection spectra in the Ni – ACO system.

Table 14. Assignment of transition bands (nm) in Ni system UV-Vis spectra

Metal complexes	$^3A_{2g} \rightarrow {}^3T_{1g}(P)$	$^3A_{2g} \rightarrow {}^3T_{1g}(F)$	$n \rightarrow \pi^*$	$\pi \rightarrow \pi^*$
$^h Ni(ACO)_2 \cdot 2H_2O$	316	525	-	268
$^a Ni(ACO)_2$	326	490	417 – 464	269
$^r Ni(ACO)_2 \cdot 2H_2O$	319	525	411 – 468	269
$^h Ni(2PCO)_2 \cdot 2H_2O$	363	473 – 674	-	264
$^a Ni(2PCO)_2$	380	472 - 674	413 – 468	267
$^r Ni(2PCO)_2 \cdot 2H_2O$	386	535	413 – 469	267
$^h Ni(PiPCO)_2 \cdot 2H_2O$	335	469 – 672	-	258 – 275
$^a Ni(PiPCO)_2$	337	469 – 672	-	258 – 275
$^r Ni(PiPCO)_2 \cdot 2H_2O$	333	469 – 672	-	257 – 272
$^h Ni(PyrCO)_2 \cdot 2H_2O$	338	530	-	252 - 278
$^a Ni(PyrCO)_2$	349	470 - 619	-	250 - 280
$^r Ni(PyrCO)_2 \cdot 2H_2O$	323	473 - 656	-	250 - 282

^{h} – Hydrated, ^{a} – anhydrous and ^{r} – rehydrated

The Ni-ACO system electronic spectra looks almost alike except for some slight changes like missing $n \rightarrow \pi^*$ transition. However, it is evident that the expected transitions in d^8 octahedral are seen in the three complexes which communicates that the environment around the Ni(II) is still octahedral.

The hydrated $Ni((2PCO)_2 \cdot 2H_2O$, anhydrous $Ni(2PCO)_2$ and rehydrated $Ni(2PCO)_2 \cdot 2H_2O$ (Figure 44) showed the three allowed transitions for a d^8 ion in an octahedral environment with two appearing on the spectra and the other found in the near IR region. Assignments are as shown in Table 14.

The electronic spectra hydrated $Ni(PiPCO)_2 \cdot 2H_2O$, anhydrous $Ni(PiPCO)_2$, and rehydrated $Ni(PiPCO)_2 \cdot 2H_2O$ (Figure 45) are in accord with the expected $d – d$ transitions (Table 14) within the wavelength range available by the instrument. Spectra

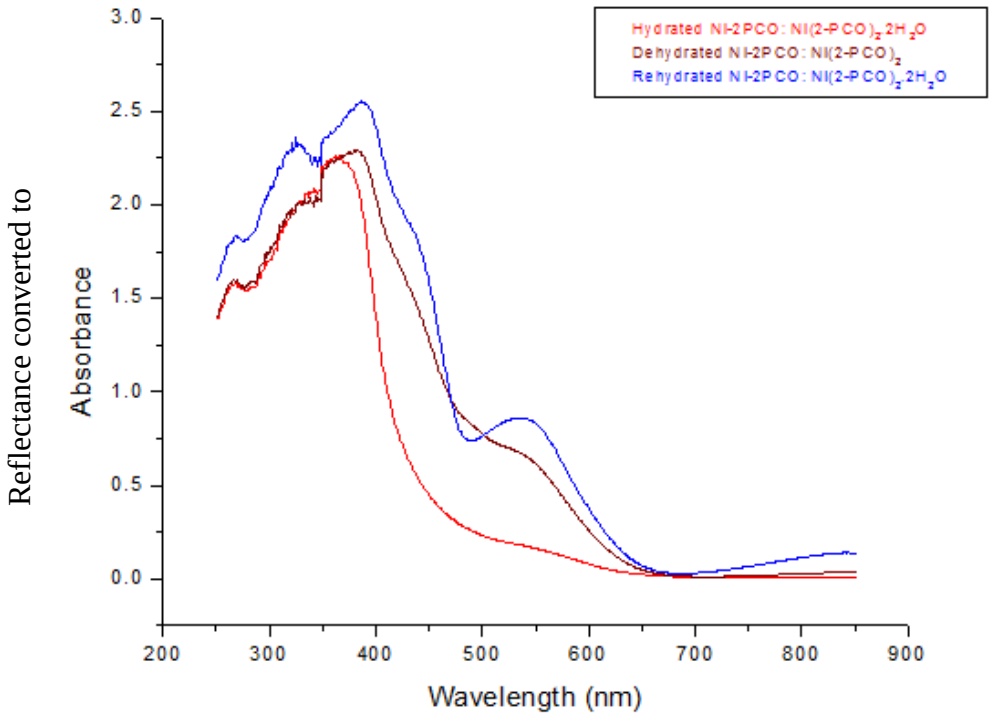

Figure 44. The solid state diffuse reflection spectra in the Ni – 2PCO system.

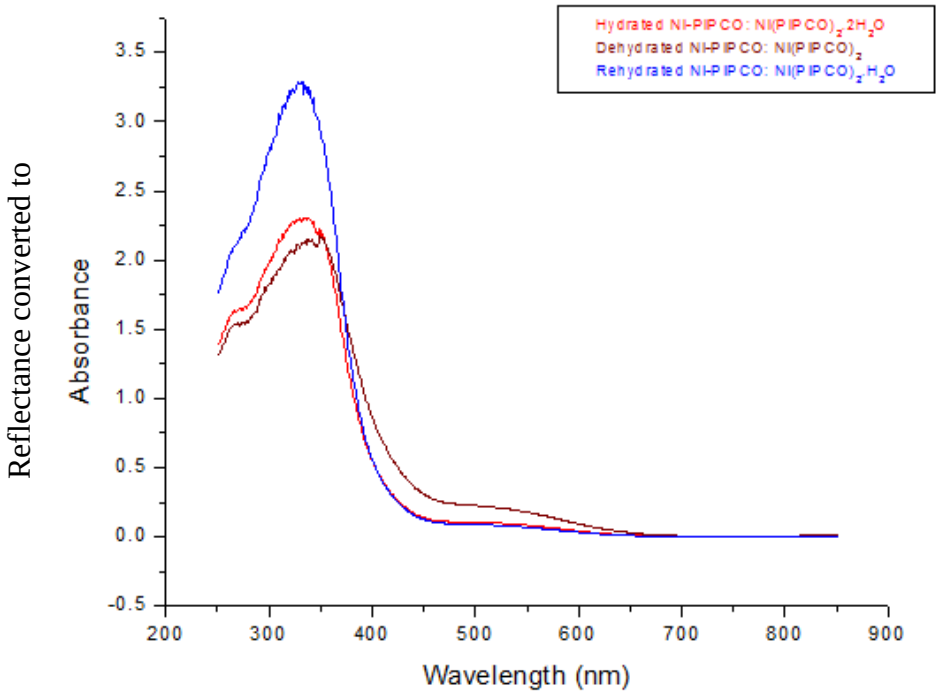

Figure 45. The solid state diffuse reflection spectra in the Ni-PiPCO system.

show that the hydrated, dehydrated and rehydrated nickel complexes have octahedral environment around the Ni(II) centers but there could be difference in the arrangement of atoms.

The electronic spectra of hydrated $Ni(PyrCO)_2 \cdot 2H_2O$, anhydrous $Ni(PyrCO)_2$, and rehydrated $Ni(PyrCO)_2 \cdot 2H_2O$ were in accord with the expected *d – d* transitions (Table 14) within the wavelength range available by the instrument. The spectra of anhydrous and rehydrated Ni(II) complexes with $PyrCO^-$ are very similar with very weak *d – d* transition bands in the range 460-630 nm unlike the fairly strong band of the hydrated complex *d – d* transition band with peak value at 530 nm (Figure 46).

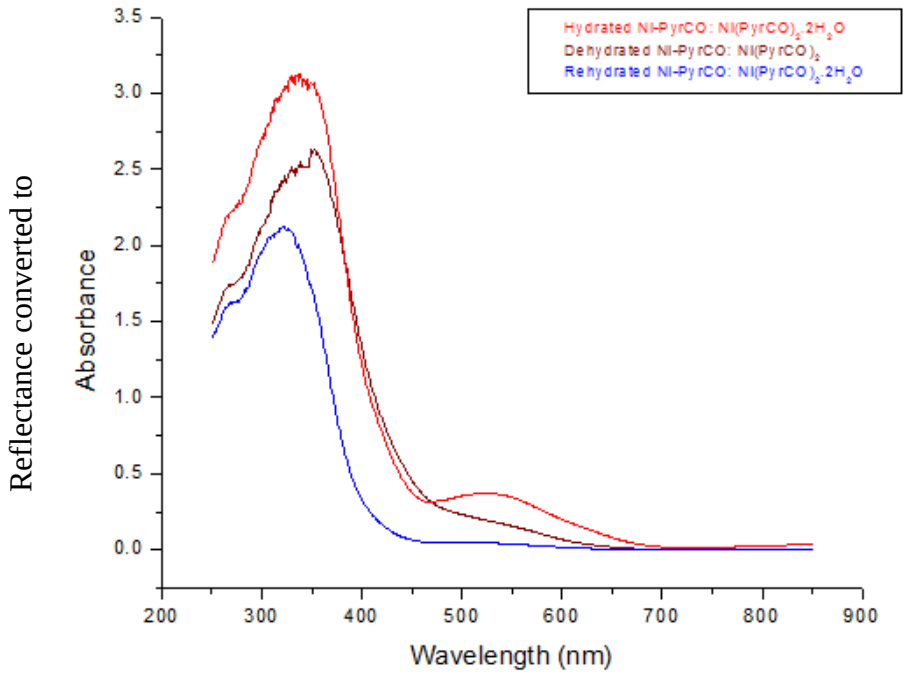

Figure 46. The solid state diffuse reflection spectra in the Ni-PyrCO system.

The solid state diffuse reflection spectra of Cu(II) complexes were also recorded.

The d^9 configuration gives rise to ^2D ground term and in an octahedral field, the ground term is ^2E_g. Octahedral Cu(II) complexes are expected to have a single absorption band corresponding to $^2E \rightarrow {}^2T_{2g}$ transition but due to Jahn-Teller distortion, six coordinates Cu(II) complexes shows spectra having broad band at greater than 10,000 cm^{-1} (below 1000 nm) resulting from several overlapping bands. In a tetrahedral field, a transition attributed to $^2E \rightarrow {}^2T_2$ is expected at below 10,000 cm^{-1} (above 1000 nm). Square-planar Cu(II) complexes usually show two absorption bands between 10,000 cm^{-1} to 20,000 cm^{-1} (1000 nm – 500 nm) with band assignments $^2B_{1g} \rightarrow {}^2A_{1g}$ and $^2B_{1g} \rightarrow {}^2E_g$ [92].

The diffuse reflection spectrum of $Cu(ACO)_2.H_2O$ (Figure 47) contain a single, asymmetric band at 579 nm (17300cm^{-1}) which is assigned to be $d - d$ transfer. There also exist a band that appears like a combination of two bands with peaks at 438 nm (22800 cm^{-1}) and 399 nm (25100 cm^{-1}) which is also a $d - d$ transfer band. There is a

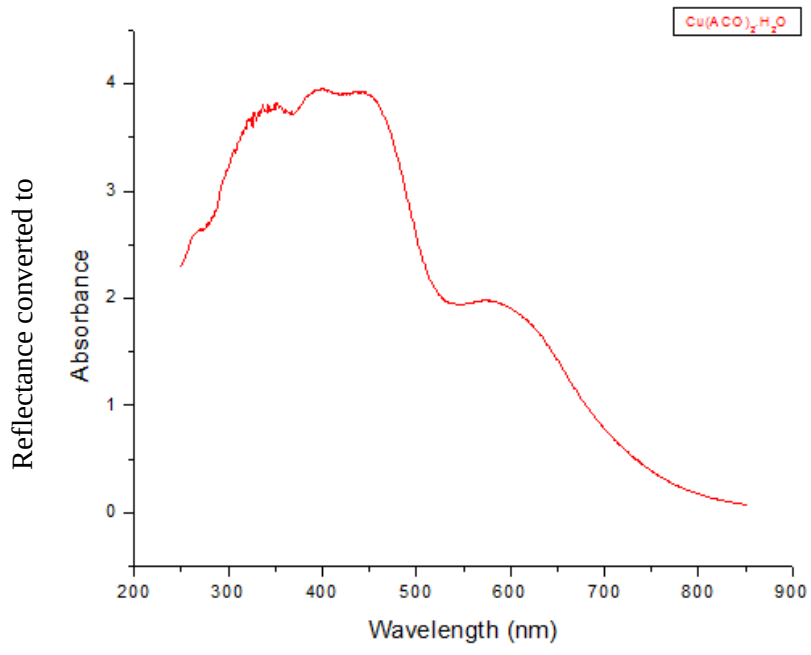

Figure 47. The solid state diffuse reflection spectrum of $Cu(ACO)_2 \cdot H_2O$.

charge transfer band with peak at 350 nm (28600 cm^{-1}) and a $\pi \rightarrow \pi^*$ band at 251 nm – 279 nm (39800 cm^{-1} – 35800 cm^{-1}). The environment around the Cu(II) ion in this complexes is distorted square pyramid.

The $Cu(2PCO)_2$ spectrum (Figure 48) shows a single broad absorption band with peak at 418 nm (23800 cm^{-1}) which is characteristic of Cu(II) ion in an octahedral environment $^2E_g \rightarrow {}^2T_{2g.}$ There also exist a $\pi \rightarrow \pi^*$ transition at 266 nm (37600 cm^{-1}). The environment around Cu(II) in this complex looks like octahedral. This suggest a polymeric compound with either direct Cu----Cu interaction or bridging coordination mode using atom(s) in the oxime.

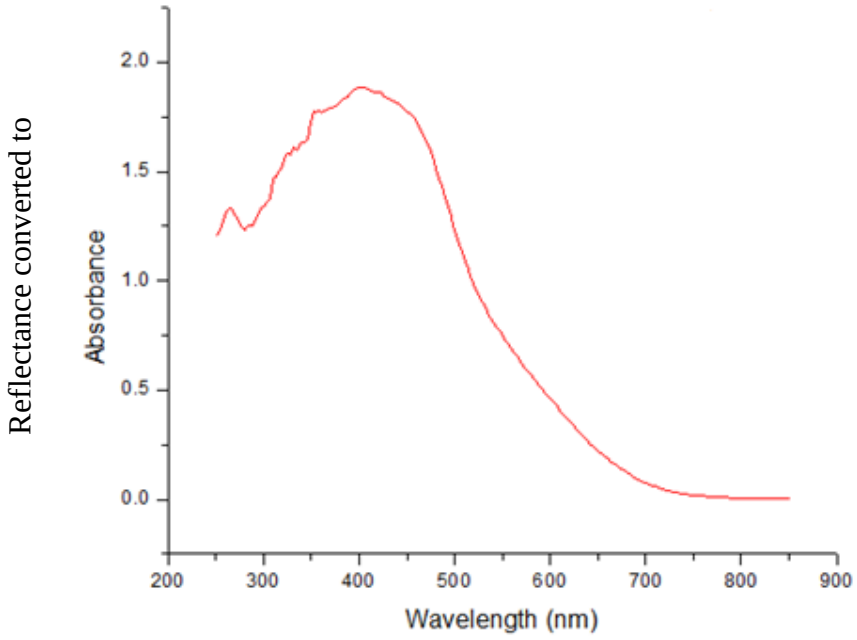

Figure 48. Solid state diffuse reflection spectrum of $Cu(2PCO)_2$**.**

The $Cu(PiCO)_2$ diffuse reflection spectrum (Figure 49) show three bands: at 529-690 nm (18900 – 14500cm^{-1}), 423-505 nm (23600-19800 cm^{-1}) and a peak at 335 nm

(29800 cm^{-1}). The first two bands are *d* – *d* transitions in square planar Cu(II) complex while the latter is a charge transfer band.

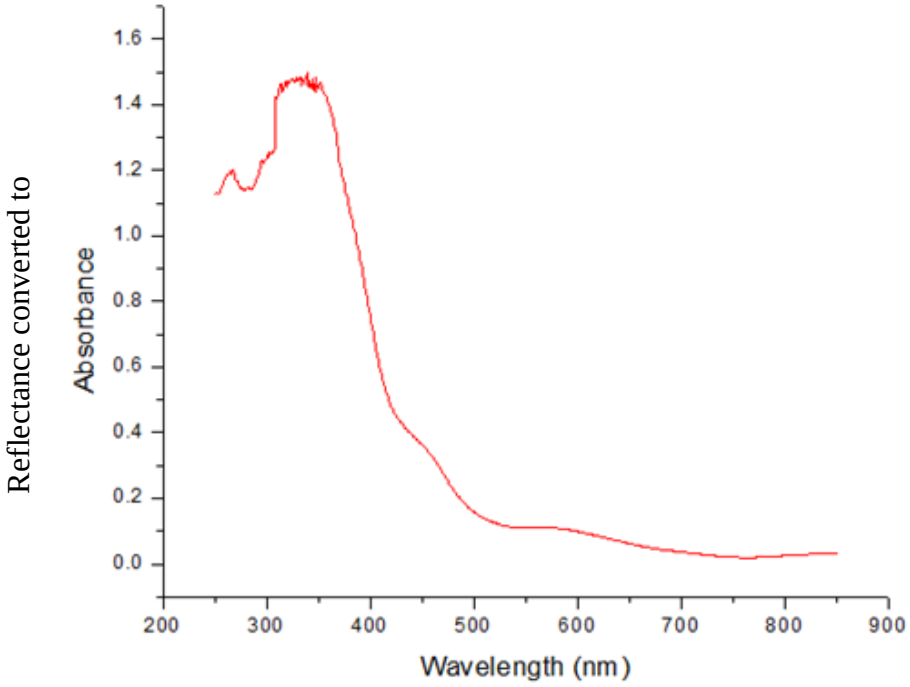

Figure 49. Solid state diffuse reflection spectrum of $Cu(PiCO)_2$.

The $Cu(PiPCO)_2 \cdot H_2O$ diffuse reflection spectrum (Figure 50) show a three distinct symmetric bands with peaks at 628 nm (15923 cm^{-1}), 390 nm (25641 cm^{-1}) and 331 nm (30211 cm^{-1}). The first two bands are *d* – *d* transition bands in a distorted square pyramidal Cu(II) complex while the latter is a charge transfer band.

The $Cu(PyrCO)_2 \cdot H_2O$ spectrum (Figure 51) shows a very weak band at 545-709 nm (18348-14104 cm^{-1}), and two distinct peaks at 410 nm (24390 cm^{-1}) and 328 nm (30487 cm^{-1}) which are $n \rightarrow \pi^*$. The band at 545-709 nm (18348-14104 cm^{-1}) is a *d* – *d* transition band. This type of spectrum for a d^9 ion is characteristic for a distorted square pyramidal structure.

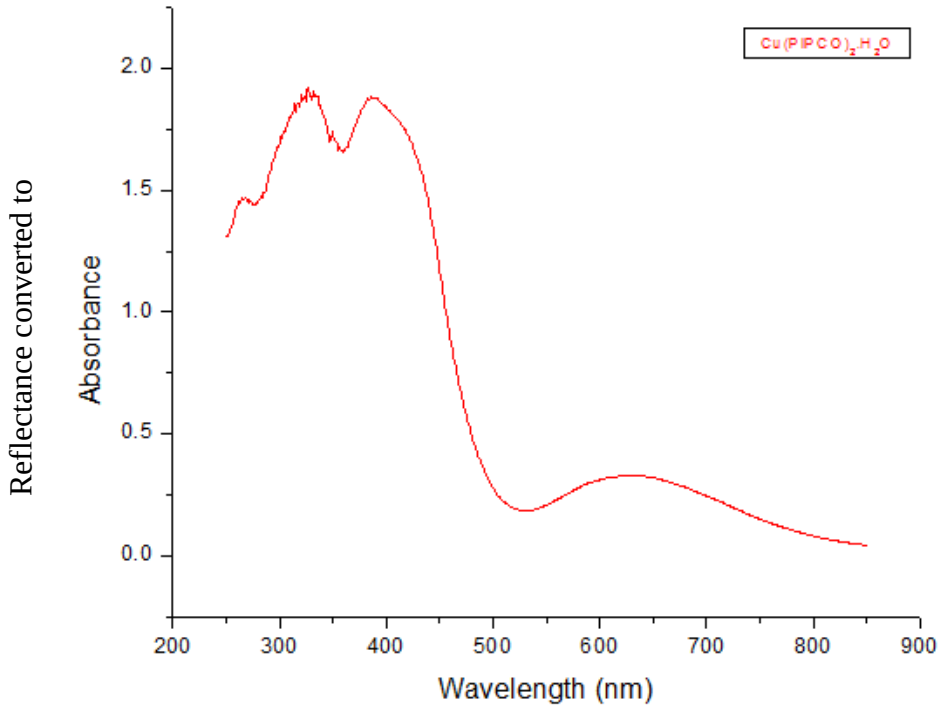

Figure 50. Solid state diffuse reflection spectrum of $Cu(PiPCO)_2 \cdot H_2O$.

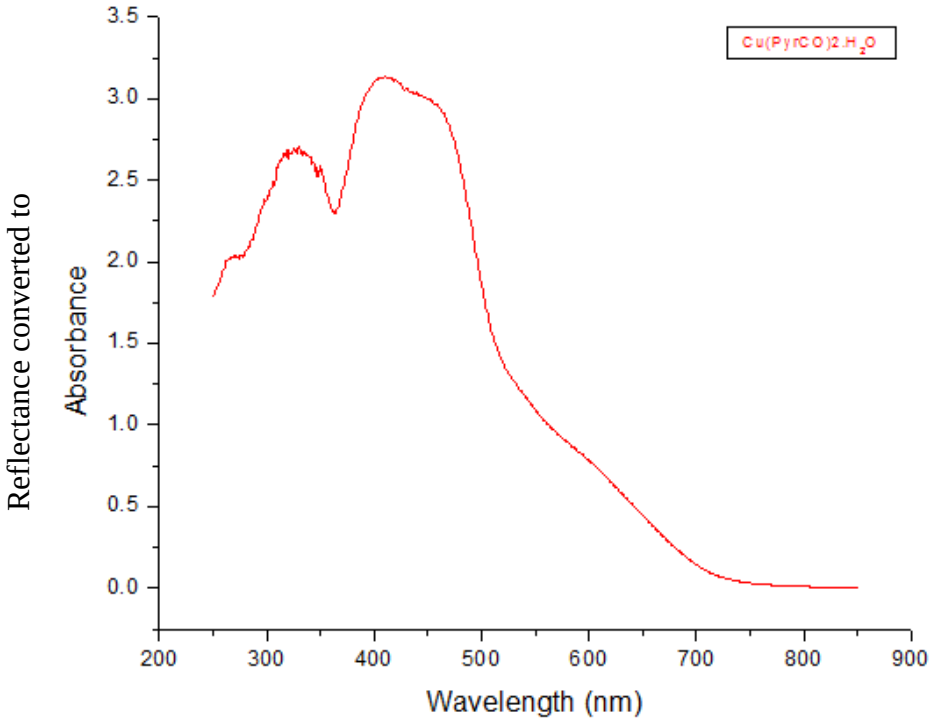

Figure 51. Solid state diffuse reflection spectrum of $Cu(PyrCO)_2 \cdot H_2O$.

V.7. Powder Diffraction

In order to see if there are any structural or lattice changes during dehydration procedure, the XRD powder diffraction data were collected for the most interesting samples in this work: Ni-cyanoximates. The diffraction pattern of the $Ni(2PCO)_2 \cdot 2H_2O$ and $Ni(2PCO)_2$ are shown in Figure 52. There are some new interplanar distances in the XRD powder of an anhydrous complex but in general the lattice seems to have small changes upon water removal. These results are certainly good news because they imply a largely retained structural motif in $Ni(2PCO)_2$, which is already adopting a stacked

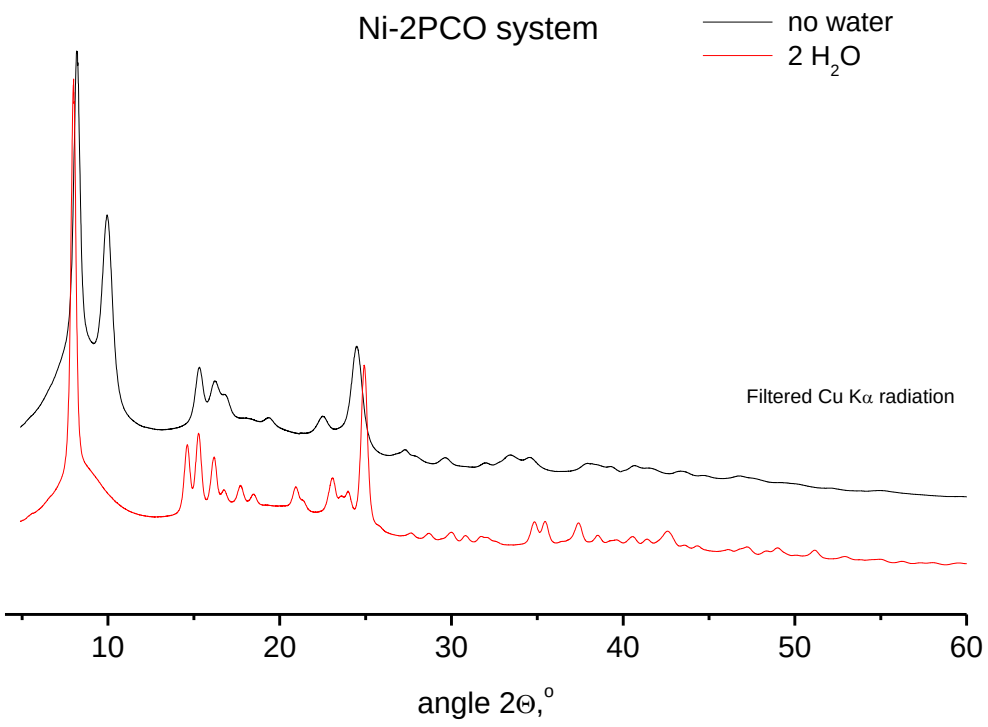

Figure 52. The powder diffraction pattern of [$Ni(2PCO)_2 \cdot 2H_2O$] (red) and [$Ni(2PCO)_2$] (black).

structure (see x-ray structures section, p. 90, 91). To the contrary, the $Ni(ACO)_2 \cdot 2H_2O$ and $Ni(ACO)_2$ diffraction patterns are different (Figure 53). This evidences the formation of a different crystal lattice when water was removed. This result indicates most likely formation of the 'ladder motiff' depicted in Figure 18 II (p.35).

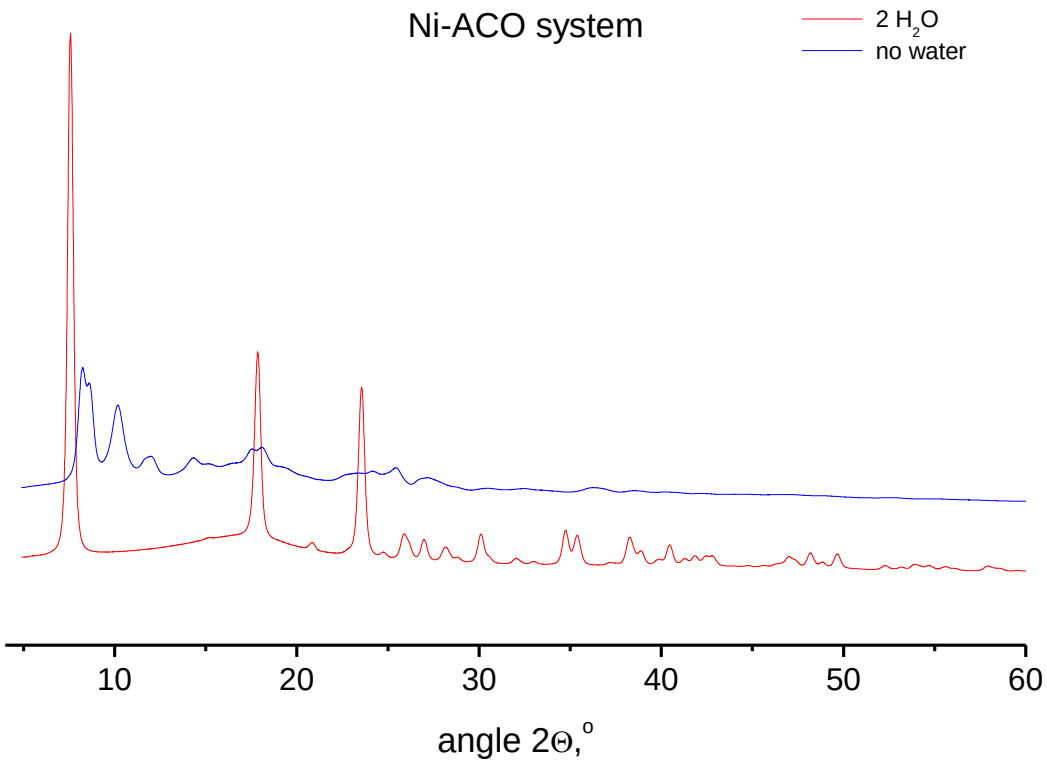

Figure 53. The powder diffraction pattern of $[Ni(ACO)_2 \cdot 2H_2O]$ (red) and $[Ni(ACO)_2]$ (blue)

The diffraction pattern of $Ni(PiPCO)_2 \cdot 2H_2O$ and $Ni(PiPCO)_2$ are almost identical except for few diffraction peaks that were missing (Figure 54). This shows that there are some similar atomic arrangements within the crystal lattice of $Ni(PiPCO)_2 \cdot 2H_2O$ and

$Ni(PiPCO)_2$ with few differences. It should be noted, though, that dehydration of the former complex leads to a substantial amorphization of its anhydrous derivative. Hence, the conclusion is that most likely there is an unchanged structural motif in $Ni(PiPCO)_2$ with the possibility of Ni-cyanoximates into 1D-extended polymeric solid.

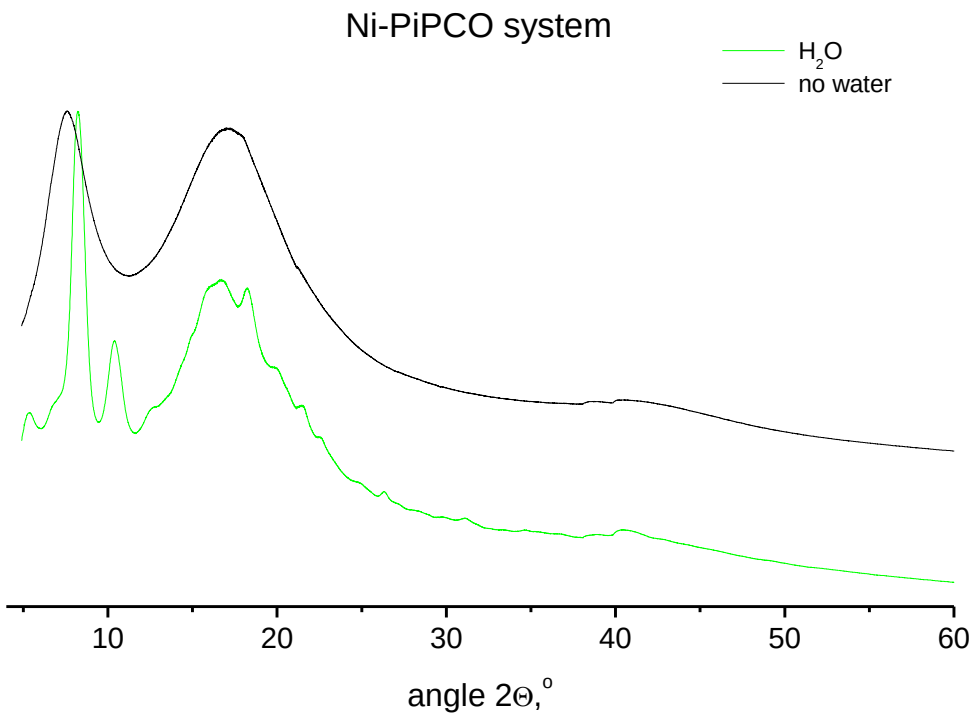

Figure 54. The powder diffraction pattern of $[Ni(PiPCO)_2.2H_2O]$ (green) and $[Ni(PiPCO)_2]$ (black).

V.8. X-ray Single Crystal Analysis

The crystals of some of the complexes were successfully grown in aqueous media and these crystals were analyzed using X-ray crystallographic technique to determine their structures. The Ni(II) complexes of HACO, HECO, HMeCO, and H(2PCO) and Cu(II) complexes of HECO and HMeCO crystals were grown and analyzed. All crystal

structures were determined by Dr. Gerasimchuk. The structures were solved using direct methods embedded into the SHELXS – 2013 and refined using Bruker SHELXTL Software Packages [93]. The drawings of molecular structures were done with ORTEP 3v2 program [94], while packing of the diagrams for structures were carried out using Mercury Program [95].

V.8.1. Crystal Structure of [Ni(ACO)$_2$·2H$_2$O]. The [Ni(ACO)$_2$·2H$_2$O] crystallized out of the aqueous solution as light pink-red plate like crystals (Figure 55) with space group Cmca. It has orthorhombic crystal system with unit cell dimension a = 7.4698(14) Å, b = 6.8635(13) Å, c = 23.379(5) Å, α = 90 °, β = 90 ° and γ = 90 ° (Table 15). The Ni(II) center is in a special position. The Ni(II) center is contained in a glide plane and mirror plane. It also has a two-fold rotational axis passing through it. The hydrogen atoms attached to the water molecules on Ni-atom were restrained using the DFIX command at idealized O-H distance of 0.9584 Å [from the molecular geometry database at U-Wisconsin-Madison]. The numbering scheme of the molecule is shown in Figure 56. The O1 atom had almost 'flat' thermal parameters and an ISOR restrain command was applied to give it a suitable appearance.

The structure of the complex has the deprotonated ligand moieties (ACO^-) coordinating in a bidentate mode in the equatorial plane of a distorted octahedron. The complex adopts *trans* – geometry, and the central Ni atom binds using the nitrogen atom of the oxime and oxygen atom of the carbonyl group. The ACO^- moieties can be described as being in *cis-anti*-configuration. It is important to notice in previous work [96, 97, 87]; HACO and NaH(ACO)$_2$ ligand were found to be in the *trans-anti*-configuration. The coordination to the Ni metal ion leads to a rotation about the C1 – C3 bond of the

Table 15. Crystal data and structure refinement of $[Ni(ACO)_2 \cdot 2H_2O]$

Parameter	$[Ni(ACO)_2 \cdot 2H_2O]$	
Chemical formula	$C_{1.50}H_2N_{1.50}Ni_{0.25}O_{1.50}$	
Formula weight	79.72 g/mol	
Temperature	119(2) K	
Wavelength	0.71073 Å	
Crystal size	0.071 x 0.107 x 0.148 mm	
Crystal habit	Clear light pink-red plate	
Crystal system	Orthorhombic	
Space group	Cmca	
Unit cell dimensions	a = 7.4698(14) Å	α = 90°
	b = 6.8635(13) Å	β = 90°
	c = 23.379(5) Å	γ = 90°
Volume	1198.6(4) $Å^3$	
Z	16	
Density (calculated)	1.767 g/cm^3	
Absorption coefficient	1.654 mm^{-1}	
F(000)	648	
Theta range for data collection	1.74 to 27.16°	
Refinement method	Full-matrix least-squares on F2	
Refinement program	SHELXL-2013 (Sheldrick, 2013)	
Function minimized	$\Sigma w(F_o^2 - F_c^2)^2$	
Goodness-of-fit on F^2	1.043	
Final R indices	570 data; I>2σ(I)	R1 = 0.0417, wR2 = 0.0926
	all data	R1 = 0.0578, wR2 = 0.1013
Weighting scheme	$w=1/[\sigma^2(F_o^2)+(0.0410P)^2+5.3599P]$	
	where $P=(F_o^2+2F_c^2)/3$	
Largest diff. peak and hole	1.129 and -0.977 $eÅ^{-3}$	
R.M.S. deviation from mean	0.112 $eÅ^{-3}$	

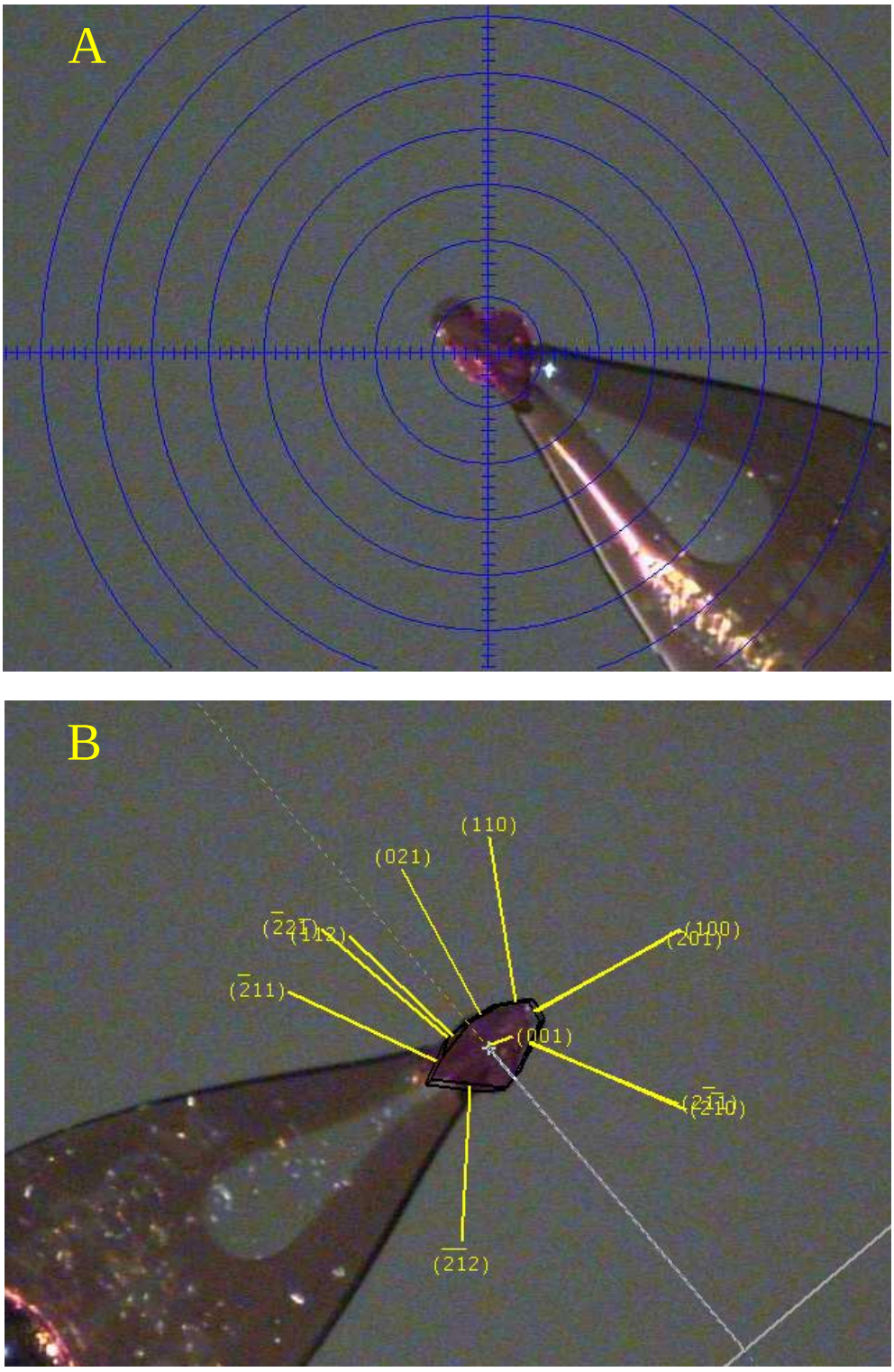

Figure 55. A video-microscope photo of centered [$Ni(ACO)_2 \cdot 2H_2O$] crystal (A) and its indexed faces (B) used for proper absorption correction.

cyanoximate ion moiety to afford coordination using the nitrogen atom of the oxime group and oxygen atom of the carbonyl groups. The ACO^- units are planar with the Ni(II) ion forming the five membered chelate rings. There are some torsions in the structure (Appendix C-5). The two water molecules are occupying the axial positions of the distorted octahedron (Figure 56).

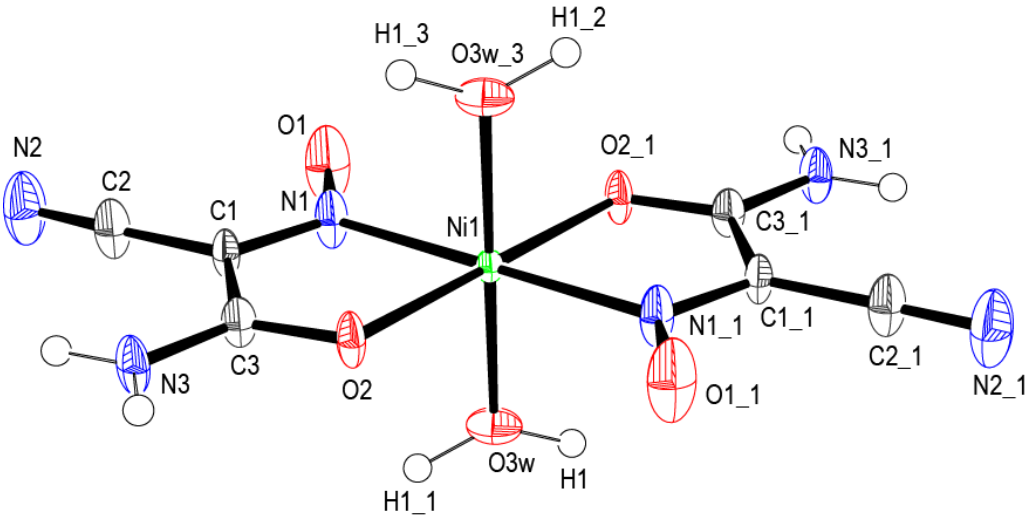

Figure 56. The GROW fragment in the structure of $[Ni(ACO)_2 \cdot 2H_2O]$. Symmetry codes for 1 :x, -y, -z; for 2: -x, y, z; for 3: -x, -y, -z.

The bond length revealed that there is delocalization of electron density in the cyanoximate anion as compared to protonated HACO [98]. The bond length of C3 – O2 is 1.252 Å (Table 16) which is longer than what is expected for a $O=C_{sp}^2$ and longer than 1.225 Å, reported for C3 – O2 in $NaH(ACO)_2$ in previous work [88]. The bond length of N1 – O1 is 1.280 Å which is shorter than the bond length of C1 – N1 of 1.320 Å and shorter than the 1.326 Å value reported for it in $NaH(ACO)_2$. This shows that the anion adopts

the *nitroso*-form upon coordination to the Ni(II). The nitrile group in ACO^- is linear with bond length of 1.141 Å expected for organic cyanides and angle N2 – C2 – C1 is 178.6°.

There are quite a number of hydrogen bonding interactions in the unit cell (Figure 58) (Appendix C-6). The molecules occupying the vertexes of the unit cell are stacked on top of each other in form of columns (Figure 57) thereby creating columnar alignment. CCDC 1473519 contains the supplementary crystallographic data for this complex.

Table 16. Selected bond lengths and angles for $[Ni(ACO)_2 \cdot 2H_2O]$

Bonds	(Å)	Angles	(°)
C1 – N1	1.320(6)	N2 – C2 – C1	178.6(5)
C1 – C3	1.482(6)	N1 – C1 – C2	124.2(4)
C3 – O2	1.252(6)	O1 – N1 – C1	118.9(4)
C1 – C2	1.417(6)	O2 – C3 – C1	118.0(4)
C2 – N2	1.141(6)	O2 – C3 – N3	122.3(4)
C3 – N3	1.310(6)	N3 – C3 – C1	119.8(4)
N1 – O1	1.280(5)	C2 – C1 – C3	124.2(4)
Ni1 – O1	2.048(3)	O2 – Ni1 – N1	101.18(14)
Ni1 – N1	2.066(4)	O2 – Ni1 – O2	180.00(17)
Ni1 – O3w	2.010(4)	N1 – Ni1 – N1	180.00(10)
		O3W – Ni1 – O3W	180.0

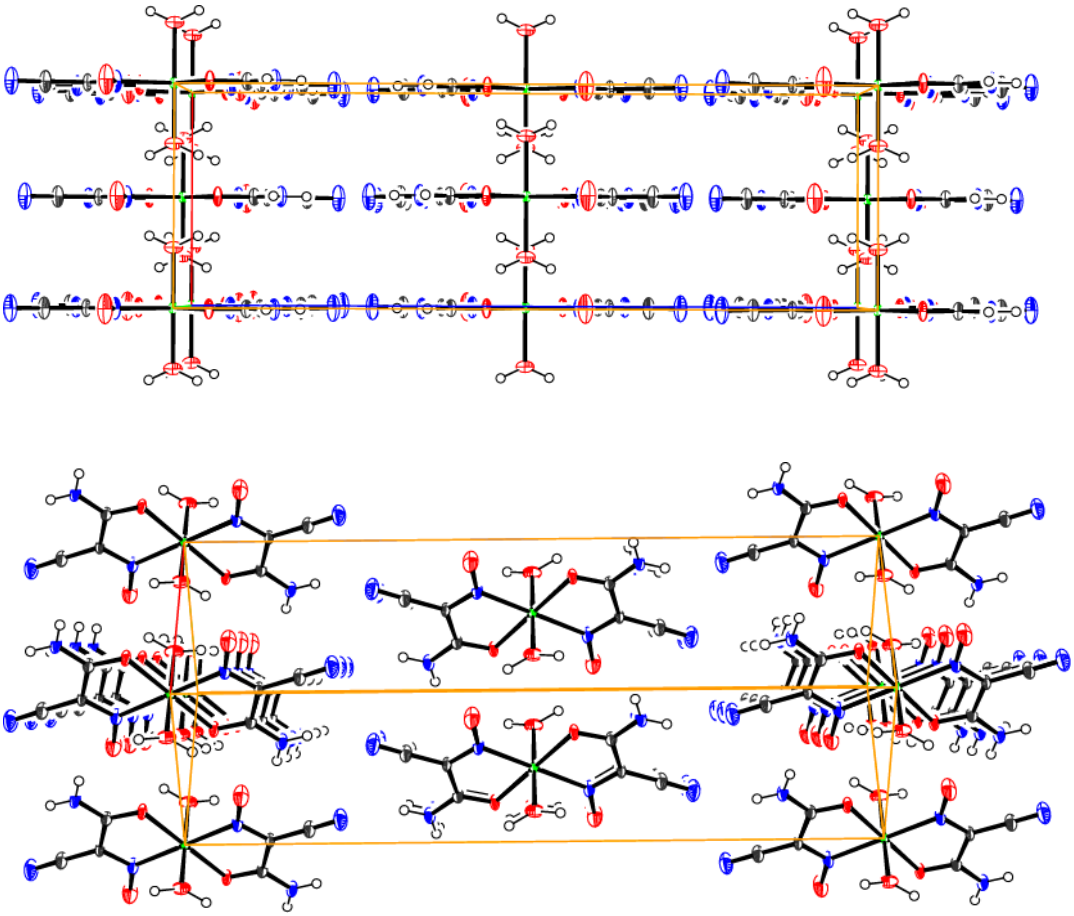

Figure 57. Two views of the unit cell content in the structure of $[Ni(ACO)_2 \cdot 2H_2O]$.

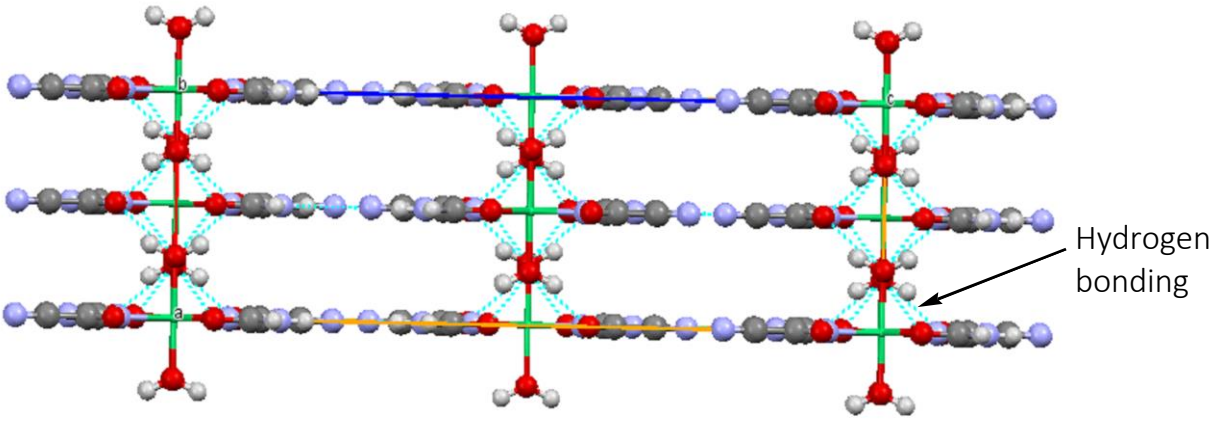

Figure 58. Packing of $[Ni(ACO)_2 \cdot 2H_2O]$ in unit cell showing hydrogen bonding.

V.8.2. Crystal Structure of [Ni(2PCO)$_2$·2H$_2$O]. The [Ni(2PCO)$_2$·2H$_2$O] crystal and refinement data are presented in Table 17. The complex crystallized as clear pink plate-like crystal (Figure 59) in triclinic system and P-1 space group. The selected bonds and angles in the structure are shown in Table 18. The coordination compound contains the deprotonated cyanoximate anions (2PCO$^-$) occupying the equatorial plane of a distorted octahedron of Ni(II) ion (Figure 60). The anion binds to the metal center via N – atom of the nitroso group and N-atom of the heterocycle forming a five membered chelate metallacycle around the Ni(II) ion. The 2PCO $^-$ ion is in *cis*-*anti*-configuration. The two 2PCO$^-$ ion are in the *trans* position to each other. In the complex, two water molecules occupied axial positions (Figure 60). The Ni(II) ion is in a special position – inversion center – in the structure. The ligand moieties in the equatorial positions are not completely coplanar relative to the center Ni(II) ion. There exist some torsions (Appendix C-9) with some atoms slightly above the mean plane. The N3 – C3 bond length is 1.351 Å, which is different and longer than the N3 – C7 bond length whose bond length is 1.337 Å (Table 18). The N3 – C7 bond length is typical of C – N bond length in pyridine [99]. The C1 – C3 bond length is 1.469 Å, which is close to that of ordinary C – C bond length. The C1 – N1 bond length is 1.312 Å, which is less than the bond length expected for C = N bond length in oxime and N1 – O1 is 1.307 Å, which is shorter than typical N – O bond. The N1 – O1 bond being shorter than C1 – N1 suggests the ligand is in the *nitroso*-form. The nitrile group is linear with bond angle of 179.7° for N2 – C2 – C1 and bond length N2 – C2 being 1.148 Å typical of organic nitrile bond length. Crystal packing is shown in Figure 61 and 62. There is extensive hydrogen bonding in the structure (Figure 63) (Appendix C-11). CCDC # for compound is 1473517.

Table 17. Crystal data and structure refinement of $[Ni(2PCO)_2 \cdot 2H_2O]$

Parameter	$[Ni(2PCO)_2 \cdot 2H_2O]$	
Chemical formula	$C_{14}H_{12}N_6NiO_4$	
Formula weight	387.01 g/mol	
Temperature	120(2) K	
Wavelength	0.71073 Å	
Crystal size	0.070 x 0.074 x 0.206 mm	
Crystal habit	Clear light pink plate	
Crystal system	Triclinic	
Space group	P -1	
Unit cell dimensions	a = 5.9748(7) Å	α = 86.128(2)°
	b = 6.2596(8) Å	β = 83.705(2)°
	c = 11.0397(13) Å	γ = 75.332(2)°
Volume	396.68(8) $Å^3$	
Z	1	
Density (calculated)	1.620 g/cm^3	
Absorption coefficient	1.257 mm^{-1}	
F(000)	198	
Theta range for data collection	1.86 to 28.17°	
Refinement method	Full-matrix least-squares on F^2	
Refinement program	SHELXL-2013 (Sheldrick, 2013)	
Function minimized	$\Sigma\, w(F_o^2 - F_c^2)^2$	
Goodness-of-fit on F^2	1.043	
Final R indices	1764 data; $I>2\sigma(I)$	R1 = 0.0324, wR2 = 0.0673
	all data	R1 = 0.0390, wR2 = 0.0703
Weighting scheme	$w=1/[\sigma^2(F_o^2)+(0.0280P)^2+0.2657P]$	
	where $P=(F_o^2+2F_c^2)/3$	
Largest diff. peak and hole	0.500 and -0.375 $eÅ^{-3}$	
R.M.S. deviation from mean	0.079 $eÅ^{-3}$	

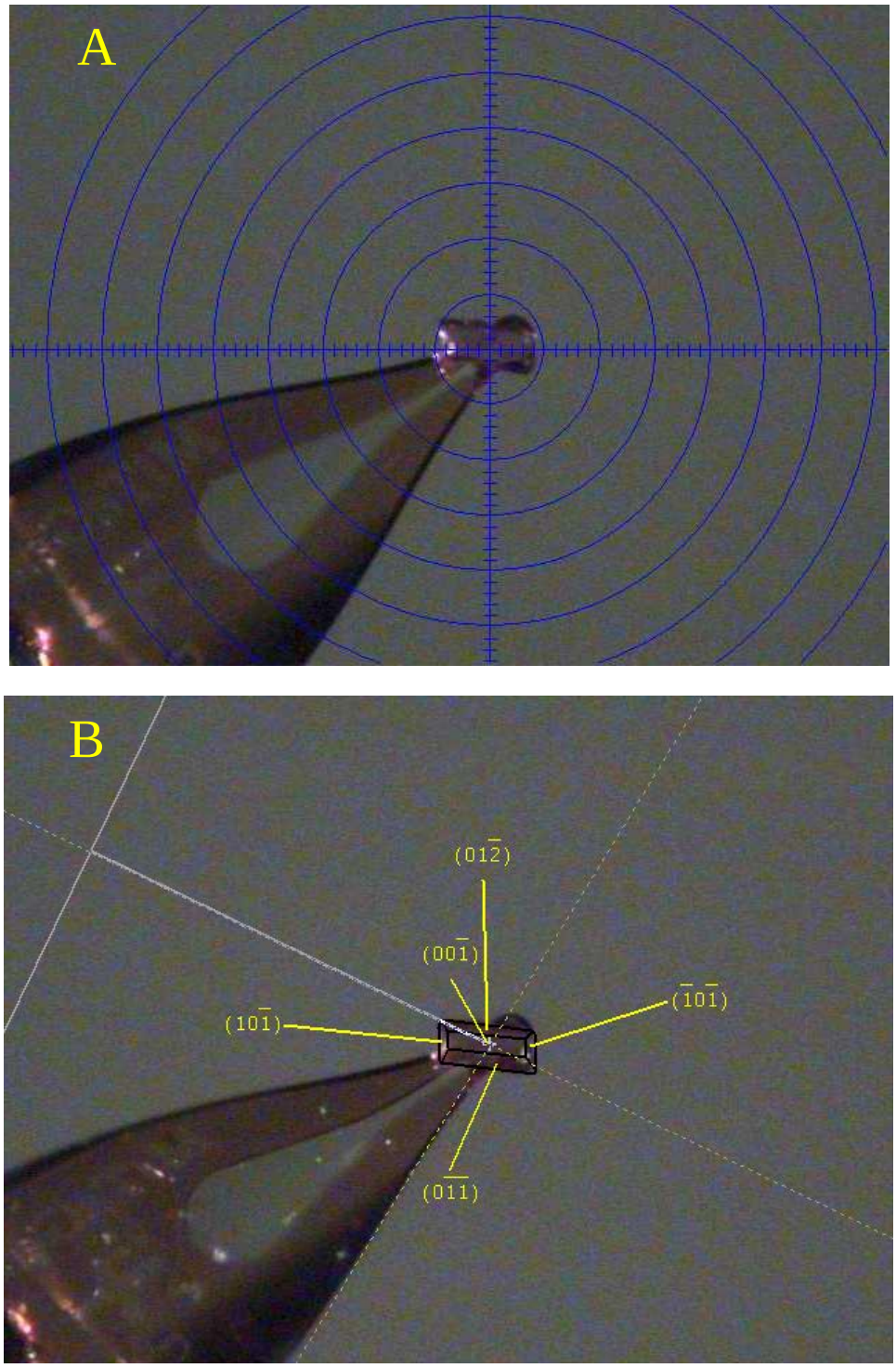

Figure 59. A video-microscope photo of centered [$Ni(2PCO)_2 \cdot 2H_2O$] crystal (A) and its indexed faces (B).

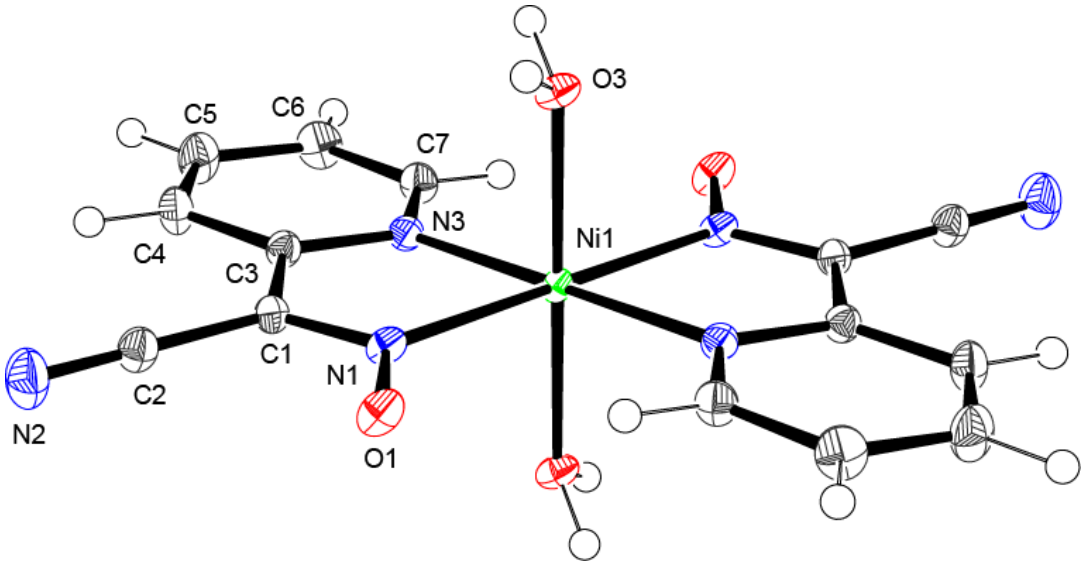

Figure 60. Molecular structure and numbering scheme for $[Ni(2PCO)_2 \cdot 2H_2O]$.

Table 18. Selected bond lengths and bond angles for $[Ni(2PCO)_2 \cdot 2H_2O]$

Bond	(Å)	Angles	(°)
C1 – N1	1.312(2)	N2 – C2 – C1	179.7(2)
C1 – C3	1.469(3)	N1 – C1 – C3	117.78(17)
C3 – N3	1.351(2)	N3 – C3 – C1	115.19(16)
N1 – O1	1.307(2)	O1 – N1 – C1	118.36(16)
C5 – C6	1.387(3)	C2 – C1 – C3	120.79(17)
C6 – C7	1.388(3)	O3 – Ni1 – O3	180.0
C7 – N3	1.336(2)	O3 – Ni1 – N3	89.90(6)
C1 – C2	1.438(3)	O3 – Ni1 – N1	87.48(6)
C2 – N2	1.148(3)	N3 – Ni1 – N1	100.99(6)
C3 – C4	1.395(3)	N3 – Ni1 – N1	79.01(6)
Ni1 – N3	2.0846(16)	N3 – Ni1 – N3	180.0
Ni1 – N1	2.0924(16)	N1 – Ni1 – N1	180.0
Ni1 – O3	2.0593(13)	O3 – Ni1 – O3	180.0

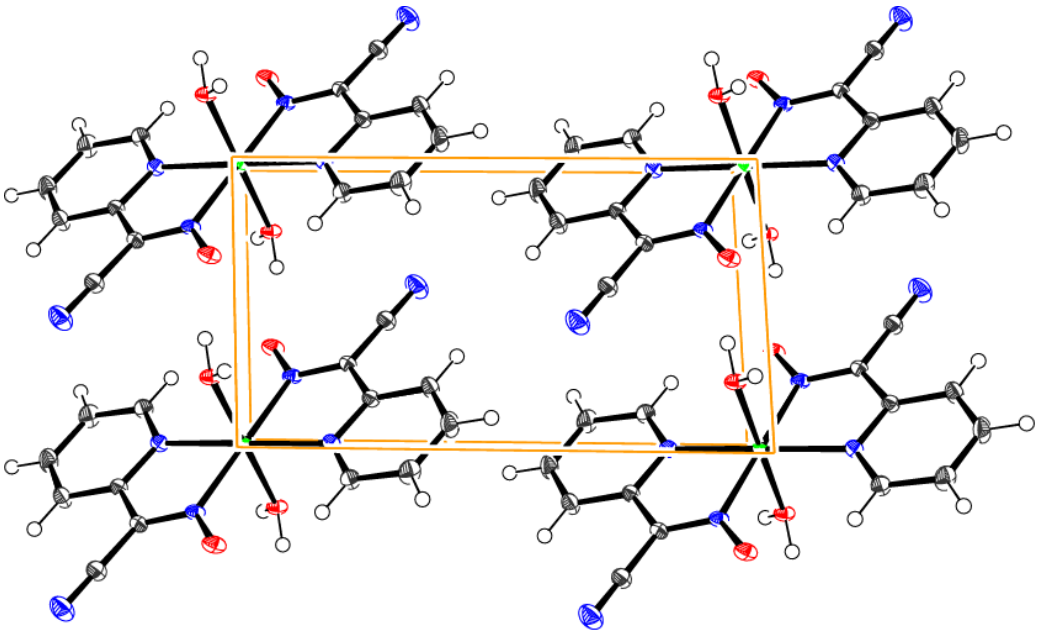

Figure 61. Projections of the unit cell with its content along crystal axes. View along a direction

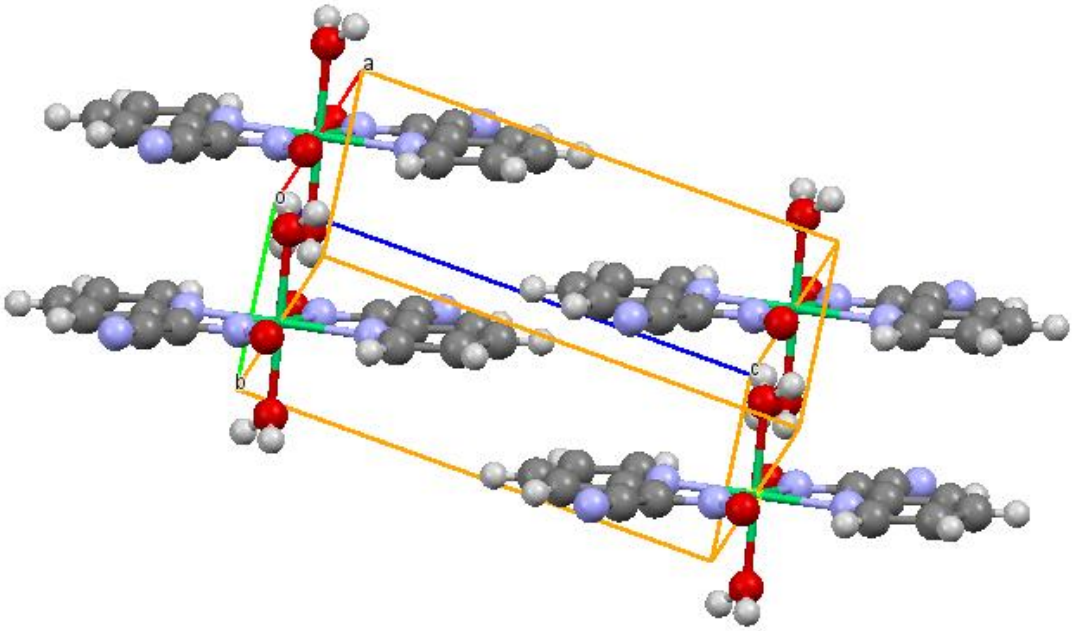

Figure 62. Projection of the unit cell showing planarity of $2PCO^-$ anions. View along b direction.

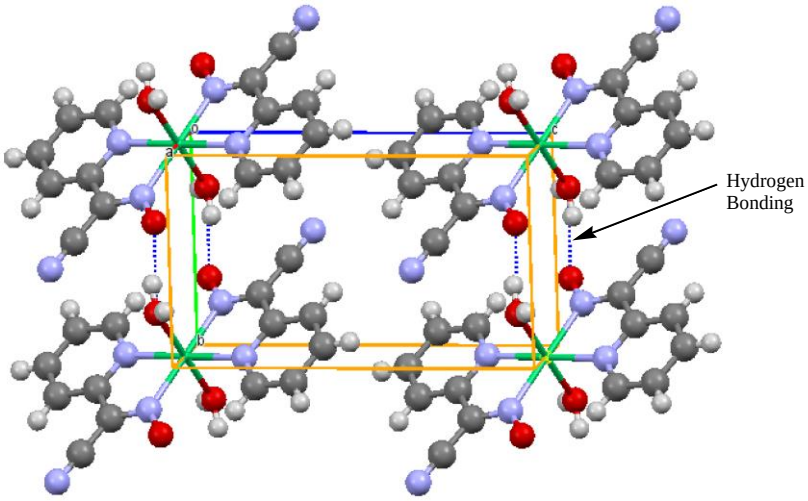

Figure 63. View of $[Ni(2PCO)_2 \cdot 2H_2O]$ unit cell showing H-bonding.

V.8.3. Crystal Structure of $[Ni(AACO) \cdot (H_2O)_3]_2 \cdot H_2O$. All attempts to synthesize Cu(II) and Ni(II) complexes with ester cyanoximes HECO and HMeCO have failed. The X-ray analysis showed that these anions in the presence of metal ions were hydrolyzed with the generation the $AACO^{2-}$. This is a dianion (Figure 64). Similar

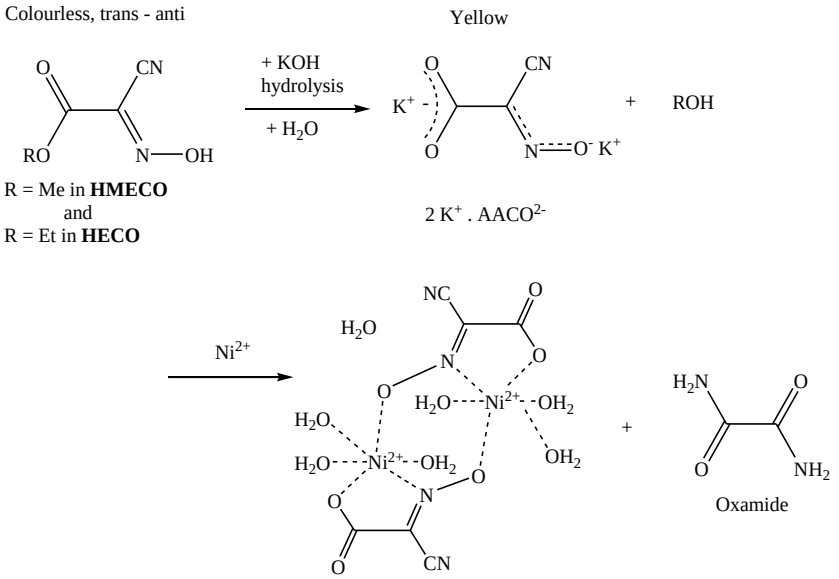

Figure 64. Formation of the $AACO^{2-}$ metal complex via hydrolysis of ester fragment.

situation has occurred in the past [81] during preparation of Pd and Pt complexes. The Ni(II) complexes with $AACO^{2-}$ represent a dimetallic complex with one water molecule outside the coordination sphere. Also, there was a side product recovered from the crystallization solution, identified by X-ray crystallography to be an oxamide ($C_2N_2O_2H_4$). This same product was observed during an attempt of making Zn(II) complex of the HECO ligand. The structure of the oxamide will be presented later in this thesis. The mechanism for the formation of oxamide (Figure 64) is unclear at this point (Appendix-D). A clear green block-type crystal of $[Ni(AACO)\cdot(H_2O)_3]_2\cdot H_2O$ grown out of the aqueous solution was used for the X-ray crystallographic analysis (Figure 65). The crystal and refinement data for this complex is displayed in Table 19, while selected bond lengths and angles are presented in Table 20. All H-atoms during structure solution of $[Ni(AACO)\cdot(H_2O)_3]_2\cdot H_2O$ were found on the electron density map.

The $AACO^{2-}$ coordinates to each nickel center using the nitrogen atom of the oxime and oxygen atom of the carboxylate group in bidentate modes. Also, this dianion acts as a bridging ligand and connects two Ni – centers via NO – group. Thus, two nickel atoms are bridged (μ^2) by the NO group of the $AACO^{2-}$, making a six membered metallacycle system with the nickel centers opposite each other. The $AACO^{2-}$ moieties occupy the equatorial position, coordinating in a *trans-anti*-configuration (oxime group *trans* to carbonyl group). This structure represents a dimetallic tricyclic system. The axial positions around the Ni(II) ions are each occupied by two water molecules *trans* to each other and an equatorial position occupied by another molecule of water, creating a distorted octahedral environment around Ni(II) ion (Figure 66). The remaining place in

Table 19. Crystal data and structure refinement of $[Ni(AACO)\cdot(H_2O)_3]_2\cdot H_2O$

Parameter	$[Ni(AACO)\cdot(H_2O)_3]_2\cdot H_2O$	
Chemical formula	$C_3H_8N_2NiO_7$	
Formula weight	242.82 g/mol	
Temperature	120(2) K	
Wavelength	0.71073 Å	
Crystal habit	Clear light green block	
Crystal system	Monoclinic	
Space group	C2/c	
Unit cell dimensions	a = 16.0508(10) Å	α = 90°
	b = 6.4725(5) Å	β = 114.2450(10)°
	c = 16.5248(13) Å	γ = 90°
Volume	1565.3(2) $Å^3$	
Z	8	
Density (calculated)	2.061 g/cm^3	
Absorption coefficient	2.492 mm^{-1}	
F(000)	992	
Theta range for data collection	2.70 to 33.02°	
Refinement method	Full-matrix least-squares on F^2	
Refinement program	SHELXL-2014 (Sheldrick, 2014)	
Function minimized	$\Sigma\, w(F_o^2 - F_c^2)^2$	
Goodness-of-fit on F^2	1.147	
Δ/σmax	0.001	
Final R indices	2446 data; I>2σ(I)	R1 = 0.0269, wR2 = 0.0570
	all data	R1 = 0.0342, wR2 = 0.0630
Weighting scheme	$w=1/[\sigma^2(F_o^2)+(0.0174P)^2+4.2033P]$	
	where $P=(F_o^2+2F_c^2)/3$	
Largest diff. peak and hole	0.520 and -0.532 $eÅ^{-3}$	
R.M.S. deviation from mean	0.105 $eÅ^{-3}$	

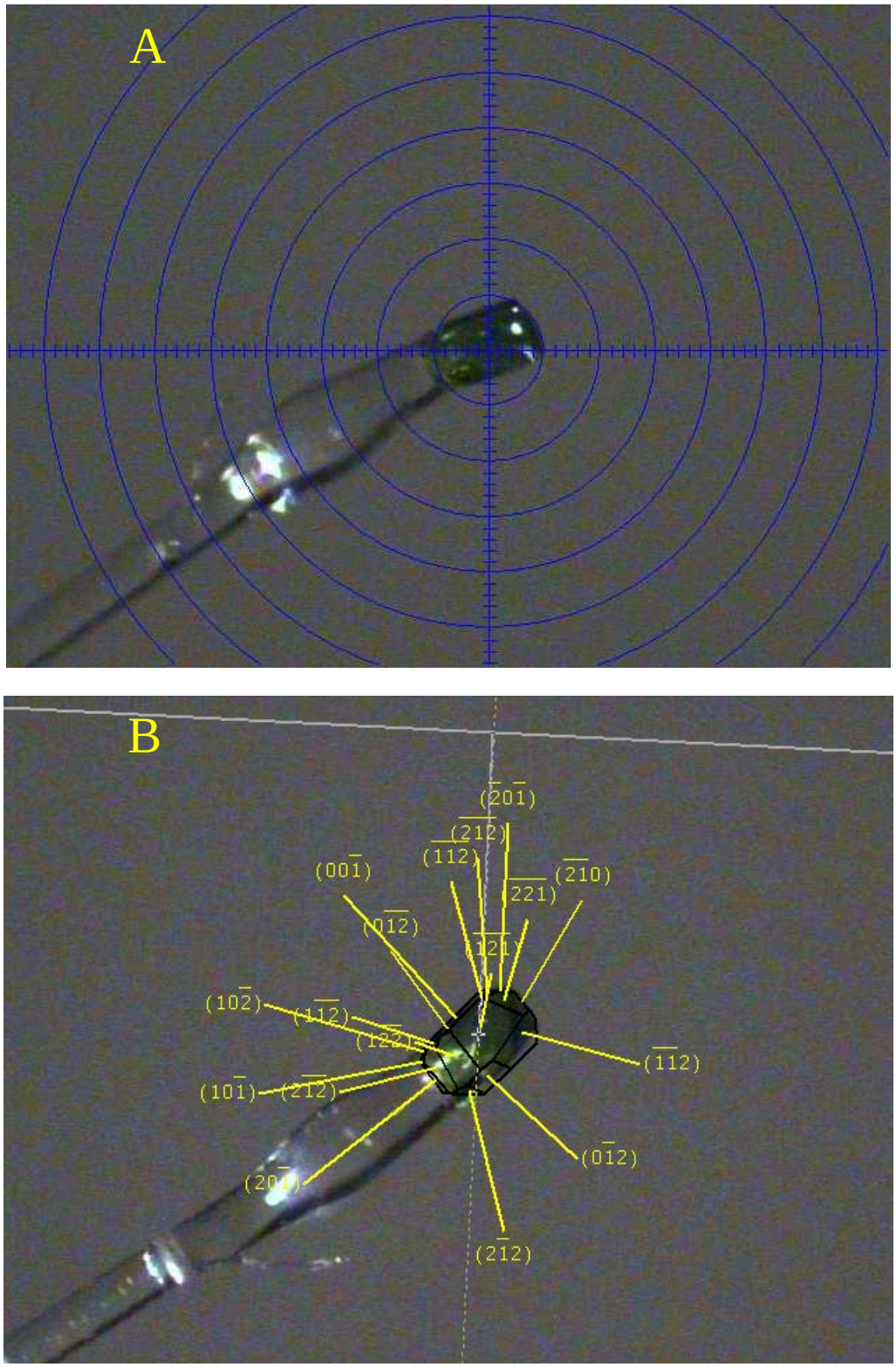

Figure 65. Actual videomicroscope image of the crystal of $[Ni(AACO)\cdot(H_2O)_3]_2\cdot H_2O$ crystal (A), and indexed faces of the crystal (B).

the equatorial plane is taken by bridging O-atoms (Figure 66). There is also a molecule of water outer outside the coordination sphere. In the unit cell, the molecule of water from

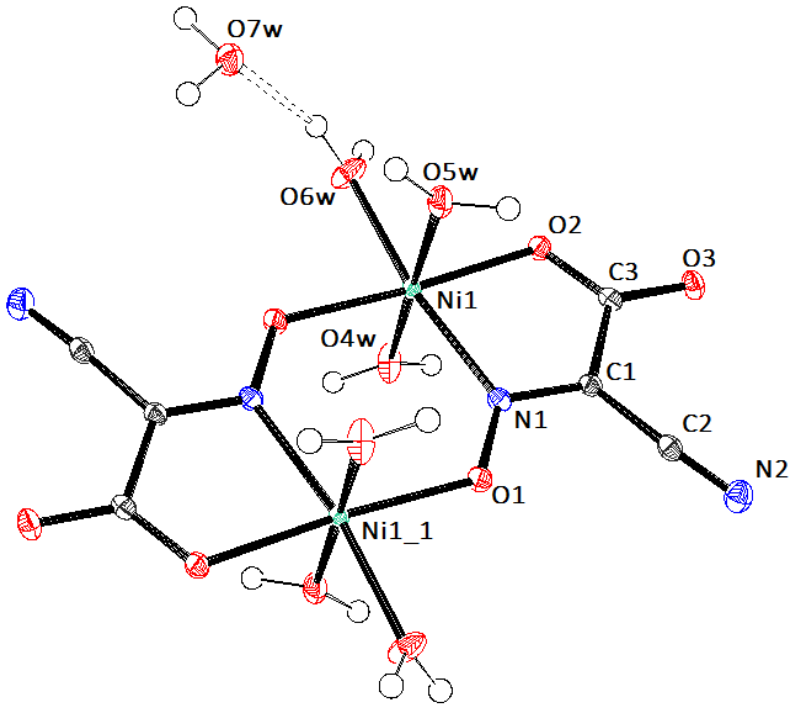

Figure 66. The GROW fragment in the dimetallic structure of $[Ni(AACO)\cdot(H_2O)_3]_2\cdot H_2O$. The inversion center is located half-way between two Ni atoms. The symmetry operation for the _1 code is –x, y, -z+1/2.

each $[Ni(AACO)(H_2O)_3]_2\cdot H_2O$ occupy channels extending along b - direction (Figure 67). The inversion center is in the middle of that Ni – N – O – Ni ring (Figure 66). This structure is a dimetallic tricyclic system.

The bond lengths of the dianion in the complex suggest delocalization of electron density. Thus, C3 – O2 bond length is 1.271 Å, which is slightly shorter when compared to typical C – O bond in an ester and C3 – O3 bond length is 1.249 Å which is slightly longer when compared to typical C=O bond of ester in oximes. The C2 – N2 bond length is 1.151 Å, which is typical of nitrile bond. The nitrile group is close to being linear with

bond angle N2 – C2 – C1 being 176.92°. The C1 – N1 bond length is 1.3101 Å and the N1 – O1 bond length is 1.308 Å (Table 20) which is shorter than the C1 – N1 bond length. The N1 – O1 bond is most likely a double bond and the $AACO^{2-}$ is in *nitroso*-form.

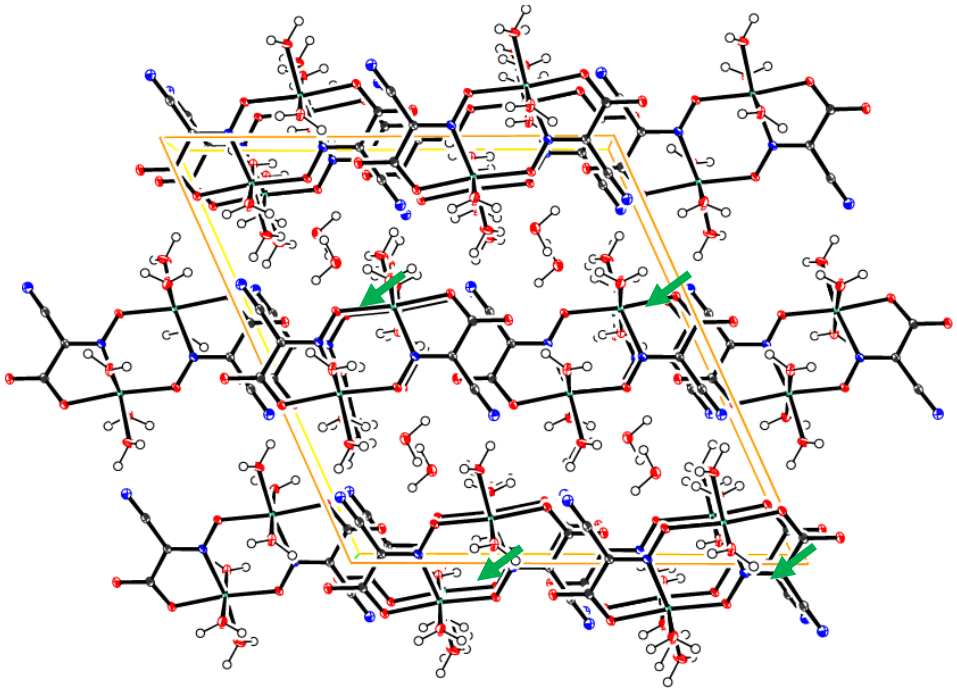

Figure 67. The unit cell content in the structure: view normal to [010] plane. Green arrows indicate water molecules occupying channels running along *b*-direction.

The bond length of Ni1 – O1 is 2.013 Å and the angle Ni1 – O1 – Ni1_1 is 123.15° while the angle between N1 – Ni1 – O1_1 is 105.74°. The axially attached water molecules are not perpendicularly attached to the nickel center. This is evident from the bond angle of 88.73° for O4w – Ni1 – O6w, 88.47° for O5w – Ni1 – O6w and 177.99° for O4w – Ni1 – O5w. There is a distorted octahedral environment around each Ni(II) ion center. The Ni1 – Ni1_1 bond length is 3.776 Å. The $AACO^{2-}$ ligand moieties are not

Table 20. Selected bond length (Å) and bond angles (°) for $[Ni(AACO)\cdot(H_2O)_3]_2\cdot H_2O$

Bonds	(Å)	Angles	(°)
C1 – N1	1.3101(19)	N2 – C2 – C1	176.92(17)
C1 – C3	1.495(2)	O3 – C3 – C1	118.74(14)
C3 – O3	1.2486(19)	O1 – N1 – C1	117.39(13)
N1 – O1	1.3084(17)	N1 – C1 – C2	122.57(14)
C1 – C2	1.433(2)	N1 – C1 – C3	117.55(14)
C2 – N2	1.151(2)	O4W – Ni1 – N1	90.86(5)
C3 – O2	1.2705(19)	O6W – Ni1 – N1	171.10(5)
Ni1 – O1	2.0127(12)	O6W – Ni1 – O4W	91.23 (6)
Ni1 – O2	2.0441(11)	O4W – Ni1 – O5W	177.99(5)
Ni1 – O4W	2.0754(14)	O2 – Ni1 – O2	173.74(5)
Ni1 – O5W	2.1135(13)	O2 –Ni1 –O4W	88.73(5)
Ni1 – O6W	2.0286(13)	O1 – Ni1 – O5W	92.93(5)
		O2 – Ni1 – O5W	89.47(5)

completely coplanar with some torsion angles (Figure 68) (Table A16). Hydrogen bonding is essential in packing of this complex into a crystal and is shown in Figure 69 (Appendix C-15). CCDC # for this complex is 1473520.

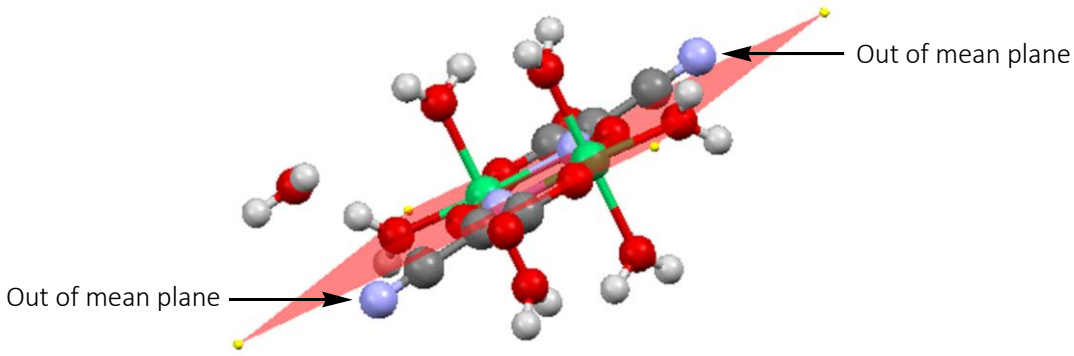

Figure 68. $[Ni(AACO)\cdot(H_2O)_3]_2\cdot H_2O$ with some $AACO^{2-}$ atoms out of mean plane.

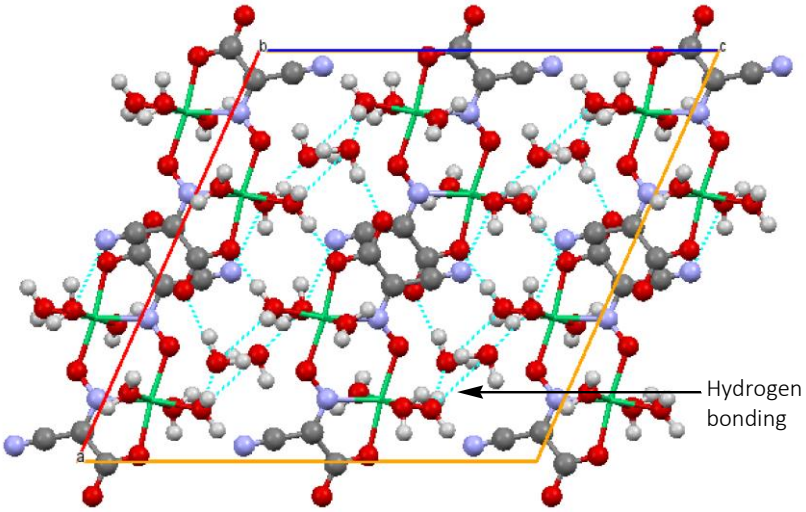

Figure 69. Hydrogen bonding in $[Ni(AACO)\cdot(H_2O)_3]_2\cdot H_2O$ unit cell view along b axes.

V.8.4. Crystal Structure of $K_2[Ni_3(AACO)_4\cdot(H_2O)_4]\cdot 4H_2O$. The reaction of HMeCO ligand in the presence of deprotonating agent K_2CO_3 or KOH and Ni(II) salt lead to hydrolysis of HMeCO ligand yielding the $AACO^{2-}$ dianion. The formed $AACO^{2-}$ coordinated to two Ni(II) ions and with several water molecules and K^+ center cations. Compound crystallized as a yellow plate of $K_2[Ni_3(AACO)_4\cdot(H_2O)_4]\cdot 4H_2O$ composition. The crystal and refinement data for the complex are shown in Table 21.

The coordination compound represents a trimetallic complex with bridging cyanoxime dianions. There are two types of Ni(II) centers in this complex with Ni2 atom being in a special position (Figure 70). Thus in the trimetallic complex, there are two centers with coordination number of five at (Ni1) and a center with coordination number of six at (Ni2). The metal ions with coordination number five have the $AACO^{2-}$ coordinated using the nitrogen atom of the oxime and oxygen atom of the carboxylate group to form a five membered metallacyle. These nickel centers have a molecule of water attached apically thereby creating a square-based pyramidal structure. The nickel

Table 21. Crystal data and structure refinement of $K_2[Ni_3(AACO)_4(H_2O)_4]\cdot 4H_2O$

Parameter	$K_2[Ni_3(AACO)_4(H_2O)_4]\cdot 4H_2O$	
Chemical formula	$C_6H_8Cu_0KN_4Ni_{1.50}O_{10}$	
Formula weight	423.33 g/mol	
Temperature	273(2) K	
Wavelength	0.71073 Å	
Crystal size	0.061 x 0.064 x 0.128 mm	
Crystal system	Monoclinic	
Space group	P21/n	
Unit cell dimensions	a = 9.750(2) Å	α = 90°
	b = 6.7291(15) Å	β = 90.508(4)°
	c = 20.616(5) Å	γ = 90°
Volume	1352.5(5) $Å^3$	
Z	4	
Density (calculated)	2.079 g/cm^3	
Absorption coefficient	2.479 mm^{-1}	
F(000)	852	
Theta range for data collection	1.98 to 25.00°	
Absorption correction	multi-scan	
Refinement method	Full-matrix least-squares on F^2	
Refinement program	SHELXL-2014/7 (Sheldrick, 2014)	
Function minimized	$\Sigma\, w(F_o^2 - F_c^2)^1$	
Goodness-of-fit on F^2	1.045	
Final R indices	1698 data; I>2σ(I)	R1 = 0.0480, wR2 = 0.1024
	all data	R1 = 0.0779, wR2 = 0.1169
Weighting scheme	$w=1/[\sigma^2(F_o^2)+(0.0275P)^2+1.3194P]$	
	where $P=(F_o^2+2F_c^2)/3$	
Largest diff. peak and hole	0.777 and -0.564 $eÅ^{-3}$	
R.M.S. deviation from mean	0.144 $eÅ^{-3}$	

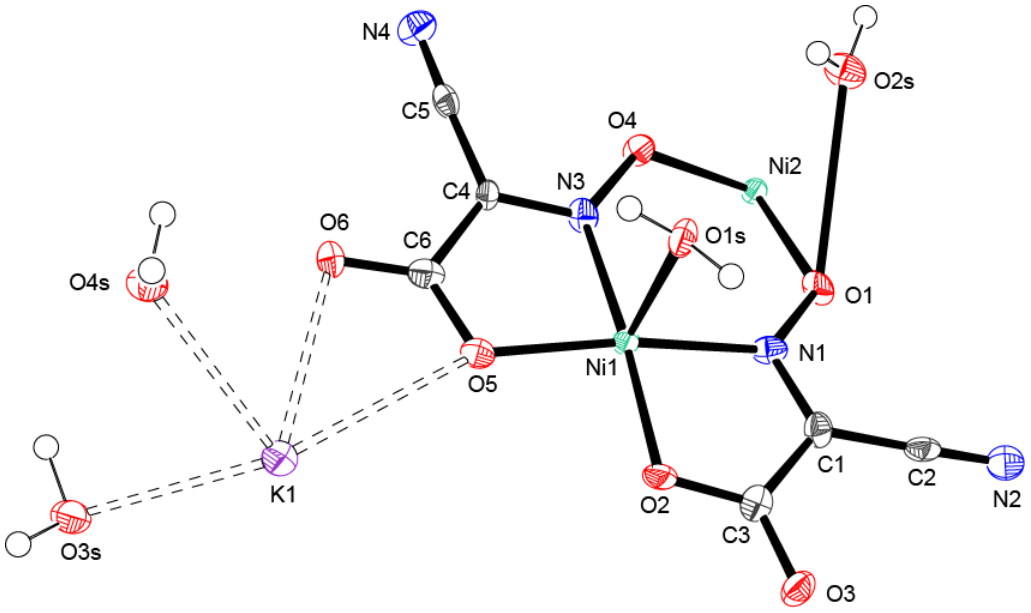

Figure 70. The ASU in the structure of $K_2[Ni_3(AACO)_4 \cdot (H_2O)_4] \cdot 4H_2O$ showing the numbering scheme. Drawing of thermal ellipsoids was done at 50% probability level. The Ni2 atom is in a special position.

center with coordination number of six (Ni2) has four oxygen atoms from the N – O group of the oxime in the basal position, bridging it with the Ni1 centers. This center has two molecules of water attached apically trans to each other, creating an octahedral configuration around the Ni(II) center (Figure 70). The coordination mode of the $AACO^{2-}$ ion to the Ni1 centers are in *trans-anti*-configurations and the ligand moieties coordinating oppositely to the nickel centers are cis to each other. The ligand displayed two coordinating properties: chelating (κ^2) and bridging (μ^2). The overall structure of the complex at Ni1 center is cis (Figure 70).

The bond lengths and angles are in Table 22 and 23. The Ni1 – N1, Ni1 – N3, Ni1 – O1s bond lengths are 1.980 Å, 1.980 Å, and 1.947 Å respectively. These show that the environment around Ni1 is a distorted square-base pyramid. The bond lengths Ni2 – O4, Ni2 – O1, Ni2 – O2S are 1.960 Å, 1.977 Å and 2.254 Å respectively. These show that the

environment around Ni2 center is a distorted octahedron. The two nickel centers (Ni1 and Ni2) are not on the same plane (Figure 71). There is a distortion creating a dihedral angle of 26.11° between the two different planes.

There are two different C – N bond lengths: C5 – N4 bond length is 1.141 Å and C2 – N2 bond length is 1.154 Å (Table 22). There exist two potassium ions outside the coordination sphere with four molecules of water. The potassium ions have electrostatic interaction with the carboxylate oxygen, carbonyl oxygen, oxygen atoms of water molecules, as well as nitrile groups. The nitrile groups are almost linear; the bond angle of N4 – C5 – C4 is 177.3° and N2 – C2 – C1 is 178.1°. The C4 –N3 bond length is 1.303 Å, which is slightly longer than the N3 – O4 bond length of 1.315 Å. This indicates that the N3 – O4 is in the oxime form. The bond length of C1 – N1 is 1.304 Å, which is

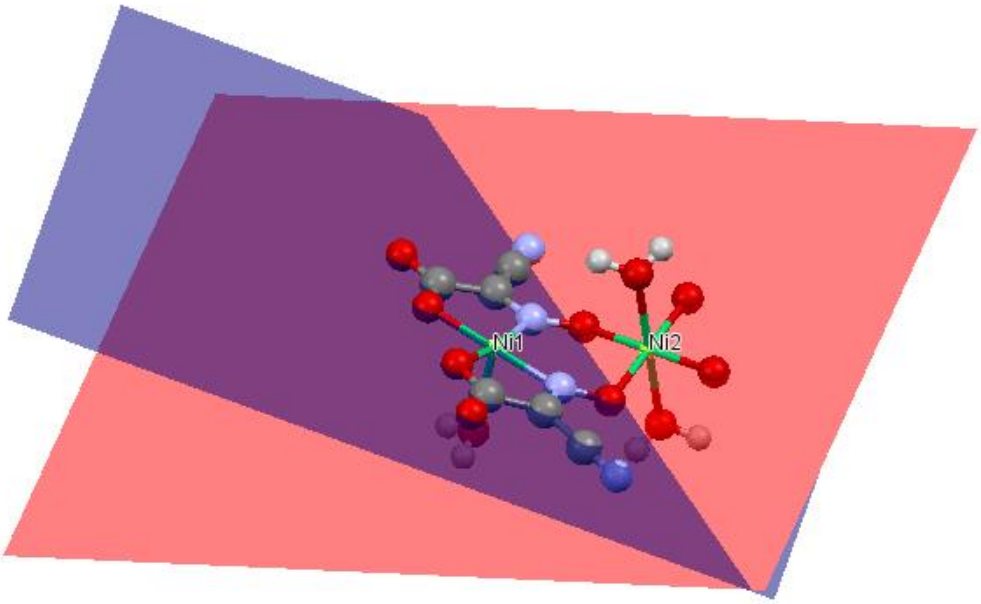

Figure 71. A fragment of the structure at adjacent Ni1 – Ni2 centers showing the dihedral angle (26.11°) between two equatorial planes at the metal centers.

Table 22. Selected bond lengths and bond angles around $AACO^{2-}$ in $K_2[Ni_3(AACO)_4 \cdot (H_2O)_4] \cdot 4H_2O$

Bonds	(Å)	Angles	(°)
C1 – N1	1.304(7)	N4 – C5 – C4	176.9
C1 – C3	1.471(9)	N2 – C2 – C1	177.2
C3 – O3	1.254(7)	C2 – C1 – C3	122.7(5)
C4 – N3	1.303(7)	C5 – C4 –C6	123.7(5)
C4 – C6	1.492(8)	O3 – C3 – O2	124.2(6)
C6 – O6	1.244(7)	O6 – C6 – O5	126.0(6)
C1 – C2	1.425(8)	N1 – C1 – C2	121.3(6)
C2 – N2	1.154(7)	N1 – C1 – C3	115.8(5)
C3 – O2	1.287(7)	N3 – C4 – C6	116.5(5)
C4 – C5	1.446(8)	N3 – C4 – C5	119.8(5)
C5 – N4	1.141(7)	C5 – C4 – C6	123.7(5)
C6 – O5	1.278(7)		

Table 23. Selected bond lengths and bond angles around Ni(II) centers in $K_2[Ni_3(AACO)_4 \cdot (H_2O)_4] \cdot 4H_2O$

Bonds	(Å)	Angles	(°)	Angles	(°)
Ni – O1	1.306(6)	N3 – Ni1 – N1	99.8(2)	O1 – Ni2 – O2S	87.00(17)
Ni1 – O1S	2.290(5)	O5 – Ni1 – O2	93.15(17)	O4 – Ni2 – O2S	91.65(17)
Ni1 – O5	1.947(4)	O5 – Ni1 – N3	83.47(18)	O1 – Ni2 – O2S	93.00(18)
N1 – Ni1	1.980(5)	O2 – Ni1 – N1	83.11(18)		
Ni1 – O2	1.959(4)	O5 – Ni1 – O1S	100.40(16)		
N3 – Ni1	1.980(5)	N3 – Ni1 – O1S	88.31(19)		
Ni2 – O2S	2.254(5)	O2 – Ni1 – O1S	95.07(18)		
Ni2 – O1	1.977(4)	N1 – Ni1 – O1S	89.00(18)		
Ni2 – O4	1.960(4)	O4 – Ni2 – O2S	88.35(17)		

slightly shorter than N1 – O1 of 1.306 Å. This also indicates the N1 – O1 is in the oxime

form. The $AACO^{2-}$ are coordinated to the Ni(II) centers in the oxime form. CCDC 1473524 contains the supplementary crystallographic data about this complex.

V.8.5. Crystal Structure of $K_2[Cu_3(AACO)_4\cdot(H_2O)_4]\cdot 4H_2O$. This compound is a product of hydrolysis of the ester (OEt) group in HECO cyanoxime in the presence of deprotonating amount of KOH and Cu^{2+} ion. The formation of the cyanoxime $AACO^{2-}$, we had observed in this work and in the past [81].

The coordination compound crystallized out as a clear light bronze-brown needle-like specimen (Appendix C-28). The crystal and refinement data for this complex are presented in Table 24. This crystal specimen was 4-component rotational twin. Only the first, main domain was used for structure solution/refinement.

The structure of this coordination compound also represents a trimetallic complex with three metal centers (Figure 72, 73). The structure of this complex is very similar to previously described analogous $K_2[Ni_3(AACO)_4\cdot(H_2O)_4]\cdot 4H_2O$. It is a complex three-dimensional framework. There are two types of environments around the different Cu(II) ion centers in terms of coordination number. Two copper (II) ion centers have coordination number of five and a copper (II) center has coordination number of six. Two molecules of the $AACO^{2-}$ ligand is coordinated to the copper centers with coordination number of five equatorially using two nitrogen atoms of the oxime groups and the oxygen atoms of the carboxylate groups to form a five membered metallacyles around those copper(II) ion centers and a molecule of water attached apically (Figure 73). The two $AACO^{2-}$ ions are coordinated to the copper (II) ion centers *cis* to each other in a *trans*-

Table 24. Crystal data and structure refinement of $K_2[Cu_3(AACO)_4 \cdot (H_2O)_4] \cdot 4H_2O$

Parameter	$K_2[Cu_3(AACO)_4 \cdot (H_2O)_4] \cdot 4H_2O$	
Chemical formula	$C_6H_8Cu_{1.50}KN_4O_{10}$	
Formula weight	430.57 g/mol	
Temperature	120(2) K	
Wavelength	0.71073 Å	
Crystal size	0.072 x 0.076 x 0.156 mm	
Crystal habit	Clear light bronze-brown needle	
Crystal system	Monoclinic	
Space group	P21/n	
Unit cell dimensions	a = 9.7412(11) Å	α = 90°
	b = 6.7282(8) Å	β = 90.543(2)°
	c = 20.585(2) Å	γ = 90°
Volume	1349.1(3) $Å^3$	
Z	4	
Density (calculated)	2.120 g/cm^3	
Absorption coefficient	2.757 mm^{-1}	
F(000)	858	
Theta range for data collection	1.98 to 28.35°	
Refinement method	Full-matrix least-squares on F^2	
Refinement program	SHELXL-2013 (Sheldrick, 2013)	
Function minimized	$\Sigma\, w(F_o^2 - F_c^2)^2$	
Goodness-of-fit on F^2	1.025	
Δ/σ_{max}	0.001	
Final R indices	2415 data; I>2σ(I)	R1 = 0.0426, wR2 = 0.0811
	all data	R1 = 0.0744, wR2 = 0.0948
Weighting scheme	$w=1/[\sigma^2(F_o^2)+(0.0279P)^2+3.1453P]$, $P=(F_o^2+2F_c^2)/3$	
Largest diff. peak and hole	0.782 and -0.901 $eÅ^{-3}$	
R.M.S. deviation from mean	0.157 $eÅ^{-3}$	

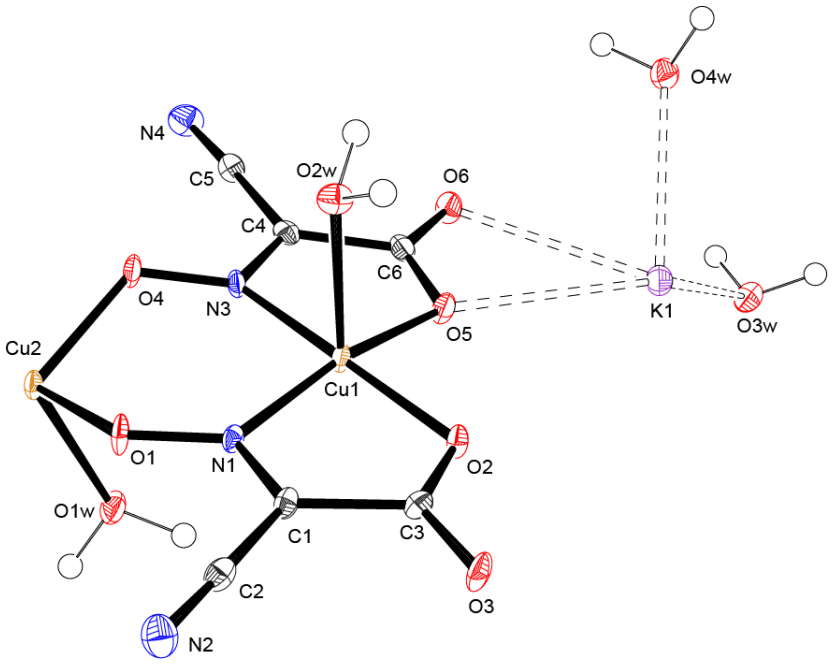

Figure 72. The ASU in the structure of $K_2[Cu_3(AACO)_4 \cdot (H_2O)_4] \cdot 4H_2O$ showing the numbering scheme. Drawing of thermal ellipsoids was done at 50% their thermal probability level. The Cu2 atoms are in the special position (inversion center) with the site occupancy 0.5.

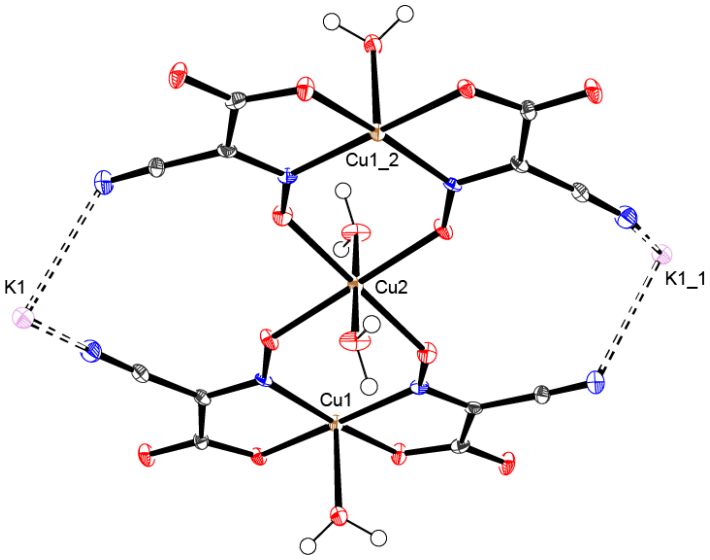

Figure 73. 6.5 Å sphere of enclosure around Cu2 atom in the structure to show connectivity of potassium ions to the $[Cu_3(AACO)_4 \cdot (H_2O)_4]^{2-}$ anion.

anti-configuration. The ligand displayed two properties upon coordination: chelation (k^2) and bridging (μ^2). The Cu(II) ion with coordination number (CN) of 6 is coordinated by using four oxygen atoms from each of the N – O groups of the four $AACO^{2-}$ ions (two $AACO^{2-}$ coordinated to each Cu(II) centers with CN = 5). The coordination to this Cu(II) ion center with C.N = 6 is in a bridging manner which afford it a CuO_4 configuration in the equatorial plane. This copper center has two molecules of water attached axially, *trans* to each other. This complex of copper (II) ion is anionic ($[Cu_3(AACO^{2-})_4{\cdot}(H_2O)_4]^{2-}$) with two cationic potassium ions outside the coordination sphere to make it neutral (Figure 73, 74). There are also four molecules of water outside the coordination sphere. As said, both Cu and Ni complexes $AACO^{2-}$ ligand are of the same composition and are isostructural.

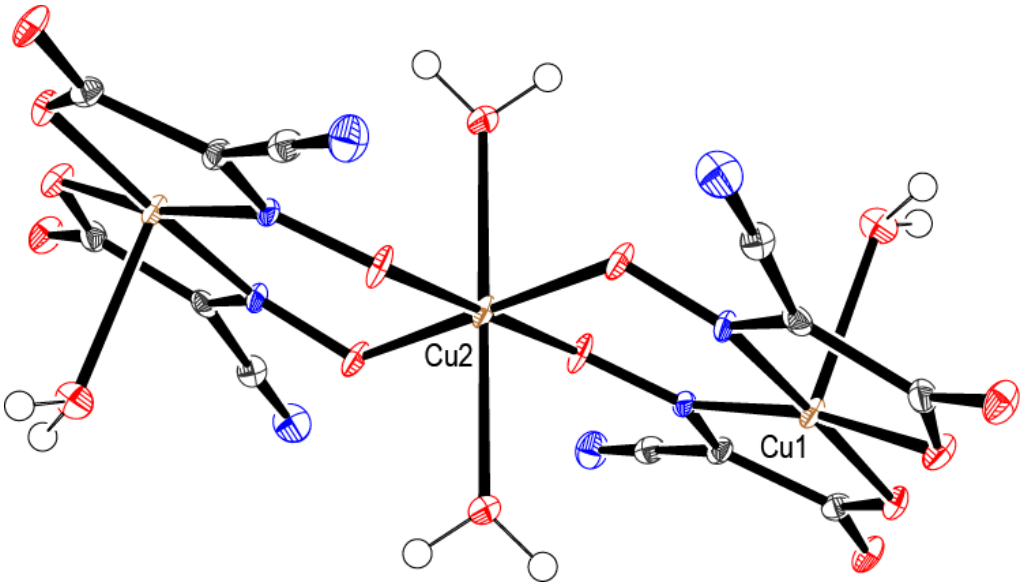

Figure 74. Side view of the anionic part of the molecule – $[Cu_3(AACO)_4{\cdot}(H_2O)_4]^{2-}$. The Cu2 atom is in a special position.

The Cu1 – N3, Cu1 – N1, Cu1 – O5 and Cu1 – O2 bond lengths are 1.977 Å,

1.977 Å, 1.942 Å and 1.960 Å respectively (Table 25) with the Cu(II) ion sitting in the same plane between the N and O atoms creating a CuN_2O_2 environment at the base and a molecule of water attached apically making a distorted square-pyramidal coordination around the Cu(II) center with C.N = 5. The Cu2 – O4, Cu2- O1, and Cu2 – O1W bond lengths are 1.962 Å, 1.978 Å and 2.250 Å respectively. This creates a distorted octahedral

Table 25. Selected bond lengths (Å) and bong angles (°) around $AACO^{2-}$ in $K_2[Cu_3(AACO)_4 \cdot (H_2O)_4] \cdot 4H_2O$

Bond	(Å)	Angle	(°)
C4 – C5	1.443(5)	N4 – C5 – C4	176.9(4)
C4 – N3	1.300(5)	C5 – C4 – N3	120.7(4)
N3 – O4	1.305(4)	C4 – N3 – O4	119.0(3)
C3 – O2	1.278(5)	O6 – C6 – C4	119.6(4)
C3 – O3	1.230(5)	O6 – C6 – C5	125.6(4)
C6 – O5	1.275(5)	N2 – C2 – C1	177.2(4)
C6 – C4	1.495(5)	C2 – C1 – C3	122.6(3)
C6 – O6	1.235(5)	O3 – C3 – C1	118.4(3)
C1 – C2	1.423(5)	O3 – C3 – O2	126.1(4)
C2 – N2	1.142(5)	N1 – C1 – C2	121.7(3)
C1 – C3	1.491(5)	C5 – C4 – C6	123.3(3)
N1 – O1	1.302(4)	O6 – C6 – O5	125.6(4)

environment around Cu(II) center with CN = 6. This distortion is like a compression along the four-fold axis. The bond lengths of C4 – C6 and C1 – C3 are 1.495 Å and 1.491 Å respectively (Table 25). These bond lengths are close to that of ordinary C – C bond. The C6 – O5 bond length is 1.275 Å and C6 – O6 bond length is 1.235 Å. C6 – O5 and C6 – O6 bond lengths are closer in value to what is expected for Csp^2 – O and that of is

characteristic of resonance in carboxylate anion. This afford the $AACO^{2-}$ coordinating to the Cu(II) centers using the carboxylate oxygen. There was a rotation across C3 – C1 bond. The nitrile groups of the oppositely coordinated $AACO^{2-}$ ions to the Cu1 centers have different bond lengths.

The bond length of C5 – N4 is 1.134 Å and the bond length of C2 – N2 is 1.142 Å. C4 – N3 bond length is 1.300 Å, which is slightly shorter than N3 – O4 bond length of 1.305 Å. The N3 – O4 has N – O group characteristic of the oxime form. C1 – N1 bond length is 1.308 Å, which is longer than N1 – O1 with bond length 1.302 Å. The N1 – O1 has double bond character of the *nitroso*-form. This is interesting to have the two $AACO^{2-}$ units coordinating in both the oxime and *nitroso*-form in the same coordination compound. The nitrile groups are almost perfectly linear with bond angles N4 – C5 – C4 = 177.3° and N2 – C2 – C1 = 178.1° (Table 26).

The distance between Cu2 – Cu1 is 3.733 Å. The magnetic susceptibility measurements for $K_2[Cu_3(AACO)_4 \cdot (H_2O)_4] \cdot 4H_2O$ gave an effective magnetic moment μ_{eff} = 1.018 B.M. at 292.5 K which shows an antiferromagnetic coupling between the Cu(II) ion centers.

The structure has some torsion angles (Appendix C-19). The copper centers with different coordination numbers are not on the same plane (Figure 75). The ring is bent and the dihedral angle between the planes containing each is 26.38°. The crystal structure features extensive system of hydrogen bonds (Appendix C-20). The structure represents a rather complex 3D network in which H-bonding is essential for the crystal packing. CCDC 1473518 contains the supplementary crystallographic data for this complex.

Table 26. Selected bond lengths (Å) and bong angles (°) around Cu(II) centers in $K_2[Cu_3(AACO)_4 \cdot (H_2O)_4] \cdot 4H_2O$

Bond	(Å)	Angle	(°)	Angle	(°)
Cu1 – O5	1.942(3)	O5-Cu1-O2	93.64(11)	O1W-Cu2-O1W	180.0
Cu2-O1	1.978(3)	O2-Cu1-N1	82.88(12)	O5-Cu1-N1	170.26(13)
Cu2-O1W	2.250(3)	O2-Cu1-N3	175.63(13)	O5-Cu1-N3	83.17(12)
Cu1-N1	1.977(3)	O5-Cu1-O2W	100.53(12)	N1-Cu1-N3	99.79(13)
Cu2-O1W	2.250(3)	N1-Cu1-O2W	88.87(12)	O2-Cu1-O2W	95.24(11)
Cu1-O2	1.960(3)	O4-Cu2-O4	180.0	N3-Cu1-O2W	88.29(13)
Cu1-N3	1.977(3)	O4-Cu2-O1	80.43(11)	O4-Cu2-O1	99.57(11)
Cu2-O4	1.962(3)	O4-Cu2-O1	99.57(11)	O4-Cu2-O1	80.43(11)
Cu2-O1	1.978(3)	O4-Cu2-O1W	91.75(12)	O1-Cu2-O1	180.0
Cu2-O1W	2.250(3)	O1-Cu2-O1W	93.23(12)	O4-Cu2-O1W	88.25(12)
		O4-Cu2-O1W	88.25(12)	O1-Cu2-O1W	86.77(12)
		O1-Cu2-O1W	86.77(12)	O4-Cu2-O1W	91.75(12)
		O1-Cu2-O1W	93.23(12)		

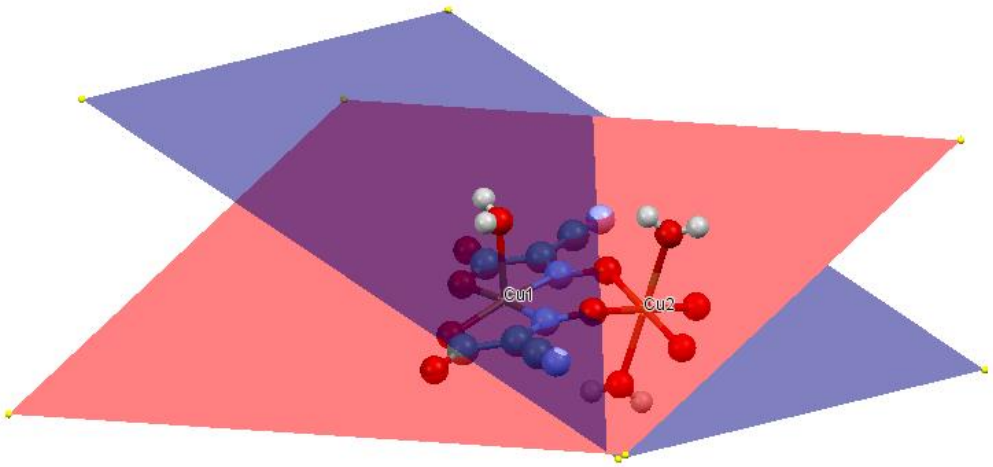

Figure 75. A fragment of the structure of $K_2[Cu_3(AACO)_4 \cdot (H_2O)_4] \cdot 4H_2O$ showing the dihedral angle between two equatorial planes at Cu1 and Cu2 centers.

V.8.6. Crystal Structure of $K_2[Cu(AACO)_2 \cdot H_2O] \cdot 2H_2O$. The complex is also a product of the hydrolysis of the cyanoxime ligand that led to the $AACO^{2-}$ dianion. The crystal was grown out of aqueous solution in a plastic centrifuge tube in a dessicator and it crystallized as a clear dark black-purple prismatic specimen (Appendix C-29). The crystal and refinement data are shown in Table 27.

The complex is monometallic with just one Cu(II) center and two K^+ counter-cations to balance charge. The $AACO^{2-}$ is coordinated to the metal ion using the nitrogen atom of the oxime group and oxygen atom of the carboxylate group. The $AACO^{2-}$ ions have a *trans-anti*-conformation around the Cu(II) ion center and they are coordinated *trans* to each other such that the Cu(II) ion have a configuration of CuN_2O_2 at the base and there is a molecule of water attached apically to create square-pyramidal coordination geometry around the Cu(II) center (Figure 76). The coordination compound is anionic $[Cu(C_3N_2O_2)_2 \cdot H_2O]^{2-}$ with two K^+ ions outside the coordination sphere to neutralize it and also displaying an electrostatic interaction with two molecules of H_2O (Figure 76).

The bond lengths and angles are summarized in Table 28 and 29. The bond length of Cu1 – O5, Cu1 – N1, Cu1 – N3 and Cu1 – O2 are 1.9659 Å, 2.0020 Å, 1.9784 Å, and 1.9388 Å respectively (Table 29). This shows that the square- pyramid geometry around the Cu1 is distorted. There is delocalization of electron density which is evident from the bond lengths. The C4 – N3 bond length is 1.3247 Å, which is longer than typical Csp^2 = N in oximes and N3 – O4 bond length is 1.2741 Å, which is shorter than typical N – O bond in oximes. This shows that the N – O group is in the *nitroso*-form (N = O). The structure has extensive hydrogen bonds that afford packing of this *trans*-complex into the crystal lattice(Appendix C-24). CCDC 1473523 contains the supplementary

Table 27. Crystal data and structure refinement of $K_2[Cu(AACO)_2 \cdot H_2O] \cdot 2H_2O$

Parameter	$K_2[Cu(AACO)_2 \cdot H_2O] \cdot 2H_2O$	
Chemical formula	$C_6H_6CuK_2N_4O_9$	
Formula weight	419.89 g/mol	
Temperature	100(2) K	
Wavelength	0.71073 Å	
Crystal habit	clear dark black-purple prism	
Crystal system	Monoclinic	
Space group	P21/c	
Unit cell dimensions	a = 8.7730(6) Å	α = 90°
	b = 12.4214(8) Å	β = 108.3500(10)°
	c = 13.1215(8) Å	γ = 90°
Volume	1357.18(15) $Å^3$	
Z	4	
Density (calculated)	2.055 g/cm^3	
Absorption coefficient	2.276 mm^{-1}	
F(000)	836	
Theta range for data collection	2.32 to 32.99°	
Refinement method	Full-matrix least-squares on F^2	
Refinement program	SHELXL-2014 (Sheldrick, 2014)	
Function minimized	$\Sigma w(F_o^2 - F_c^2)^2$	
Goodness-of-fit on F^2	1.002	
Δ/σmax	0.002	
Final R indices	4310 data; I>2σ(I)	R1 = 0.0242, wR2 = 0.0574
	all data	R1 = 0.0285, wR2 = 0.0605
Weighting scheme	$w=1/[\sigma^2(F_o^2)+(0.0198P)^2+2.4243P]$	
	where $P=(F_o^2+2F_c^2)/3$	
Largest diff. peak and hole	0.660 and -0.679 $eÅ^{-3}$	
R.M.S. deviation from mean	0.093 $eÅ^{-3}$	

crystallographic data for this complex.

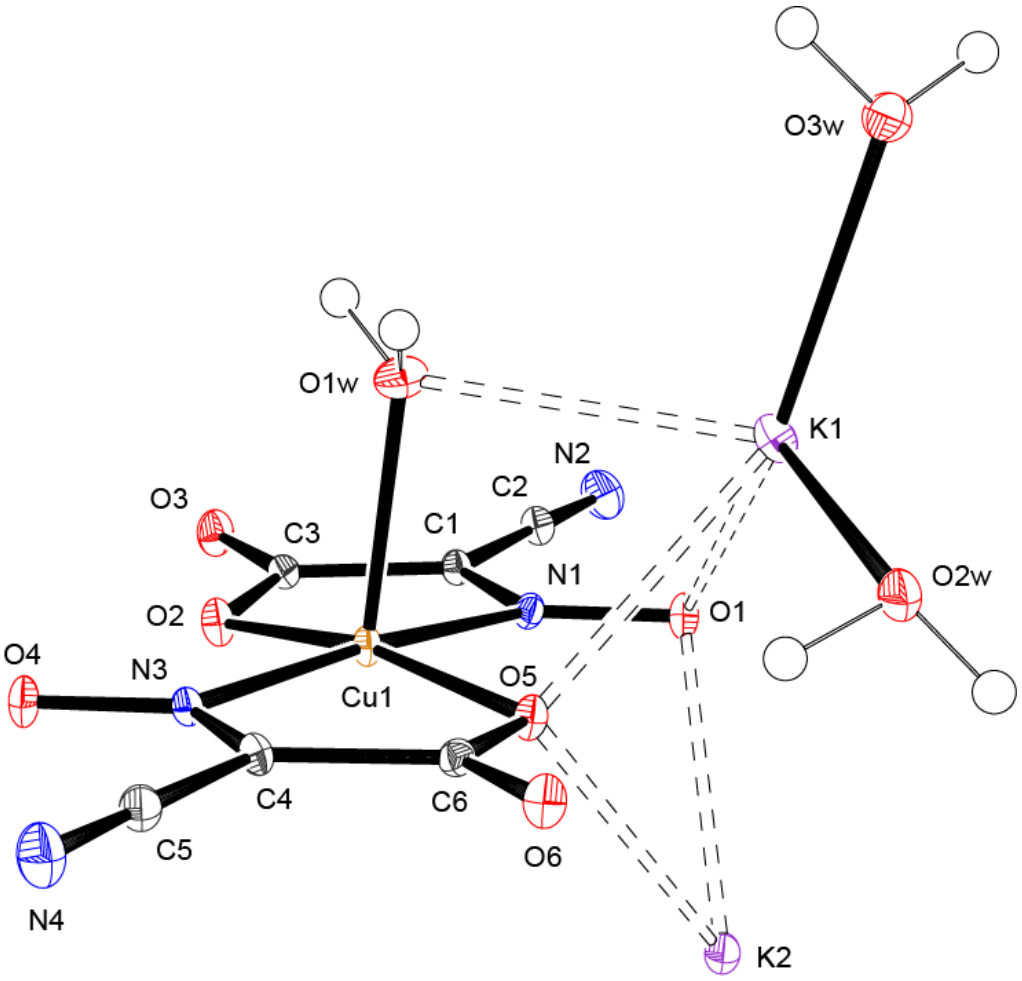

Figure 76. The ASU in the structure of $K_2[Cu(AACO)_2 \cdot H_2O] \cdot 2H_2O$: an ORTEP drawing at 50% thermal ellipsoids parameters. Clearly shown trans-geometry of chelating $AACO^-_2$ anion in the complex. Dotted lines indicate long electrostatic contacts between water molecules and K-cations.

Table 28. Selected bond lengths (Å) and angles for $AACO^{2-}$ ion in $K_2[Cu(AACO)_2 \cdot H_2O] \cdot 2H_2O$.

Bond	(Å)	Angle	(°)	Angle	(°)
C1-N1	1.3140(18)	N1-C1-C2	121.92(13)	O6-C6-O5	123.94(13)
C1-C3	1.4952(19)	C2-C1-C3	122.22(12)	O5-C6-C4	116.23(12)
C3-O3	1.2361(17)	O3-C3-O2	124.97(13)	O1-N1-C1	121.79(12)
C4-N3	1.3247(18)	O2-C3-C1	114.86(12)		
C4-C6	1.4826(19)	N3-C4-C6	116.01(12)		
C6-O6	1.2481(17)	N4-C5-C4	179.67(17)		
C1-C2	1.432(2)	O6-C6-C4	119.84(12)		
C2-N2	1.151(2)	N1-C1-C3	115.84(12)		
C3-O2	1.2839(17)	N2-C2-C1	178.38(16)		
C4-C5	1.432(2)	O3-C3-C1	120.16(13)		
C5-N4	1.149(2)	N3-C4-C5	121.80(12)		
C6-O5	1.2841(17)	C5-C4-C6	122.17(12)		

Table 29. Selected bond lengths (Å) and angles for Cu(II) ion centers in $K_2[Cu(AACO)_2 \cdot H_2O] \cdot 2H_2O$.

Bond	(Å)	Angle	(°)	Angle	(°)
Cu1-O2	1.9388(11)	O2-Cu1-O5	169.61(5)	C1-N1-Cu1	110.58(9)
Cu1-N3	1.9784(12)	O5-Cu1-N3	83.69(5)	O1-N1-Cu1	127.33(9)
Cu1-O1W	2.2141(11)	O5-Cu1-N1	97.21(5)		
Cu1-O5	1.9659(10)	O2-Cu1-O1W	101.20(4)		
Cu1-N1	2.0020(12)	N3-Cu1-O1W	96.67(5)		
		O2-Cu1-N3	95.23(5)		
		O2-Cu1-N1	82.86(5)		
		N3-Cu1-N1	174.31(5)		
		O5-Cu1-O1W	89.19(4)		
		N1-Cu1-O1W	88.97(5)		

V.8.7. Crystal Structure of the Side Product, the Oxamide. The oxamide crystallized out of the aqueous solution of Ni(II) complexes during attempts of syntheses of complexes with the HECO ligand. As shown earlier, the HECO and HMeCO cyanoxime hydrolyzed to the $AACO^-$ dianion. The oxamide showed up as clear light colourless block-like crystals on the plastic test-tube walls. A suitable crystal was used for X-ray crystallographic analysis. The crystal turned out to be multi-component twin (8 domains) with clearly seen major components with greater than 80 % reflections. Structure solution was successfully carried out and subsequently refined using only the main domain. The crystal and refinement data for the oxamide are presented in Table 30, while bond angles and bond lengths are presented in Table 31. The structure is as shown in Figure 77. There are two molecules in the unit cell (Z = 2) (Figure 78). The molecule is planar, with a system of hydrogen bonds helping in its crystal packing (Appendix C-27). CCDC 1473522 contains the supplementary crystallographic data for this compound. The first (and only) mentioning of the oxamide crystal structure was in the work by Sly, William Glenn [100].

Table 30. Crystal data and structure refinement of oxamide

Parameter	Oxamide	
Chemical formula	CHNO	
Formula weight	43.03 g/mol	
Temperature	119(2) K	
Wavelength	0.71073 Å	
Crystal size	0.268 x 0.282 x 0.533 mm	
Crystal habit	Clear light colourless block	
Crystal system	Triclinic	
Space group	P -1	
Unit cell dimensions	a = 3.5592(7) Å	α = 90.842(2)°
	b = 4.8685(10) Å	β = 103.472(2)°
	c = 5.2934(10) Å	γ = 106.075(2)°
Volume	85.40(3) $Å^3$	
Z	2	
Density (calculated)	1.673 g/cm^3	
Absorption coefficient	0.150 mm^{-1}	
F(000)	44	
Theta range for data collection	3.97 to 27.81°	
Refinement method	Full-matrix least-squares on F^2	
Refinement program	SHELXL-2014 (Sheldrick, 2014)	
Function minimized	$\Sigma w(F_o^2 - F_c^2)^2$	
Goodness-of-fit on F^2	1.211	
Final R indices	401 data; $I>2\sigma(I)$	R1 = 0.0265, wR2 = 0.0789
	all data	R1 = 0.0272, wR2 = 0.0796
Weighting scheme	$w=1/[\sigma^2(F_o^2)+(0.0430P)^2+0.0210P]$	
	where $P=(F_o^2+2F_c^2)/3$	
Extinction coefficient	0.4700(1100)	
Largest diff. peak and hole	0.489 and -0.208 $eÅ^{-3}$	
R.M.S. deviation from mean	0.045 $eÅ^{-3}$	

Table 31. Selected bond lengths (Å) and bond angles (°) in oxamide.

Bonds	(Å)	Angles	(°)
C1-O1	1.2397(12)	O1-C1-N1	125.60(9)
C1-C1	1.5428(18)	N1-C1-C1	114.17(10)
N1-H1N1	0.908(16)	C1-N1-H1N1	117.4(9)
C1-N1	1.3226(11)	O1-C1-C1	120.23(10)
N1-H2N	0.862(17)	C1-N1-H2N	119.8(10)
		H2N-N1-H1N1	122.7(14)

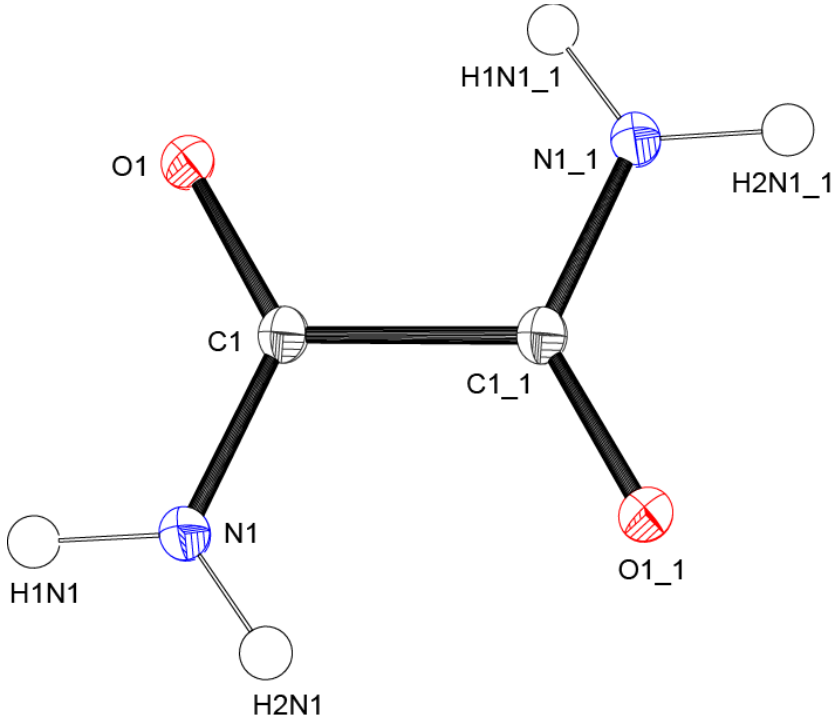

Figure 77. The GROW fragment in the structure of oxamide. An ORTEP drawing at 50% thermal ellipsoids probability. Symmetry code for _1 position: -x, -y, -z.

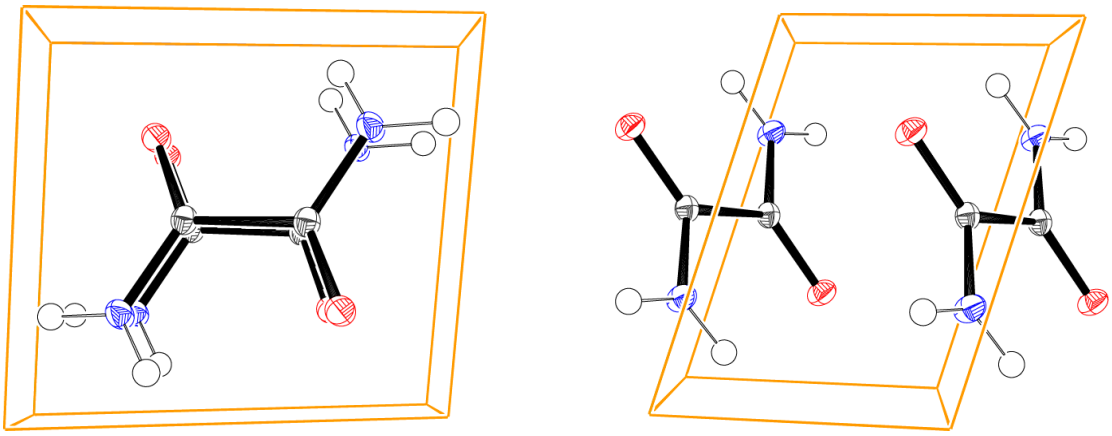

Figure 78. The unit cell content in the structure of oxamide: two prospective views.

VI. SUMMARY AND CONCLUSION

The results from this study can be summarized as follow and the following conclusions can be drawn:

- We obtained 23 compounds: 3 organic and 20 metal complexes of bivalent Cu (7) and Ni (13). Two organic ligands – HECO and HMCO – were known before and prepared in the research group, while the oxamide, $C_2N_2O_2H_4$, was obtained as a side product. Our goal of preparation of a series of transition metal cyanoximates was accomplished, albeit not to the desired level. The main obstacle was a hydrolysis reaction of the ether-cyanoximates HECO and HMeCO that lead to the formation of another cyanoxime – $AACO^{2-}$ dianion $C_3N_2O_3^{2-}$, which formed elegant dimetallic and trimetallic complexes with Cu(II) and Ni(II).

- Synthesized metal complexes were characterized by elemental analysis, thermal analysis, IR and electronic (solid state, diffuse reflectance) spectroscopies and X-ray analysis. The latter technique included both powder diffraction, and single crystal diffraction studies. Thus, crystal and molecular structures of 8 compounds were determined: 6 for transition metal complexes and 2 for organic compounds – HECO cyanoxime and side product such as oxamide. The origin of appearance of this compound is postulated (Appendix D).

- Two metal complexes – $[Ni(ACO)_2\cdot(H_2O)_2]$ and $[Ni(2PCO)_2\cdot(H_2O)_2]$ – form molecular, island type structures with rhombically distorted octahedral Ni(II) environment. In both complexes the cyanoximes act as chelating ligands, adopting *trans-anti*, *nitroso-* structures and form complexes with *cis*-geometry of mutually oriented anions in equatorial plane. Water molecules occupy axial positions. These water molecules are involved in a system of H-bonding that helps molecules to pack into crystals.

- Three metal complexes –$[Ni(AACO)\cdot(H_2O)_3]_2\cdot H_2O$, $K_2[Ni_3(AACO)_4\cdot(H_2O)_4]\cdot 4H_2O$ and $K_2[Cu_3(AACO)_4\cdot(H_2O)_4]\cdot 4H_2O$ – were found to form a multimetallic species. In all these cases the $AACO^{2-}$ dianions perform bridging function via the oxygen atoms of nitroso-group with the nitrogen atoms being part of the five-membered chelate rings. Two out of three complexes are anionic, while one is neutral ($[Ni(AACO)\cdot(H_2O)_3]_2\cdot H_2O$). Two trimetallic complexes are isostructural, with the *cis*-orientation of the $AACO^{2-}$ dianions. The compounds $K2[Cu(AACO)_2\cdot H_2O]\cdot 2H_2O$, $[Ni(AACO)\cdot(H_2O)_3]_2\cdot H_2O$ are very different: the first one has *trans*-geometry of the cyanoximes in the anionic complex, while the second one just forms neutral dimetallic complex with bridging dianion.

- Transition metals in polynuclear complexes have two different environments: penta- and hexa-coordinated, which correspond to distorted square pyramidal and octahedral geometries.

- In all these Cu(II) and Ni(II) complexes, there are both coordinated and crystallization water molecules. All are essential for the crystal packing via complex system of H-bonding.

- Careful heating of several Ni(II) complexes, such as $[Ni(ACO)_2 \cdot (H_2O)_2]$, $[Ni(2PCO)_2 \cdot (H_2O)_2]$, $[Ni(PyrCO)_2 \cdot (H_2O)_2]$ and $[Ni(PiPCO)_2 \cdot (H_2O)_2]$, at temperatures pre-determined by the DSC/TG analysis, allowed removal of coordinated water. The process is reversible for the first three complexes. Data of the XRD powder diffraction shows that in some cases the lattice is changed upon dehydration.

- Data of solid state electronic spectroscopy evidenced the retention of the geometry of central atoms during dehydration process in as $[Ni(ACO)_2]$, $[Ni(2PCO)_2]$, $[Ni(PyrCO)_2]$ and $[Ni(PiPCO)_2]$, which suggests developing bridging function of cyanoximes in the lattice upon water loss.

- Results of room temperature measurements of magnetic moment for the trimetallic complex, $K_2[Cu_3(AACO)_4(H_2O)_4] \cdot 4H_2O$, clearly indicates an extensive antiferromagnetic interactions between the cyanoxime-bridged metal centers.

- No one-dimensional solids were obtained at this point. Some compounds characterized by the X-ray analysis possess columnar structures and some represent 3D complex H-bonded networks. However, studies of dehydrated compounds clearly showed that the formation of stacks of complexes is feasible and arrangement of those in 1D solids achievable.

VII. FUTURE WORK

As a result of the time constraints, we were unable to perform crystallization of the obtained anhydrous Ni(II) complexes [$Ni(ACO)_2$], [$Ni(2PCO)_2$], [$Ni(PyrCO)_2$] and [$Ni(PiPCO)_2$] in the presence of an inert organic solvent using an autoclave or sealed ampoule method. When crystal structures will be determined then the binding mode of the cyanoximes in these complexes will be established, and it can be used for further design of conditions for the formation of 1D solids that form stacks. At that point the oxidation reactions to form mixed valence Ni(II)---Ni(III) coordination polymers will be conducted. As oxidants, the plan is to use H_2O_2 and organic t-butyl-hydroperoxide. The monitoring of the progress and studies of properties of such complexes will be done using the UV-visible and NIR spectroscopies. Hence, this work will be carried out in the group in the future.

VIII. LITERATURE CITED

1. Stevens, G., & Bloor, D. (1977, October). One-dimensional solids. New Scientist, 27, 213-215.

2. Leong. W.L., & Vittal, J.J. (2011). One-dimensional coordination polymers: complexity and diversity in structures, properties, and applications. *Chemical Reviews, 111*(2), 688-764.

3. Berlinsky, A.J. (1979). Introduction to highly conducting One-Dimensional solids. In J. Devreese (Ed.), *Highly conducting One-Dimensional solids*. pp 1-16. Newyork and London: Plenum Press.

4. Stevens, G.C. (1979). The platinum metals in quasi one-dimensional solids. Novel materials with a potential for new solid state technology. *Platinum Metals Review*, *23*(1), 23-28.

5. Greenwood, N.N., & Earnshaw, A. (1997). *Chemistry of the elements*. Burlington, MA: Butterworth-heinemann.

6. Campbell, M.G., Zheng, S., & Ritter, T. (2013). One-dimensional palladium wires: Influence of supramolecular structure. *Inorganic Chemistry*, *52*(23), 13295-13297.

7. Gopalakrishnan, J., & Nanjundaswamy, K. S. (1983). Transition metal chalcogenides exhibiting quasi-one-dimensional behavior. *Bulletin of Materials Science, 5*(3&4), 287-306.

8. Georgiev, V.P., & McGrady, J.E. (2011). Influence of low-symmetry distortions on electron transport through metal atom chains: When is a molecular wire really 'broken'. *Journal of the American Chemical Society, 133*(32), 12590-12599.

9. Jang, K., Jung, I.G., Nam, H.J., Jung, D.Y., & Son, S.U. (2009). One-dimensional organometallic molecular wires via assembly of $Rh(CO)_2Cl$(amine): Chemical control of interchain distances and optical properties. *Journal of the American Chemical Society, 131*(34), 12046-12047.

10. Swager, T.M. (1998). The molecular wire approach to sensory signal amplification. *Accounts of Chemical Research*, *31*(5), 201-207.

11. Liu, Y., Bauer, A.Q., Akers, W.J., Sudlow, G., Liang, K., Shen, D., Berezin, M.Y., Culver, J.P., & Achilefu, S. (2011). Hands-free, wireless goggles for near-infrared fluorescence and real-time image-guided surgery. *American Journal of Surgery, 149*(5), 689-698.

12. Thomas, T.W., & Underhill, A.E. (1972). Metal-metal interactions in transition-metal complexes containing infinite chains of metal atoms. *Chemical Society Reviews*, 1, 99-120.

13. Qian, G., Zhong, Z., Luo, M., Yu, D., Zhang, Z., Wang, Z. Y., & Ma, D. (2009). Simple and efficient near-infrared organic chromophores for light-emitting diodes with single electroluminescent emission above 1000 nm. *Advanced Materials*, *21*(1), 111-116.

14. Schaafsma, B.E., Mieog, J.S., Hutteman, M., van der Vorst, J.R., Kuppen, P.J., Lowik, C. W., Frangioni, J.V., van de Velde, C.J., & Vahrmeijer, A. L. (2011). The clinical use of indocyanine green as a near-infrared fluorescent contrast agent for image-guided oncology survey. *Journal of Surgical Oncology*, *104*(3), 323-332. doi: 10.1002/jso.21943

15. Barone, P.W., Baik, S., Heller, D. A., & Strano, M. S. (2005). Near-infrared optical sensors based on single-walled carbon nanotubes. *Nature Materials*, *4*(1), 86-92.

16. Cao, Q., Zhegalova, N.G., Wang, S.T., Akers, W.J., & Berezin, M. (2013). Multispectral imaging in the extended near-infrared window based on endogenous chromophores. *Journal of Biomedical Optics*, *18*(10), 101318. doi: 10.1117/1.JBO.18.10.101318

17. Salo, D., Zhang, H., Kim, D.M., & Berezin, M.Y. (2014). Multispectral measurement of contrast in tissue-mimicking phantoms in near-infrared spectral range of 650 to 1600 nm. *Journal of Biomedical Optics*, *19*(8), 086008. doi: 10.1117/1.JBO.19.8.086008

18. Klaus, D.R., Keene, M., Silchenko, S., Berezin, M., & Gerasimchuk, N. (2015). 1D polymeric cyanoximate: A strategy toward luminescence in the near-infrared region beyond 1000 nm. *Inorganic Chemistry, 54*(4), 1890-900.

19. Mokhir, A.A., Gerasimchuk, N.N., Pol'shin, E.V., & Domasevich, K.V. (1993). Synthesis, IR, and Mossbauer study of bisorganotin complexes with cyanoximes. *Inorganic Chemistry, 39*(2), 289-293.

20. Gerasimchuk, N.N., Nagy, L., Schmidt, H.G., Noltemeyer, M., Bohra, R., & Roesky, H. (1992). Preparation, IR and x-ray crystal structure studies of Tl(I)-2-pyridyl-cyanoxime complex. *Zeitschrift fur Naturforschung*, *47*(b), 1741-1745.

21. Domasevich, K.V., Gerasimchuk, N.N., & Mokhir, A. (2000). Organoantimony(V)cyanoximates: Synthesis, spectra and crystal structures. *Inorganic Chemistry, 39*(6), 1227-1237.

22. Gerasimchuk, N.N, Simonov,Y.A., Dvorkin A.A., & Rebrova, O.N. (1993). Synthesis, IR spectra and structure of lead(II) complex with amide-cyanoximate-

ion $ONC(CN)C(O)NH_2^-$. *Russian Journal of Inorganic Chemistry*, *38*(2), 247-252.

23. Domasevich, K.V., & Gerasimchuk, N.N. (1992). 2-Cyano-2-isonitroso-N,N-dimethyl-thioacetamide HONC(CN)C(S)N(CH3)2 – Member of a family of nonlinear cyanoxime acidoligands. *Ukrainskii Khimicheskii Zhurnal* (Russian Edition), *58*(8), 603 – 607.

24. Maher, T., Gerasimchuk, N.N., Durham P., Domasevitch, K.V., Wilking, J., & Mokhir, A. (2007). Tin (IV) cyanoximates: Synthesis, characterization and cytotoxicity. *Inorganic Chemistry*, *46*(18), 7268-7284.

25. Mokhir, A.A., Domasevich, K.V., Dalley, N.K., Kou, X., Gerasimchuk, N.N., & Gerasimchuk, O.A. (1999). Syntheses, crystal structures and coordination compounds of some 2-hetarylcyanoximes. *Inorganica Chimica Acta*, *284*(1), 85-89.

26. Ponomareva, V.V., Dalley, N.K., Kou, X., Gerasimchuk, N.N., & Domasevitch, K.V. (1996). Synthesis, spetcra and crystal structures of complexes of ambidentate $C_6H_5C(O)C(NO)CN^-$. *Journal of Chemical Society, Dalton Transaction*, 11, 2351-2359.

27. Gerasimchuk, N. N., & Dalley, N.K. (2004). Demetallation of a Ni(II) tetraazamacrocyclic complex by cyanoxime resulting in the formation of a stereospecific trinuclear compound $[Na(H2O)6]^+[NaNi2L6]^-$ (L= NC – C(NO) – C(O)NH2-]. *Journal of Coordination of Chemistry*, *57*(6), 1431 – 1445.

28. Sliva, T.Y., Dobosz, A., Jerzykiewicz, L., Karaczyn, A., Moreeuw, A.M., Swiatek – Kozlowska, J., Glowiak, T., & Kozlowski, H. (1998). Copper (II) and nickel (II) complexes with oxime analogues of amino acids, potentiometric, spectroscopic and x-ray studies of complexes with 2-cyano-2-(hydroxyimino)acetic acid and its ethane-1,2-diamine derivative. *Journal of Chemical Society, Dalton Transaction*, 11, 18

29. Sliva, T.Y., Duda, A.M., Glolak, T., Fristsky, I.O., Amirkhanov, V.M., Mokhir, A.A., & Kozlowski, H. (1997). Coordination ability of amino acid oximes, potentiometric, spectroscopic and structural studies of complexes of 2-cyano-2-(hydroxyimino)acetamide. *Journal of Chemical Society, Dalton Transaction*, 2 273-276. doi: 10.1039/a605125a

30. Gerasimchuk, N.N., Skopenko, V.V., Ponomareva, V.V., & Domasevich, V.V. (1993). The benzoylcyanoximate ion and its properties as a ligand. *Russian Journal of Inorganic Chem*istry, *38*(6), 1042 – 1048.

31. Feuer, H. (1970). *The Chemistry of nitro and nitroso Groups*. New York: Wiley.

32. Skopenko, V.V., Zub, V.Y., & Lampeka, R.D. (1983). *Doklady Akademii Nauk Ukrainskoj SSR Serija B: Geol., Khim. Biol. Nauki*, No. 4, pp. 60 – 62.

33. Gerasimchuk, N.N., & Bowman-James, K. (1994). Mixed Donor Ligands. In *Encyclopedia of Inorganic Chemistry*. (Vol. 5, pp.2254 – 2270). England: John Wiley & Sons.

34. Cheadle C., Gerasimchuk, N.N., Barnes C.L., Tyukhtenko S.I., & Silchenko, S. (2013). The first bis-cyanoxime: Synthesis and properties of a new versatile and accessible polydentate bifunctional building block for coordination and supramolecular chemistry. *Dalton Trans*action, *42*(14), 4931-4946.

35. Sidman, J.W. (1957). Electroic and vibrational states of the nitrite ion. I. electronic states[1]. *Journal of American Chemical Society*, *79*(11), 2669-2675.

36. Gerasimchuk, N.N., Nagy, L., Schmidt, H-G., Noltmeyer, M., Bohra, R., & Roesky, H.W. (1992). Preparation, IR and x-ray crystal structural studies of Tl(I)-2-pyridyl-cyanoxime complex. *Zeitschrift fur Naturforschung*, 47b, 1741-1745.

37. Gerasimchuk, N.N., Zhmurko, O.A., & Tyukhtenko, S.I. (1993). 2-Pyridylcyanoxime and related complex compounds of Cu(II) and Ni(II). *Russian Journal of Inorganic Chemistry*, *38*(2), 301-306.

38. Domashevskaya, O.A., Simonov, Y.A., Gerasimchuk, N.N., Dvorkin, A.A., & Mazus, M.D. (1990). Synthesis and crystal structure of nickel(II) complex with a tetraamino-aliphatic ligand and an $ONC(CN)C(S)NH_2^-$ ion. *Russian Journal Coordination Chemistry*, *16*(11), 1544-1548.

39. Simonov, Y.A., Domashevskaya, O.A., Skopenko, V.V., Dvorkin, A.A., & Gerasimchuk, N.N. (1991). Crystal and molecular structure of the $[Cu(dipy)Br\{ONC(CN)C(S)NH_2\}]$*(1,4-dioxane) complex. *Koordinatsionnaya Khimiy*

40. Skopenko, V.V., Palii, G.K., Gerasimchuk, N.N., & Makatas, E.P. (1986). Outer-sphere tris-diamine complexes of iron(II) and their antimicrobial activity. *Dopovidi Academii Nauk ukrainskoi RSR*, *B*(2), 45-48.

41. Lampeka, R.D. (1983). Doctoral dissertation: Kiev State University.

42. Hubele, A., & Kuhne, M. (1978). USA Pat. No 4063921.

43. Gerasimchuk, N.N., & Charlier, H.A. (1982). Austria Pat. No 367268.

44. Gus'kova, T.V., Chernoiv'yantz, M.S., & Bagdasarov, K.N. (1984). *Ukrainskii Khimicheskii Zhurnal*, *50*(9), 982.

45. Cronstedt, Axel F. (1751). Rön och försök, gjorde med en malm-art från Los kobolt grufvor i farila socken och helsingeland. *Kongl. Svenska Veenskapas Academians Handlingar*, *12*, 287-292.

46. Cronstedt, Axel F. (1754). Fortsättning af rön och försök, gjorde med en malm-art från los kobolt grufvor". *Kongl. Svenska Veenskapas Academians Handlingar, 15,* 38-45.

47. Lee, J.D. 2009. *Concise Inorganic Chemistry*. Delhi, India: S.P Printers.

48. Latimer diagrams in acid and in basic solution. (2016, March 28). Retrieved from http://www.yorku.ca/stynes/Latimer09.pdf

49. Kuck, P.H. (2015, January). Nickel. United States Geological Survey, mineral commodity summaries. pp. 108-109.

50. Kuck, P.H. (2015, May). Nickel (advance release). 2012 Minerals yearbook: United States Geological Survey. pp 51.1 - 51.39.

51. Sigel, A., Sigel, H., & Sigel, R.K.O. (2007). *Nickel and its surprising impact in nature: Metal ions in life sciences*. *Vol.2*. Chichester, West Sussex: John Wiley & Sons.

52. Sydor, A.M., & Zamble, D.B. (2013). Nickel Metallomics: General themes guiding nickel homeostasis. *Metal ions in life sciences, 12*, 375-416. doi: 10.1007/978-94-007-5561-1_11

53. Ragsdale, S.W. (2014). Biochemisirty of methyl-coenzyme M reductase: The nickel metalloenzyme that catalyzes the final step in synthesis and the first step in anaerobic oxidation of the greenhouse gas methane. *Metals Ions in Life Science, 14*, 125 - 145. doi:10.1007/978-94-017-9269-1_6.

54. Greig, N., Wyllie, S., Vickers, T.J., & Fairlamb, A.H. (2006). Tryanothione-dependent glyoxalase I in *Trypanosoma cruzi. Biochemical Journal, 400*(2), 217-223.

55. Thornallety, P.J. (2003). Glyoxalase I - structure, unction and a critical role in the enzymatic defense against glycation. *Biochemical Society Transactions, 31*(6), 1343-1348.

56. Ridderstrom, M., & Mannervik, B. (1996). Optimized heterologous expression of the human zinc enzyme glyoxalase I. *Biochemical Journal, 314* (Pt 2), 463-467.

57. Aronsson A-C., Marmstal, E., & Mannervik, B. (1978). Glyoxalase I, a zinc metalloenzyme of mammals and yeast. *Biochemical and Biophysical Research Comminucations, 81*(4), 1235-1240.

58. Lev Tschugaeff. (1905). Über ein neues, empfindliches reagens auf nickel. *Berichte der deutschen chemischen Gesellschaft, 38* (3), 2520–2522.

59. Dohring, A., Goddard, R., Jolly, P.W., Kruger, C., & Polyakov, V.R. (1997). Monomer-trimer isomerism in 3-substituted pentane-2,4-dione derivatives of nickel(II). *Inorganic Chemistry, 36*(2), 177 – 183.

60. Wielandt, J.W., & Ruckerbauer, D. (2010). Bis(1,5-cyclooctadiene)nickel(0). In T.B. Rauchfuss (Ed) *Inorganic Syntheses, Vol. 35* (pp. 120). Hoboken, New Jersey: John Wiley & Sons, Inc.

61. Ginsberg, A.P., Martin, R.L., & Sherwood, R.C. (1967). Ferromagnetic Ni – Ni interaction in trimeric bis(acetylacetonato)nickel (II). *Chemical Communications (London)*, 17, 856-858. doi**:** 10.1039/C19670000856

62. Atanasov, A., Hitchman, M.A., Hoppe, R., Murray, K.S., Moubaraki, B., Reinen, D., & Stratemeier, H. (1993). The compressed tetragonal hexafluorocuprate(4-) (CuF64-) complex in potassium aluminium copper fluoride (KAlCuF6): An angular overlap treatment of the electronic structure and magnetic exchange coupling. *Inorganic Chemistry, 32*(16), 3397-3401.

63. Gerloch, M. (1981). The sense of Jahn-Teller distortions in octahedral copper(II) and other transition-metal complexes. *Inorganic Chemistry, 20*(2), 638-640.

64. Joseph, G., Kundig, K.J.A., & International Copper Association. (1999). *Copper: Its trade, manufacture, use, and environmental status*. (pp. 144-192 & pp. 331-375). Materials Park, Ohio: *ASM International*.

65. Seale, W. 2007. The role of copper, brass and bronze in architecture and design; *Metal Architecture*.

66. Erik P. (2012). Simple method of copper analysis using monosodium glutamate and its application in ore analysis. *Mineralogia, 43*(1-2), 137-146.

67. Onindo, C.O., Sliva, T.Y., Kowalik-Jankowska, T., Fritsky, I.O., Buglyo, P., Pettit, L.D., Kozlowski, H., & Kiss, T. (1995). Copper(II) coordination by oxime analogues of amino acids and peptides. *Journal of Chemical Society, Dalton Transactions*, 23, 3911-3915.

68. Sliva, T.Y., Kowalik-Jankowska, T., Amirkhanov, V.M., Glowiak, T., Pettit, L.D., Fritsky, I.O., & Kozlowski, H. (1997). Coordination ability of amino-acid oximes – potentiometric, spectroscopic and structural studies of complexes of 2-cyano-2-(hydroxyimino)acetamide. *Journal of Chemical Society. Dalton Transactions*, 2, 273-276.

69. Pettit, L.D., Gregor, J.E., & Kozlowski, H. (1991). In perspectives in Bioinorganic Chemistry, eds. Hay, R.W.; Dilworth, J.R.; Nolan, K.B. JAI Press, London, p.1.

70. Malek, K., Kozlowski, H., & Proniewicz, L.M. (2005). Interaction of Na(I), Ni(II) and Cu(II) with 2-cyano-2-(hydroxyimino)acetic acid: Spectroscopic and theoretical studies. *Polyhedron*, *24*, 1175 -1184.

71. Domasevich, K.V., Lindeman, S.V., Struchkov, Y.T., Gerasimchuk, N.N., & Zhurmko, O A. (1993). The synthesis and investigation of copper (II) complexes with N, N- dimethylacetamidocyanooximates ion. *Rusian Journal of Inorganic Chemistry*, *38*(1), 98-103.

72. Storhoff, B.N., & Lewis, H.C. (1977). Organonitrile complexes of transition metals. *Coordination Chemistry Reviews*., *23*(1), 1-29.

73. Mokhir, A.A., Gumienns-Kontecka, E., Swiatek-Kozlowska, J., Petkova, E.G., Fritsky, I.O., Jerzykiwicz, L., Kapshuk, A.A., & Sliva, T.Y. (2002). Study of complex formation with 2-hydroxyiminocarboxylates: specific metal binding ability of 2-(4-methylthiazol-2-yl)-2-(hydroxyimino)acetic acid. *Inorganica Chimica Acta*, *329*(1), 113-121.

74. Gerasimchuk, N., Zhmurko, O., & Tyukhtenko, S. (1993). 2-pyridylcyanoxime and related complex compounds of Cu(II) and Ni(II). *Russian journal of Inorganic Chemistry, 38*(2), 283-287.

75. Neiding, A.B. (1970). Magnitokhimiyaa, Itogi Nauki, Ser. Fiz. Khim. (Magnetochemistry, Advances in Science. Physics and Chemistry Series), Mosc

76. Hedwig, G.R., Love, J.L., & Powell, H.J. (1970). Electronic absorption spectra for copper(II) polyamine complexes. *Australian Journal of Chemistry*, *23*(5), 981-987.

77. Duda, A.M., Karaczyn, A., Kozlowski, H., Fritsky, I.O., Glowiak, T., Prisyazhnaya, E.V., Sliva, T.Y., & Swiatek-Kozlowska, J. (1997). Coordination of copper (II) and nickel (II) ions by a novel open chain oxime ligand. *Journal of Chemical Society, Dalton Transaction*, 20, 3853-3859. doi: 10.1039/A703202A

78. Fedorenko, D., Gerasimchuk, N.N., & Domasevich, K. (1993). 2-Oxyiminopivaloylacetonitrile, the first α - ketocyanoxime: Synthesis and donor properties. *Russian Journal of Inorganic Chemistry, 38*(9), 1535-1539.

79. Domashevskaya, O.A. (1989). Cand. Sci. (Chem) Dissertation, Kiev.

80. Riddles, N. C., Whited, M., Lotlikar, S. R., Still, K., Patrauchan, M., Silchenko, S., & Gerasimchuk, N. (2014). Synthesis and characterization of two cyanoxime ligands, their precursors, and light insensitive antimicrobial silver(I) cyanoximates. *Inorganica Chimica Acta, 412*(1), 94-103.

81. Eddings, D., Barnes, C., Gerasimchuk, N., Durham, P., & Domasevich, K. (2004). First bivalent palladium cyanoximates synthesis, characterization, and biological activity. *Inorganic Chemistry*, *43*(13), 3894-3909.

82. Sheldrick, G. M. (2001). *CELL NOW* program for unit cell determination.

83. Sheldrick, G. M. (2002). *TWINABS*. Bruker-AXS, Madison, Wisconsin, USA.

84. Hilton M., Gerasimchuk, N., Silchenko, S., & Charlier, H.A. (2013). Synthesis, properties and crystal structure of the 2, 4-dichlorophenyl-cyanoxime: A powerful carbonyl reductase inhibitor. *Journal of Chemical Crystallography*, *43* (3), 157-164.

85. APEX2 Software Suit. (2013). Bruker AXS, Madison, Wisconsin.

86. Minacheva, L.Kh.; Raspetova, I.V.; Sliva, T.Y.; Lampeka, R.D. (2000). *Russian Journal of Coordination Chemistry*, *26*(3), 235-237.

87. Morton, J. (2010). Further Investigation of Silver(I) cyanoximates (M.S. thesis).

88. Maher, T.R. (2004). Synthesis, characterization and anti-cancer properties of organotin(IV) cyanoximates (M.S. thesis).

89. Ratcliff, J.L. (2007). Further Investigations of cytotoxic metallo cyanoximates (M.S. Thesis).

90. Eddings, D. (2003). The synthesis, characterization, spectroscopic and biological activity studies of Pt(II) and Pd(II) cyanoximates (M.S. Thesis).

91. Lever, A.B.P. (1984). *Inorganic Electronic Spectroscopy. Studies in Physical and Theoretical Chemistry*. Newyork, NY: Elsevier.

92. Opalade, A. A. (2014). *Spectroscopy of First Transition Metal Complexes*. Personal Collection of Dr. Osowole, A., University of Ibadan, Ibadan, Oyo State, NG.

93. SHELXTL, Crystallographic Software Package, version 5.1.

94. Burnett, M.N., & Johnson, C.K. (1996). OR TEP-III: Oak Ridge Thermal-Ellipsoid Plot Program for Crystal Structure Illustration, Oak Ridge National Laboratory Report ORNL-6895.

95. Macrae, C.F, Edginton, P.R., McCabe, P., Pidcock, E., van de Streek, J, Bruno, I.J., Taylor, R., Chisholm, J.A., & Wood, P.A. (2008). Mercury CSD 2.0 – New Features for the Visualization and Investigation of Crystal Structures. *Journal of Applied Crystallography, 41*, 466 – 470.

96. Robertson, D. (2006). Thallium (I) Coordination Polymers Based on Monosubstituted Arylcyanoximes (M.S. Thesis).

97. Lynam, M., & Vites, J.C. (1997). Manganese 1994. *Coordination Chemistry Reviews*, *162*, 275-304.

98. Gerasimchuk, N., Esaulenko, A.N., Dalley, K.N., & Moore, C. (2010). 2-Cyano-2-isonitroso acetamide and its Ag(I) complexes. Silver(I) cyanoximate as a non-electric gas sensor. *Dalton Transactions, 39*, 749-764.

99. Allen, F.H., Kennard, O., Watson, D.G., Brammer, L., & Orpen, A.G. (1987). Tables of bond Lengths determined by X-Ray and Neutron Diffraction. Part 1. Bond Lengths in Organic Compounds. *Journal of Chemical Society Perkin Transactions II*, S1-S19.

100. Sly, W.G. (1955). *The crystal structure of oxamide. II. The crystal structure of 15, 15'-dehydrobetacarotene* (Doctoral dissertation). Retrieved from http://resolver.caltech.edu/CaltechETD:etd-01262004-143104.

APPENDICES

Appendix A

UV-Visible Spectroscopy

Appendix A-1. A custom-built high vacuum station Dream-1

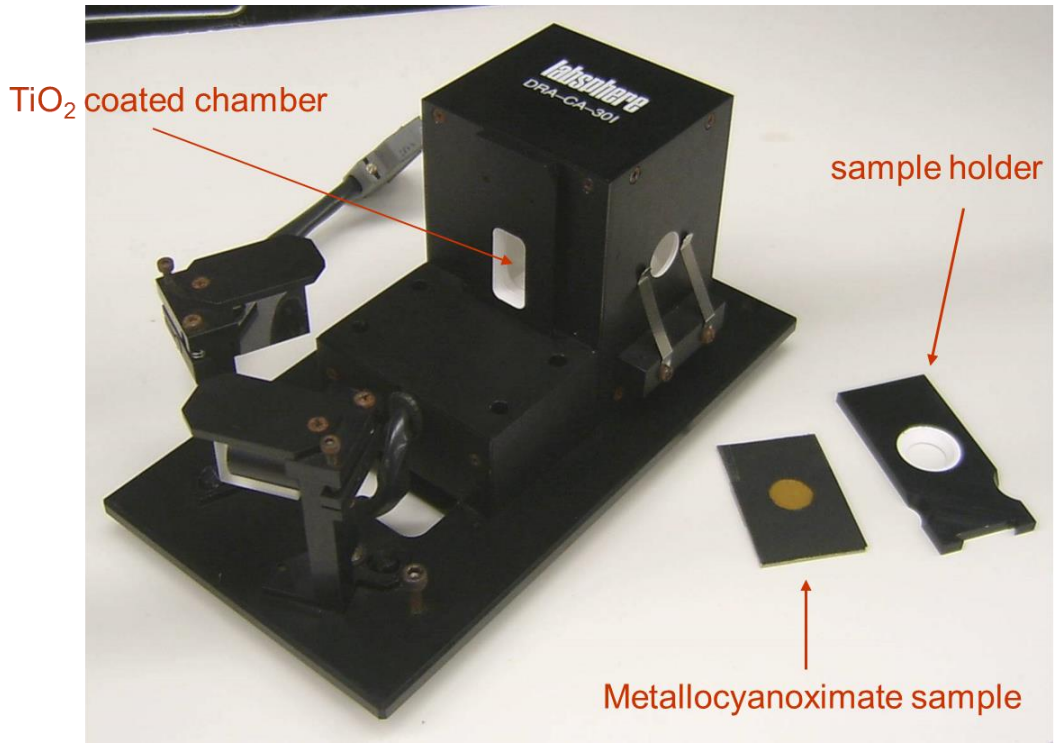

Appendix A-2. Experimental setup for recording the reflectance spectra of solid samples.

Appendix A-3. Metallocyanoximate sample adhered to a membrane Millipore with Scotch tape.

Appendix B

Data of TG/DSC Analysis

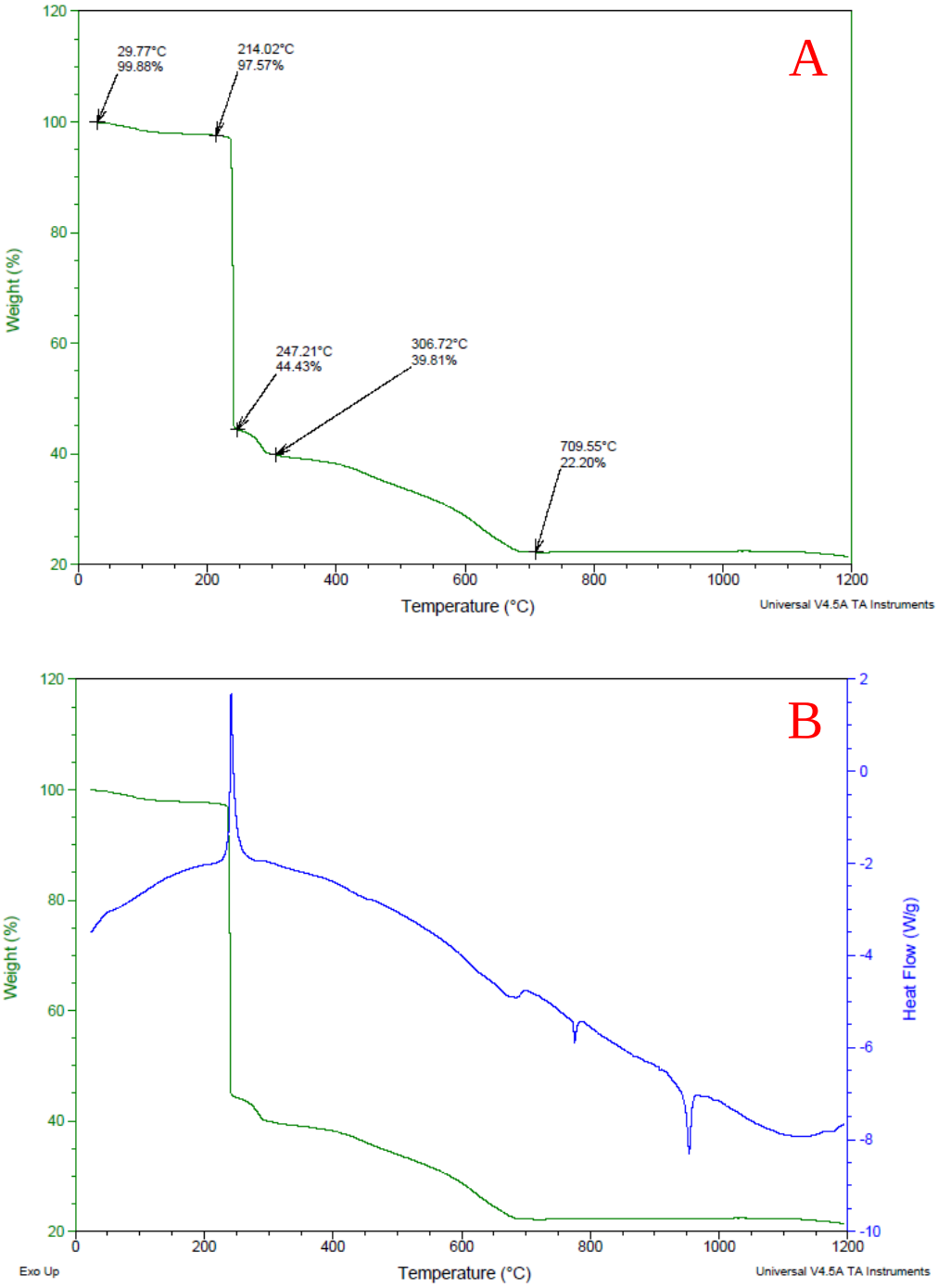

Appendix B-1. Results of thermal analysis study of $Cu(ACO)_2 \cdot H_2O$. Mass loss trace (A); Combined weight loss and the heat flow curves (B).

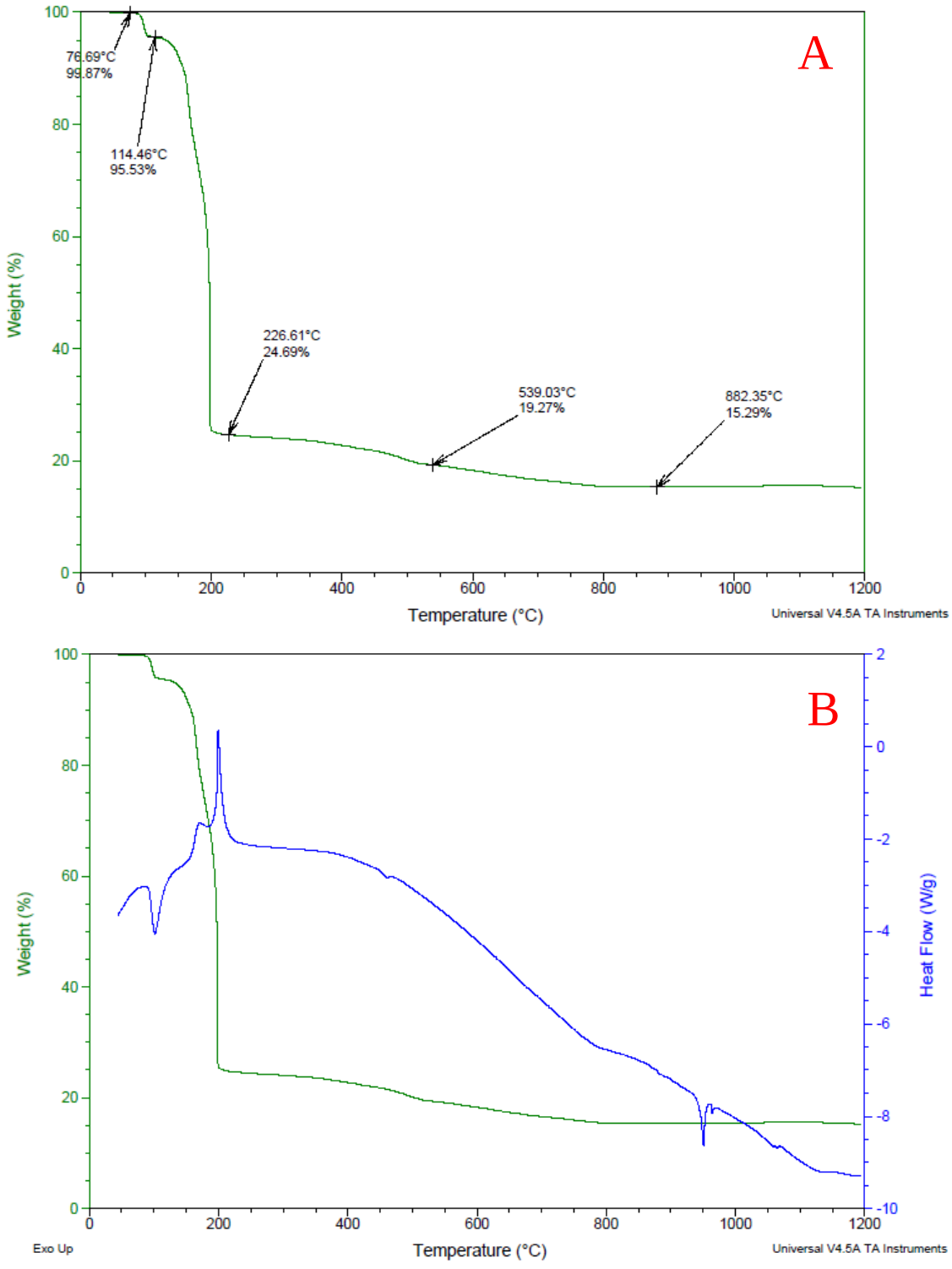

Appendix B-2. Results of thermal analysis study of $Ni(PiCO)_2 \cdot H_2O$. Mass loss trace (A); Combined weight loss and the heat flow curves (B).

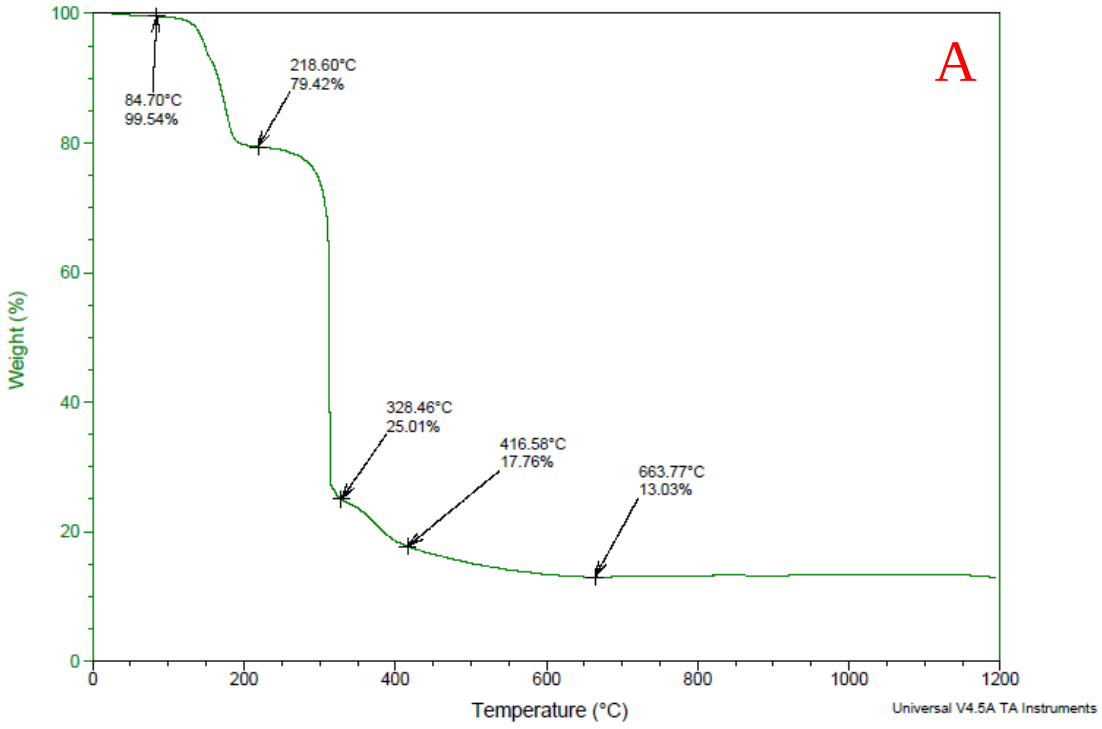

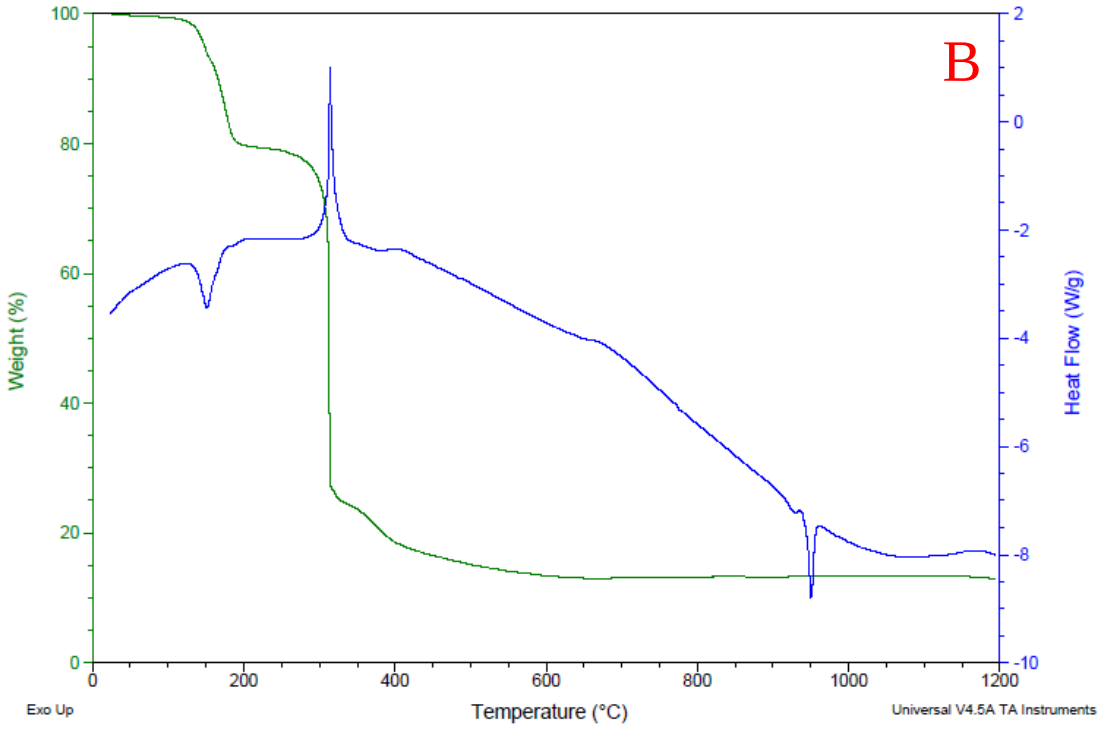

Appendix B-3. Results of thermal analysis study of $Cu(PiCO)_2$. Mass loss trace (A); Combined weight loss and the heat flow curves (B).

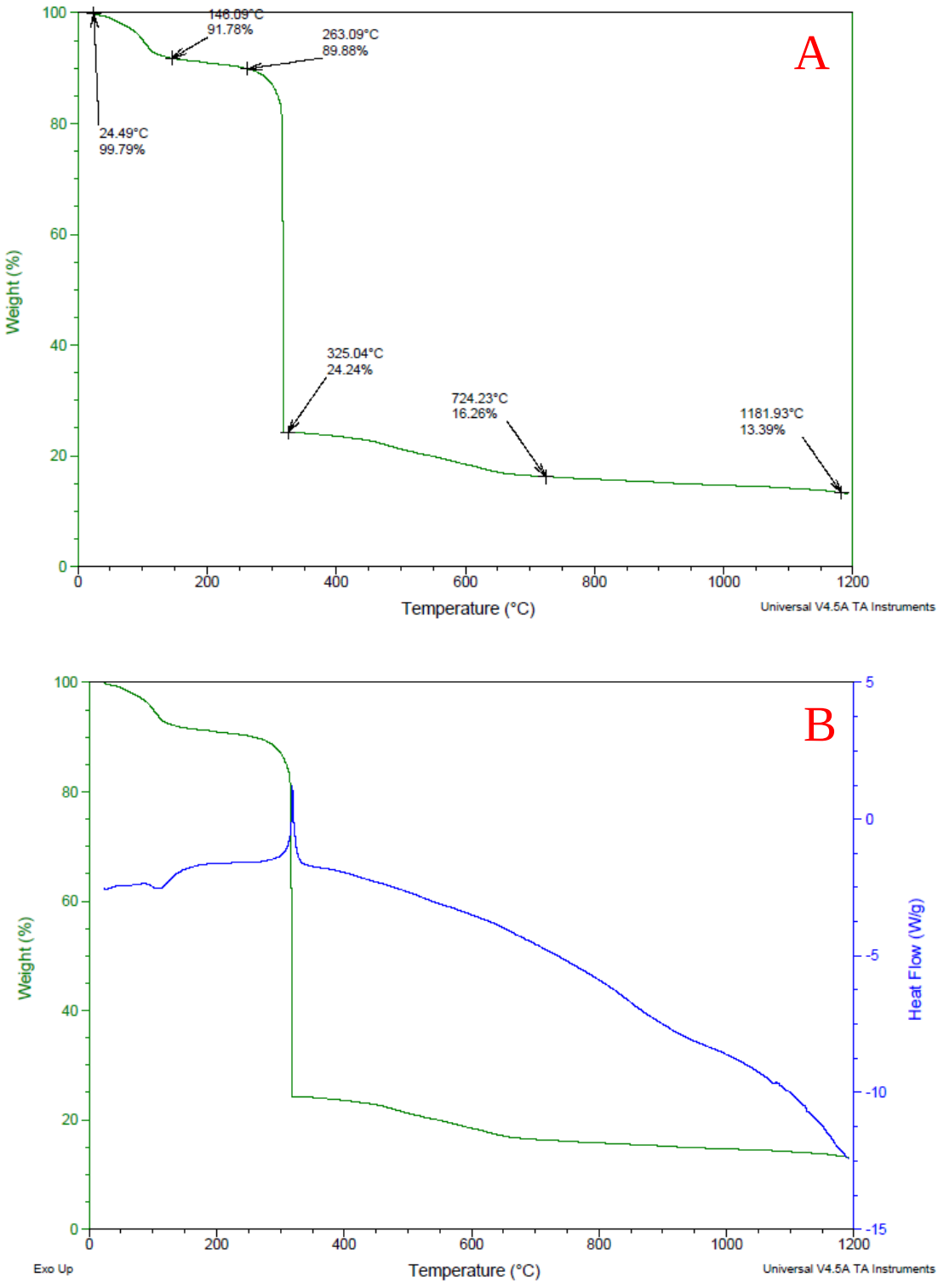

Appendix B-4. Results of thermal analysis study of $[Ni(2PCO)_2 \cdot 2H_2O] \cdot 2H_2O$. Mass loss trace (A); Combined weight loss and the heat flow curves (B).

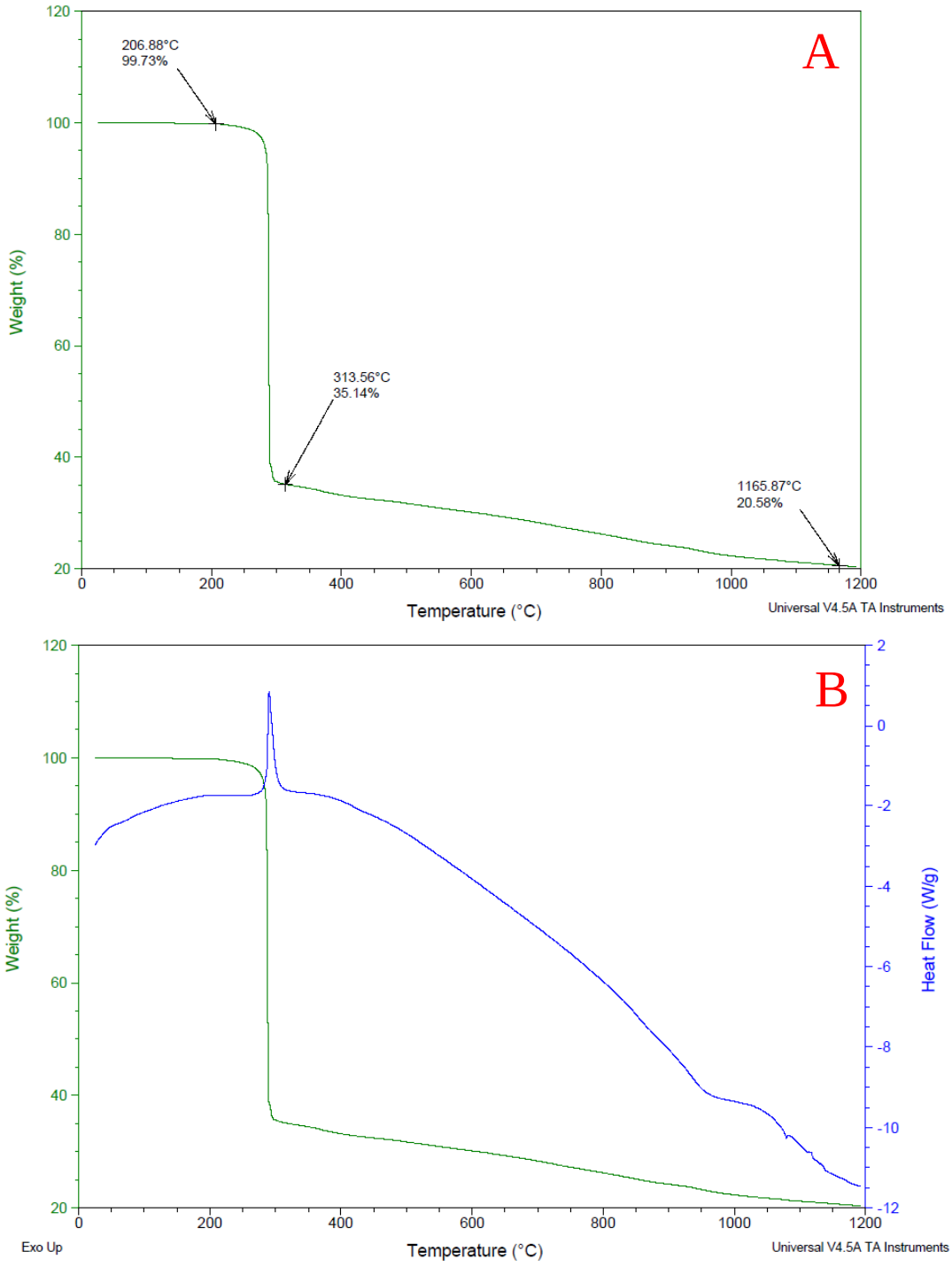

Appendix B-5. Results of thermal analysis study of $Cu(2PCO)_2$. Mass loss trace (A); Combined weight loss and the heat flow curves (B).

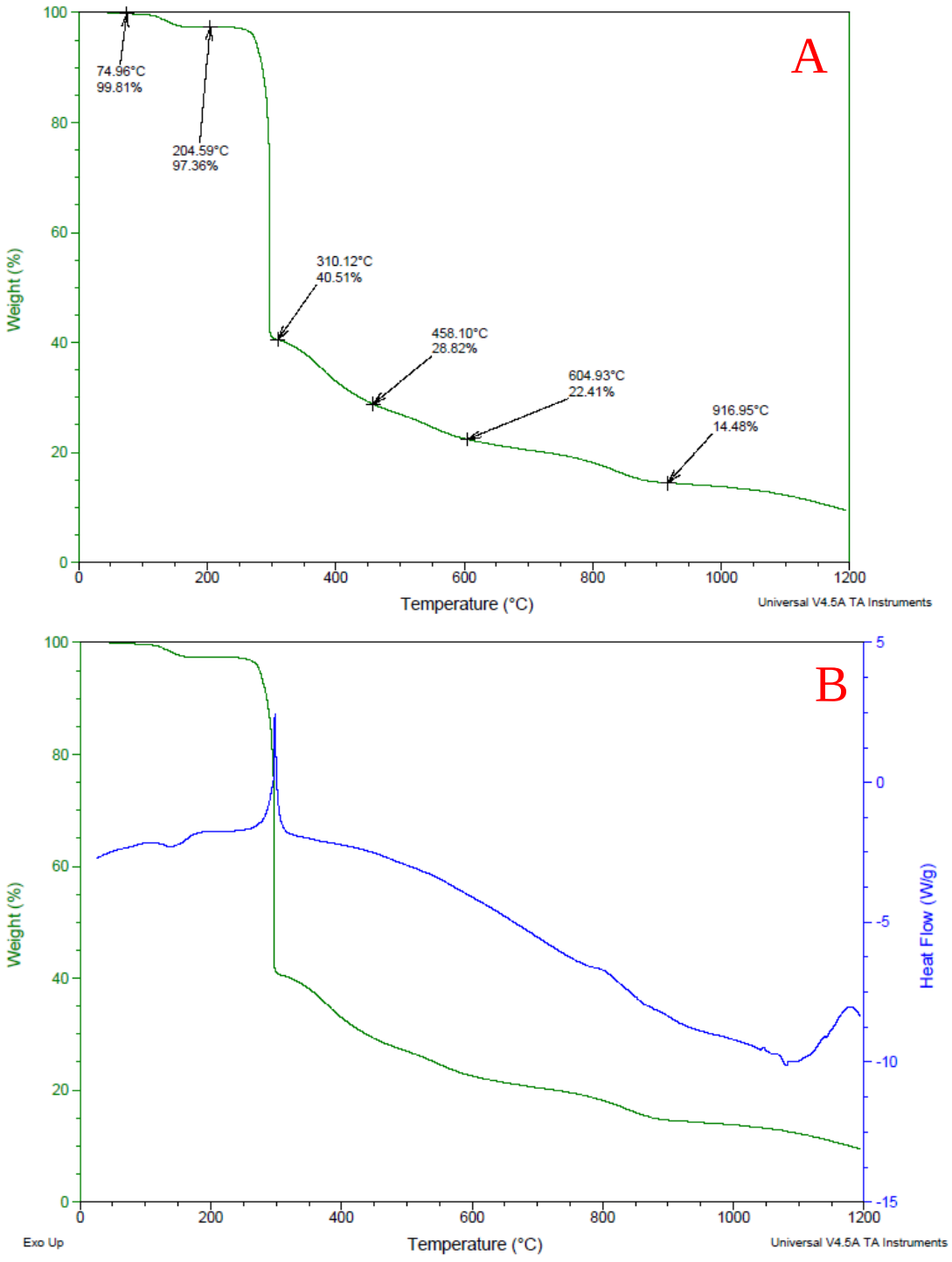

Appendix B-6. Results of thermal analysis study of $Ni(PyrCO)_2 \cdot 2H_2O$. Mass loss trace (A); Combined weight loss and the heat flow curves (B).

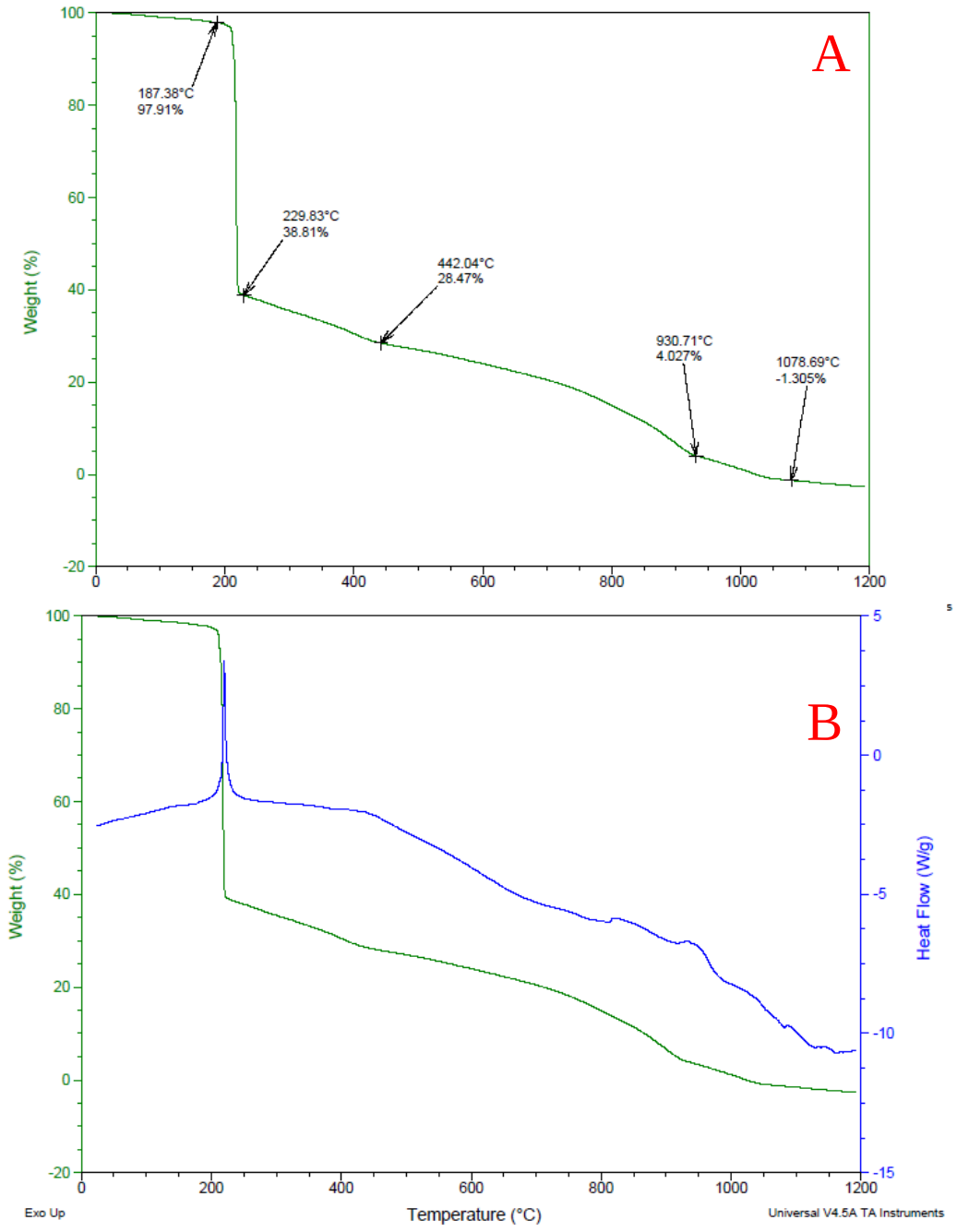

Appendix B-7. Results of thermal analysis study of $Cu(PyrCO)_2 \cdot H_2O$. Mass loss trace (A); Combined weight loss and the heat flow curves (B).

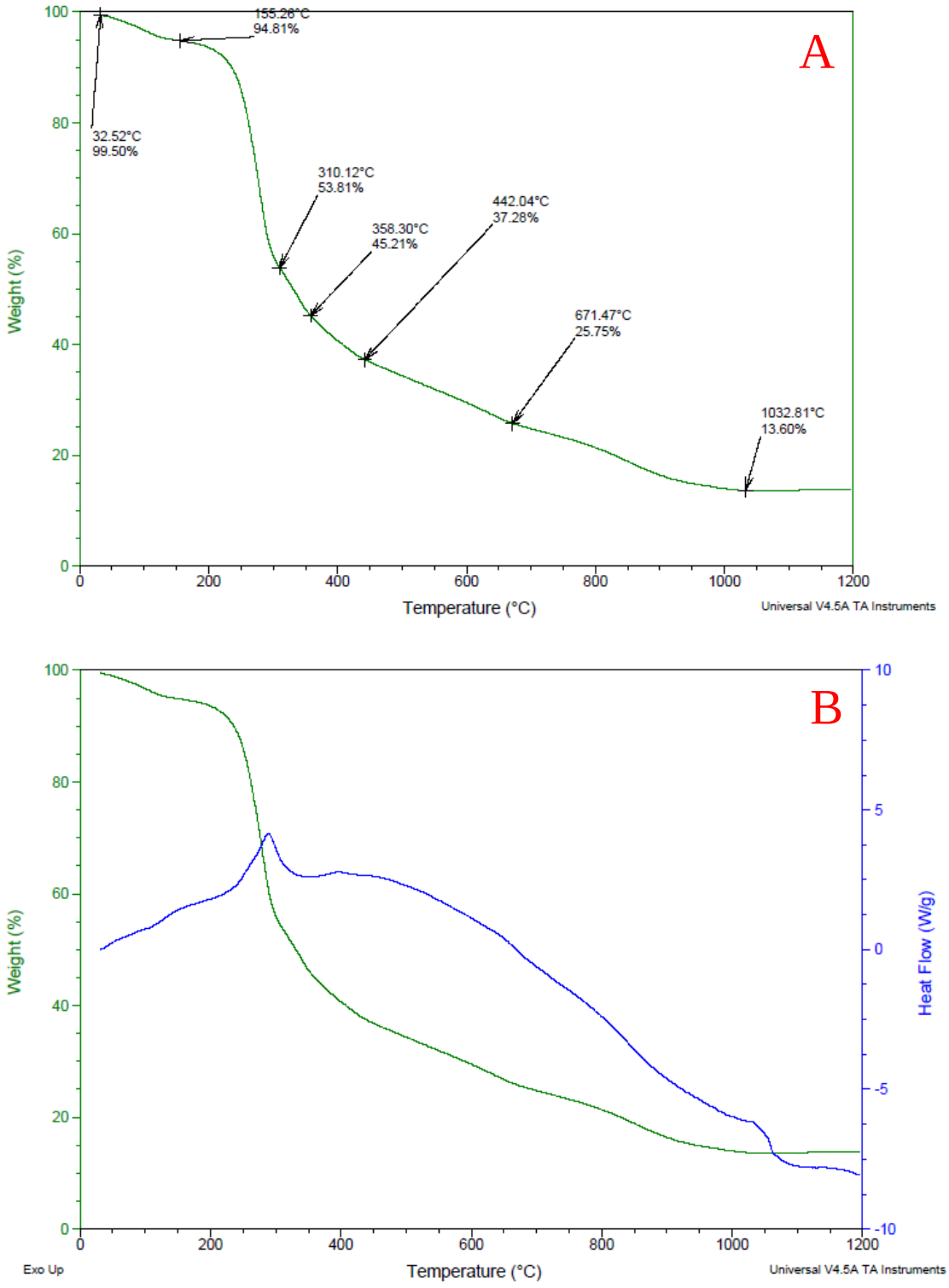

Appendix B-8. Results of thermal analysis study of $Ni(PiPCO)_2 \cdot 2H_2O$. Mass loss trace (A); Combined weight loss and the heat flow curves (B).

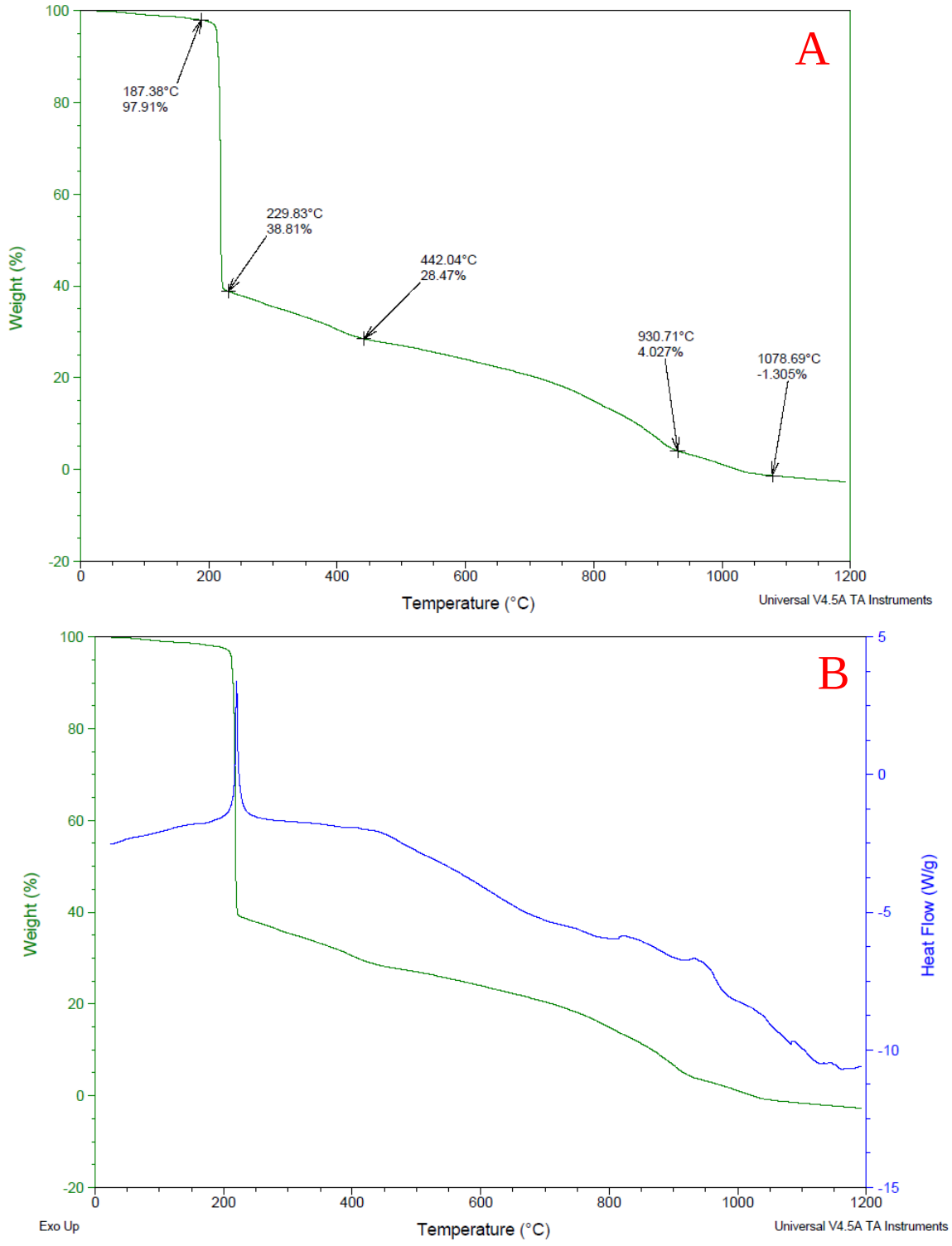

Appendix B-9. Results of thermal analysis study of $Cu(PiPCO)_2 \cdot H_2O$. Mass loss trace (A); Combined weight loss and the heat flow curves (B).

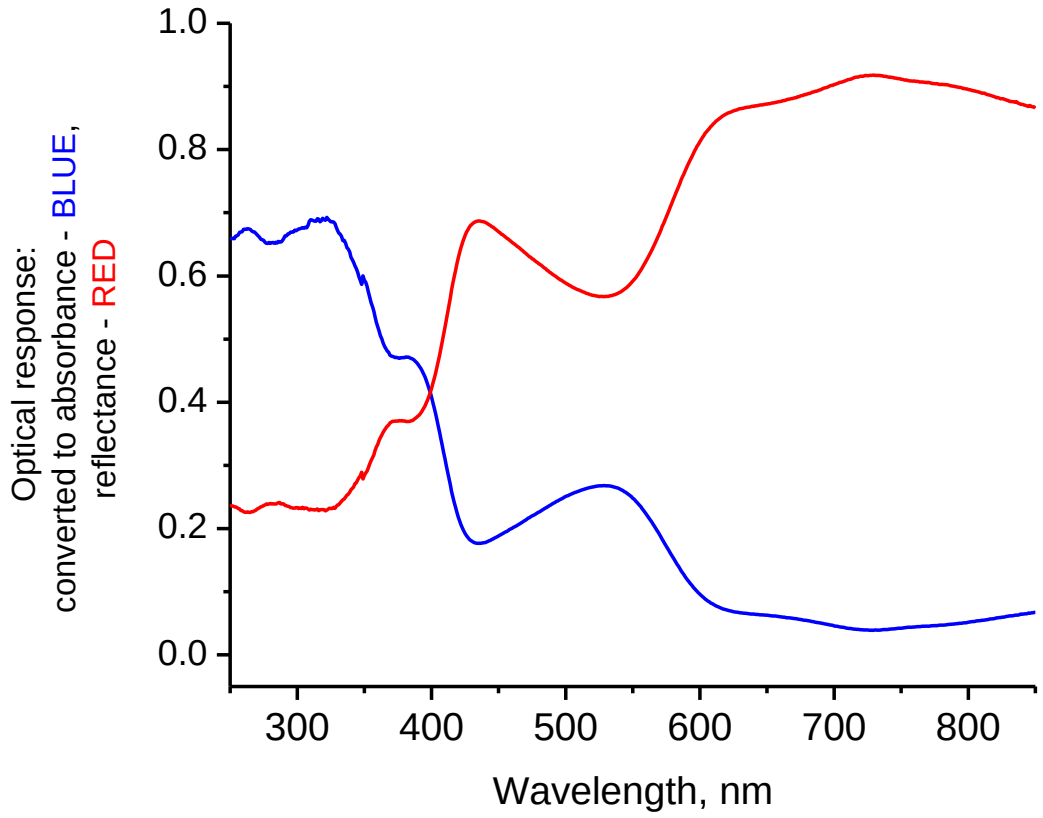

Appendix B-10. The solid state reflectance spectrum of powdery [$Ni(ACO)_2 \cdot 2H_2O$]: comparison of true reflectance spectrum (red trace) with converted into "absorbance" mode for convenient viewing and analysis (blue trace).

Appendix C

Crystal Data for Studied Complexes

HECO

Appendix C-1. Atomic coordinates and equivalent isotropic atomic displacement parameters ($Å^2$) for HECO.

U(eq) is defined as one third of the trace of the orthogonalized U_{ij} tensor.

	x/a	y/b	z/c	U(eq)
C1	0.2656(4)	0.41665(16)	0.4499(3)	0.0179(5)
C2	0.2403(4)	0.48828(17)	0.5816(3)	0.0199(5)
C3	0.2726(4)	0.45053(17)	0.2716(3)	0.0198(5)
C4	0.2719(6)	0.5919(2)	0.0939(3)	0.0318(7)
C5	0.2162(5)	0.6982(2)	0.1099(4)	0.0330(7)
N1	0.2799(3)	0.32326(14)	0.4783(2)	0.0220(5)
N2	0.2180(4)	0.54517(16)	0.6857(3)	0.0270(5)
O1	0.2710(3)	0.30200(14)	0.6454(2)	0.0266(4)
O2	0.2809(3)	0.39515(12)	0.1516(2)	0.0270(5)
O3	0.2682(3)	0.54768(11)	0.26378(19)	0.0217(4)

Appendix C-2. Hydrogen bond distances (Å) and angles (°) for HECO.

	Donor-H	Acceptor-H	Donor-Acceptor	Angle
O1-H1O1···O2	0.92(4)	1.76(4)	2.672(3)	178.(3)
C4-H4B···O2	0.98(3)	2.67(3)	3.565(4)	152.(2)
C4-H4A···N2	0.96(3)	2.72(3)	3.293(4)	119.(2)
C4-H4B···O2	0.98(3)	2.67(3)	3.565(4)	152.(2)

Appendix C-3. Anisotropic atomic displacement parameters ($Å^2$) for HECO.

The anisotropic atomic displacement factor exponent takes the form: $-2\pi^2[h^2 a^{*2} U_{11} + ... + 2 h k a^* b^* U_{12}]$.

	U_{11}	U_{22}	U_{33}	U_{23}	U_{13}	U_{12}
C1	0.0214(13)	0.0153(12)	0.0169(13)	-0.0021(9)	0.0012(9)	-0.0010(9)
C2	0.0222(13)	0.0185(12)	0.0187(12)	0.0040(10)	0.0001(9)	-0.0002(10)
C3	0.0235(13)	0.0181(12)	0.0180(13)	-0.0009(10)	0.0026(9)	-0.0016(10)
C4	0.055(2)	0.0241(15)	0.0163(14)	0.0055(11)	0.0067(13)	0.0014(13)
C5	0.0433(19)	0.0239(15)	0.0322(18)	0.0107(12)	0.0047(13)	0.0069(13)
N1	0.0264(11)	0.0198(10)	0.0202(11)	0.0034(8)	0.0045(8)	0.0001(9)
N2	0.0393(14)	0.0230(12)	0.0188(11)	-0.0016(9)	0.0023(9)	0.0016(10)
O1	0.0395(11)	0.0198(10)	0.0210(10)	0.0056(7)	0.0048(7)	0.0007(8)
O2	0.0432(11)	0.0201(9)	0.0185(10)	-0.0047(7)	0.0068(8)	-0.0008(8)
O3	0.0379(11)	0.0168(9)	0.0108(9)	0.0011(6)	0.0047(7)	-0.0003(7)

[Ni(ACO)$_2$·2H$_2$O]

Appendix C-4. Atomic coordinates and equivalent isotropic atomic displacement parameters (Å^2) for [Ni(ACO)$_2$·2H$_2$O].

	x/a	y/b	z/c	U(eq)
C1	0.5	0.0264(6)	0.37756(19)	0.0185(11)
C2	0.5	0.0999(7)	0.3209(2)	0.0272(13)
C3	0.5	0.1837(7)	0.6078(2)	0.0201(11)
N1	0.5	0.1437(6)	0.42233(17)	0.0259(11)
N2	0.5	0.1629(7)	0.27575(19)	0.0437(14)
N3	0.5	0.3142(6)	0.64864(17)	0.0243(10)
Ni1	0.5	0.0	0.5	0.0109(3)
O1	0.5	0.3280(5)	0.41405(16)	0.0468(12)
O2	0.5	0.2296(4)	0.55593(13)	0.0218(8)
O3W	0.2310(5)	0.0	0.5	0.0252(8)

Appendix C-5. Torsion angles (°) for [Ni(ACO)$_2$·2H$_2$O].

C2-C1-N1-O1	0.000(2)	C3-C1-N1-O1	180.0000(10)
C2-C1-N1-Ni1	180.0000(10)	C3-C1-N1-Ni1	0.0000(10)
N3-C3-O2-Ni1	180.000(2)	C1-C3-O2-Ni1	0.000(2)

Appendix C-6. Hydrogen bond distances (Å) and angles (°) for [Ni(ACO)$_2$·2H$_2$O].

	Donor-H	Acceptor-H	Donor-Acceptor	Angle
N3-H3B···N2	0.88	2.17	2.976(6)	152.2
N3-H3A···O1	0.88	2.04	2.860(5)	154.8
O3W-H1···O1	0.9583(11)	2.00(2)	2.900(4)	156.(4)

Appendix C-7. Anisotropic atomic displacement parameters ($Å^2$) for $[Ni(ACO)_2 \cdot 2H_2O]$.

The anisotropic atomic displacement factor exponent takes the form: $-2\pi^2[h^2 a^{*2} U_{11} + ... + 2 h k a^* b^* U_{12}]$

	U_{11}	U_{22}	U_{33}	U_{23}	U_{13}	U_{12}
C1	0.035(3)	0.012(2)	0.008(2)	-0.0001(17)	0	0
C2	0.055(4)	0.012(2)	0.015(3)	0.0012(19)	0	0
C3	0.035(3)	0.012(2)	0.013(2)	0.0003(18)	0	0
N1	0.056(3)	0.0089(18)	0.013(2)	0.0016(15)	0	0
N2	0.083(4)	0.027(2)	0.021(3)	0.004(2)	0	0
N3	0.049(3)	0.0113(19)	0.013(2)	-0.0034(16)	0	0
Ni1	0.0156(5)	0.0079(4)	0.0092(4)	0.0004(3)	0	0
O1	0.104(3)	0.0119(17)	0.0243(19)	0.0037(15)	0	0
O2	0.045(2)	0.0105(15)	0.0099(16)	-0.0017(13)	0	0
O3W	0.0164(18)	0.0193(16)	0.040(2)	-0.0013(18)	0	0

[Ni(2PCO)$_2$·2H$_2$O]

Appendix C-8. Atomic coordinates and equivalent isotropic atomic displacement parameters (Å^2) for [Ni(2PCO)$_2$·2H$_2$O].

U(eq) is defined as one third of the trace of the orthogonalized U_{ij} tensor.

	x/a	y/b	z/c	U(eq)
C1	0.4013(3)	0.7181(3)	0.20585(17)	0.0141(4)
C2	0.3094(3)	0.5610(3)	0.28403(18)	0.0179(4)
C3	0.5556(3)	0.8379(3)	0.25075(17)	0.0144(4)
C4	0.6332(4)	0.7968(3)	0.36678(18)	0.0198(4)
C5	0.7752(4)	0.9208(4)	0.40195(19)	0.0242(5)
C6	0.8351(4)	0.0824(4)	0.32208(19)	0.0228(5)
C7	0.7507(3)	0.1128(3)	0.20824(18)	0.0174(4)
N1	0.3456(3)	0.7640(3)	0.09369(15)	0.0137(3)
N2	0.2364(3)	0.4360(3)	0.34682(17)	0.0276(4)
N3	0.6160(3)	0.9931(3)	0.17188(14)	0.0141(3)
Ni1	0.5	0.0	0.0	0.01034(11)
O1	0.2045(2)	0.6620(2)	0.05355(13)	0.0183(3)
O3	0.2029(2)	0.2349(2)	0.05468(12)	0.0156(3)

Appendix C-9. Torsion angles (°) for [Ni(2PCO)$_2$·2H$_2$O].

N1-C1-C3-N3	3.0(3)	C2-C1-C3-N3	-175.11(17)
N1-C1-C3-C4	-177.55(18)	C2-C1-C3-C4	4.3(3)
N3-C3-C4-C5	0.5(3)	C1-C3-C4-C5	-178.92(18)
C3-C4-C5-C6	0.5(3)	C4-C5-C6-C7	-0.5(3)
C5-C6-C7-N3	-0.4(3)	C2-C1-N1-O1	-0.4(3)
C3-C1-N1-O1	-178.55(15)	C2-C1-N1-Ni1	179.42(14)

Appendix C-10. Anisotropic atomic displacement parameters ($Å^2$) for $[Ni(2PCO)_2 \cdot 2H_2O]$.

The anisotropic atomic displacement factor exponent takes the form: $-2\pi^2[h^2 a^{*2} U_{11} + ... + 2 h k a^* b^* U_{12}]$

	U_{11}	U_{22}	U_{33}	U_{23}	U_{13}	U_{12}
C1	0.0148(9)	0.0131(9)	0.0146(9)	0.0014(7)	-0.0010(7)	-0.0043(7)
C2	0.0193(10)	0.0184(10)	0.0179(10)	0.0015(8)	-0.0050(8)	-0.0071(8)
C3	0.0149(9)	0.0139(9)	0.0148(9)	0.0007(7)	-0.0020(7)	-0.0043(7)
C4	0.0239(11)	0.0226(10)	0.0156(10)	0.0039(8)	-0.0039(8)	-0.0111(8)
C5	0.0289(12)	0.0315(12)	0.0159(10)	0.0008(9)	-0.0083(8)	-0.0121(10)
C6	0.0237(11)	0.0282(11)	0.0223(11)	-0.0029(9)	-0.0069(8)	-0.0143(9)
C7	0.0181(10)	0.0185(10)	0.0177(10)	-0.0001(8)	-0.0029(8)	-0.0083(8)
N1	0.0132(8)	0.0108(7)	0.0188(8)	0.0001(6)	-0.0052(6)	-0.0044(6)
N2	0.0330(11)	0.0283(10)	0.0256(10)	0.0076(8)	-0.0054(8)	-0.0161(9)
N3	0.0133(8)	0.0143(8)	0.0151(8)	0.0008(6)	-0.0021(6)	-0.0042(6)
Ni1	0.0118(18)	0.0081(17)	0.0127(18)	0.0010(12)	-0.00362(12)	-0.0050(12)
O1	0.0192(7)	0.0144(7)	0.0256(8)	0.0027(6)	-0.0105(6)	-0.0094(6)
O3	0.0132(6)	0.0115(6)	0.0225(7)	-0.0007(5)	-0.0052(5)	-0.0021(5)

Appendix C-11. Hydrogen bond distances (Å) and angles (°) for $[Ni(2PCO)_2 \cdot 2H_2O]$.

	Donor-H	Acceptor-H	Donor-Acceptor	Angle
O3-H4B···O1	0.87	1.82	2.6748(19)	166.2
O3-H3B···O1	0.87	1.88	2.7402(18)	172.2

$[Ni(AACO)(H_2O)_3]_2 \cdot H_2O$

Appendix C-12. Atomic coordinates and equivalent isotropic atomic displacement parameters ($Å^2$) for $[Ni(AACO)(H_2O)_3]_2 \cdot H_2O$.

U(eq) is defined as one third of the trace of the orthogonalized U_{ij} tensor

	x/a	y/b	z/c	U(eq)
O7W	0.23977(8)	0.18392(19)	0.29011(9)	0.0177(2)
C1	0.07043(9)	0.7692(2)	0.51635(9)	0.0098(2)
C2	0.05444(9)	0.8255(2)	0.59263(9)	0.0119(2)
C3	0.99273(9)	0.6967(2)	0.43391(9)	0.0104(2)
N1	0.15191(8)	0.77220(19)	0.51616(8)	0.0104(2)
N2	0.03779(9)	0.8667(2)	0.65209(9)	0.0166(2)
Ni1	0.15008(2)	0.65279(3)	0.39873(2)	0.00889(5)
O1	0.21977(7)	0.83527(18)	0.58842(7)	0.0134(2)
O2	0.01378(7)	0.64046(17)	0.37105(7)	0.01219(19)
O3	0.91423(7)	0.69494(18)	0.43213(7)	0.0141(2)
O4W	0.12988(9)	0.9453(2)	0.34298(9)	0.0206(3)
O5W	0.16586(9)	0.3521(2)	0.45265(9)	0.0167(2)
O6W	0.12845(9)	0.5213(2)	0.28050(8)	0.0207(3)

Appendix C-13. Torsion angles (°) for $[Ni(AACO)(H_2O)_3]_2 \cdot H_2O$**.**

N1-C1-C3-O3	-179.11(15)	C2-C1-C3-O3	2.9(2)
N1-C1-C3-O2	1.2(2)	C2-C1-C3-O2	-176.72(14)
C2-C1-N1-O1	-2.0(2)	C3-C1-N1-O1	-179.86(13)
C2-C1-N1-Ni1	174.22(12)	C3-C1-N1-Ni1	-3.68(17)
C1-N1-O1-Ni1	179.19(11)	Ni1-N1-O1-Ni1	3.91(19)
O3-C3-O2-Ni1	-177.61(13)	C1-C3-O2-Ni1	2.02(17)

Appendix C-14. Anisotropic atomic displacement parameters ($Å^2$) for $[Ni(AACO)(H_2O)_3]_2 \cdot H_2O$

The anisotropic atomic displacement factor exponent takes the form: $-2\pi^2[h^2 a^{*2} U_{11} + ... + 2 h k a^* b^* U_{12}]$

	U_{11}	U_{22}	U_{33}	U_{23}	U_{13}	U_{12}
O7W	0.0132(5)	0.0210(6)	0.0190(6)	-0.0012(5)	0.0064(5)	0.0006(5)
C1	0.0084(6)	0.0100(6)	0.0106(6)	0.0000(5)	0.0029(5)	-0.0003(5)
C2	0.0086(6)	0.0123(7)	0.0136(7)	0.0012(5)	0.0029(5)	-0.0002(5)
C3	0.0090(6)	0.0093(6)	0.0123(6)	0.0011(5)	0.0031(5)	-0.0006(5)
N1	0.0086(5)	0.0117(6)	0.0099(5)	0.0003(5)	0.0022(4)	-0.0002(4)
N2	0.0147(6)	0.0203(7)	0.0157(6)	0.0008(6)	0.0065(5)	0.0021(5)
Ni1	0.00662(9)	0.0119(10)	0.0081(9)	-0.0011(7)	0.0024(7)	0.0000(7)
O1	0.0078(5)	0.0213(6)	0.0097(5)	-0.0039(4)	0.0016(4)	-0.0020(4)
O2	0.0081(5)	0.0166(5)	0.0112(5)	-0.0022(4)	0.0027(4)	-0.0005(4)
O3	0.0088(5)	0.0194(6)	0.0145(5)	0.0012(4)	0.0045(4)	-0.0009(4)
O4W	0.0165(6)	0.0261(7)	0.0220(6)	0.0104(5)	0.0115(5)	0.0069(5)
O5W	0.0130(5)	0.0180(6)	0.0208(6)	-0.0003(5)	0.0091(5)	0.0011(5)
O6W	0.0169(6)	0.0280(7)	0.0111(5)	-0.0061(5)	-0.0002(4)	0.0092(5)

Appendix C-15. Hydrogen bond distances (Å) and angles (°) for $[Ni(AACO)(H_2O)_3]_2 \cdot H_2O$.

	Donor-H	Acceptor-H	Donor-Acceptor	Angle
O7W-H7B...O3	0.9582(10)	1.876(5)	2.8202(17)	168.1(19)
O6W-H6B...O7W	0.9582(10)	1.851(8)	2.7852(18)	164.(2)
O5W-H5B...O3	0.9582(10)	1.761(3)	2.7157(17)	174.(2)
O4W-H4B...N2	0.9581(10)	2.155(17)	2.983(2)	144.(2)
O5W-H5A...O5W	0.9583(10)	2.02(4)	2.829(3)	141.(5)
O4W-H4A...O7W	0.9582(10)	1.794(5)	2.7435(19)	171.(2)

$K_2[Ni_3(AACO)_4(H_2O)_4]\cdot 4H_2O$

Appendix C-16. Atomic coordinates and equivalent isotropic atomic displacement parameters ($Å^2$) for $K_2[Ni_3(AACO)_4(H_2O)_4]\cdot 4H_2O$.

U(eq) is defined as one third of the trace of the orthogonalized U_{ij} tensor.

	x/a	y/b	z/c	U(eq)
C1	0.6254(6)	0.2527(9)	0.0366(3)	0.0188(14)
C2	0.6450(6)	0.3207(9)	0.1015(3)	0.0178(14)
C3	0.4905(6)	0.2517(9)	0.0042(3)	0.0199(14)
C4	0.8279(6)	0.9376(8)	0.8214(3)	0.0147(13)
C5	0.9469(6)	0.8810(9)	0.7843(3)	0.0176(13)
C6	0.6846(6)	0.9300(9)	0.7956(3)	0.0195(14)
K1	0.36416(14)	0.9176(2)	0.73603(6)	0.0214(3)
N1	0.7258(5)	0.1752(7)	0.0038(2)	0.0171(11)
N2	0.6643(5)	0.3727(8)	0.1541(3)	0.0258(13)
N3	0.8431(5)	0.9995(7)	0.8809(2)	0.0168(11)
N4	0.0436(6)	0.8359(8)	0.7573(2)	0.0244(13)
Ni1	0.66721(7)	0.10163(11)	0.91480(3)	0.0135(2)
Ni2	0.0	0.0	0.0	0.0129(3)
O1	0.8473(4)	0.1673(6)	0.03091(19)	0.0200(10)
O2	0.4866(4)	0.1841(6)	0.94577(19)	0.0199(10)
O3	0.3876(4)	0.3132(6)	0.03422(19)	0.0220(10)
O4	0.9670(4)	0.0136(6)	0.90616(18)	0.0192(10)
O5	0.5928(4)	0.9923(6)	0.83443(19)	0.0194(10)
O6	0.6640(4)	0.8632(6)	0.7401(2)	0.0240(10)
O1S	0.7306(5)	0.4118(7)	0.8804(2)	0.0217(10)
O2S	0.1233(5)	0.2821(7)	0.9920(2)	0.0250(11)
O3S	0.2518(5)	0.6205(7)	0.6558(2)	0.0239(11)
O4S	0.4766(5)	0.0133(8)	0.6115(2)	0.0232(11)

Appendix C-17. Anisotropic atomic displacement parameters ($Å^2$) for $K_2[Ni_3(AACO)_4(H_2O)_4]\cdot 4H_2O$.

The anisotropic atomic displacement factor exponent takes the form: $-2\pi^2[h^2 a^{*2} U_{11} + ... + 2 h k a^* b^* U_{12}]$

	U_{11}	U_{22}	U_{33}	U_{23}	U_{13}	U_{12}
C1	0.021(3)	0.014(3)	0.021(3)	-0.003(3)	0.000(3)	-0.001(3)
C2	0.009(3)	0.017(3)	0.027(4)	0.001(3)	0.004(3)	0.002(3)
C3	0.023(4)	0.018(3)	0.019(4)	0.000(3)	0.001(3)	0.003(3)
C4	0.018(3)	0.016(3)	0.011(3)	-0.003(2)	0.000(2)	-0.002(3)
C5	0.017(3)	0.020(3)	0.015(3)	0.000(3)	-0.007(3)	-0.001(3)
C6	0.015(3)	0.019(4)	0.024(4)	0.001(3)	0.002(3)	0.000(3)
K2	0.0194(7)	0.0237(8)	0.0210(8)	-0.0003(6)	-0.0003(6)	-0.0005(6)
N1	0.013(3)	0.020(3)	0.018(3)	0.004(2)	0.001(2)	0.003(2)
N2	0.019(3)	0.030(3)	0.029(3)	-0.004(3)	0.001(2)	0.002(2)
N3	0.016(3)	0.017(3)	0.017(3)	0.001(2)	-0.005(2)	0.004(2)
N4	0.024(3)	0.029(3)	0.021(3)	0.003(2)	0.003(3)	0.004(3)
Ni1	0.0097(4)	0.0182(4)	0.0125(4)	-0.0020(3)	-0.0006(3)	0.0017(3)
Ni2	0.0097(6)	0.0172(6)	0.0117(6)	-0.0012(4)	-0.0009(4)	0.0023(5)
O1	0.010(2)	0.026(3)	0.024(2)	-0.004(19)	-0.008(18)	0.0036(18)
O2	0.009(2)	0.031(3)	0.020(2)	-0.002(2)	0.0004(17)	-0.0014(19)
O3	0.019(2)	0.028(3)	0.019(2)	-0.006(2)	0.0021(19)	0.007(2)
O4	0.012(2)	0.031(3)	0.014(2)	0.0005(19)	-0.003(18)	0.0046(19)
O5	0.013(2)	0.024(2)	0.021(2)	-0.001(19)	-0.000(18)	-0.0004(19)
O6	0.021(2)	0.034(3)	0.017(2)	-0.007(2)	-0.002(19)	-0.004(2)
O1S	0.028(3)	0.022(3)	0.016(2)	-0.007(2)	0.002(2)	0.001(2)
O2S	0.018(3)	0.029(3)	0.028(3)	0.006(2)	-0.006(2)	0.000(2)
O3S	0.018(3)	0.028(3)	0.026(3)	0.002(2)	0.002(2)	-0.002(2)
O4S	0.018(3)	0.026(3)	0.026(3)	0.003(2)	0.001(2)	-0.002(2)

$K_2[Cu_3(AACO)_4(H_2O)_4]\cdot 4H_2O$

Appendix C-18. Atomic coordinates and equivalent isotropic atomic displacement parameters ($Å^2$) for $K_2[Cu_3(AACO)_4(H_2O)_4]\cdot 4H_2O$.

U(eq) is defined as one third of the trace of the orthogonalized U_{ij} tensor.

	x/a	y/b	z/c	U(eq)
C1	0.6252(4)	0.7490(6)	0.03723(19)	0.0101(8)
C2	0.6449(4)	0.6794(6)	0.10195(19)	0.0120(8)
C3	0.4885(4)	0.7478(6)	0.00404(19)	0.0110(8)
C4	0.8291(4)	0.0630(6)	0.82150(19)	0.0109(8)
C5	0.9474(4)	0.1202(6)	0.78423(19)	0.0117(8)
C6	0.6855(4)	0.0701(6)	0.79536(19)	0.0125(8)
Cu1	0.66734(5)	0.89854(7)	0.91477(2)	0.00992(13)
Cu2	0.0	0.0	0.0	0.00986(16)
K1	0.36431(9)	0.08223(14)	0.73601(4)	0.0147(2)
N1	0.7259(3)	0.8251(5)	0.00379(15)	0.0090(7)
N2	0.6647(4)	0.6297(5)	0.15424(17)	0.0178(8)
N3	0.8431(3)	0.0001(5)	0.88092(15)	0.0100(7)
N4	0.0440(4)	0.1633(6)	0.75731(17)	0.0193(8)
O1	0.8474(3)	0.8312(4)	0.03057(13)	0.0130(6)
O2	0.4866(3)	0.8169(4)	0.94620(13)	0.0109(6)
O3	0.3887(3)	0.6870(4)	0.03440(13)	0.0148(6)
O4	0.9663(3)	0.9856(4)	0.90599(13)	0.0134(6)
O5	0.5940(3)	0.0082(4)	0.83435(13)	0.0132(6)
O6	0.6637(3)	0.1366(4)	0.74028(13)	0.0154(6)
O3W	0.2518(3)	0.3798(5)	0.65603(15)	0.0182(7)
O4W	0.4762(3)	0.9863(5)	0.61149(15)	0.0172(6)
O1W	0.8767(3)	0.2815(5)	0.00813(16)	0.0187(7)
O2W	0.7309(3)	0.5873(5)	0.88055(14)	0.0149(6)

Appendix C-19. Torsion angles (°) for $K_2[Cu_3(AACO)_4(H_2O)_4]\cdot 4H_2O$.

Angle	(°)	Angle	(°)
N1-C1-C3-O3	-176.4(4)	C2-C1-C3-O3	1.2(6)
N1-C1-C3-O2	1.6(5)	C2-C1-C3-O2	179.3(4)
N3-C4-C6-O6	176.8(4)	C5-C4-C6-O6	-3.6(6)
N3-C4-C6-O5	-1.7(5)	C5-C4-C6-O5	177.9(4)
C2-C1-N1-O1	1.9(6)	C3-C1-N1-O1	179.5(3)
C2-C1-N1-Cu1	177.9(3)	C3-C1-N1-Cu1	-4.4(4)
C5-C4-N3-O4	-1.4(6)	C6-C4-N3-O4	178.2(3)
C5-C4-N3-Cu1	-172.1(3)	C6-C4-N3-Cu1	7.5(4)
C1-N1-O1-Cu2	-162.9(3)	Cu1-N1-O1-Cu2	21.9(4)
O3-C3-O2-Cu1	-180.0(3)	C1-C3-O2-Cu1	2.1(4)
C4-N3-O4-Cu2	154.6(3)	Cu1-N3-O4-Cu2	-36.6(4)
O6-C6-O5-Cu1	176.4(3)	C4-C6-O5-Cu1	-5.2(4)
O6-C6-O5-K1	2.1(4)	C4-C6-O5-K1	-179.4(3)
O5-C6-O6-K1	-2.2(5)	C4-C6-O6-K1	179.4(3)

Appendix C-20. Hydrogen bond distances (Å) and angles (°) for $K_2[Cu_3(AACO)_4(H_2O)_4]\cdot 4H_2O$.

	Donor-H	Acceptor-H	Donor-Acceptor	Angle
O3W-H8···O2	0.84(4)	2.34(4)	3.148(4)	162.(6)
O3W-H7···O4	0.85(4)	2.32(4)	3.122(4)	157.(5)
O4W-H6···O1	0.85(4)	2.19(4)	2.979(4)	155.(5)
O4W-H5···O2W	0.86(4)	2.11(4)	2.936(4)	162.(5)
O2W-H4···O6	0.88(4)	1.88(4)	2.720(4)	160.(5)
O2W-H3···O3	0.83(4)	2.12(4)	2.805(4)	140.(4)
O1W-H2···O4W	0.86(4)	1.96(4)	2.805(4)	166.(6)
O1W-H1···O3	0.88(4)	1.88(4)	2.730(4)	162.(5)

Appendix C-21. Anisotropic atomic displacement parameters ($Å^2$) for $K_2[Cu_3(AACO)_4(H_2O)_4]\cdot 4H_2O$.

The anisotropic atomic displacement factor exponent takes the form: $-2\pi^2[h^2 a^{*2} U_{11} + ... + 2 h k a^* b^* U_{12}]$

	U_{11}	U_{22}	U_{33}	U_{23}	U_{13}	U_{12}
C1	0.0072(18)	0.009(2)	0.014(2)	0.0006(15)	-0.000(15)	-0.000(15)
C2	0.0096(19)	0.0095(19)	0.017(2)	0.0009(16)	0.0019(16)	-0.000(15)
C3	0.0091(18)	0.0116(19)	0.0122(19)	0.0009(15)	0.0020(15)	0.0002(15)
C4	0.0138(19)	0.0065(19)	0.0123(19)	-0.002(15)	-0.000(16)	-0.000(15)
C5	0.0146(19)	0.011(2)	0.0100(19)	0.0034(16)	-0.001(15)	-0.000(16)
C6	0.0140(19)	0.012(2)	0.0110(19)	-0.001(16)	-0.002(16)	0.0005(16)
Cu1	0.0057(2)	0.0138(3)	0.0103(2)	0.0016(2)	-0.001(17)	-0.000(19)
Cu2	0.0058(3)	0.0138(4)	0.0100(3)	0.0018(3)	-0.0015(2)	-0.0021(3)
K1	0.0129(4)	0.0150(5)	0.0163(4)	-0.0007(4)	-0.0014(3)	-0.0004(4)
N1	0.0060(15)	0.0077(16)	0.0133(17)	-0.001(13)	-0.000(13)	-0.001(12)
N2	0.0177(18)	0.018(2)	0.0179(19)	0.0029(15)	-0.002(15)	-0.001(15)
N3	0.0078(15)	0.0120(17)	0.0102(16)	-0.000(14)	-0.004(12)	0.0004(13)
N4	0.021(2)	0.021(2)	0.0165(19)	0.0010(15)	0.0051(16)	-0.004(16)
O1	0.0058(13)	0.0169(15)	0.0163(15)	0.0063(12)	-0.004(11)	-0.003(11)
O2	0.0072(13)	0.0129(14)	0.0127(14)	0.0026(12)	-0.002(11)	-0.002(11)
O3	0.0056(13)	0.0214(16)	0.0174(15)	0.0049(13)	0.0012(11)	-0.002(12)
O4	0.0060(13)	0.0207(16)	0.0134(14)	0.0023(12)	-0.003(11)	0.0004(12)
O5	0.0077(13)	0.0201(15)	0.0118(14)	0.0037(12)	-0.000(11)	0.0009(12)
O6	0.0135(14)	0.0237(17)	0.0091(14)	0.0053(12)	-0.001(11)	0.0010(12)
O3W	0.0132(15)	0.0201(17)	0.0212(17)	0.0001(14)	0.0018(13)	0.0001(13)
O4W	0.0145(16)	0.0162(16)	0.0210(16)	-0.001(14)	0.0001(13)	-0.002(13)
O1W	0.0118(15)	0.0171(17)	0.0271(18)	-0.008(14)	-0.005(13)	0.0048(13)
O2W	0.0171(15)	0.0131(15)	0.0146(15)	0.0007(13)	0.0037(12)	-0.002(13)

$K_2[Cu(AACO)_2H_2O]\cdot 2H_2O$

Appendix C-22. Atomic coordinates and equivalent isotropic atomic displacement parameters ($Å^2$) for $K_2[Cu(AACO)_2H_2O]\cdot 2H_2O$.

U(eq) is defined as one third of the trace of the orthogonalized U_{ij} tensor.

	x/a	y/b	z/c	U(eq)
C1	0.66581(16)	0.17236(11)	0.16717(11)	0.0087(2)
C2	0.77344(17)	0.26145(12)	0.20161(11)	0.0112(2)
C3	0.49014(17)	0.18744(11)	0.11140(11)	0.0093(2)
C4	0.39243(16)	0.76968(11)	0.09533(11)	0.0089(2)
C5	0.28061(17)	0.68259(12)	0.06298(11)	0.0111(2)
C6	0.56688(16)	0.75149(11)	0.14672(11)	0.0085(2)
Cu2	0.53038(2)	0.97010(2)	0.13669(2)	0.00805(4)
K1	0.86027(4)	0.88574(3)	0.38152(3)	0.01362(6)
K2	0.89746(4)	0.88641(3)	0.06412(2)	0.01154(6)
N1	0.71632(14)	0.07217(10)	0.18030(10)	0.0087(2)
N2	0.86291(17)	0.33136(12)	0.23015(12)	0.0175(3)
N3	0.34629(14)	0.87148(10)	0.07871(9)	0.0088(2)
N4	0.19143(16)	0.61242(11)	0.03690(12)	0.0164(2)
O1	0.86640(12)	0.04853(9)	0.22512(9)	0.01163(19)
O2	0.41095(12)	0.10002(8)	0.08054(9)	0.01152(19)
O3	0.43197(13)	0.27896(9)	0.09695(9)	0.0135(2)
O4	0.19999(12)	0.89745(9)	0.03364(9)	0.01267(19)
O5	0.65560(12)	0.83601(8)	0.16756(8)	0.00965(18)
O6	0.61936(13)	0.65787(8)	0.16696(9)	0.01154(19)
O1W	0.52508(14)	0.97125(9)	0.30427(9)	0.0140(2)
O2W	0.89779(14)	0.66025(11)	0.36033(9)	0.0169(2)
O3W	0.89155(14)	0.84144(10)	0.59006(9)	0.0160(2)

Appendix C-23. Anisotropic atomic displacement parameters ($Å^2$) for $K_2[Cu(AACO)_2H_2O]\cdot 2H_2O$.

The anisotropic atomic displacement factor exponent takes the form: $-2\pi^2[h^2 a^{*2} U_{11} + ... + 2 h k a^* b^* U_{12}]$

	U_{11}	U_{22}	U_{33}	U_{23}	U_{13}	U_{12}
C1	0.0071(5)	0.0092(5)	0.0093(5)	-0.0002(4)	0.0017(4)	-0.0005(4)
C2	0.0099(6)	0.0115(6)	0.0111(6)	0.0006(5)	0.0019(5)	0.0004(5)
C3	0.0085(5)	0.0107(6)	0.0083(5)	0.0001(4)	0.0020(4)	0.0003(4)
C4	0.0071(5)	0.0096(6)	0.0090(5)	-0.0005(4)	0.0009(4)	-0.0014(4)
C5	0.0096(6)	0.0124(6)	0.0110(6)	0.0002(5)	0.0028(5)	0.0001(5)
C6	0.0080(5)	0.0098(6)	0.0082(5)	0.0007(4)	0.0032(4)	0.0004(4)
Cu2	0.0056(7)	0.00720(7)	0.01030(8)	0.00039(6)	0.00112(6)	-0.0002(5)
K1	0.013(13)	0.0143(14)	0.0112(13)	0.0016(10)	0.0009(10)	0.0003(10)
K2	0.008(12)	0.0147(13)	0.0108(12)	0.0005(10)	0.0026(10)	0.0012(10)
N1	0.0063(5)	0.0106(5)	0.0095(5)	0.0006(4)	0.0027(4)	0.0001(4)
N2	0.0162(6)	0.0160(6)	0.0179(6)	-0.0003(5)	0.0018(5)	-0.0027(5)
N3	0.0063(5)	0.0107(5)	0.0084(5)	-0.0004(4)	0.0012(4)	-0.0005(4)
N4	0.0119(6)	0.0160(6)	0.0194(6)	-0.0002(5)	0.0022(5)	-0.0017(5)
O1	0.0068(4)	0.0127(5)	0.0139(5)	0.0018(4)	0.0011(4)	0.0015(3)
O2	0.0083(4)	0.0096(4)	0.0145(5)	0.0012(4)	0.0005(4)	-0.0004(3)
O3	0.0118(5)	0.0093(5)	0.0173(5)	-0.0003(4)	0.0017(4)	0.0025(4)
O4	0.0060(4)	0.0153(5)	0.0148(5)	0.0008(4)	0.0006(4)	0.0016(4)
O5	0.0071(4)	0.0083(4)	0.0130(4)	0.0002(3)	0.0024(3)	0.0001(3)
O6	0.0099(4)	0.0089(4)	0.0152(5)	0.0012(4)	0.0031(4)	-0.0004(3)
O1W	0.0193(5)	0.0102(5)	0.0146(5)	0.0007(4)	0.0082(4)	0.0016(4)
O2W	0.0096(5)	0.0271(6)	0.0128(5)	-0.0001(4)	0.0020(4)	0.0011(4)
O3W	0.0124(5)	0.0218(6)	0.0140(5)	-0.0009(4)	0.0046(4)	-0.0023(4)

Appendix C-24. Hydrogen bond distances (Å) and angles (°) for $K_2[Cu(AACO)_2H_2O]\cdot 2H_2O$.

	Donor-H	Acceptor-H	Donor-Acceptor	Angle
O3W-H2O3···O1	0.9583(10)	2.053(4)	3.0026(16)	170.5(18)
O2W-H2O2···O1	0.9583(10)	2.040(4)	2.9872(16)	169.7(19)
O1W-H2O1···O6	0.9580(10)	1.792(6)	2.7245(15)	163.5(18)
O3W-H1O3···O6	0.9583(10)	1.920(5)	2.8701(16)	171.(3)
O2W-H1O2···O6	0.9583(10)	1.984(9)	2.9161(16)	164.(3)

OXAMIDE

Appendix C-25. Atomic coordinates and equivalent isotropic atomic displacement parameters ($Å^2$) for oxamide.

U(eq) is defined as one third of the trace of the orthogonalized U_{ij} tensor.

	x/a	y/b	z/c	U(eq)
C1	0.1420(3)	0.50735(19)	0.63607(17)	0.0106(3)
N1	0.0428(2)	0.27681(17)	0.76303(16)	0.0131(3)
O1	0.4344(2)	0.72197(14)	0.71779(13)	0.0135(3)

Appendix C-26. Anisotropic atomic displacement parameters ($Å^2$) for oxamide.

The anisotropic atomic displacement factor exponent takes the form: $-2\pi^2[h^2 a^{*2} U_{11} + ... + 2 h k a^* b^* U_{12}]$

	U_{11}	U_{22}	U_{33}	U_{23}	U_{13}	U_{12}
C1	0.0099(5)	0.0120(5)	0.0099(5)	0.0006(3)	0.0018(3)	0.0037(3)
N1	0.0127(5)	0.0121(5)	0.0113(5)	0.0028(3)	-0.0002(3)	0.0009(3)
O1	0.0127(4)	0.0120(4)	0.0123(4)	0.0018(3)	0.0001(3)	0.0002(3)

Appendix C-27. Hydrogen bond distances (Å) and angles (°) for oxamide.

	Donor-H	Acceptor-H	Donor-Acceptor	Angle
N1-H1N1¨O1	0.908(16)	2.030(16)	2.9371(11)	178.1(13)
N1-H2N¨O1	0.862(17)	2.149(16)	2.9228(12)	149.2(13)

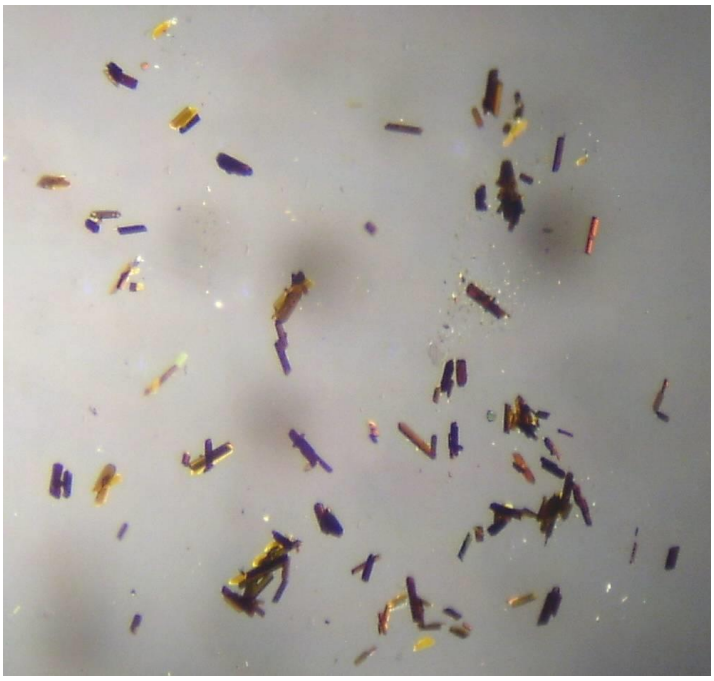

Appendix C-28. Crystals of $K_2[Cu_3(AACO)_4(H_2O)_4]\cdot 4H_2O$ under the microscope x10.

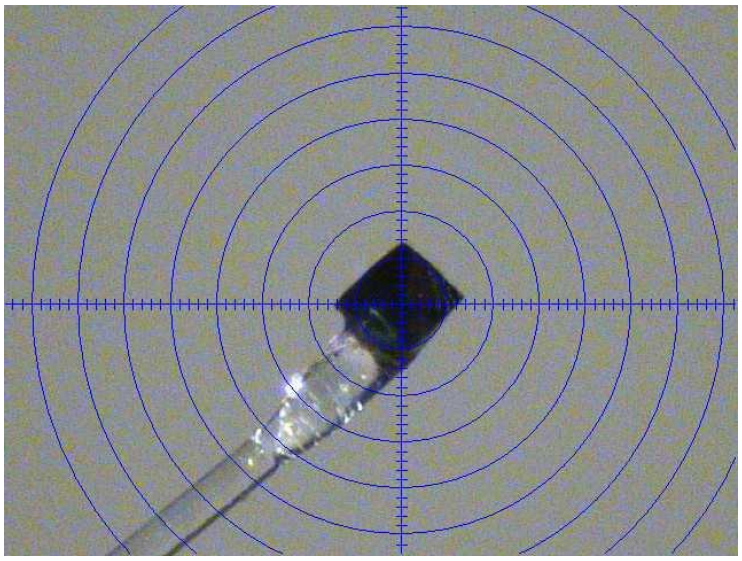

Appendix C-29. Actual videomicroscope image of $K_2[Cu(AACO)_2H_2O]\cdot 2H_2O$.

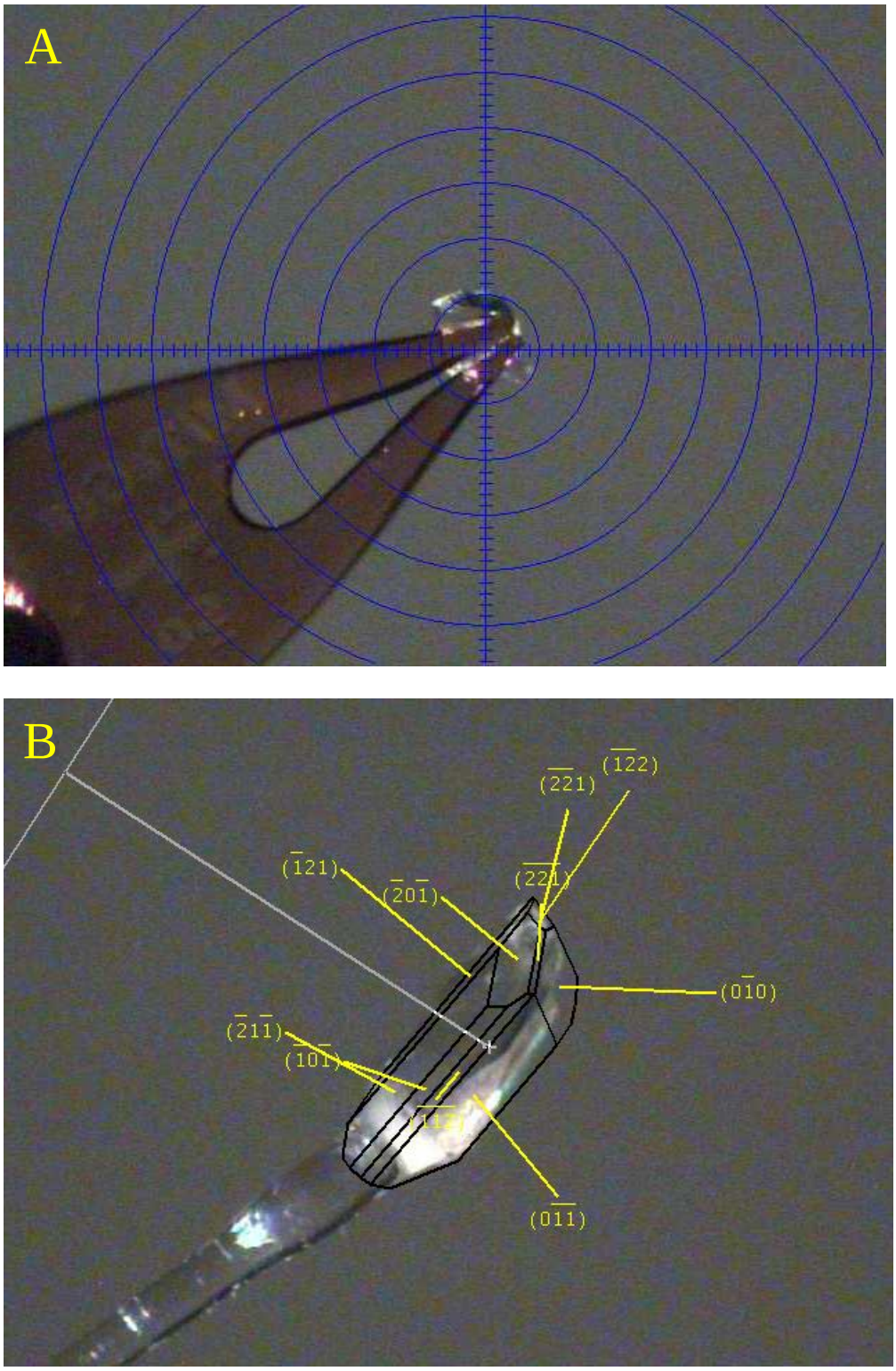

Appendix C-30. Actual videomicroscope image of the crystal of oxamide (A), and indexed faces of the crystal (B).

Appendix C-31. checkCIF-reports for HECO

```
Bond precision:      C-C = 0.0033 A              Wavelength=0.71073
Cell:         a=6.336(2)     b=13.549(4)    c=7.938(3)
              alpha=90       beta=94.418(5) gamma=90
Temperature: 120 K
                    Calculated                      Reported
Volume              679.4(4)                        679.4(4)
Space group         P 21/c                          P 21/c
Hall group          -P 2ybc                         -P 2ybc
Moiety formula      C5 H6 N2 O3                     ?
Sum formula         C5 H6 N2 O3                     C5 H6 N2 O3
Mr                  142.12                          142.12
Dx,g cm-3           1.389                           1.389
Z                   4                               4
Mu (mm-1)           0.117                           0.117
F000                296.0                           296.0
F000'               296.17
h,k,lmax            7,16,9                          0,0,0
Nref                1381                            1377
Tmin,Tmax           0.973,0.987                     0.917,0.993
Tmin'               0.961
Correction method= # Reported T Limits: Tmin=0.917
Tmax=0.993 AbsCorr = MULTI-SCAN
Data completeness= 0.997        Theta(max)= 26.369
R(reflections)= 0.0545( 1016)      wR2(reflections)= 0.1118( 1377)
S = 1.146              Npar= 115
```

The following ALERTS were generated. Each ALERT has the format
test-name_ALERT_alert-type_alert-level.
Click on the hyperlinks for more details of the test.

Alert level C

PLAT030_ALERT_1_C _diffrn_reflns_number < _reflns_number_total Please Check
PLAT480_ALERT_4_C Long H...A H-Bond Reported H4B .. O2 .. 2.67 Ang.
And 9 other PLAT480 Alerts
More ...
PLAT906_ALERT_3_C Large K value in the Analysis of Variance ..... 15.265 Check
PLAT906_ALERT_3_C Large K value in the Analysis of Variance ..... 2.493 Check

Alert level G

PLAT194_ALERT_1_G Missing _cell_measurement_reflns_used Datum .... Please Add
PLAT195_ALERT_1_G Missing _cell_measurement_theta_max Datum .... Please Add
PLAT196_ALERT_1_G Missing _cell_measurement_theta_min Datum .... Please Add
PLAT720_ALERT_4_G Number of Unusual/Non-Standard Labels ..... 1 Note
PLAT912_ALERT_4_G Missing # of FCF Reflections Above STh/L= 0.600 4 Note
PLAT961_ALERT_5_G Dataset Contains no Negative Intensities ..... Please Check

0 **ALERT level A** = Most likely a serious problem - resolve or explain
0 **ALERT level B** = A potentially serious problem, consider carefully
13 **ALERT level C** = Check. Ensure it is not caused by an omission or oversight
6 **ALERT level G** = General information/check it is not something unexpected

4 ALERT type 1 CIF construction/syntax error, inconsistent or missing data
0 ALERT type 2 Indicator that the structure model may be wrong or deficient
2 ALERT type 3 Indicator that the structure quality may be low
12 ALERT type 4 Improvement, methodology, query or suggestion
1 ALERT type 5 Informative message, check

Appendix C-32. checkCIF-reports for $[Ni(ACO)_2 \cdot 2H_2O]$

```
Bond precision:      C-C = 0.0060 A              Wavelength=0.71073
Cell:         a=7.4698(14)    b=6.8635(13)    c=23.379(5)
              alpha=90        beta=90         gamma=90
Temperature:119 K
                    Calculated                      Reported
Volume              1198.6(4)                       1198.6(4)
Space group         C m c a                         C m c a
Hall group          -C 2bc 2                        -C 2bc 2
Moiety formula      C6 H6 N6 Ni O6                  ?
Sum formula         C6 H6 N6 Ni O6                  C1.50 H2 N1.50 Ni0.25 O1.50
Mr                  316.86                          79.72
Dx,g cm-3           1.756                           1.767
Z                   4                               16
Mu (mm-1)           1.654                           1.654
F000                640.0                           648.0
F000'               641.64
h,k,lmax            9,8,30                          9,8,30
Nref                723                             721
Tmin,Tmax           0.809,0.889                     0.678,0.746
Tmin'               0.783
Correction method= # Reported T Limits: Tmin=0.678
Tmax=0.746 AbsCorr = MULTI-SCAN
Data completeness= 0.997        Theta(max)= 27.160
R(reflections)= 0.0417( 570)       wR2(reflections)= 0.1013( 721)
S = 1.043             Npar= 62
```

The following ALERTS were generated. Each ALERT has the format
test-name_ALERT_alert-type_alert-level.
Click on the hyperlinks for more details of the test.

Alert level C

PLAT041_ALERT_1_C Calc. and Reported SumFormula Strings Differ Please Check
PLAT043_ALERT_1_C Calculated and Reported Mol. Weight Differ by .. 2.02 Check
PLAT048_ALERT_1_C MoietyFormula Not Given ..... Please Do !
PLAT068_ALERT_1_C Reported F000 Differs from Calcd (or Missing)... Please Check
PLAT213_ALERT_2_C Atom O1 has ADP max/min Ratio ..... 3.1 prolat
PLAT250_ALERT_2_C Large U3/U1 Ratio for Average U(i,j) Tensor .... 3.7 Note
PLAT752_ALERT_4_C Angle Calc 90.00, Rep 90.00 ..... Senseless su
O3W -NI1 -O2 1.555 1.555 1.555 # 15
PLAT911_ALERT_3_C Missing # FCF Refl Between THmin & STh/L= 0.600 2 Report
PLAT975_ALERT_2_C Check Calcd Residual Density 0.97A From O3W 0.44 eA-3

Alert level G

FORMU01_ALERT_2_G There is a discrepancy between the atom counts in the
_chemical_formula_sum and the formula from the _atom_site* data.
Atom count from _chemical_formula_sum:C1.5 H2 N1.5 Ni0.25 O1.5
Atom count from the _atom_site data: C1.5 H1.5 N1.5 Ni0.25 O1.5
CELLZ01_ALERT_1_G Difference between formula and atom_site contents detected.
CELLZ01_ALERT_1_G WARNING: H atoms missing from atom site list. Is this intentional?
From the CIF: _cell_formula_units_Z 16
From the CIF: _chemical_formula_sum C1.50 H2 N1.50 Ni0.25 O1.50
TEST: Compare cell contents of formula and atom_site data

atom	Z*formula	cif sites	diff
C	24.00	24.00	0.00
H	32.00	24.00	8.00

N 24.00 24.00 0.00
Ni 4.00 4.00 0.00
O 24.00 24.00 0.00
PLAT002_ALERT_2_G Number of Distance or Angle Restraints on AtSite 2 Note
PLAT003_ALERT_2_G Number of Uiso or Uij Restrained non-H Atoms ... 1 Report
PLAT007_ALERT_5_G Number of Unrefined Donor-H Atoms ..... 2 Report
PLAT045_ALERT_1_G Calculated and Reported Z Differ by ..... 0.25 Ratio
PLAT083_ALERT_2_G SHELXL Second Parameter in WGHT Unusually Large. 5.36 Why
?
PLAT172_ALERT_4_G The CIF-Embedded .res File Contains DFIX Records 1 Report
PLAT300_ALERT_4_G Atom Site Occupancy of *H1 is Constrained at 0.500 Check
And 3 other PLAT300 Alerts
More ...
PLAT860_ALERT_3_G Number of Least-Squares Restraints ..... 7 Note

---

0 **ALERT level A** = Most likely a serious problem - resolve or explain
0 **ALERT level B** = A potentially serious problem, consider carefully
9 **ALERT level C** = Check. Ensure it is not caused by an omission or oversight
14 **ALERT level G** = General information/check it is not something unexpected

7 ALERT type 1 CIF construction/syntax error, inconsistent or
missing data
7 ALERT type 2 Indicator that the structure model may be wrong or deficient
2 ALERT type 3 Indicator that the structure quality may be low
6 ALERT type 4 Improvement, methodology, query or suggestion
1 ALERT type 5 Informative message, check

Appendix C-33. checkCIF-reports for [Ni(2PCO)$_2$·2H$_2$O]

```
Bond precision:      C-C = 0.0030 A              Wavelength=0.71073
Cell:         a=5.9748(7)     b=6.2596(8)     c=11.0397(13)
              alpha=86.128(2) beta=83.705(2) gamma=75.332(2)
Temperature: 120 K
                    Calculated                      Reported
Volume              396.68(8)                       396.68(8)
Space group         P -1                            P -1
Hall group          -P 1                            -P 1
Moiety formula      C14 H12 N6 Ni O4                C14 H12 N6 Ni O4
Sum formula         C14 H12 N6 Ni O4                C14 H12 N6 Ni O4
Mr                  386.99                          387.01
Dx,g cm-3           1.620                           1.620
Z                   1                               1
Mu (mm-1)           1.257                           1.257
F000                198.0                           198.0
F000'               198.41
h,k,lmax            7,8,14                          7,8,14
Nref                1945                            1935
Tmin,Tmax           0.894,0.916                     0.845,0.983
Tmin'               0.772
Correction method= # Reported T Limits: Tmin=0.845
Tmax=0.983 AbsCorr = NUMERICAL
Data completeness= 0.995        Theta(max)= 28.171
R(reflections)= 0.0324( 1764)      wR2(reflections)= 0.0703( 1935)
S = 1.043              Npar= 115
```

The following ALERTS were generated. Each ALERT has the format
test-name_ALERT_alert-type_alert-level.
Click on the hyperlinks for more details of the test.

Alert level C

PLAT415_ALERT_2_C Short Inter D-H..H-X H3B .. H7 .. 2.12 Ang.
PLAT911_ALERT_3_C Missing # FCF Refl Between THmin & STh/L= 0.600 3 Report
PLAT975_ALERT_2_C Check Calcd Residual Density 1.03A From O1 0.42 eA-3

Alert level G

PLAT007_ALERT_5_G Number of Unrefined Donor-H Atoms ..... 2 Report
PLAT154_ALERT_1_G The su's on the Cell Angles are Equal ..... 0.00200 Degree
PLAT232_ALERT_2_G Hirshfeld Test Diff (M-X) Ni1 -- N1 .. 6.5 su
PLAT912_ALERT_4_G Missing # of FCF Reflections Above STh/L= 0.600 7 Note

0 **ALERT level A** = Most likely a serious problem - resolve or explain
0 **ALERT level B** = A potentially serious problem, consider carefully
3 **ALERT level C** = Check. Ensure it is not caused by an omission or oversight
4 **ALERT level G** = General information/check it is not something unexpected

1 ALERT type 1 CIF construction/syntax error, inconsistent or missing data
3 ALERT type 2 Indicator that the structure model may be wrong or deficient
1 ALERT type 3 Indicator that the structure quality may be low
1 ALERT type 4 Improvement, methodology, query or suggestion
1 ALERT type 5 Informative message, check

Appendix C-34. checkCIF-reports for $[Ni(AACO)\cdot(H_2O)_3]_2\cdot H_2O$

```
Bond precision:      C-C = 0.0020 A              Wavelength=0.71073
Cell:         a=16.0508(10)  b=6.4725(5)     c=16.5248(13)
              alpha=90       beta=114.245(1) gamma=90
Temperature: 120 K
                    Calculated                      Reported
Volume              1565.3(2)                       1565.3(2)
Space group         C 2/c                           C 2/c
Hall group          -C 2yc                          -C 2yc
Moiety formula      C6 H12 N4 Ni2 O12, 2(H2 O)      ?
Sum formula         C6 H16 N4 Ni2 O14               C3 H8 N2 Ni O7
Mr                  485.61                          242.82
Dx,g cm-3           2.061                           2.061
Z                   4                               8
Mu (mm-1)           2.492                           2.492
F000                992.0                           992.0
F000'               995.29
h,k,lmax            24,9,25                         24,9,25
Nref                2953                            2791
Tmin,Tmax           0.586,0.723                     0.607,0.751
Tmin'               0.528
Correction method= # Reported T Limits: Tmin=0.607
Tmax=0.751 AbsCorr = MULTI-SCAN
Data completeness= 0.945        Theta(max)= 33.021
R(reflections)= 0.0269( 2446)      wR2(reflections)= 0.0630( 2791)
S = 1.147             Npar= 150
```

The following ALERTS were generated. Each ALERT has the format
test-name_ALERT_alert-type_alert-level.
Click on the hyperlinks for more details of the test.

Alert level A

PLAT417_ALERT_2_A Short Inter D-H..H-D H5A .. H5A .. 1.42 Ang.

Alert level C

PLAT222_ALERT_3_C Large Non-Solvent H Uiso(max)/Uiso(min) ... 5.3 Ratio
PLAT975_ALERT_2_C Check Calcd Residual Density 0.61A From O6W 0.47 eA-3
And 2 other PLAT975 Alerts
More ...

Alert level G

PLAT002_ALERT_2_G Number of Distance or Angle Restraints on AtSite 12 Note
PLAT045_ALERT_1_G Calculated and Reported Z Differ by ..... 0.50 Ratio
PLAT172_ALERT_4_G The CIF-Embedded .res File Contains DFIX Records 8 Report
PLAT232_ALERT_2_G Hirshfeld Test Diff (M-X) Ni1 -- O4W .. 9.3 su
And 2 other PLAT232 Alerts
More ...
PLAT432_ALERT_2_G Short Inter X...Y Contact C2 .. C3 .. 3.17 Ang.
PLAT860_ALERT_3_G Number of Least-Squares Restraints ..... 12 Note
PLAT912_ALERT_4_G Missing # of FCF Reflections Above STh/L= 0.600 162 Note

1 **ALERT level A** = Most likely a serious problem - resolve or explain
0 **ALERT level B** = A potentially serious problem, consider carefully
4 **ALERT level C** = Check. Ensure it is not caused by an omission or oversight
9 **ALERT level G** = General information/check it is not something unexpected

1 ALERT type 1 CIF construction/syntax error, inconsistent or missing data
9 ALERT type 2 Indicator that the structure model may be wrong or deficient
2 ALERT type 3 Indicator that the structure quality may be low
2 ALERT type 4 Improvement, methodology, query or suggestion
0 ALERT type 5 Informative message, check

Appendix C-35. checkCIF-reports for $K_2[Ni_3(AACO)_4(H_2O)_4]\cdot 4H_2O$

```
Bond precision:      C-C = 0.0083 A              Wavelength=0.71073
Cell:         a=9.750(2)      b=6.7291(15)    c=20.616(5)
              alpha=90        beta=90.508(4)  gamma=90
Temperature: 100 K
                    Calculated                      Reported
Volume              1352.5(5)                       1352.6(5)
Space group         P 21/n                          P 21/n
Hall group          -P 2yn                          -P 2yn
Moiety formula      C12 H16 K2 N8 Ni3 O20           C12 H16 K2 N8 Ni3 O20
Sum formula         C12 H16 K2 N8 Ni3 O20           C12 H16 K2 N8 Ni3 O20
Mr                  846.60                          846.60
Dx,g cm-3           2.079                           2.079
Z                   2                               2
Mu (mm-1)           2.479                           2.479
F000                852.0                           852.0
F000'               855.27
h,k,lmax            11,8,24                         11,8,24
Nref                2379                            2377
Tmin,Tmax           0.827,0.860                     0.868,0.963
Tmin'               0.728
Correction method= # Reported T Limits: Tmin=0.868
Tmax=0.963 AbsCorr = MULTI-SCAN
Data completeness= 0.999        Theta(max)= 24.999
R(reflections)= 0.0477( 1696)      wR2(reflections)= 0.1159( 2377)
S = 1.043             Npar= 231
```

The following ALERTS were generated. Each ALERT has the format
test-name_ALERT_alert-type_alert-level.
Click on the hyperlinks for more details of the test.

Alert level C

PLAT222_ALERT_3_C Large Non-Solvent H Uiso(max)/Uiso(min) ... 4.4 Ratio
PLAT341_ALERT_3_C Low Bond Precision on C-C Bonds ..... 0.0083 Ang.
PLAT911_ALERT_3_C Missing # FCF Refl Between THmin & STh/L= 0.595 3 Report
PLAT975_ALERT_2_C Check Calcd Residual Density 1.03A From O4 0.41 eA-3

Alert level G

PLAT002_ALERT_2_G Number of Distance or Angle Restraints on AtSite 12 Note
PLAT004_ALERT_5_G Polymeric Structure Found with Maximum Dimension 3 Info
PLAT007_ALERT_5_G Number of Unrefined Donor-H Atoms ..... 2 Report
PLAT172_ALERT_4_G The CIF-Embedded .res File Contains DFIX Records 8 Report
PLAT720_ALERT_4_G Number of Unusual/Non-Standard Labels ..... 8 Note
PLAT764_ALERT_4_G Overcomplete CIF Bond List Detected (Rep/Expd) . 1.24 Ratio
PLAT774_ALERT_1_G Suspect X-Y Bond in CIF: K2 -- K2 .. 4.08 Ang.
PLAT774_ALERT_1_G Suspect X-Y Bond in CIF: K2 -- K2 .. 4.08 Ang.
PLAT860_ALERT_3_G Number of Least-Squares Restraints ..... 12 Note z
PLAT909_ALERT_3_G Percentage of Observed Data at Theta(Max) still 50 %

---

0 **ALERT level A** = Most likely a serious problem - resolve or explain

0 **ALERT level B** = A potentially serious problem, consider carefully
4 **ALERT level C** = Check. Ensure it is not caused by an omission or oversight
10 **ALERT level G** = General information/check it is not something unexpected

2 ALERT type 1 CIF construction/syntax error, inconsistent or missing data
2 ALERT type 2 Indicator that the structure model may be wrong or deficient
5 ALERT type 3 Indicator that the structure quality may be low
3 ALERT type 4 Improvement, methodology, query or suggestion
2 ALERT type 5 Informative message, check

Appendix C-36. checkCIF-reports for $K_2[Cu_3(AACO)_4(H_2O)_4]\cdot 4H_2O$

```
Bond precision:      C-C = 0.0060 A              Wavelength=0.71073
```

```
Cell:         a=9.7412(11)    b=6.7282(8)     c=20.585(2)
              alpha=90        beta=90.543(2)  gamma=90
Temperature: 120 K
                    Calculated                      Reported
Volume              1349.1(3)                       1349.1(3)
Space group         P 21/n                          P 21/n
Hall group          -P 2yn                          -P 2yn
Moiety formula      C12 H16 Cu3 K2 N8 O20           ?
Sum formula         C12 H16 Cu3 K2 N8 O20           C6 H8 Cu1.50 K N4 O10
Mr                  861.18                          430.57
Dx,g cm-3           2.120                           2.120
Z                   2                               4
Mu (mm-1)           2.757                           2.757
F000                858.0                           858.0
F000'               861.15
h,k,lmax            13,8,27                         13,8,27
Nref                3355                            3356
Tmin,Tmax           0.778,0.820                     0.659,0.746
Tmin'               0.650
Correction method= # Reported T Limits: Tmin=0.659
Tmax=0.746 AbsCorr = NUMERICAL
Data completeness= 1.000        Theta(max)= 28.354
R(reflections)= 0.0426( 2415)      wR2(reflections)= 0.0948( 3356)
S = 1.025              Npar= 237
```

The following ALERTS were generated. Each ALERT has the format
test-name_ALERT_alert-type_alert-level.
Click on the hyperlinks for more details of the test.

Alert level C

PLAT048_ALERT_1_C MoietyFormula Not Given ..... Please Do !
PLAT975_ALERT_2_C Check Calcd Residual Density 1.03A From O2W 0.50 eA-3
PLAT975_ALERT_2_C Check Calcd Residual Density 0.65A From O3W 0.44 eA-3
PLAT976_ALERT_2_C Check Calcd Residual Density 1.08A From O6 -0.45 eA-3
PLAT976_ALERT_2_C Check Calcd Residual Density 0.88A From O2W -0.45 eA-3

Alert level G

PLAT002_ALERT_2_G Number of Distance or Angle Restraints on AtSite 12 Note
PLAT004_ALERT_5_G Polymeric Structure Found with Maximum Dimension 3 Info
PLAT045_ALERT_1_G Calculated and Reported Z Differ by ..... 0.50 Ratio
PLAT172_ALERT_4_G The CIF-Embedded .res File Contains DFIX Records 8 Report
PLAT173_ALERT_4_G The CIF-Embedded .res File Contains DANG Records 4 Report
PLAT764_ALERT_4_G Overcomplete CIF Bond List Detected (Rep/Expd) . 1.24 Ratio
PLAT774_ALERT_1_G Suspect X-Y Bond in CIF: K1 -- K1 .. 4.08 Ang.
PLAT774_ALERT_1_G Suspect X-Y Bond in CIF: K1 -- K1 .. 4.08 Ang.
PLAT794_ALERT_5_G Tentative Bond Valency for Cu1 (II) ..... 2.23 Note
PLAT794_ALERT_5_G Tentative Bond Valency for Cu2 (II) ..... 2.25 Note
PLAT860_ALERT_3_G Number of Least-Squares Restraints ..... 12 Note

---

0 **ALERT level A** = Most likely a serious problem - resolve or explain
0 **ALERT level B** = A potentially serious problem, consider carefully
5 **ALERT level C** = Check. Ensure it is not caused by an omission or oversight
11 **ALERT level G** = General information/check it is not something unexpected

4 ALERT type 1 CIF construction/syntax error, inconsistent or missing data
5 ALERT type 2 Indicator that the structure model may be wrong or deficient

1 ALERT type 3 Indicator that the structure quality may be low
3 ALERT type 4 Improvement, methodology, query or suggestion
3 ALERT type 5 Informative message, check

Appendix C-37. checkCIF-reports for $K_2[Cu(AACO)_2H_2O]\cdot 2H_2O$

Bond precision: C-C = 0.0020 A Wavelength=0.71073
Cell: a=8.7730(6) b=12.4214(8) c=13.1215(8)

```
            alpha=90       beta=108.350(1) gamma=90
Temperature: 100 K
                  Calculated                    Reported
Volume            1357.18(15)                   1357.18(15)
Space group       P 21/c                        P 21/c
Hall group        -P 2ybc                       -P 2ybc
Moiety formula    C6 H6 Cu K2 N4 O9             C6 H6 Cu K2 N4 O9
Sum formula       C6 H6 Cu K2 N4 O9             C6 H6 Cu K2 N4 O9
Mr                419.90                        419.89
Dx,g cm-3         2.055                         2.055
Z                 4                             4
Mu (mm-1)         2.276                         2.276
F000              836.0                         836.0
F000'             839.29
h,k,lmax          13,19,20                      12,18,13
Nref              5105                          4756
Tmin,Tmax         0.625,0.724                   0.628,0.747
Tmin'             0.613
Correction method= # Reported T Limits: Tmin=0.628
Tmax=0.747 AbsCorr = MULTI-SCAN
Data completeness= 0.932       Theta(max)= 32.987
R(reflections)= 0.0242( 4310)     wR2(reflections)= 0.0605( 4756)
S = 1.002            Npar= 223
```

The following ALERTS were generated. Each ALERT has the format
test-name_ALERT_alert-type_alert-level.
Click on the hyperlinks for more details of the test.

Alert level C

PLAT911_ALERT_3_C Missing # FCF Refl Between THmin & STh/L= 0.600 2 Report

---

Appendix C-38. checkCIF-reports for Oxamide

```
Bond precision:     C-C = 0.0013 A              Wavelength=0.71073
Cell:         a=3.5592(7)     b=4.8685(10)    c=5.2934(10)
              alpha=90.842(2) beta=103.472(2) gamma=106.075(2)
Temperature: 119 K
```

	Calculated	Reported
Volume	85.40(3)	85.40(3)
Space group	P -1	P -1
Hall group	-P 1	-P 1
Moiety formula	C2 H4 N2 O2	C2 H4 N2 O2
Sum formula	C2 H4 N2 O2	C2 H4 N2 O2
Mr	88.07	88.03
Dx,g cm-3	1.712	1.673
Z	1	1
Mu (mm-1)	0.152	0.150
F000	46.0	44.0
F000'	46.03	
h,k,lmax	4,6,6	4,6,6
Nref	410	411
Tmin,Tmax	0.951,0.961	0.701,0.746
Tmin'	0.923	

Correction method= # Reported T Limits: Tmin=0.701 Tmax=0.746 AbsCorr = NUMERICAL

Data completeness= 1.002 Theta(max)= 27.813

R(reflections)= 0.0265(401) wR2(reflections)= 0.0796(411)

S = 1.211 Npar= 37

The following ALERTS were generated. Each ALERT has the format
test-name_ALERT_alert-type_alert-level.
Click on the hyperlinks for more details of the test.

Alert level C

ABSMU01_ALERT_1_C The ratio of given/expected absorption coefficient lies outside the range 0.99 <> 1.01
Calculated value of mu = 0.152
Value of mu given = 0.150

DENSD01_ALERT_1_C The ratio of the submitted crystal density and that calculated from the formula is outside the range 0.99 <> 1.01
Crystal density given = 1.673
Calculated crystal density = 1.712

PLAT046_ALERT_1_C Reported Z, MW and D(calc) are Inconsistent 1.712

PLAT068_ALERT_1_C Reported F000 Differs from Calcd (or Missing)... Please Check

PLAT094_ALERT_2_C Ratio of Maximum / Minimum Residual Density .... 2.35 Report

PLAT369_ALERT_2_C Long C(sp2)-C(sp2) Bond C1 - C1_a .. 1.54 Ang.

Alert level G

PLAT154_ALERT_1_G The s.u.'s on the Cell Angles are Equal ..(Note) 0.002 Degree

PLAT172_ALERT_4_G The CIF-Embedded .res File Contains DFIX Records 1 Report

PLAT173_ALERT_4_G The CIF-Embedded .res File Contains DANG Records 1 Report

PLAT720_ALERT_4_G Number of Unusual/Non-Standard Labels ..... 1 Note

---

0 **ALERT level A** = Most likely a serious problem - resolve or explain
0 **ALERT level B** = A potentially serious problem, consider carefully
6 **ALERT level C** = Check. Ensure it is not caused by an omission or oversight
4 **ALERT level G** = General information/check it is not something unexpected

5 ALERT type 1 CIF construction/syntax error, inconsistent or missing data
2 ALERT type 2 Indicator that the structure model may be wrong or deficient
0 ALERT type 3 Indicator that the structure quality may be low
3 ALERT type 4 Improvement, methodology, query or suggestion
0 ALERT type 5 Informative message, check

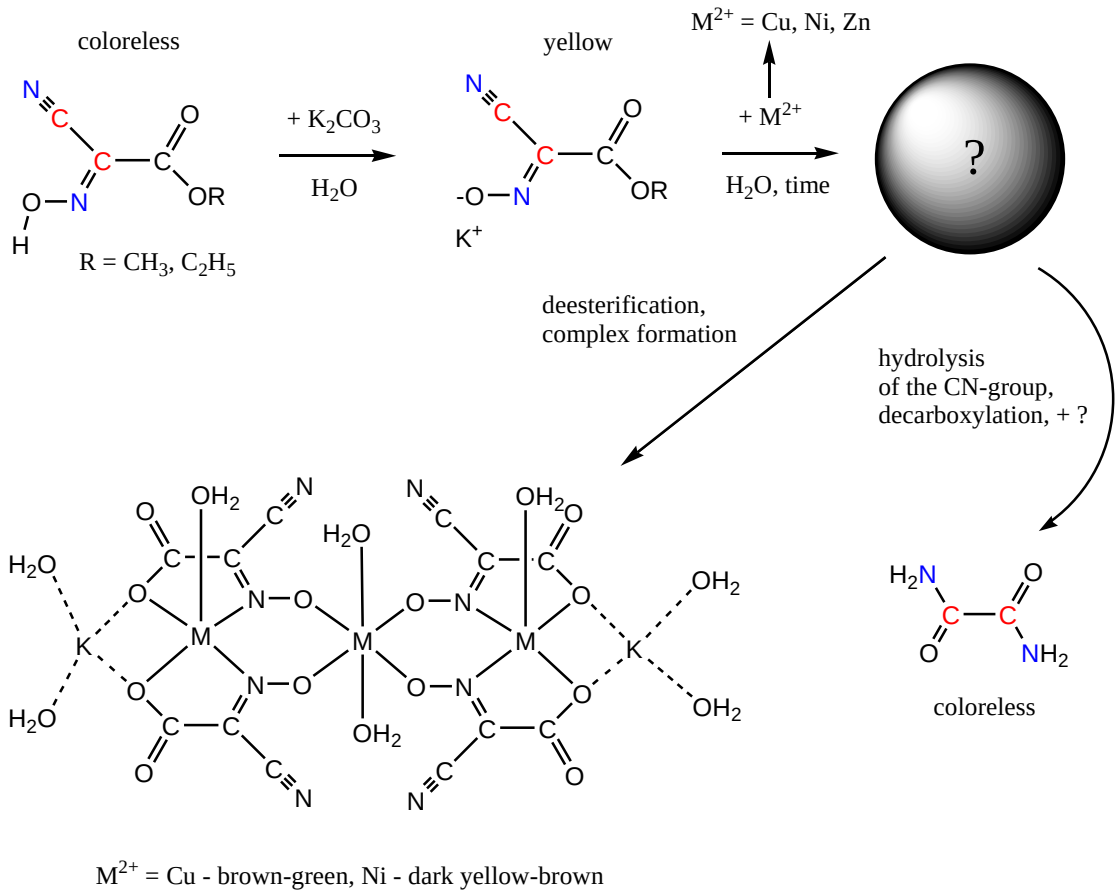

Appendix D. Formation of multinuclear complexes and oxamide side product.